

UNIVERSITÀ
DEGLI STUDI
DI PADOVA

Sede Amministrativa: Università degli Studi di Padova

Dipartimento di Scienze Statistiche
Corso di Dottorato di Ricerca in Scienze Statistiche
Ciclo XXXI

Competition and Substitution in Energy: Old Scenarios and Emerging Technologies

Coordinatore del Corso: Prof. Nicola Sartori

Supervisore: Prof. Cinzia Mortarino

Co-supervisore: Prof. Claudia Furlan

Dottorando: Mohammad Salim Zahangir

Abstract

The diffusion of an innovation in a social system is characterised as a dynamic that typically gives rise to a finite lifecycle. The pioneering approach by Bass (1969), called the Bass model (BM), has been widely used because it considers the internal rules of the social system. The model has been extended in several directions. The generalised Bass model (GBM), by Bass *et al.* (1994), is the most popular extension describing the exogenous interventions acting on the timing of the diffusion process. Another important extension is the Guseo and Guidolin (2009) model (GGM), which defines the dynamic nature of the latent market potential. However, these univariate time series models do not consider the competitive environment, in which two or more concurrent innovations enter the market, possibly at different times, and target the main set of potential adopters or subgroups of potential adopters with possible interaction effects.

The model proposed by Guseo and Mortarino (2014) allows a flexible behaviour in describing the diffusion of two products under competition, where interaction effects, namely word-of-mouth (WOM), are split into within-product and cross-product effects. This thesis proposes an extended diffusion model for three products in a competitive framework that may be able to improve the description of mutual interactions (either competition or cooperation), along with defining specific features of each product. To examine the improvement of the proposed three-competitor model (3CM) compared with the bivariate model (2CM), both models are applied to energy data to describe competition among energy sources. The intervention functions (e.g. the external shocks) are incorporated in the models when necessary to estimate the effect of incentives and policy measures, which are crucial tools in the expansion of renewables and nonrenewable energy technologies.

Without incorporating intervention functions, models based on the assumption of a constant market potential are virtually unable to capture the wide variety of shapes of products in a diffusion process. Following the model proposed by Guseo and Mortarino (2015), this thesis further proposes a diffusion model for three competing products that are sufficiently similar to share a common market potential, where the size increases over time. Models 2CM and 3CM with dynamic market potential (DMP) are also applied to the same energy data studied in the preceding part of this work. The obtained results highlight the efficacy of the models with DMP over similar models with fixed market potential. Overall, the proposed models (3CM), either with a fixed market potential, m , or DMP, prove to be useful in applied contexts, for example, in describing the lifecycle of products and evaluating predictions.

Sommario

La diffusione di un'innovazione in un sistema sociale si caratterizza come una dinamica che dà origine a un ciclo di vita finito. L'approccio pionieristico di Bass (1969), chiamato Bass model (BM), è stato ampiamente utilizzato in quanto tiene conto delle regole interne del sistema sociale. Il BM è stato esteso in molteplici direzioni. Il modello di Bass Generalizzato (GBM), Bass *et al.* (1994), è l'estensione più popolare e descrive gli interventi esogeni che agiscono sui tempi del processo di diffusione. Un'altra estensione importante è il modello Guseo and Guidolin (2009), (GGM), che definisce la natura dinamica del potenziale di mercato latente. Questi modelli per serie storiche univariate non considerano l'ambiente competitivo, in cui due o più innovazioni concorrenti entrano nel mercato, eventualmente in tempi diversi, e descrivono il gruppo principale di potenziali adottanti o sottogruppi di potenziali adottanti con possibili effetti di interazione.

Il modello proposto da Guseo and Mortarino (2014) consente di ottenere maggiore flessibilità nella descrizione della diffusione di due prodotti in competizione, dal momento che gli effetti di interazione, ovvero il passaparola (WOM), sono suddivisi in interni e incrociati.

Questa tesi propone un modello a diffusione esteso a tre prodotti in un quadro competitivo in grado di migliorare la descrizione delle interazioni reciproche (competizione o cooperazione), e di definire le caratteristiche specifiche di ciascun prodotto. Per valutare il miglioramento del modello proposto (3CM) rispetto al modello bivariato (2CM), entrambi i modelli sono applicati ai dati energetici per descrivere la competizione tra le diverse fonti energetiche. Le funzioni di intervento (ad es. gli shock esterni) sono integrate nei modelli per stimare l'effetto di incentivi e misure politiche, che sono strumenti cruciali per l'espansione delle energie rinnovabili e delle tecnologie energetiche non rinnovabili.

Senza incorporare le funzioni di intervento, i modelli basati sull'assunzione di un potenziale di mercato costante non sono virtualmente in grado di catturare un'ampia varietà di forme di prodotti in un processo di diffusione. Seguendo il modello proposto da Guseo and Mortarino (2015), nella seconda parte di questa tesi si propone un modello di diffusione per tre prodotti concorrenti che sono sufficientemente simili per condividere un potenziale di mercato comune, ma variabile nel tempo. I modelli 2CM e 3CM con potenziale di mercato dinamico (DMP) sono applicati agli stessi dati energetici esaminati nella prima parte di questo lavoro. I risultati ottenuti evidenziano l'efficacia dei modelli con DMP rispetto agli altri modelli simili con un potenziale di mercato fisso. Nel complesso, i modelli proposti (3CM) si dimostrano molto efficaci nelle applicazioni, nel descrivere il ciclo di vita dei prodotti e calcolare le corrispondenti previsioni.

Dedicated to my father
Late Md. Sayyed Ahammad

Acknowledgements

First and foremost, praise is to ALLAH, the Almighty, the most Merciful and the most Beneficent, for making me who I am today. I would like to thank Almighty Allah for giving me the opportunity, determination, strength, and wisdom to set off this research task and enabling me to its completion. I firmly believe that his eternal love and mercy are with me throughout my life and that was ever more during the tenure of this research.

Now, I would like to thank and express my deep and sincere gratitude to my supervisor Prof. Cinzia Mortarino for her continuous support, patience guidance, unflinching encouragement, and valuable advice during the period of my PhD studies. It is indeed honorable and invaluable to me that I have got an opportunity to work alongside and gain experiences from her flourish acumen as a great academician and excellent researcher. My deepest thanks go to my cosupervisor Prof. Claudia Furlan, who suggested me to think critically about the facts and findings of my research. Her quick feedback and logical inquisitions with constructive comments were really inspiring and helpful.

I would especially like to thank the academic committee of the PhD course and respective course instructors for sharing their esteemed knowledge and experiences that, with refining my ability of thinking, boosted my level of confidence for the successful completion of my studies here in Padova. My sincere thanks to the PhD course coordinators: Prof. Monica Chiogna who was during the first year and Prof. Nicola Sartori for the last two years of my PhD studies. It's my pleasure to acknowledge the contribution of all the departmental staffs in the PhD course of Statistical Sciences, who were responding very cordially to any of my academic, administrative and technical provisions. I especially acknowledge to Mrs. Patrizia Piacentini for her cooperation and fruitful assistance during my PhD tenure. I cannot forget to express my deep thanks to Prof. Gunnar Andersson and Prof. Juho Harkonen at Stockholm University, who were actively contributed as my referees for having this PhD position.

I raise the value of my classmates of XXXI PhD cycle: Gioia Di Credico, Ahabab Mohammad Fazle Rabbi, Grzegorz Michal Kotkowski, Waldir Leoncio Netto, Luca Maestrini, Sally Paganin, Thi Huong Phan, Massimiliano Russo, Margherita Silan and Charlotte Taglioni, who felt my loneliness and tried to make my moments enjoyable with their active presence and support. I will miss them and their worth company. Now, I would like to appreciate a post-doctoral fellow Lucia Zanotto from Italy and my junior PhD colleague Md Moinuddin from Bangladesh. They both, especially Md Moinuddin was very cordial to assist me when I suffered from illness for time and again. I remember my first year at Residenza Colombo, where from the first day I found my PhD mate Fazle Rabbi from Bangladesh. Hence, the days were not lonely and dull. I will never forget my next two years with G. K. Murad Bhai

and his family who always treated me as a family member and gave me a flavor of home away from home. I also remember my junior and senior PhD colleagues, especially Mohammad Adil from Pakistan, Mohammed Elseidi from Egypt, To Duc Khanh and Kim Hue Nguyen from Vietnam for inspiring me.

I wish to express my thanks and gratitude to my mother, the one who can never ever be thanked enough, for the overwhelming love and care she bestows upon me and for all her sacrifices that she has made on my behalf. Her diligent prayers for me were what sustained me so far. My special, profound and affectionate thanks, love, affectionate gratitude and deep indebtedness are due to my wife, Mrs. Kamrunnahar, who sacrificed a lot to secure and shape my brighter future; especially I cannot thank her enough for encouraging me throughout this experience. At the same time, I would like to express my love and thanks to ‘the beats of my heart’, my son, Kaisan Zahangir, who is the only source of inspiration to me, but due to an abnormal and complicated family visa policy for Bangladeshis’ in Italy, I missed enjoying his love and innocent smiles staying beside him during my PhD tenure. I am sincerely thankful to my mother-, father- and brother-in-law for constantly supporting me, especially for their love and care for my wife and son whom I kept to them during my PhD studies. My deep love and thanks to my sisters and their kids for adoring me and taking responsibility for my mother in my absence. Cordial thanks to my friend Zouhirul Quayem Badal and my cousins, especially elder brother Md. Abdul Baten and younger brother Md. Mozibur Rahman for their love and mental support.

Now, I acknowledge to the respected authority of the University of Chittagong, Bangladesh for granting me leave from my job and allowing me to stay abroad for more than three years. I express my deep thanks to my colleagues, especially Prof. Md. Abdul Karim, Prof. Soma Chowdhury Biswas, Prof. Md. Imam Hussain, Prof. Md. Emdadual Hoque, Prof. Md. Abdul Malek, Prof. Md. Monirul Islam, Asso.Prof. Md. Shakhawat Hossain and Assis.Prof. Mst. Zamilun Nahar for their wishes and administrative support from the department. My friend and colleague Asso.Prof. Md Rokonuzzaman Azad deserves a special mention in the series of my study for his tireless encouragements. Special thanks to my ex-colleague Dr. Md Masud Hasan, who constantly pushed me until not having this PhD position, and ever more fortified me during my PhD studies. Last, but not the least, I remember my CU friends – especially Azad, Liton, Mahfuz, Maruf, Mizan, Pasha, Saiful, Tofayel, and others – the bonding will never be faded. Honestly speaking, I tried to acknowledge all people for their love and support, but I sincerely apologize for any omissions here.

Padova
October 1, 2018

Mohammad Salim Zahangir

Contents

List of Figures	xiii
List of Tables	xvii
Introduction	1
Overview	1
Main contributions of the thesis	3
1 Review of innovation diffusion models	7
1.1 Introduction	7
1.2 Univariate diffusion models	9
1.2.1 The Bass Model	9
1.2.2 The Generalised Bass Model (GBM)	10
1.2.3 Guseo and Guidolin (2009) model (GGM)	13
1.3 Competition diffusion models	14
1.3.1 The two-competitor model with fixed m	14
1.3.2 The two-competitor model with dynamic market potential	16
1.4 Inferential aspects	18
1.4.1 Parameter estimates	18
1.4.2 Predictions and confidence bands	19
1.4.3 Forecasting accuracy	20
1.4.4 Comparison with alternative models	22
2 The three-competitor diffusion model with a fixed m	23
2.1 Introduction	23
2.2 The model	24
3 Applications of the three-competitor diffusion model with a fixed m	27
3.1 Introduction	27
3.2 The Data	29
3.3 Analysis	30
3.3.1 Belgium	32
3.3.2 Sweden	38
3.3.3 Switzerland	44
3.3.4 The United Kingdom	50
3.3.5 The United States	55

3.4	Remarks	60
4	The three-competitor diffusion model with dynamic market potential	63
4.1	Introduction	63
4.2	The Model	64
5	Applications of the three-competitor diffusion model with dynamic market potential	67
5.1	Introduction	67
5.2	Analysis	67
5.2.1	Belgium	68
5.2.1.1	2CM and 3CM DMP	68
5.2.1.2	Comparison between models with two and three competitors	70
5.2.1.3	Comparison among the alternative 3CM models	74
5.2.2	Finland	75
5.2.2.1	2CM and 3CM DMP	75
5.2.2.2	Comparison between models with two and three competitors	78
5.2.2.3	Comparison among the alternative 3CM models	81
5.2.3	France	82
5.2.3.1	2CM and 3CM DMP	82
5.2.3.2	Comparison between models with two and three competitors	84
5.2.3.3	Comparison among the alternative 3CM models	87
5.2.4	Germany	89
5.2.4.1	2CM and 3CM DMP	89
5.2.4.2	Comparison between models with two and three competitors	91
5.2.4.3	Comparison among the alternative 3CM models	94
5.3	Remarks	95
	Conclusions	99
	Discussion	99
	Future directions for research	103
	Appendix A Models with fixed m	105
	Appendix B Applications of the three-competitor diffusion model with a fixed m to other countries	109
B.1	China	109
B.1.1	An alternative partition of energy sources as two competitors	114
B.2	Finland	116
B.3	France	121
B.4	Germany	126

B.5 India	131
B.6 Japan	135
B.7 Spain	140
Appendix C Models with dynamic market potential	145
Appendix D A short essential bibliography	147
Bibliography	147

List of Figures

1.1	Simulated data according to assumption (1.18).	19
3.1	Belgium, 2CM. Energy consumption (Mtoe) from CGON sources (squares) and renewables (triangles). The solid lines correspond to the BSC fitted model with four shocks (three for CGON and one for renewables). The broken lines represent 2σ predictions' confidence bands.	32
3.2	Belgium, 3CM. Energy consumption (Mtoe) from CGO sources (circles), renewables (triangles) and nuclear (diamonds). The solid lines correspond to the BSC fitted model with five shocks (three for CGO, one for renewables and one for nuclear). The broken lines represent 2σ predictions' confidence bands.	34
3.3	Sweden, 2CM. Energy consumption (Mtoe) from CGON sources (squares) and renewables (triangles). The solid lines correspond to the USC fitted model with two shocks (one for each competitor). The broken lines represent 2σ predictions' confidence bands.	38
3.4	Sweden, 3CM. Energy consumption (Mtoe) from CGO sources (circles), renewables (triangles) and nuclear (diamonds). The solid lines correspond to the restricted UCRCF fitted model with three shocks (one for each competitor). The broken lines represent 2σ predictions' confidence bands.	41
3.5	Switzerland, 2CM. Energy consumption (Mtoe) from CGON sources (squares) and renewables (triangles). The solid lines correspond to the USC fitted model with two shocks (one for each competitor). The broken lines represent 2σ predictions' confidence bands.	45
3.6	Switzerland, 3CM. Energy consumption (Mtoe) from CGO sources (circles), renewables (triangles) and nuclear (diamonds). The solid lines correspond to the restricted UCRCF fitted model with three shocks (one for each competitor). The broken lines represent 2σ predictions' confidence bands.	47
3.7	The United Kingdom, 2CM. Energy consumption (Mtoe) from CGON sources (squares) and renewables (triangles). The solid lines correspond to the UUC fitted model with two shocks (one for each competitor). The broken lines represent 2σ predictions' confidence bands.	51
3.8	The United Kingdom, 3CM. Energy consumption (Mtoe) from CGO sources (circles), renewables (triangles) and nuclear (diamonds). The solid lines correspond to the USC fitted model with three shocks (one for each competitor). The broken lines represent 2σ predictions' confidence bands.	52
3.9	The United States, 2CM. Energy consumption (Mtoe) from CGON sources (squares) and renewables (triangles). The solid lines correspond to the BSC fitted model with four shocks (three for CGON and one for renewables). The broken lines represent 2σ predictions' confidence bands.	55

3.10	The United States, 3CM. Energy consumption (Mtoe) from CGO sources (circles), renewables (triangles) and nuclear (diamonds). The solid lines correspond to the BSC fitted model with five shocks (three for CGO, one for renewables and one for nuclear). The broken lines represent 2σ predictions' confidence bands.	58
5.1	Belgium. Plot of estimated market potential function, $\hat{m}(t)$, for two and three competitors.	69
5.2	Belgium. Observed data and fitted trajectories with predictions' 2σ confidence bands (thin lines): (a) 2CM, (b) 3CM.	72
5.3	Belgium, 3CM. Energy consumption (in Mtoe) form CGO sources (circles), renewables (triangles) and nuclear (diamonds). Solid (red) lines for the model with DMP, dashed (brown) lines for the model with fixed m and dotted (orange) lines for the model with fixed m and shocks.	75
5.4	Finland. Plot of estimated market potential function, $\hat{m}(t)$, for two and three competitors.	76
5.5	Finland. Observed data and fitted trajectories with predictions' 2σ confidence bands (thin lines): (a) 2CM, (b) 3CM.	79
5.6	Finland, 3CM. Energy consumption (in Mtoe) form CGO sources (circles), renewables (triangles) and nuclear (diamonds). Solid (red) lines for the model with DMP, dashed (brown) lines for the model with fixed m and dotted (orange) lines for the model with fixed m and shocks.	81
5.7	France. Plot of estimated market potential function, $\hat{m}(t)$, for two and three competitors.	83
5.8	France. Observed data and fitted trajectories with predictions' 2σ confidence bands (thin lines): (a) 2CM, (b) 3CM.	86
5.9	France, 3CM. Energy consumption (in Mtoe) form CGO sources (circles), renewables (triangles) and nuclear (diamonds). Solid (red) lines for the model with DMP, dashed (brown) lines for the model with fixed m and dotted (orange) lines for the model with fixed m and shocks.	88
5.10	Germany. Plot of estimated market potential function, $\hat{m}(t)$, for two and three competitors.	90
5.11	Germany. Observed data and fitted trajectories with predictions' 2σ confidence bands (thin lines): (a) 2CM, (b) 3CM.	93
5.12	Germany, 3CM. Energy consumption (in Mtoe) form CGO sources (circles), renewables (triangles) and nuclear (diamonds). Solid (red) lines for the model with DMP, dashed (brown) lines for the model with fixed m and dotted (orange) lines for the model with fixed m and shocks.	95
B.1	China, 2CM. Energy consumption (Mtoe) from CGON sources (squares) and renewables (triangles). The solid lines correspond to the UUC fitted model with two shocks (one for each competitor). The broken lines represent 2σ predictions' confidence bands.	110
B.2	China, 3CM. Energy consumption (Mtoe) from CGO sources (circles), renewables (triangles) and nuclear (diamonds). The solid lines correspond to the UCRCF fitted model with two shocks (one for CGO and the other for renewables). The broken lines represent 2σ predictions' confidence bands.	112

B.3	China, 2CM. Energy consumption (Mtoe) from CGO sources (circles) and Ren-Nuc (triangles). The solid lines correspond to the UUC fitted model with two shocks (one for each competitor). The broken lines represent 2σ predictions' confidence bands.	115
B.4	Finland, 2CM. Energy consumption (Mtoe) from CGON sources (squares) and renewables (triangles). The solid lines correspond to the UUC fitted model with two shocks (one for each competitor). The broken lines represent 2σ predictions' confidence bands.	117
B.5	Finland, 3CM. Energy consumption (Mtoe) from CGO sources (circles), renewables (triangles) and nuclear (diamonds). The solid lines correspond to the UCRCF fitted model with three shocks (one for each competitor). The broken lines represent 2σ predictions' confidence bands.	118
B.6	France, 2CM. Energy consumption (Mtoe) from CGON sources (squares) and renewables (triangles). The solid lines correspond to the BSC fitted model with three exponential shocks (two for CGON and one for renewables). The broken lines represent 2σ predictions' confidence bands.	122
B.7	France, 3CM. Energy consumption (Mtoe) from CGO sources (circles), renewables (triangles) and nuclear (diamonds). The solid lines correspond to the USC fitted model with three shocks (one for each competitor). The broken lines represent 2σ predictions' confidence bands.	125
B.8	Germany, 2CM. Energy consumption (Mtoe) from CGON sources (squares) and renewables (triangles). The solid lines correspond to the USC fitted model with three shocks (two for CGON and one for renewables). The broken lines represent 2σ predictions' confidence bands.	127
B.9	Germany, 3CM. Energy consumption (Mtoe) from CGO sources (circles), renewables (triangles) and nuclear (diamonds). The solid lines correspond to the USC fitted model with four shocks (two for CGO, one for renewables and one for nuclear). The broken lines represent 2σ predictions' confidence bands.	130
B.10	India, 2CM. Energy consumption (Mtoe) from CGON sources (squares) and renewables (triangles). The solid lines correspond to the BSC fitted model. The broken lines represent 2σ predictions' confidence bands.	132
B.11	India, 3CM. Energy consumption (Mtoe) from CGO sources (circles), renewables (triangles) and nuclear (diamonds). The solid lines correspond to the CRCF fitted model. The broken lines represent 2σ predictions' confidence bands.	133
B.12	Japan, 2CM. Energy consumption (Mtoe) from CGON sources (squares) and renewables (triangles). The solid lines correspond to the BSC fitted model with three shocks (three for CGON and one for renewables). The broken lines represent 2σ predictions' confidence bands.	137
B.13	Japan, 3CM. Energy consumption (Mtoe) from CGO sources (circles), renewables (triangles) and nuclear (diamonds). The solid lines correspond to the USC fitted model with five shocks (three for CGO, one for renewables and one for nuclear). The broken lines represent 2σ predictions' confidence bands.	137

-
- B.14 Spain, 2CM. Energy consumption (Mtoe) from CGON sources (squares) and renewables (triangles). The solid lines correspond to the UUC fitted model with two shocks (one for each competitor). The broken lines represent 2σ predictions' confidence bands. 141
- B.15 Spain, 3CM. Energy consumption (Mtoe) from CGO sources (circles), renewables (triangles) and nuclear (diamonds). The solid lines correspond to the CRCDD fitted model with three shocks (one for each competitor). The broken lines represent 2σ predictions' confidence bands. 144

List of Tables

3.1	Belgium, 2CM. Estimates, standard errors and marginal linearised 95% confidence intervals of the BSC model with four shocks (three for CGON sources and one for renewables).	33
3.2	Belgium, 3CM. Estimates, standard errors and marginal linearised 95% confidence interval of the BSC model with five shocks (three for CGO sources, one for renewables and one for nuclear).	35
3.3	Belgium. Confidence band width of 2CM and 3CM predictions in 2016–2020.	37
3.4	Sweden, 2CM. Estimates, standard errors and marginal linearised 95% confidence intervals of the USC model with two shocks (one for each competitor).	39
3.5	Sweden, 3CM. Estimates, standard errors and marginal linearised 95% confidence interval of restricted UCRC model with three shocks (one for each competitor).	40
3.6	Sweden. Confidence band width of 2CM and 3CM predictions in 2016–2020.	42
3.7	Sweden. Forecasting accuracy measures for CGON predictions by 2CM and RW.	43
3.8	Sweden. Forecasting accuracy measures for CGO and nuclear predictions by 3CM and RW.	43
3.9	Sweden. Comparison of forecasting accuracy measures for renewables predictions by 2CM and 3CM.	44
3.10	Switzerland, 2CM. Estimates, standard errors and marginal linearised 95% confidence interval of the USC model with two shocks (one for each competitor).	45
3.11	Switzerland, 3CM. Estimates, standard errors and marginal linearised 95% confidence intervals of the restricted UCRC model with three shocks (one for each competitor).	46
3.12	Switzerland. Confidence band width of 2CM and 3CM predictions in 2016–2020.	48
3.13	Switzerland. Forecasting accuracy measures for CGON predictions by 2CM and RW.	49
3.14	Switzerland. Forecasting accuracy measures for CGO and nuclear predictions by 3CM and RW.	49
3.15	Switzerland. Comparison of forecasting accuracy measures for renewables predictions by 2CM and 3CM.	49
3.16	The United Kingdom, 2CM. Estimates, standard errors and marginal linearised 95% confidence interval of the UUC model with two shocks (one for each competitor).	51

3.17	The United Kingdom, 3CM. Estimates, standard errors and marginal linearised 95% confidence interval of the USC model with three shocks (one for each competitor).	53
3.18	The United Kingdom. Confidence band width of 2CM and 3CM predictions in 2016–2020.	54
3.19	The United States, 2CM. Estimates, standard errors and marginal linearised 95% confidence intervals of the BSC model with four shocks (three for CGON sources and one for renewables).	56
3.20	The United States, 3CM. Estimates, standard errors and marginal linearised 95% confidence intervals of the BSC model with five shocks (three for CGO sources, one for renewables and one for nuclear).	57
3.21	The United States. Confidence band width of 2CM and 3CM predictions in 2016–2020.	59
5.1	Belgium, 2CM-DMP. Estimates, standard errors and marginal linearised 95% confidence intervals of the UUC model with DMP for two competitors.	69
5.2	Belgium, 3CM-DMP. Estimates, standard errors and marginal linearised 95% confidence intervals of the UUC model with DMP for three competitors.	70
5.3	Belgium. Values of R^2 of the 2CM and 3CM with FMP and DMP. The F -ratio values to compare DMP models with the corresponding FMP version are also shown.	71
5.4	Belgium. Comparison among all 2CM and 3CM models: predictions' confidence band width.	73
5.5	Belgium, 3CM. Comparison among models with DMP, fixed m and fixed m with shocks.	74
5.6	Finland, 2CM-DMP. Estimates, standard errors and marginal linearised 95% confidence intervals of the USC model with DMP for two competitors.	76
5.7	Finland, 3CM-DMP. Estimates, standard errors and marginal linearised 95% confidence intervals of the unrestricted UCRC model with DMP for three competitors.	77
5.8	Finland. Values of R^2 of the 2CM and 3CM with FMP and DMP. The F -ratio values to compare DMP models with the corresponding FMP version are also shown.	78
5.9	Finland. Comparison among all 2CM and 3CM models: predictions' confidence band width.	80
5.10	Finland, 3CM. Comparison among models with DMP, fixed m and fixed m with shocks.	81
5.11	France, 2CM-DMP. Estimates, standard errors and marginal linearised 95% confidence intervals of the UUC model with DMP for two competitors.	83
5.12	France, 3CM-DMP. Estimates, standard errors and marginal linearised 95% confidence intervals of the UUC model with DMP for three competitors.	84
5.13	France. Values of R^2 of the 2CM and 3CM with FMP and DMP. The F -ratio values to compare DMP models with the corresponding FMP version are also shown.	85
5.14	France. Comparison among all 2CM and 3CM models: predictions' confidence band width.	85

5.15	France, 3CM. Comparison among models with DMP, fixed m and fixed m with shocks.	88
5.16	Germany, 3CM-DMP. Estimates, standard errors and marginal linearised 95% confidence intervals of the USC model with DMP for two competitors.	89
5.17	Germany, 3CM-DMP. Estimates, standard errors and marginal linearised 95% confidence intervals of the UUC model with DMP for three competitors.	90
5.18	Germany. Values of R^2 of the 2CM and 3CM with FMP and DMP. The F -ratio values to compare DMP models with the corresponding FMP version are also shown.	91
5.19	Germany. Comparison among all 2CM and 3CM models: predictions' confidence band width.	92
5.20	Germany, 3CM. Comparison among models with DMP, fixed m and fixed m with shocks.	94
B.1	China, 2CM. Estimates, standard errors and marginal linearised 95% confidence intervals of the UUC model with two exponential shocks (one for each competitor).	111
B.2	China, 3CM. Estimates, standard errors and marginal linearised 95% confidence intervals of the UCRC model with two shocks (one for CGO sources and the other for renewables).	113
B.3	China. Confidence band width of 2CM and 3CM predictions in 2016–2020.	114
B.4	China, 2CM. Estimates, standard errors and marginal linearised 95% confidence intervals of the UUC model with two exponential shocks (one for each competitor) for an alternative partition of energy sources.	115
B.5	China. Confidence band width of 2CM (CGO and RenNuc) and 3CM predictions in 2016–2020.	116
B.6	Finland, 2CM. Estimates, standard errors and marginal linearised 95% confidence interval of the UUC model with two exponential shocks (one for each competitor).	118
B.7	Finland, 3CM. Estimates, standard errors and marginal linearised 95% confidence interval of the UCRC model with three shocks, one for each competitor.	119
B.8	Finland. Confidence band width of 2CM and 3CM predictions in 2016–2020.	121
B.9	France, 2CM. Estimates, standard errors and marginal linearised 95% confidence intervals of the BSC model with three shocks (two for CGON sources and one for renewables).	123
B.10	France, 3CM. Estimates, standard errors and marginal linearised 95% confidence intervals of the USC model with three shocks (one for each competitor).	124
B.11	France. Confidence band width of 2CM and 3CM predictions in 2016–2020.	126
B.12	Germany, 2CM. Estimates, standard errors and marginal linearised 95% confidence intervals of the USC model with three shocks (two for CGON sources and one for renewables).	127
B.13	Germany, 3CM. Estimates, standard errors and marginal linearised 95% confidence intervals of the USC model with four shocks (two for CGO sources, one for renewables and one for nuclear).	129

B.14 Germany. Confidence band width of 2CM and 3CM predictions in 2016–2020.	131
B.15 India, 2CM. Estimates, standard errors and marginal linearised 95% confidence intervals of the BSC model.	132
B.16 India, 3CM. Estimates, standard errors and marginal linearised 95% confidence intervals of the CRCDC model.	133
B.17 India. Confidence band width of 2CM and 3CM predictions in 2016–2020.	134
B.18 Japan, 2CM. Estimates, standard errors and marginal linearised 95% confidence intervals of the BSC model with four shocks (three for CGON sources and one for renewables).	136
B.19 Japan, 3CM. Estimates, standard errors and marginal linearised 95% confidence intervals of the USC model with five shocks (three for CGO sources, one for renewables and one for nuclear).	138
B.20 Japan. Confidence band width of 2CM and 3CM predictions in 2016–2020.	140
B.21 Spain, 2CM. Estimates, standard errors and marginal linearised 95% confidence intervals of the UUC model with two shocks (one for each competitor). .	142
B.22 Spain, 3CM. Estimates, standard errors and marginal linearised 95% confidence intervals of the CRCDC model with three shocks (one for each competitor).	143
B.23 Spain. Confidence band width of 2CM and 3CM predictions in 2016–2020.	144

Introduction

Overview

Consistent energy supply through a reliable and well-established infrastructure is a precondition for a nation's balanced economic growth. In contrast, an inadequate or unreliable setup, as observed in most developing countries, inhibits sustainable development. In this context, global energy consumption is expected to increase by 28% between 2015 and 2040 (Energy Information Administration (EIA), 2017). However, the use of popular sources of energy, such as fossil fuels and uranium, generates pollution, greenhouse effects and climate change. Renewable energy sources appear as a viable option that guarantees the availability of electricity produced in a safer way.

Renewable energy has often been used in human civilisation. Examples include the use of firewood to cook food or produce heat or the use of energy from wind as an input for transport vehicles. Renewables were used as a major source of energy in the preindustrial era, playing a pivotal role in the pace of economic development. With the exponential growth since the industrial revolution, the use of nonrenewable sources of energy became a nearly universal phenomenon around the globe, especially for most of the developed nations. However, in recent decades, an increasing trend in the use of renewable sources of energy has been observed. The magnitude of this trend is different across countries, and it depends highly on country-specific characteristics, such as the market structure, political tendency and population's perception of technological change and substitution. The adoption of renewables has been generally facilitated by specific policy instruments like feed-in-tariffs (FiT) and other incentive mechanisms.

The use of traditional sources of energy is expected to reach the last phase of the lifecycle. However, new technological innovations can unpredictably alter the lifecycle of a source, at least temporarily. For example, the extended application of fracking technologies in the United States has heavily modified internal and external energy policies due to the unexpected growth of shale oil and shale gas (Wang and Krupnick, 2015). Even when extending the lifecycle of a specific source is possible through a

technological discovery, a sensible choice could be to consider the safety aspects of such innovation (Furlan and Mortarino, 2018). For instance, due to the negative effects of shale gas on the environment through hydraulic fracturing (Melikoglu, 2014; Wang *et al.*, 2014; Vengosh *et al.*, 2014), cautions should be taken in considering shale gas as the bridge for renewables (Klein and Whalley, 2015). In fact, the effects of shale gas on the environment are worse than those of natural gas from conventional sources (Wang *et al.*, 2014).

Renewable sources of energy have emerged as an important component in the world energy consumption mix because of fossil fuel's negative environmental consequences, high and unstable prices and depleting sources (Apergis and Payne, 2012). In the first decade of the 21st century, the growth rate of renewables was 4.40%, including hydropower (3.18%) and non-hydropower (12.89%; Pao and Fu, 2013). In 2011, an estimated 16.7% of global final energy consumption was supplied by renewable energy sources. Due to reductions in costs and technological innovations, global new investment in renewables increased by 17%. Cost-competitive renewables have been established as a mainstream source of energy around the world (Renewable Energy Policy Network for the 21st Century (REN21), 2016). However, further research and development are required to achieve a technological breakthrough in the near future.

With different motivations, a nuclear power renaissance is especially being sustained in the energy economies, contributing 11% of the global electricity production (Nuclear Power (NP), 2017). The operating externalities of the source are relatively low, as nuclear power produces low levels of air pollution and greenhouse gas (GHG) emissions. Although the burning of nuclear energy releases zero CO₂ into the atmosphere, the byproduct is extremely hazardous. The invisible nuclear pollution is considered dangerous because the source of nuclear energy is not categorised as clean. Considering the safety issues, nuclear power plants are probably the most vulnerable of all sources of energy used to produce electricity (Furlan *et al.*, 2016). For example, three major accidents have occurred during the commercial use of nuclear fission since 1950. The first occurred in 1979 at Three Mile Island (USA), causing limited damage. The second one, the Chernobyl disaster in the western Union of Soviet Socialist Republics (USSR) and Europe in 1986, is considered the worst ever nuclear accident. This has been classified at the maximum level (Level 7) on the International Nuclear Event Scale (INES). The third accident occurred in Fukushima (Japan), in March 2011 and it was also classified as Level 7. In addition, nuclear energy may not be a good economic investment, as the establishment of nuclear plants is more expensive and their construction usually takes longer than is the case for renewable energy sources like solar or wind. However,

nuclear energy has been considered as an alternative source to fossil fuels. For instance, after the oil boycott in 1973, France decided to achieve greater energy independence. In the two subsequent decades, the majority of energy-generating capacity in France was converted from fossil-fuel-based to uranium-based systems (Brook *et al.*, 2014).

Overall, the use of various energy sources is changing with time, and the different sources behave as competitors in the market niche. Their availability, sustainability and cost effectiveness change over time, and each has dynamic shares. The new technological innovations may restrict the usual behaviour of pre-existing technologies, and at the same time, foster the expansion of the market potential, especially for emerging states. Moreover, the speed of competition depends on the entry time of new technologies and the lifecycle of pre-existing technologies. Hence, the diffusion of energy sources in a competitive framework may be a broader research topic that can enrich the existing literature.

The competition effect of a new technology with existing ones may be studied using diffusion models. However, studies on competition modelling are limited in contemporary literature (Krishnan *et al.*, 2000; Savin and Terwiesch, 2005; Guseo and Mortarino, 2012, 2014, 2015). Describing the competition requires complex mathematical/statistical tools, especially with diffusion models requiring nonlinear estimation. The models studying competition between two energy sources with different data include the logistic model (Vestrucci *et al.*, 2015), diffusion model (Huh and Lee, 2014), Lotka–Volterra model (Duan *et al.*, 2014), extended Lotka–Volterra model (Guidolin and Guseo, 2016) and two-wave diffusion model (Furlan and Mortarino, 2018). These studies are restricted to explaining the competition between two rivals. The development of diffusion models for more than two competitors may be a notable input in the literature, and their applications, especially to energy issues, may have valuable implications in designing policies.

Main contributions of the thesis

The central goal of this thesis is developing a novel model explaining the diffusion of a new technology with more than two products under competition. Following a brief introduction, Chapter 1 reviews existing univariate and bivariate diffusion models. The univariate models include the Bass model, the generalised Bass model (GBM) and the Guseo and Guidolin (2009) model (GGM). Among the bivariate models, the models proposed by Guseo and Mortarino (2014, 2015) are briefly discussed. The examination

mainly focusses on the structure of the models and their adaptability to specific situations. Where necessary, the limitations of the models are also considered. In addition, various aspects of existing models and the models proposed in this thesis, which are useful for drawing inferences, are also discussed.

The main contributions of the thesis are presented in Chapters 2–5. A three-competitor diffusion model (3CM) is proposed in Chapter 2. The model assumes an invariant market potential over the entire diffusion process. The proposed 3CM may improve the description of mutual interactions, whether through competition or cooperation of the products, over the existing two-competitor models (2CM). The 2CM models entail information loss due to the aggregation of data relating to similar products or the simplified description of the market by the two leading products.

Applications (e.g. parameter estimation and short-period predictions) of the proposed 3CM are discussed in Chapter 3 using energy consumption data from 12 selected countries. The consumptions are partitioned into three sources, as follows: coal, gas and oil (CGO), renewables and nuclear. Using the same energy data, a comparison of the 3CM with the 2CM (proposed by Guseo and Mortarino, 2014) is performed. The 2CM is applied to the energy data, contrasting renewable and nonrenewable sources. The forecasting accuracy of the models is compared both in terms of in-sample (training data) performances based on multi-step forecasts and out-of-sample performances (test data). In the latter case, we compare the entire sample performances based on the width of prediction confidence bands. The improvement of 3CM over 2CM is assessed using the confidence bands for all 12 countries. This improvement is also verified using forecasting accuracy measures for two countries.

A three-competitor diffusion model with the assumption of a non-constant or dynamic market potential (DMP) is proposed in Chapter 4. With the entrance of a new product into the market, the knowledge and awareness do not disperse instantly throughout the eligible adopters. In such a situation, as compared with the models with fixed market potential, the proposed model with DMP assumption is more flexible to follow the observed data and achieve more reliable forecasts.

In Chapter 5, the model proposed in Chapter 4 is discussed through an application using energy data. The same dataset and partitioning as mentioned for applications of Chapter 3 is used. However, some of the countries are excluded from the analysis. Considering the number of parameters, the models with DMP are relatively more complex than similar models with a fixed market potential. In this context, we quantify the benefits of using relatively complex models over the simpler models. This is done by comparing the efficacy of 3CM with DMP models with their bivariate structure, as

proposed by Guseo and Mortarino (2015).

Overall discussion of the results obtained through the proposed and existing diffusion models for competition is presented in the concluding chapter. Here, we highlight the relative flexibility of our proposed models over the existing models used in this field of research. We also mention the potential limitations of the models. Finally, we suggest some research directions that may help in further contributing to the diffusion of innovations literature.

Chapter 1

Review of innovation diffusion models

1.1 Introduction

In the last several decades, the innovation diffusion models have gained considerable interests among scholars working on modelling and forecasting the diffusion of innovative ideas and technologies. The over 4000 scholarly publications in this broad research area since 1940 is indicative of the progression of its theoretical underpinnings. Contemporary researchers in this research area have been developing innovative modelling approaches to capture the character of innovation diffusion models. One of the significant innovations is the extension of models to describe the diffusion in a competitive approach for bivariate data.

In addition to the basic usage of forecasting the lifecycles of products, the models have been used for descriptive and normative purposes (Guseo *et al.*, 2007). The recent research on diffusion theory has focussed on administrative diagnostics, including divulging the basic structures of a market, generating comparisons with other contexts, helping organisations to forge ahead and preparing for potential manoeuvres in the future (Muller *et al.*, 2009). Diffusion of innovation is basically a social phenomenon, and the classic diffusion of innovations theories have applications in the marketing and management disciplines. However, the complex nature of the diffusion of innovations demands interdisciplinary research by incorporating knowledge from economics, social sciences, physics, mathematics, statistics, organisational behaviour, technological management and technological forecasting disciplines (Guseo *et al.*, 2007).

In a diffusion process, innovation is communicated among the members of a social

system through certain networks (Rogers, 2003). The process comprises four essential elements, namely the innovation, communication networks, time and social system. According to Mahajan *et al.* (1990) the focus of diffusion theory should be the communication channels, which determine how information about innovation is spread to the social system within which an innovation is implemented and practiced. These channels may be formal or informal. The formal channel includes the mass media and advertising, whereas, interpersonal communication is a basic informal channel. Nonverbal observations, a component of interpersonal communications, has a great influence in determining the speed and shape of the diffusion process in a social system (Mahajan *et al.*, 1990).

Earlier contributors to this dynamic research area explicated diffusion as a process that is mostly governed by learning through imitation. Tarde (1890), a French lawyer, claimed that the imitation process can represent a general law of social change. In support of the claim, he argued that, although invention is a necessary condition of change, the actual change occurs only when a large number of individuals instigates the adoption process.

Imitation plays the central role in explaining the diffusion processes, and the process is commonly represented by logistic curves (Kijek and Kijek, 2010). However, several studies indicate that the diffusion of an innovation follows an S-shaped curve over time (Rogers, 2003). For example, the Bass model, BM (Bass, 1969) is deemed to be the most known and widely used diffusion model offering the theoretical and empirical evidence for the S-shaped pattern. Later, many reviews of innovation diffusion models have been developed (Mahajan and Muller, 1979; Mahajan *et al.*, 1990, 1995, 2000; Meade and Islam, 2001, 2006; Hauser *et al.*, 2006; Muller *et al.*, 2009).

Following research for univariate lifecycles, several models have been developed and applied to describe the diffusion of products under competition, such as those of Peterson and Mahajan (1978), Mahajan *et al.* (1993), Kalish *et al.* (1995), Krishnan *et al.* (2000), Savin and Terwiesch (2005), Libai *et al.* (2009) and Guseo and Mortarino (2012, 2014). All these models assume that the market potential is invariant throughout the diffusion process. However, the assumption has been reasonably relaxed in the recent literature (see Guseo and Guidolin, 2009 for univariate and Guseo and Mortarino, 2015 for bivariate diffusion of innovations).

In this chapter, we make a brief review of the BM, its extensions, the GBM (Bass *et al.*, 1994) and GGM. While all three models explain the diffusion process of an innovation, the GGM works differently from the other two in terms of market potential. We also review the general competition models developed for explaining two competitors'

diffusion and proposed by Guseo and Mortarino (2014) and Guseo and Mortarino (2015). The models are dissimilar in terms of their market potential framework.

1.2 Univariate diffusion models

1.2.1 The Bass Model

The BM (Bass, 1969) describes the diffusion of a novelty by portraying the launch, growth, maturity and decline phases, that is, the S-shaped diffusion dynamics. Let $y(t)$ denote the relative cumulative number of adoptions at time t with corresponding instantaneous adoptions $y'(t) = dy(t)/dt$. The BM can be defined through its hazard function, that is, the probability that an adoption of a new product or service occurs at time t , given that it has not been adopted yet. We have

$$y'(t)/[1 - y(t)]. \quad (1.1)$$

The function can be expanded through the theorem of total probability. Equation (1.1) is a combination of three factors, following the conditional probability law. These are as follows:

- i) The conditional probability of adoption of innovators: 1;
- ii) The analogous conditional probability of imitators: $y(t)$; and
- iii) The conditional probability of neutral agents: 0.

Mathematically,

$$y'(t)/[1 - y(t)] = p \cdot 1 + q \cdot y(t) + 0 \cdot (1 - p - q) = p + qy(t), \quad (1.2)$$

where $p > 0$ and $q > 0$ are coefficients of innovation (measuring the propensity of potential adopters to become adopters) and imitation (measuring the propensity of potential adopters to imitate previous adopters), respectively. Van den Bulte (2002) gave a different interpretation of the parameters, where p represents the effect of external influence due to mass media communication and q measures the effect of internal influence, both acting on the same agent. Combining Equations (1.2) and (1.1), we see that the BM can be expressed by the normalised equation

$$y'(t) = [p + q \cdot y(t)] [1 - y(t)]. \quad (1.3)$$

Under the initial condition $y(0) = 0$, as proven in Bass (1969), the solution of Equation (1.3) can be expressed as:

$$y(t) = \frac{1 - e^{-(p+q)t}}{1 + \frac{q}{p}e^{-(p+q)t}}, \quad t \geq 0, \quad p, q > 0. \quad (1.4)$$

Here, $y(t)$, the proportion of adoptions, describes the dynamics of the diffusion process. The number of adoptions at time t , expressed as $z(t)$, can be obtained by multiplying both sides of Equation (1.4) by the scale parameter, m . This parameter represents the *market potential* or carrying capacity. Hence, we have,

$$z(t) = m \frac{1 - e^{-(p+q)t}}{1 + \frac{q}{p}e^{-(p+q)t}}, \quad t \geq 0. \quad (1.5)$$

The structure (1.5) is the closed-form solution of the BM, a special cumulative distribution. For instantaneous adoptions, the BM can be expressed with the following first-order differential equation:

$$z'(t) = \left[p + q \frac{z(t)}{m} \right] [m - z(t)]. \quad (1.6)$$

From this formulation, we can appreciate that $z'(t)$, the amount of new adoptions, is proportional to the residual market, $[m - z(t)]$ at time t . The market potential, m , representing the maximum number of adoptions in the lifecycle, is assumed to be fixed along the entire diffusion process.

The BM is considered the seminal contribution that separates innovators and imitators in the innovation diffusion process. One of the model's advantages is the tangible possibility of describing the initialising phase of diffusion, due to the presence of innovators. Although an ample body of literature has recognised the role of innovators, also called 'early adopters' (Rogers, 2003), or 'opinion leaders' (Katz and Lazarsfeld, 1955) in the process, the BM was the first to formalise their action.

1.2.2 The Generalised Bass Model (GBM)

The BM is criticised for its inability to incorporate marketing mix variables under managerial control, like price strategies and advertising (Mahajan and Muller, 1979; Mahajan, 1986; Mahajan *et al.*, 1990), into the framework. Another criticism of the model, as indicated by Muller *et al.* (2009), is what is regarded as a conceptual conflict. With assumptions on consumers' behaviour, the BM provides good-fit models to real-life data, leading to reliable forecasts. Marketing mix decisions have a notable influence

on the growth of new products, and hence, the variable(s) should be included in the model. Moreover, shortening of lifecycles due to the evolution of successive generations (see Norton and Bass, 1987), especially for high-technology products, demands adopting models that can incorporate control variables.

According to Bass *et al.* (2000), a diffusion model with decision variables should have several desirable properties. The model should have empirical support and a closed-form solution, be easy to implement and managerially useful and allow a direct explanation of parameters and comparisons with competing models. The GBM (Bass *et al.*, 1994), an important extension of the standard BM, possesses all these properties. The GBM is obtained by multiplying the basic structure of the BM by an intervention or control function, $x(t) = x(t; \theta)$, $\theta \in \mathbb{R}^k$. The model depicts the possible effect of price and advertising strategies as exogenous variables on the diffusion process. Thus, as an extension of Equation (1.6), the GBM is represented as:

$$z'(t) = \left[p + q \frac{z(t)}{m} \right] [m - z(t)] x(t), \quad (1.7)$$

and its closed-form solution, under the initial condition $z(0) = 0$, is

$$z(t) = m \frac{1 - e^{-(p+q) \int_0^t x(\tau) d\tau}}{1 - \frac{q}{p} e^{-(p+q) \int_0^t x(\tau) d\tau}}, \quad 0 \leq t < +\infty. \quad (1.8)$$

Function $x(t)$ is called the ‘current marketing effort’, and it acts on the natural shape of diffusion, modifying its temporal structure without affecting its internal parameters. As a result, the important effect of $x(t)$ is to accelerate or delay adoptions but not to increase or decrease them. More explicitly, if $x(t) > 1$, we observe an acceleration of the diffusion process, while a delay in adoptions is implied by $x(t) < 1$. If there are no external influences on the diffusion process, that is, if $x(t) = 1$, $\forall t \in \mathbb{R}^+$, the GBM reduces to the standard BM. According to Guseo and Dalla Valle (2005), the intervention function, $x(t)$, with exponential shocks can be expressed as:

$$x(t) = 1 + c_1 e^{b_1(t-a_1)} I_{[t \geq a_1]}, \quad (1.9)$$

where a_1 represents the starting time of the shock, b_1 indicates how rapidly the shock decays toward 0 (it usually has negative values) and c_1 denotes the intensity of the shock. Another possible form of $x(t)$ is suggested by Guseo and Dalla Valle (2005). The

form is called rectangular shock and can be presented as:

$$x(t) = 1 + c_1 I_{[a_1 \leq t \leq b_1]}, \quad (1.10)$$

where a_1 and b_1 delimit the time interval when the shock affects diffusion and c_1 indicates the shock's intensity. Although function $x(t)$ was originally perceived to represent marketing mix variables, its configuration is so common and simple that it can take various forms, to portray external influences other than marketing strategies. The possibility of estimating its parameters simultaneously with the model's main parameters gives further advantages to this model.

The market potential of both the BM and GBM is assumed to be fixed in the whole diffusion process. With the aim of achieving more flexible models to describe real data, a plausible extension, the dynamic market potential (DMP), $m(t)$, is introduced in the models proposed by Guseo and Guidolin (2009, 2010, 2011).

Despite recent developments, the standard BM and GBM suffer from conceptual limitations in operational and predictional terms. Both the models assume that the internal influence (word-of-mouth, WOM, effect) remains static throughout the diffusion process. In practice, later adopters may not be as prompt in discussing the product, and they may be less inclined to exhibit the interest in discussing the new product with non-adopters compared with the early adopters. In many situations, late adopters are found to have different characteristics from early adopters, and consequently, they respond differently (Rogers, 2003). Furthermore, Bass-type models consider more specific assumptions regarding the social interactions, maintaining the social structure as a fully connected network. Consequently, the effect of adopters on non-adopters is a linear function of the number of adopters during the diffusion timeline (Shaikh *et al.*, 2006). Nonetheless, the control function, $x(t)$, may not be flexible enough to cover the entire range of agents' heterogeneity.

Both the BM and GBM have been employed in a wide range of applications in social sciences, applied sciences, business and marketing research. Special applications of the GBM have been used in the energy sector, especially for crude oil (Guseo and Dalla Valle, 2005; Guseo *et al.*, 2007; Guseo, 2011) and solar photovoltaic (PV) (Guidolin and Mortarino, 2010). The motivation for these applications is based on the related diffusion of technologies consuming energy. This topic is discussed in more detail in Chapter 3.

1.2.3 Guseo and Guidolin (2009) model (GGM)

The BM and GBM proved to be valuable for describing the diffusion of an innovation. However, both models assume the market potential or carrying capacity, m , as a constant along the entire diffusion process. This assumption conflicts with the common concept that knowledge is time varying. Attempts have been proposed in the literature to overcome this constraint.

In some studies, the DMP is defined as a function of exogenous variables (see, e.g. Mahajan and Peterson, 1978; Kalish, 1985; Kamakura and Balasubramanian, 1988; Horsky, 1990; Jain and Rao, 1990; Parker, 1992, 1993; Kim *et al.*, 1999), whereas other studies assume this as an exponential function of time only (e.g. Sharif and Ramanathan, 1981; Meyer and Ausubel, 1999; Centrone *et al.*, 2007). Guseo and Guidolin (2009) assumed that the market potential is a function of time that may assume various levels throughout the product lifecycle.

As Guseo and Guidolin (2009) define it, the adoption of an innovation in a social system is a direct indication of an existing absorptive capacity. The ability to assimilate and accept an innovation depends on the accumulation of prior knowledge. They observed that accumulating knowledge involves learning dynamics, which can be explained through an evolutionary model, rather than a cross-sectional model, as proposed by Cohen and Levinthal (1990). Consequently, by adopting an evolutionary perspective, they represented a communication structure as a set of informational linkages among the units of the system. The progress of collective knowledge can be considered an evolving network, where some linkages exist, some rise and some others perish. This happens when individual knowledge creates connecting ideas and concepts between them and demolishes existing networks. The market potential proposed by Guseo and Guidolin (2009) is a function of this knowledge process depending on a network of connections that changes over time. The DMP is defined through the following form:

$$m(t) = K \sqrt{\frac{1 - e^{-(p_c+q_c)t}}{1 + \frac{q_c}{p_c} e^{-(p_c+q_c)t}}}, \quad K, p_c, q_c > 0, t > 0, \quad (1.11)$$

where K is the upper asymptotic potential, $K = \lim_{t \rightarrow \infty} z(t)$, and p_c and q_c are evolutionary parameters describing how rapidly communication spreads through the network. For large values of p_c and q_c , the DMP $m(t)$ rapidly approaches K . In contrast, smaller values of p_c and q_c negatively affect $m(t)$, so that it reaches K much more slowly.

In Equation (1.11), the expression under the square root represents the core of a BM describing the latent diffusion process of communication. Hence, the model proposed

by Guseo and Guidolin (2009), called GGM – an extension of BM (Bass, 1969) – can be defined as

$$z'(t) = m(t) \left[p_s + q_s \frac{z(t)}{m(t)} \right] \left[1 - \frac{z(t)}{m(t)} \right] + z(t) \frac{m'(t)}{m(t)}, \quad p_s, q_s > 0, \quad t > 0, \quad (1.12)$$

where $z(t)$ and $z'(t)$ represent the mean cumulative sales and the mean instantaneous sales at time t , respectively, and $m(t) \geq z(t)$. The parameters p_s and q_s are evolutionary parameters that describe how rapidly the product is adopted, while p_c and q_c , as mentioned above, are related to the spread of knowledge. The last term on the right-hand side in Equation (1.12) – which would obviously vanish for a constant $m(t)$ – represents a *self-reinforcing* effect, which is common in marketing behavioural studies (see, e.g. Sydow and Schreyogg, 2013). This point is further discussed in Subsection 1.3.2.

1.3 Competition diffusion models

1.3.1 The two-competitor model with fixed m

The model proposed by Guseo and Mortarino (2014) is a generalisation or modification of all available bivariate models (e.g. Krishnan Bass Kumar Diachronic, KBKD, model by Krishnan *et al.*, 2000, Savin Terwiesch Diachronic, STD, model by Savin and Terwiesch, 2005, Libai Muller Peres Diachronic, LMPD, model by Libai *et al.*, 2009 and Competition and Regime Change Diachronic, CRCDD, model by Guseo and Mortarino, 2012) that have been developed through the concept of the Bass diffusion of an innovation. The model refers to a category based on substitute products; that is, the products represent a homogeneous category competing for the same customers. In this case, the specific diffusion process of each product under competition is driven at the product-category level (Parker and Gatignon, 1994).

Let $z_i(t)$ be the cumulative sales of product i , $i = 1, 2$ and $z(t) = z_1(t) + z_2(t)$ be the category cumulative sales. Let $z'_i(t) = dz_i(t)/dt$ be the instantaneous sales of the i -th product. Suppose we examine a two-product competition with the late entrance of the second product at time $t = c_2$ with $c_2 > 0$, where $t = 0$ indicates the time origin for the first product. Therefore, the model proposed by Guseo and Mortarino (2014) can

be expressed with a system of differential equations:

$$\begin{aligned}
z_1'(t) &= m \left\{ \left[p_{1a} + q_{1a} \frac{z(t)}{m} \right] (1 - I_{t > c_2}) + \left[p_{1c} + (q_{1c} + \delta) \frac{z_1(t)}{m} + q_{1c} \frac{z_2(t)}{m} \right] I_{t > c_2} \right\} \times \\
&\quad \times \left[1 - \frac{z(t)}{m} \right], \\
z_2'(t) &= m \left[p_2 + (q_2 - \gamma) \frac{z_1(t)}{m} + q_2 \frac{z_2(t)}{m} \right] \left[1 - \frac{z(t)}{m} \right] I_{t > c_2}, \\
m &= m_a (1 - I_{t > c_2}) + m_c I_{t > c_2}, \\
z(t) &= z_1(t) + z_2(t) I_{t > c_2}.
\end{aligned} \tag{1.13}$$

Here, m is the limiting state of $z(t)$ as $t \rightarrow +\infty$, representing the aggregate market potential. System (1.13) describes a twofold model, called an unrestricted unbalanced competition and regime change diachronic (unrestricted UCRCD) model. It considers different aspects of *diachronic* competition (sequential market entries of the competing products). Until $t \leq c_2$, the stand-alone period, the first product is characterised by the three parameters, as follows: an innovation coefficient, p_1 , and imitation coefficient, q_1 , and market potential, m_a .

For the competition period, $t > c_2$, the market potential takes a new value m_c . The first product is characterised by a new innovation coefficient p_{1c} and two imitation coefficients based on the decomposition of WOM. These are the within-product imitation coefficient, $(q_1 + \delta)$, modulating the sales of the first product through the relative diffusion level z_1/m (the market fraction already controlled by the first competitor at time t) and the cross-product imitation coefficient, q_1 , which is driven by z_2/m (the market fraction already controlled by the second competitor at time t) and measures the effect on sales of the first product due to WOM by adopters of the second product. Likewise, the second product is characterised by the three following parameters: the innovation coefficient, p_2 , within-product imitation coefficient, q_2 , and cross-product imitation coefficient, $(q_2 - \gamma)$, which measures the effect on sales of the second product due to WOM by adopters of the first product.

The unrestricted UCRCD model is flexible as the parameters δ and γ can eventually be different. They are unrestricted in the model, since δ refers uniquely to the first product and γ to the second product. Specifically, δ represents the difference between within-product effect and cross-product effect for the first product, and γ represents the similar difference for the second product. Parameters δ and γ are positive (negative) if the within-product effect is stronger (weaker) than the cross-product effect for the corresponding product.

Under the constraint $\delta = \gamma$, the model in Equation (1.13) reduces to a specific unbalanced model discussed in Guseo and Mortarino (2014), based on a kind of symmetry that leads to a BM for the aggregate consumptions of the homogeneous category. The model with this constraint admits a closed-form solution, differently from the unrestricted UCRC. With the further restriction $\delta = \gamma = 0$, the model in Equation (1.13) reduces to a balanced model (for details, see Guseo and Mortarino, 2012), where the WOM has no specific decomposition between product levels; in this situation, the within-product WOM is equal to the cross-product WOM.

The first two equations of system (1.13), for $t > c_2$, can be rearranged in the following way:

$$\begin{aligned} z_1(t)I_{t>c_2} &\propto p_{1c} + q_{1c} \frac{z_1(t) + z_2(t)}{m} + \delta \frac{z_1(t)}{m}, \\ z_2(t)I_{t>c_2} &\propto p_2 + (q_2 - \gamma) \frac{z_1(t) + z_2(t)}{m} + \gamma \frac{z_2(t)}{m}. \end{aligned}$$

The above rearrangement of system (1.13) highlights that the diffusion of each product is characterised by a category-level imitation coefficient, q_{1c} for the first entrant and $q_2 - \gamma$ for the second, and a product-level imitation coefficient, δ or γ .

It is possible to construct the aggregate hazard of Equation (1.13) for $t > c_2$ (for $t \leq c_2$, the result is straightforward), that is,

$$h(t) = \frac{z'(t)/m}{1 - z(t)/m} = (p_{1c} + p_2) + [(q_{1c} - \delta) + (q_2 - \gamma)] \frac{z_1(t)}{m} + (q_{1c} - q_2) \frac{z_2(t)}{m}, \quad t > c_2.$$

Here, the cumulative sales of the homogeneous category, $z(t)$, behaves as a BM if the hazard assumes the form $h(t) = P + Qz(t)/m$ for appropriate P and Q values.

1.3.2 The two-competitor model with dynamic market potential

The models proposed by Guseo and Mortarino (2014) and models previously published in the literature to describe the diffusion of two competing products in a common market stand on the assumption that the market potential is invariant throughout the lifecycle from the products' takeoff. Guseo and Mortarino (2015) noticed that this assumption is impracticable in almost all situations. Thus, they proposed a diffusion model for two competing products, where the products are supposed to be sufficiently similar to share a common market potential, where the size increases over time. The assumption of a common market potential is suitable in situations where the products

are perfect substitutes. Whenever the competing products are sufficiently different to preserve product-specific market potentials, Abramson and Zanette (1998) suggested relying on Lotka–Volterra models. While Guseo and Mortarino (2015) presented their model by both the closed-form solution and the form of differential equations, we represent their model with the latter formulation, which is suitable for instantaneous data. The model is defined as

$$\begin{aligned} z_1'(t) &= m(t) \left[p_1 + (q_1 + \delta) \frac{z_1(t)}{m(t)} + q_1 \frac{z_2(t)}{m(t)} \right] \left[1 - \frac{z(t)}{m(t)} \right] + z_1(t) \frac{m'(t)}{m(t)}, \\ z_2'(t) &= m(t) \left[p_2 + (q_2 - \gamma) \frac{z_1(t)}{m(t)} + q_2 \frac{z_2(t)}{m(t)} \right] \left[1 - \frac{z(t)}{m(t)} \right] + z_2(t) \frac{m'(t)}{m(t)}, \\ z(t) &= z_1(t) + z_2(t), \end{aligned} \quad (1.14)$$

where $z_i(t)$ denotes the mean cumulative sales and $z_i'(t) = \partial z_i(t)/\partial t$ the instantaneous mean sales at time t of the i -th product, $i = 1, 2$; $z(t)$ indicates the category cumulative sales of both the products; and $z(t) \leq m(t)$, for all t .

The parameters related to innovation effects (p_1 and p_2) and imitation effects (q_1 , q_2 , δ and γ) may be different for describing products with different strengths in the market. Observe that the structure of the model in Equation (1.14) is analogous to the second phase of model (1.13), allowing for different within-product WOMs ($q_1 + \delta$ and q_2 for two products, respectively) in relation to their respective cross-product WOMs (q_1 and $q_2 - \gamma$). In model (1.13), however, unlike model (1.14), $m(t)$ is supposed to be constant throughout the diffusion process, that is, $m(t) = m$ for all t .

Similar to the GGM, the final additive terms in Equation (1.14), which are the self-reinforcing components, will disappear for a constant $m(t)$. The mean sales of both products are enhanced when $m(t)$ increases more quickly, that is, when awareness of the product category spreads rapidly based on the agents' mutual performance. In contrast, the mean sales are further reduced by a diminishing potential persuaded by disapproving signals, and in this case, $m(t)$ would be a nonmonotonic function, with a negative self-reinforcing term when the market potential endures a reduction (Guseo and Mortarino, 2015). It is important to mention that model (1.14) is the more general structure of diffusion model for two competitors, while Guseo and Mortarino (2015) proposed its restricted version with only one parameter as discrimination, that is, $\delta = \gamma$. The restricted version has a closed-form solution, while the general one does not. The differences between the two cases in terms of inference are discussed in Section 1.4.

The sum of the equations in (1.14) is equivalent to model (1.12). In addition, the model can be used with an expression for $m(t)$ that is dissimilar from Equation (1.11).

Guseo and Mortarino (2015) suggested the following two alternative functions of (1.11):

$$m(t) = K \frac{1 - e^{-(p_c+q_c)t}}{1 + \frac{q_c}{p_c} e^{-(p_c+q_c)t}} \quad (1.15)$$

and

$$m(t) = K.F(t) = K. \int_0^t \frac{1}{\Gamma(\alpha_1)} \alpha_0^{\alpha_1} t^{\alpha_1-1} e^{-\alpha_0 t} dt, \quad (1.16)$$

where $\Gamma(\alpha_1) = \int_0^\infty t^{\alpha_1-1} e^{-t} dt$, and $\alpha_0, \alpha_1, t > 0$. The function in (1.15) expresses a modification of (1.11), while (1.16) defines the evolution of the DMP as proportional to $F(t)$, the cumulative distribution function of a Gamma random variable with mean α_1/α_0 and variance α_1/α_0^2 .

1.4 Inferential aspects

1.4.1 Parameter estimates

The BM and GBM can be expressed either in a closed-form solution or with a differential equation. Here, the GGM is represented by a differential equation, although it also has a closed-form solution. Moreover, models (1.13) and (1.14), under restriction $\delta = \gamma$, can be represented by a closed-form solution or with a system of differential equations. Notice that models with a closed-form solution are suitable for cumulative data, and models defined by differential equations are appropriate for instantaneous data. In the latter case, forecasts cannot be evaluated directly, as we will show in the next subsection. Given that, in this dissertation, we deal mostly with models without a closed-form solution, we will focus now on this kind of model.

The structure of a nonlinear regression model for instantaneous data can be expressed as:

$$s(t) = z'(t) + \epsilon(t), \quad (1.17)$$

where $s(t)$ represents observed data, namely instantaneous adoptions or sales of product at time t , and $z'(t) = z'(t; \beta)$ represents the deterministic component of the model. Structure (1.17) is adequate for univariate data. It will be the same structure for two or more variables as well. The second component in Equation (1.17), $\epsilon(t)$, is the residual or error term. The set of parameters of the diffusion models, β , can be estimated through a nonlinear least square (NLS) algorithm without allowing detailed assumptions, from the beginning, about the structure of $\epsilon(t)$. In order to avoid convergence on local minima,

a large grid of initial values for all the parameters is explored. For further details about inference for nonlinear models, see Seber and Wild (1989).

1.4.2 Predictions and confidence bands

Beside estimating parameters, forecasting is crucial for the diffusion process. When we use instantaneous data, because of lacking of a closed-form solution, to predict the future values of diffused products or technologies, we follow Euler's method for the numerical solution of differential equations (see, e.g. Atkinson, 1962).

To compute confidence bands for the predicted values, we follow Boswijk and Franses (2005), assuming heteroscedasticity in $\epsilon(t)$:

$$\epsilon(t) = z'(t; \beta)u(t),$$

where $u(t)$ is supposed to be distributed as normal with a zero mean and constant variance, σ_u^2 . Thus, Equation (1.17) can be rewritten as

$$s(t) = z'(t; \beta) + z'(t; \beta)u(t). \quad (1.18)$$

Structure (1.18) provides low variability around the mean trajectory, both at the beginning and end of the diffusion cycle, with higher variability when the diffusion peaks. Figure 1.1 represents an example of simulated data (blue triangles) with heteroscedastic deviations from the mean trajectory (red line). After parameter estimation, the estimate of $u(t)$ is obtained as follows:

$$\hat{u}(t) = [s(t) - z'(t; \hat{\beta})] / z'(t; \hat{\beta}). \quad (1.19)$$

We call $\hat{u}(t)$ 'scaled residuals'. To confirm the hypothesis that scaled residuals follow a Gaussian distribution, we use the Kolmogorov–Smirnov test for normality. Then, the

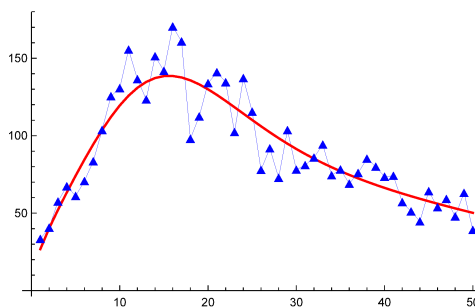


FIGURE 1.1: Simulated data according to assumption (1.18).

confidence bands for the predictions $\hat{z}(t) = z(t; \hat{\beta})$ can be computed as

$$\hat{z}(t) \pm 2 \hat{\sigma}_u \hat{z}'(t), \quad t = T + 1, T + 2, \dots, \quad (1.20)$$

where $\hat{\sigma}_u^2$ represent the variance estimate and T is the number of observations used to estimate the parameters (for details, see Guseo and Mortarino, 2015).

Given the confidence bands definition of Equation (1.20), their width is equal to:

$$4 \hat{\sigma}_u \hat{z}'(t), \quad t = T + 1, T + 2, \dots \quad (1.21)$$

This highlights that width is affected both by residuals' variability, $\hat{\sigma}_u$, and the fitted trajectory, $\hat{z}'(t)$. Both may depend on model choice, but while low residuals' variability always represents an improvement, the role of $\hat{z}'(t)$ may be controversial, as highlighted in the applications in Chapter 3 and Chapter 5.

1.4.3 Forecasting accuracy

In addition to confidence bands, forecasting accuracy (FA) measures are also useful alternative techniques for assessing a model's predictions. It is an assessment of the in-sample (training data) performances based on multistep forecasts to the out-of-sample (test data), which is performed by a 'rolling-origin evaluation' process, proposed by Tashman (2000). Consequently, we have different training data sets, each containing one more observation compared with the previous set.

There are various measures for computing the errors between the observed data and parallel forecasts. Many researchers (Armstrong and Collopy, 1992; Makridakis, 1993; Armstrong and Fildes, 1995) claimed that no single measure can be superior to all others, and the performance of forecasting methods varies according to the accuracy measure being used (Makridakis and Hibon, 2000). Although root mean square error (RMSE) is not unit-free, it has been used frequently to draw conclusions about forecasting methods (Armstrong and Collopy, 1992). However, it is sensible to use scale-independent error measures. The mean absolute percentage error (MAPE) can be used when there are no zeros or extremely small values in a data. Although the symmetric MAPE (sMAPE) is widely criticised as an asymmetric measure (Goodwin and Lawton, 1999), it does not have the problems of being excessively large or infinite.

The relative absolute errors (RAEs), especially the geometric mean RAE (GMRAE) and median RAE (MdRAE) proposed by Armstrong and Collopy (1992), also have a serious deficiency when the benchmark method – the random walk (RW) – can be small (Hyndman and Koehler, 2006). Armstrong and Collopy (1992) suggested the use

of ‘Winsorising’ to trim extreme values and avoid the difficulties associated with small values of the naïve (RW) method, but this adds some complications to the computation.

Instead of using the average of relative errors, one can use the relative of average errors obtained using a base measure proposed by Armstrong and Collopy (1992). For instance, when the base measure is mean absolute error (MAE), the relative MAE (RelMAE) is the ratio of MAE to MAE*, where MAE* denotes the MAE from the benchmark method. Hyndman and Koehler (2006) noticed as an advantage of these measures that they are interpretable. For instance, when RelMAE < (>) 1, the proposed forecast method is better (worse) than the benchmark method. However, the measures require several forecasts on the same series to enable an MAE (or RMSE) to be computed (Hyndman and Koehler, 2006).

The mean absolute scaled error (MASE), a new measure proposed by Hyndman and Koehler (2006), is suitable in those situations where the previously mentioned measures are problematic to use. The measure can be defined as

$$\text{MASE} = \text{mean} \left(\frac{e_t}{\frac{1}{n-1} \sum_{i=2}^n |Z_i - Z_{i-1}|} \right),$$

where $e_t = Z_t - F_t$ is the forecast error at time t and $\frac{1}{n-1} \sum_{i=2}^n |Z_i - Z_{i-1}|$ is the in-sample MAE from the naïve forecast method. Notice that MASE will not be infinite unless all historical data are equal. When MASE < 1, the errors from the proposed method are, on average, smaller than the errors from the one-step naïve method. However, MASE is also vulnerable to outliers (Davydenko and Fildes, 2013).

Another accuracy measure, called the unscaled mean bounded relative absolute error (UMBRAE), has recently been proposed by Chen *et al.* (2017). The RAE is used as the base to derive this new measure. Since $\text{RAE} = \frac{|e_t|}{|e_t^*|}$ has no upper bound, it can be extremely large or infinite when $|e_t^*|$, one-step naïve method, is small or equal to zero. This issue can easily be solved by adding an $|e_t|$ to the denominator of RAE, which is addressed as a bounded RAE (BRAE) and is defined as $\text{BRAE} = \frac{|e_t|}{|e_t^*| + |e_t|}$. The average of BRAE is called mean BRAE (MBRAE). Finally, the unscaled MBRAE can be defined as

$$\text{UMBRAE} = \frac{\text{MBRAE}}{1 - \text{MBRAE}}.$$

When UMBRAE is equal to 1, the proposed method performs roughly the same as the naïve method. When UMBRAE < (>) 1, the proposed model performs roughly $(1 - \text{UMBRAE}) \times 100\%$ better ($(\text{UMBRAE} - 1) \times 100\%$ worse) than the naïve method.

UMBRAE would be particularly useful for cases where the forecasting method performance is not expected to be dominated by forecasting outliers.

1.4.4 Comparison with alternative models

As explained in Subsection 1.2.2, the model may incorporate external shocks whose parameters are estimated jointly with the remaining ones. In particular, through the general grid of initial values, models with an increasing number of shocks are fitted starting from different initial values about a_i , which describe the starting points for the shocks. The least square algorithm designates the optimal allocation of any shock. In order to decide whether further shocks provide a significant improvement, we exploit the theory of nested models. For dealing with the comparison of models from different families, Akaike's Information Criterion (AIC), Akaike (1974), or Bayesian Information Criterion (BIC), Schwarz (1978), would be adequate. Conversely, the models with a lower number of shocks are nested within larger models with more shocks. For this reason, we can exploit this relationship to obtain more powerful statistical tests as follows (Seber, 1980; Seber and Wild, 1989; Guseo and Mortarino, 2015).

Suppose M_1 and M_2 are two different models, where M_2 is nested in M_1 ; then, the normalised squared multiple partial correlation coefficient can be computed as

$$\tilde{R}^2 = (R_{M_1}^2 - R_{M_2}^2) / (1 - R_{M_2}^2),$$

where $R_{M_1}^2$ and $R_{M_2}^2$ are the standard determination index of models M_1 and M_2 , respectively. The improvement between M_1 and M_2 can be assessed by using the traditional F -ratio, which has a one-to-one monotone correspondence with \tilde{R}^2 , that is,

$$F = [\tilde{R}^2(N - k)] / [(1 - \tilde{R}^2)v], \quad (1.22)$$

where N is the total number of observations, k is the number of parameters of M_1 and v is the number of parameters of M_1 not in M_2 . Under the null hypothesis H_0 , models M_1 and M_2 are equivalent, and the F -ratio is distributed as a Snedecor's F with $(v, N - k)$ degrees of freedom, $F \sim F_{v, N-k}$ if the error term $\epsilon(t)$ is independently and identically distributed normal. Nevertheless, without strong assumptions about error distributions, the F -ratio (1.22) can be used as an approximate robust criterion to check the null hypothesis by considering the threshold of 4 (Guseo *et al.*, 2007).

In the next chapters, we propose some extensions of the existing diffusion models for competition and discuss their applications in the energy market.

Chapter 2

The three-competitor diffusion model with a fixed m

2.1 Introduction

Contemporary researchers across disciplines (e.g. marketing, social sciences, physics, mathematics, statistics, biology and epidemiology) have been contributing to either theoretical extension or novel applications of diffusion models (Krishnan *et al.*, 2000; Rogers, 2003; Meade and Islam, 2006; Peres *et al.*, 2010; Guseo and Mortarino, 2012, 2014). Existing models in the diffusion of innovations literature explains the competition between two products (as discussed in Chapter 1). To apply these models, data from two or more similar products are aggregated or only the two leading products are considered. This aggregation may hide specific features of some of the products, resulting in lost information. Indeed, the higher number of products are aggregated, the more the possibility is to have a new path for the aggregated products. In such a situation, there is a higher chance to lose the usual patterns and behaviors of individual products. To avoid loss information on leading products, the aggregation can be applied to non-leading products. However, any kind of aggregation determines information waste. Thus, an extended model for dealing with additional competitors may be an important contribution to the diffusion literature. However, higher dimension models with extra parameters and a composite structure of the interactions among competitors demand greater computational effort.

With the aim of improving the description of mutual interactions of three competing products (either competition or cooperation), a higher dimension diffusion model is proposed. In contemporary literature, alternative options for two-product competition models include, balanced or unbalanced versions and models for synchronic or diachronic

competition. We propose a diffusion model for three competitors following the model proposed by Guseo and Mortarino (2014), which is a general model of competition between two products with a fixed market potential. The competing products share a common residual market.

2.2 The model

We assume that all the products belong to a homogeneous category and they will compete in the same customer segment. Hence, we assume a common market potential m , and consequently, a common residual market $m - z(t)$. Here, $z(t) = \sum_i z_i(t)$ denotes the aggregate cumulative consumptions, while $z_i(t)$, $i = 1, 2, 3$ represents the cumulative consumptions of product i . Considering that observing three simultaneous products is uncommon, we focus on situations where two products exist in the market from the beginning, while the third enters the market later.

Let us consider a twofold case with the late entrance of the third competitor at time $t = c_2$ with $c_2 > 0$, where $t = 0$ represents the time of origin for the first two competitors. Our proposed new model, as an extension of the models proposed by Guseo and Mortarino (2014), can be expressed through the following system of differential equations:

$$\begin{aligned}
z'_1(t) &= m \left\{ \left[p_{1\alpha} + (q_{1\alpha} + \delta_\alpha) \frac{z_1(t)}{m} + q_{1\alpha} \frac{z_2(t)}{m} \right] (1 - I_{t>c_2}) + \right. \\
&\quad \left. + \left[p_{1\beta} + (q_{1\beta} + \varepsilon_\beta) \frac{z_1(t)}{m} + (q_{1\beta} + \eta_\beta) \frac{z_2(t)}{m} + q_{1\beta} \frac{z_3(t)}{m} \right] I_{t>c_2} \right\} \left[1 - \frac{z(t)}{m} \right], \\
z'_2(t) &= m \left\{ \left[p_{2\alpha} + (q_{2\alpha} - \delta_\alpha) \frac{z_1(t)}{m} + q_{2\alpha} \frac{z_2(t)}{m} \right] (1 - I_{t>c_2}) + \right. \\
&\quad \left. + \left[p_{2\beta} + (q_{2\beta} + \theta_\beta) \frac{z_1(t)}{m} + (q_{2\beta} + \xi_\beta) \frac{z_2(t)}{m} + q_{2\beta} \frac{z_3(t)}{m} \right] I_{t>c_2} \right\} \left[1 - \frac{z(t)}{m} \right], \quad (2.1) \\
z'_3(t) &= m \left\{ \left[p_3 + (q_3 - \varepsilon_\beta - \theta_\beta) \frac{z_1(t)}{m} + (q_3 - \eta_\beta - \xi_\beta) \frac{z_2(t)}{m} + q_3 \frac{z_3(t)}{m} \right] I_{t>c_2} \right\} \left[1 - \frac{z(t)}{m} \right], \\
m &= m_\alpha (1 - I_{t>c_2}) + m_\beta I_{t>c_2}, \\
z(t) &= z_1(t) + z_2(t) + z_3(t) I_{t>c_2},
\end{aligned}$$

where $z'_i(t) = \partial z_i(t) / \partial t$, $i = 1, 2, 3$, represents instantaneous consumptions of product i . The system of Equation (2.1) indicates a competition among three products in two phases. During the first phase, until $t \leq c_2$, it is assumed that the first two products are characterised separately by three parameters each (denoted with subscript α). The parameters of the first product are $p_{1\alpha}$, $q_{1\alpha} + \delta_\alpha$ and $q_{1\alpha}$. The second product has three

corresponding parameters, as follows: $p_{2\alpha}$, $q_{2\alpha}$ and $q_{2\alpha} - \delta_\alpha$. Thus, in the first phase, we assume an unrestricted unbalanced (synchronic) competition (UUC) model with the constraint $\delta_\alpha = \gamma_\alpha$.

The second phase of the model begins when the third product enters the market, at time $t = c_2$. We allow the first two products to be characterised by new parameters. The parameters of the second phase are denoted with β as subscript. In case of the first product, the new parameters are as follows: the innovation coefficient, $p_{1\beta}$; the imitative one due to the WOM, split into three parts, the within-product imitation coefficient, $(q_{1\beta} + \varepsilon_\beta)$, modulating the sales of the first product through the relative knowledge z_1/m ; the cross-product imitation coefficient $(q_{1\beta} + \eta_\beta)$, powered by z_2/m and the cross-product imitation coefficient, $q_{1\beta}$, powered by z_3/m . The second product has the corresponding four new parameters, as follows: the innovation coefficient, $p_{2\beta}$; the within-product imitation coefficient $(q_{1\beta} + \xi_\beta)$; the cross-product imitation coefficient $(q_{2\beta} + \theta_\beta)$, which measures the effect of the first product on sales of the second product and the cross-product imitation coefficient $q_{2\beta}$, which measures the effect of the third product on sales of the second product. Finally, the third product has four parameters with the same meaning, as follows: the innovation coefficient, p_3 ; the within-product imitation coefficient q_3 ; the cross-product imitation coefficient $(q_3 - \varepsilon_\beta - \theta_\beta)$, which measures the effect of the first product on sales of the third product and the cross-product imitation coefficient $(q_3 - \eta_\beta - \xi_\beta)$, which measures the effect of the second product on sales of the third product. As before, ε_β , η_β , θ_β and ξ_β are called discriminations, where ε_β and η_β represent the differences between within-product and cross-product WOM effect of the first product, θ_β and ξ_β represent the similar differences in the second product, and all together represent those differences for the third product. The discriminations ε_β , η_β , θ_β and ξ_β may be either positive or negative, depending on whether the within-product effects of a specific product is stronger or weaker than the cross-product effects of the corresponding product. The common market potential, m , is equal to m_α in the first phase and is allowed to change to m_β in the second phase. A restricted version of model (2.1), with $\varepsilon_\beta = \xi_\beta$ and $\eta_\beta = \theta_\beta = 0$, has been proposed and applied in Furlan *et al.* (2018a) and Furlan *et al.* (2018b).

In the second phase, the first three equations of system (2.1) may be reorganised in the following way:

$$\begin{aligned} z'_1(t)I_{t>c_2} &\propto p_{1\beta} + q_{1\beta} \frac{z_1(t) + z_2(t) + z_3(t)}{m} + \varepsilon_\beta \frac{z_1(t)}{m} + \eta_\beta \frac{z_2(t)}{m}, \\ z'_2(t)I_{t>c_2} &\propto p_{2\beta} + q_{2\beta} \frac{z_1(t) + z_2(t) + z_3(t)}{m} + \theta_\beta \frac{z_1(t)}{m} + \xi_\beta \frac{z_2(t)}{m}, \\ z'_3(t)I_{t>c_2} &\propto p_3 + (q_3 - \varepsilon_\beta - \theta_\beta - \eta_\beta - \xi_\beta) \frac{z_1(t) + z_2(t) + z_3(t)}{m} + \\ &\quad + (\eta_\beta + \xi_\beta) \frac{z_1(t)}{m} + (\varepsilon_\beta + \theta_\beta) \frac{z_2(t)}{m} + (\varepsilon_\beta + \theta_\beta + \eta_\beta + \xi_\beta) \frac{z_3(t)}{m}. \end{aligned}$$

The restructuring of system (2.1) shows that the diffusion of each product is characterised by a category level imitation coefficient, specifically, $q_{1\beta}$ for the first, $q_{2\beta}$ for the second and $(q_3 - \varepsilon_\beta - \theta_\beta - \eta_\beta - \xi_\beta)$ for the third product, and product-level imitation coefficients, namely ε_β and θ_β or η_β and ξ_β . As a result, the aggregate hazard of the first three equations of system (2.1) for $t > c_2$, is

$$h(t) = \frac{z'(t)/m}{1 - z(t)/m} = (p_{1\beta} + p_{2\beta} + p_3) + (q_{1\beta} + q_{2\beta} + q_3) \left[\frac{z_1(t) + z_2(t) + z_3(t)}{m} \right], \quad t > c_2.$$

The hazard assumes the form $h(t) = P + Qz(t)$ for $P = p_{1\beta} + p_{2\beta} + p_3$ and $Q = q_{1\beta} + q_{2\beta} + q_3$, as it behaves as a BM for the cumulative sales $z(t)$ of the homogeneous category. The parameters ε_β , η_β , θ_β and ξ_β denote the equivalence discriminations for the first three equations of system (2.1) for $t > c_2$. Following Guseo and Mortarino (2014), the equations of system (2.1) may be called a UCRC model for the competitors.

If all three products are launched simultaneously, the first phase of the equations of system (2.1) disappears. Then, only the second phase of the Equation (2.1) system, with a minor change due to the fixed market potential, m , can be termed an unbalanced synchronic competition (USC) model (for details, see Appendix A). If the competing products in the market niche are extremely similar, that is, there is a homogeneous market, it is not necessary to split the WOM for each product from those of competing products. In such a situation, the equations of system (2.1) reduce to a balanced model, the same as proposed in Guseo and Mortarino (2012) for two competitors.

We may incorporate intervention functions in model (2.1) for one or more products. The number of intervention functions in the lifecycle can be three or more, if necessary (for details, see Subsection 1.2.2).

Chapter 3

Applications of the three-competitor diffusion model with a fixed m

3.1 Introduction

Since the 1960s, various diffusion models have been used to capture the usual S-shaped pattern of the process (Meade and Islam, 2006). The diffusion rates are context specific, and they are either facilitated or prevented by socioeconomic, technological and institutional factors (Rao and Kishore, 2010). These interrelated factors influencing the process demand the development of complex models. For example, renewable energy technologies (RETs) are boosted by impending environmental and energy security considerations arising from the use of fossil fuels (e.g. CGO). The issue has appeared at the front line because of the consideration that the fossil fuel-based energy sources are not unlimited. Moreover, RETs are promoted and adopted through financial and fiscal incentives from the government and private agencies (Rao and Kishore, 2010). Although RETs are inherently advantageous for the environment and receive financial support, the share of RETs in the energy market mix is not increasing to a desired rate. Indeed, the lifecycle of renewables may be influenced by alternative energy sources. For instance, the nonrenewables may have a more prominent lifecycle compared with renewables. Since diffusion of innovations models are able to explain how, why and at what rate new ideas and technology spread, the models can suitably be used in the energy market.

Marchetti (1980) was one of the first to employ the diffusion of innovation framework (logistic model) to analyse energy dynamics. Later, several researchers employed diffusion models, especially Bass models (the BM, Bass, 1969 and GBM, Bass *et al.*, 1994) and proposed their potential modifications to describe and forecast energy sources

and technologies. Rao and Kishore (2009) applied the BM for investigating growth patterns of wind power technology in several Indian states. They noticed that the diffusion model is suitable for the study of consumer markets and capital-intensive equipment, such as wind power generators. Davies and Diaz-Rainey (2011) studied the diffusion of wind power in 25 Organisation for Economic Co-operation and Development (OECD) countries by testing several assumptions related to the logistic and Bass models. The authors examined the difference between induced diffusion patterns when interventions exist and conventional diffusion patterns without any interventions. They revealed how the effects of induced diffusion could be modelled through a series of analyses and proposed several policy implications for inducing the diffusion of wind power. Guidolin and Mortarino (2010) analysed adoption patterns of solar photovoltaic (PV) for 11 countries to select a model, among the several Bass modifications, suitable to each country. They modelled the intervention function of the GBM through two types of shock function, as follows: an exponential function for describing a drastic perturbation and a rectangular function for a more stable perturbation. To describe the lifecycles of wind power in the United States and some European countries, Dalla Valle and Furlan (2011) introduced incentive influences as exogenous dynamics in the GBM. They found that, among several diffusion models, GBM performed the best in terms of forecasting accuracy. Duan *et al.* (2014) employed a revised Lotka–Volterra model to explore the diffusion patterns of wind and PV solar technologies in the United States, China, Japan and some European countries. They examined the possible relationships (competition or cooperation) between the two technological innovations. Through equilibrium calculation, they made some short-term predictions for equilibrium-stable countries.

The GBM was also profitably used to analyse the adoption of nonrenewable energy sources, such as oil (Guseo *et al.*, 2007; Brandt, 2007), natural gas (Aguilera and Aguilera, 2012; Wang *et al.*, 2013) and nuclear (Guidolin and Guseo, 2012). Furthermore, Guseo *et al.* (2015) introduced two separate heterogeneity effects in a GBM through Bemmaor’s approach and applied them to conventional Algerian natural gas production. In contrast, Furlan and Mortarino (2018) studied the lifecycles of renewable and nonrenewable energy sources as two competitors. They proposed a two-wave diffusion model that offers a competition between two products. To describe external influences with internal dynamics, they incorporated shock functions into the model.

Although the diffusion of innovation methodology is not new for the energy sector, the existing research on the diffusion of energy sources or technologies may be improved; especially, the competitive relationship among three or more sources of energy has never been investigated. Hence, we are interested in studying the possible relationship among

three energy competitors by introducing some powerful diffusion models.

In contemporary literature, renewable and nonrenewable energy sources are observed as perfect substitutes (see, e.g. Tsur and Zemel, 2003; Chakravorty *et al.*, 2006, 2012; Van der Ploeg and Withagen, 2012). Understanding the relationship is critical when the fossil fuels (CGO), a major source of nonrenewable energy, are depleting and may run out over time. Complete dependency on such energy sources could spell disaster for a country's future energy security. Moreover, the negative effects of these sources on the environment is a well-established scientific fact. Nuclear energy is an alternative energy source that may reduce the consumption of fossil fuels. The established nuclear plants provide energy for an indefinitely long time, and hence, nuclear power is being considered as a feasible energy source by several nations. However, considering economic viability, environmental friendliness and safety issues, the use of nuclear energy is being restricted. The nuclear sources are not considered clean because of environmental degradation. Alternatively, 'renewable' sources (energy derived from hydro, solar, wind, geothermal and biomass resources) are appearing as the most feasible alternative (Brook *et al.*, 2014). The share of renewable sources in energy consumption has been increasing over time, especially among the developed countries.

This study considers energy sources as (two or three) competitors of substitute products competing for the same adopters (consumers). Thus, models with a common market potential appear as an adequate solution. Here, energy represents the category of products, and adopters are the ultimate consumers. The sales are considered as annual energy consumptions. The market potential (or carrying capacity) is the entire size of the market (total consumptions), and the residual market is the additional amount that the sources can still ensure will be produced.

3.2 The Data

In this study, we analyse energy consumption (in million tonnes of oil equivalent, Mtoe) data for both nonrenewable (coal, gas, oil and nuclear: CGON) and renewables (hydro, solar, wind, geothermal and biomass) sources as provided by British Petroleum (2016). Information from 12 countries, namely Belgium, China, Finland, France, Germany, India, Japan, Spain, Sweden, Switzerland, the United Kingdom and the United States are utilised. The data cover the period from 1965 to 2015, with a few exceptions. At the beginning of the study period, the use of traditional energy sources (coal, natural gas and oil) were nearly universal in most of the studied countries. Since the beginning of the study period, Belgium, France, Germany, Japan, the United Kingdom and the

United States have been using nuclear sources along with fossil fuels. The other studied countries introduced the nuclear source at a later time. Hydroelectricity, a renewable energy source, came into use in all countries in or before 1965. The other renewable sources, such as solar, wind, geothermal and biomass, were launched at a later time. Geothermal and biomass sources were introduced at a relatively early stage compared with solar and wind sources.

First, we aggregate consumptions (in Mtoe) into two competitors, CGON and renewables. The competition in all the studied countries turns out to be synchronic, as at least one of the sources of energy has been used since the beginning of the study period. Hence, in the first step, the two-competitor diffusion model is adopted to explain the competition between CGON sources and renewables. For the alternative categorisation of competition among the aggregate consumptions (in Mtoe) of CGO sources, renewables and nuclear, the three competitors may be synchronic or diachronic depending on the launch time of nuclear energy. A synchronic model can suitably be used when nuclear energy is launched simultaneously with CGO sources and renewables; otherwise, a diachronic model is appropriate. To describe nuclear consumptions with CGO sources and renewables, we subsequently analyse each country via the diffusion models for three competitors.

3.3 Analysis

When the energy sources are categorised as CGON and renewables, it should be understood that sources were present from the beginning of the study. In such a situation, only the second phase of the model (1.13) is applicable. However, grouping the sources into three categories (CGO, renewables and nuclear) would provide better information. In such case, we may observe two situations, as follows:

- i) CGO and renewables were available from the beginning and nuclear sources entered the market later (e.g. China, Finland, India, Spain, Sweden and Switzerland); and
- ii) All three sources were present at the beginning of the study (as in Belgium, France, Germany, Japan, the United Kingdom and the United States).

For the former situation, both the phases of model (2.1) are used. For the latter situation, only the second phase of the model is applicable. All available versions (balanced, unbalanced and unrestricted unbalanced) of models (1.13) and (2.1) are fitted to the energy data partitioned into two and three competitors, respectively. Additionally, one or

more exponential shocks (control functions) are added to the model. This introduction is intended to improve the fitting of the models by incorporating the effect of financial crisis and incentives that are externalities to the diffusion process. The performance of the models is compared to achieve the best fit within the models included in the study. Only renewables are common in both the two- (2CM) and three-competitor (3CM) models. Hence, in both the models (2CM and 3CM), we targeted having essentially the same raising point for the shocks for renewables. This choice was made to avoid introducing bias into the comparison between the performance of the 2CM and 3CM. However, for the price of achieving a good-fitted model, in some cases, we accepted, as a compromise, an insignificant variation between the raising point for the shocks for renewables in the 2CM and 3CM.

Since we are dealing with nonlinear models, a general discussion on their structural settings and inferential aspects is very relevant although, in Section 1.4, we have discussed in details how to make inference for these models. Nonlinear regression models can take many different forms. There are almost no restrictions on how parameters can be used in a nonlinear model. The positive side is that this flexibility allows nonlinear regression to provide the most flexible curve-fitting functionality. The weakness is that the correct null hypothesis value for each parameter depends on the expectation function, the parameter's location in it, and the field of study. Because the expectation functions can be so wildly different, it is not possible to create a single hypothesis test that works for all nonlinear models.

Simpler models are better, in the sense that, models with a large number of parameters demand complex mathematical computation. However, we are explaining complex market situations where a large number of products compete for the same customers. In such situation, relatively complex models with additional parameters (e.g. an increasing number of shocks) is preferred. While choosing a model, we make a balance by considering a minimum number of parameters but not excluding any parameter with physical importance or statistical significance. In practice, while fitting a model with large number of parameters, all the confidence intervals for respective parameters may not include the null value. Though, as Kalinowski and Fidler (2010) mentioned, statistically insignificant parameters may have practical (contextual) importance. Hence, some of the statistically insignificant parameters with importance in market philosophy were included in the models fitted in this study.

Naturally, diffusion models for cumulative data give an extremely high R^2 value. The R^2 value is also very large even if the model is fitted to instantaneous data. Because, in a comparison, with the mean response, growth curves as nonlinear diffusion models,

perform obviously extremely well. This is the reason why we need a better benchmark as simple diffusion model. The approach described in Subsection 1.4.4, of comparing a model with its simplified version, represents thus a good strategy for model choice.

Both 2CM and 3CM models are fitted to the data from all 12 countries. The structure of data may differ from country to country. Accordingly, each country can require a different model among available versions. Notice that the fitted model for each country is found to be globally significant, however, its all parameters are not locally important. In this chapter only five countries are presented in detail. A complete discussion on the rest of countries is found to be in Appendix B. Here, it is important to mention that the 2CM model is also applied to an alternative partition of energy sources and the findings are compared with the 3CM. This comparison is executed only for a country (e.g. for China) where CGO sources as a leading product compete with other energies.

3.3.1 Belgium

In 1965, the use of renewables was rare, with only 0.06 Mtoe of such sources used against 35.0 Mtoe of nonrenewables (see source-specific data in British Petroleum, 2016). Hydroelectric was the only renewable source of energy until the launch of geothermal and biomass in 1973. Wind and solar sources were added to the renewable energy mix in 1987 and 2004, respectively. To date, renewables contribute only a minor share (3.27 Mtoe) of Belgium’s total energy consumption (53.20 Mtoe). Energy production from renewable sources is intermittent, dispersed and weather dependent (Energy Outlook, 2013), leading to grid stability issues, such as congestions and imbalances. Figure 3.1 shows that energy consumptions from renewables were almost trivial until 2010,

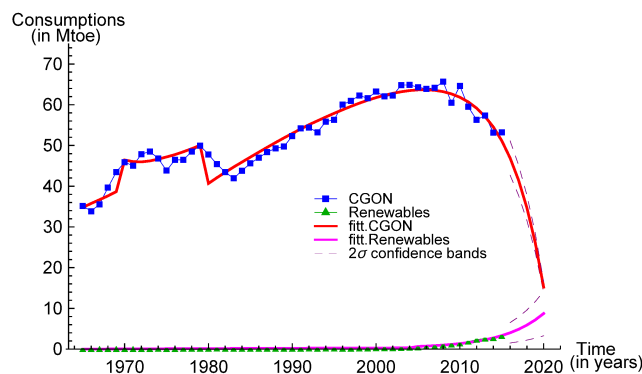


FIGURE 3.1: Belgium, 2CM. Energy consumption (Mtoe) from CGON sources (squares) and renewables (triangles). The solid lines correspond to the BSC fitted model with four shocks (three for CGON and one for renewables). The broken lines represent 2σ predictions’ confidence bands.

TABLE 3.1: Belgium, 2CM. Estimates, standard errors and marginal linearised 95% confidence intervals of the BSC model with four shocks (three for CGON sources and one for renewables).

Parameter	Estimate	Standard error	95% Confidence interval
m	5925.11	1802.93	{2340.40, 9509.82}
p_1	0.00587	0.00171	{0.00246, 0.00928}
q_1	0.03323	0.00767	{0.01797, 0.04848}
c_1	0.19133	0.04605	{0.09977, 0.28289}
b_1	-0.28437	0.20522	{-0.69240, 0.12367}
a_1	5.55485	0.00251	{5.54987, 5.55983}
c_2	-0.21730	0.02375	{-0.26453, -0.17007}
b_2	-0.07552	0.04266	{-0.16035, 0.00930}
a_2	15.0000	0.00039	{14.9992, 15.0008}
c_3	-0.00092	0.00320	{-0.00728, 0.00545}
b_3	0.23169	0.13364	{-0.03403, 0.49741}
a_3	27.1793	$6.78 * 10^{-7}$	{27.1793, 27.1793}
p_2	$3.52 * 10^{-6}$	0.00008	{-0.00016, 0.00017}
q_2	0.00023	0.00052	{-0.00081, 0.00127}
c_4	0.97486	2.68338	{-4.36042, 6.31014}
b_4	0.20187	0.16742	{-0.13100, 0.53475}
a_4	40.3508	0.52808	{39.3008, 41.4007}
R^2	0.99712		

at which point a substantial increasing trend could be observed. Fluctuations in the consumption of CGON sources were observed between the early 1980s and mid-'90s. Afterward, CGON sharply increased as the share of oil and nuclear in the energy mix remained stable. While coal consumption was reduced, the use of natural gas almost doubled. After a sharp increase between 1985 and 2005, a decreasing trend in overall CGON consumption has been observed since 2005. In this interim, the Belgium Federal Commission for Electricity and Gas Regulation (CREG), as well as other authorities and consultants, concluded that Belgium was facing security problems because of low electricity generation (Deloitte, 2015a). In fact, the country heavily depends on imported CGO energy. Moreover, in 2012–2013, Belgium's energy production capacity was compromised due to cold weather (Deloitte, 2015a).

Belgium has a long industrial history in the nuclear sector; however, its first commercial nuclear power reactor started functioning in 1974. Currently, about half of the domestically generated electricity comes from nuclear power (Nuclear Power in Belgium (NPB), 2018). According to British Petroleum (2016), Belgium's nuclear consumption

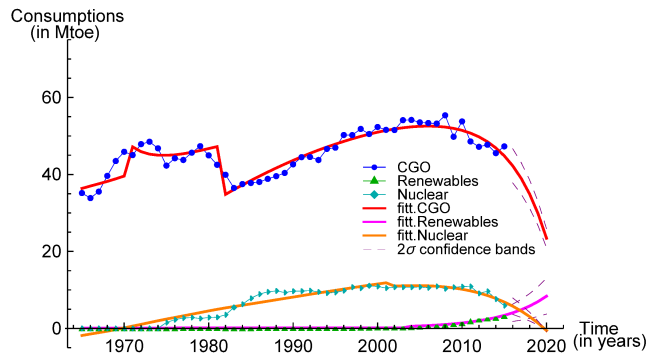


FIGURE 3.2: Belgium, 3CM. Energy consumption (Mtoe) from CGO sources (circles), renewables (triangles) and nuclear (diamonds). The solid lines correspond to the BSC fitted model with five shocks (three for CGO, one for renewables and one for nuclear). The broken lines represent 2σ predictions' confidence bands.

amounted as 1.5 Mtoe in 1975, when the consumption of CGO sources was approximately 42 Mtoe and the use of renewables was negligible (< 0.05 Mtoe). Figure 3.2 indicates that CGO consumption largely fluctuated until 1985. A consistent sharp increasing trend was observed for the period between 1986 and 2005, following a sharp decline lasting until recent years. Between 1975 and 1988, nuclear energy consumptions increased at a high rate. However, it was almost stable for the next two decades or more, and it has been declining since 2011.

When the data from Belgium are separated into CGON and renewables, model (A.3), illustrating balanced synchronic competition (BSC; see Appendix A), with four exponential shocks, Equation (1.9) (three for CGON and one for renewables) is suitably fitted. The rising time of the shocks has been estimated simultaneously with other parameters. The shocks minimise the deviance of residuals (globally as well as locally) of the model. The shocks are significantly incorporated into the model, as the F -ratio of the fitted model with the BSC model without shocks is larger than the threshold of 4 (for details, see Subsection 1.4.4). The value of $R^2=0.99712$ is adequate for proving that the model's overall fit is good.

Now, the data are separated into three sources (products or competitors), as follows: CGO, renewables and nuclear. For this country, they were simultaneously launched. Hence, only the second phase of model (2.1) is appropriate for describing these data. Model (A.7), BSC, with five exponential shocks (three for CGO sources, one for renewables and one for nuclear) is applied. The overall fitting is good ($R^2 = 0.99514$). The shocks are significant, as the value of the F -statistic obtained when comparing the fitted model with the BSC model without shocks is larger ($\hat{F} = 22.24465$) than the threshold of 4. For CGO sources, the three shocks occurred at times $1965 + \hat{a}_1 \simeq 1972$,

TABLE 3.2: Belgium, 3CM. Estimates, standard errors and marginal linearised 95% confidence interval of the BSC model with five shocks (three for CGO sources, one for renewables and one for nuclear).

Parameter	Estimate	Standard error	95% Confidence interval
m	6059.81	1571.47	{2951.07, 9168.55}
p_1	0.00600	0.00152	{0.00300, 0.00900}
q_1	0.02383	0.00417	{0.01558, 0.03208}
c_1	0.16966	0.03545	{0.09953, 0.23979}
b_1	-0.35364	0.17609	{-0.70198, -0.00529}
a_1	7.00000	0.00213	{6.99579, 7.00421}
c_2	-0.27100	0.02227	{-0.31505, -0.22695}
b_2	-0.07330	0.02301	{-0.11882, -0.02777}
a_2	18.0000	0.00044	{17.9991, 18.0009}
c_3	-0.00025	0.00132	{-0.00285, 0.00236}
b_3	0.23112	0.17376	{-0.11261, 0.57485}
a_3	22.5871	$7.41 * 10^{-8}$	{22.5871, 22.5871}
p_2	0.00001	0.00008	{-0.00015, 0.00018}
q_2	0.00009	0.00053	{-0.00096, 0.00114}
c_4	1.82989	6.22416	{-10.4830, 14.14280}
b_4	0.18918	0.12618	{-0.06044, 0.43880}
a_4	39.0587	2.15466	{34.7963, 43.3212}
p_3	-0.00030	0.00015	{-0.00059, -0.00002}
q_3	0.01054	0.00103	{0.00850, 0.01258}
c_5	-0.08619	0.05561	{-0.19620, 0.02383}
b_5	0.13345	0.04593	{0.04259, 0.22430}
a_5	37.3546	0.00064	{37.3534, 37.3559}
R^2	0.99514		

1965 + $\hat{a}_2 \simeq 1983$ and 1965 + $\hat{a}_3 \simeq 1988$. The first shock was estimated as positive ($\hat{c}_1 = 0.16966$) and decaying over time (negative \hat{b}_1). The second and third shocks were estimated as negative ($\hat{c}_2 = -0.27100$, $\hat{c}_3 = -0.00025$). The former shock decayed over time (negative \hat{b}_2) but the latter did not (positive \hat{b}_3). The first shock was observed immediately after 1971. The year is prominent for discharging the highest percentage of CO₂ emissions from liquid fuel consumption in Belgium's 50-year CO₂ emissions record. The second shock happened during the oil crisis 1979, which abruptly reduced CGO consumption in Belgium. The third shock was quite mild, and may have been due to a long-term effect of the oil crisis of 1979. One shock arose for renewables at time 1965 + $\hat{a}_4 \simeq 2004$. It is estimated to be positive ($\hat{c}_4 = 1.82989$) and not yet faded over time (positive \hat{b}_4). The shock can be explained in that several subsidies and tax incentives encouraged both Belgian and foreign private companies to invest in wind or solar

energy. A negative shock ($\hat{c}_5 = -0.08619$) arose for nuclear at time $1965 + \hat{a}_5 \simeq 2002$, which did not decay over time (positive \hat{b}_5). The shock may be due to the fact that the Belgian Senate approved the Federal Act of 31 January 2003, which limited the operating lives of existing nuclear power plants to 40 years and prohibited the building of new plants (NPB, 2018).

The 3CM's findings are more specific and informative than those of the 2CM models, and hence, we focus on the parameters estimated through the 3CM. Table 3.2 indicates that the effect of the innovative component corresponding to CGO sources ($\hat{p}_1 = 0.00637$) is notably larger than the effect for competitors ($\hat{p}_2 = 0.00001$ for renewables and $\hat{p}_3 = -0.00031$ for nuclear). This indicates that Belgium is somewhat more motivated for the innovation of clean and safe energy (renewables) technology compared with nuclear technology. By substituting the estimated parameter values in the BSC model, the following three equations can be obtained:

$$\begin{aligned} z'_1(t) &\propto 0.00600 + 0.02383 z(t)/m \\ z'_2(t) &\propto 0.00001 + 0.00009 z(t)/m \\ z'_3(t) &\propto -0.00031 + 0.01054 z(t)/m. \end{aligned}$$

Here, all three sources exploited the WOM effect of the whole category. It shows that the innovative effect of nuclear is negative, whereas it experiences a positive imitative (WOM) effect with other sources. More specifically, the diffusion spread of CGO sources is high ($\hat{q}_1 = 0.02383$) and that of nuclear is also high ($\hat{q}_3 = 0.01054$). Conversely, renewable diffusion spread is extremely low ($\hat{q}_2 = 0.00009$).

The solid lines in Figures 3.1 and 3.2, representing fitted models, show satisfactory fit of the models to the observed data. Here, we make a short period of predictions (5 years after 2015) for each competitor. Both the 2CM and 3CM predictions suggest increasing trends in renewables in 2016–2020, when the use of other energies may decline. In fact, over the last 10 years, the share of renewables in Belgium's final energy consumption has increased from 2% in 2005 to 8% in 2014. That is, the country is progressing through the way to meet its 2020 objective of 13% increase in the use of renewables (Energy Transition, 2016).

Although fitted lines are found be consistent with the observed data, we observe worse fit in the first part of renewables in 2CM and nuclear in 3CM. For this reason, the estimate of the variance of the stochastic component, based on residuals that are inflated by a partial lack of fit, is biased. To build credible confidence bands for future assessment of the series, we excluded the first two residuals for renewables and the first 17 residuals

for nuclear. As the renewables are common to both 2CM and 3CM, we also omitted the first two residuals of renewables for the 3CM. No residuals were omitted for other sources (CGON in 2CM and CGO in 3CM). Then, we computed ‘scaled residuals’ of each competitor in the two models (for details, see Subsection 1.4.2). The Kolmogorov–Smirnov test confirms the hypothesis that scaled residuals follow a Gaussian distribution. The standard deviations of scaled residuals ($\hat{\sigma}_u$) through 2CM are 0.04483 for CGON and 0.31263 for renewables, and those obtained with 3CM are 0.05254 for CGO, 0.27749 for renewables and 0.18512 for nuclear. Now, using the properties of normal distributions, we computed 95% confidence bands for predictors with 2σ bands (represented by broken lines in Figures 3.1 and 3.2) and the corresponding confidence band width (Table 3.3).

The first column of Table 3.3 represents the prediction years. The next two columns represent the confidence band width of 2CM predictions, and the last three columns represent the confidence band width of 3CM predictions. Since 2CM and 3CM use different data, it is not appropriate to compare them through global goodness-of-fit measures (standard deviation, residual diagnostics and the R^2 value). Thus, we decided to assess the improvement of the 3CM with respect to 2CM, focussing on the common time series, for example, renewables.

The confidence bands of predictions for renewables using 3CM are narrower than those obtained through 2CM. However, the band width from the first to the subsequent prediction years increased for both the 2CM and 3CM. While both the models suggest increasing renewables in 2016–2020, the predictions obtained with 3CM are more reliable. CGO predictions suggest a sharp decline of traditional energies (CGO sources) in 2016–2020. According to nuclear predictions, the use of nuclear may decline or stop between 2016 and 2020. Above all, the planned nuclear phase-out and implied embargo on new investments in coal for power generation will change the diversity of electricity

TABLE 3.3: Belgium. Confidence band width of 2CM and 3CM predictions in 2016–2020.

Year	2CM		3CM		
	CGON ($\hat{\sigma}_u=0.04483$)	Renewables ($\hat{\sigma}_u=0.31263$)	CGO ($\hat{\sigma}_u=0.05254$)	Renewables ($\hat{\sigma}_u=0.27749$)	Nuclear ($\hat{\sigma}_u=0.18512$)
2016	8.40890	5.01686	8.87624	4.50149	4.27832
2017	7.44140	6.07902	8.19142	5.38906	3.34565
2018	6.21916	7.38121	7.33420	6.45810	2.26483
2019	4.67646	8.97784	6.26243	7.74632	1.01773
2020	2.72858	10.93599	4.92237	9.29982	–

Confidence band width is not shown when the fitted trajectory is negative.

supply beyond 2025 (International Energy Agency (IEA), 2016a). The energy sector will then depend on natural gas and various renewable sources. Moreover, the large share of renewables will entail substantial capital investments to cope with the variability of wind and solar energy availability.

3.3.2 Sweden

There are few countries in the world with higher per capita energy consumption than Sweden, while Swedish carbon emissions are lower than those of other countries. According to the latest statistics from the IEA, Sweden releases, on average, 4.25 tonnes of CO₂ into the atmosphere yearly, compared with the EU average of 6.91 tonnes and the US average of 16.15 tonnes (Sweden.se, 2018). Apparently, Sweden is on the front line of efficient energy use. In 1965, the share of renewables was one-third of the total energy consumption, when hydroelectricity was the sole renewable source (British Petroleum, 2016). Sweden started to use geothermal and biomass energy in 1970, wind in 1983 and solar power in 1993. In Figure 3.3, with regular fluctuations, the consumption of CGON sources gradually increased until 2000 and declined after that year. The use of renewables continuously increased, with regular instabilities.

Sweden has been using nuclear energy since 1972. As Figure 3.4 shows, nuclear consumption sharply increased until 1987. After this time, it was almost stable or trivially declined with regular fluctuations. According to the Nuclear Power in Sweden (NPS; 2018), about 40% of the Swedish domestic electricity comes from nuclear energy. Still, Sweden has three nuclear plants with 10 nuclear reactors in commercial operation, making it the world's sole country that has more than one reactor per million people

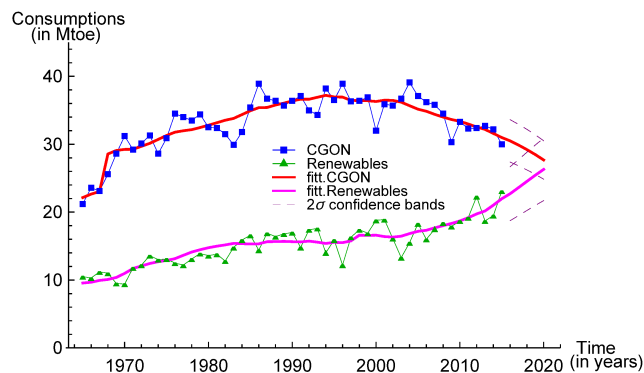


FIGURE 3.3: Sweden, 2CM. Energy consumption (Mtoe) from CGON sources (squares) and renewables (triangles). The solid lines correspond to the USC fitted model with two shocks (one for each competitor). The broken lines represent 2σ predictions' confidence bands.

TABLE 3.4: Sweden, 2CM. Estimates, standard errors and marginal linearised 95% confidence intervals of the USC model with two shocks (one for each competitor).

Parameter	Estimate	Standard error	95% confidence interval
m	3498.97	418.868	{2666.82, 4331.12}
p_1	0.00633	0.00085	{0.00463, 0.00802}
q_1	0.13153	0.06685	{-0.00127, 0.26434}
δ	-0.16301	0.09086	{-0.34352, 0.01751}
c_1	0.21120	0.06588	{0.08032, 0.34208}
b_1	0.01569	0.02587	{-0.03571, 0.06708}
a_1	3.11651	0.00022	{3.11608, 3.11694}
p_2	0.00273	0.00032	{0.00210, 0.00338}
q_2	-0.10260	0.06430	{-0.23035, 0.02516}
c_2	0.05254	0.03101	{-0.00906, 0.11414}
b_2	0.17576	0.02615	{0.12381, 0.22771}
a_2	33.1467	0.00029	{33.1461, 33.1473}
R^2	0.97506		

(Sweden.se, 2018). The consumption of CGO sources sharply increased until 1974. Later, it sharply declined for a decade and gradually declined after 1983.

First, the data from Sweden were partitioned as CGON sources and renewables. Model (A.2), USC, with two exponential shocks (one for each competitor) is fitted. The F -ratio, comparing the fitted model with and without shocks, provides a large value ($\hat{F} = 7.05260$). This suggests that the shocks are significantly incorporated into the model.

Later, the data were partitioned into three sources (CGO, renewables and nuclear), and we observed that the first two sources existed from the beginning and the third entered the market later. Hence, model (A.4), restricted UCRCO, with three exponential shocks (one for each competitor) is applied. The shocks are significant, as the value of the F -ratio obtained by comparing the fitted model with and without shocks is large ($\hat{F} = 16.07882$). The shocks occurred at time $1965 + \hat{a}_1 = 1982$ for the CGO time series, time $1965 + \hat{a}_2 \simeq 1999$ for renewables and time $1965 + \hat{a}_3 \simeq 1986$ for nuclear sources. The shock for CGO sources was estimated as negative ($\hat{c}_1 = -0.21129$) and not absorbed in time (positive \hat{b}_1). The next two shocks were estimated to be positive ($\hat{c}_2 = 0.03203$ and $\hat{c}_3 = 0.43093$). The shock for renewables has not yet decayed (positive \hat{b}_2), while that of nuclear energy decayed over time (negative \hat{b}_3). The negative shock for CGO sources may be related to the 1980s oil price hike, which also had an effect on the Swedish economy. The positive shock for renewables may be due to Swedish Parliament's 1999 decision to

TABLE 3.5: Sweden, 3CM. Estimates, standard errors and marginal linearised 95% confidence interval of restricted UCRC model with three shocks (one for each competitor).

Parameter	Estimate	Standard error	95% Confidence interval
m_α	1459.83	$7.02 * 10^{-9}$	{1459.83, 1459.83}
$p_{1\alpha}$	0.01438	0.00063	{0.01314, 0.01563}
$q_{1\alpha}$	0.30682	0.17885	{-0.04720, 0.66084}
δ_α	-0.37089	0.25191	{-0.86952, 0.12775}
$p_{2\alpha}$	0.00753	0.00063	{0.00629, 0.00878}
$q_{2\alpha}$	-0.26222	0.17885	{-0.61625, 0.09180}
m_β	3941.92	580.513	{2792.83, 5091.01}
$p_{1\beta}$	0.00875	0.00114	{0.00650, 0.01100}
$q_{1\beta}$	0.04038	0.02603	{-0.01115, 0.09191}
δ_β	-0.06425	0.04356	{-0.15047, 0.02196}
c_1	-0.21129	0.03477	{-0.28011, -0.14247}
b_1	0.00439	0.04225	{-0.07923, 0.08802}
a_1	17.0000	0.00003	{16.9999, 17.0001}
$p_{2\beta}$	0.00255	0.00037	{0.00183, 0.00327}
$q_{2\beta}$	0.02969	0.01182	{0.00630, 0.05308}
c_2	0.03203	0.02481	{-0.01707, 0.08113}
b_2	0.18170	0.03724	{0.10799, 0.25541}
a_2	33.8456	0.00014	{33.8454, 33.8459}
p_3	-0.00225	0.00043	{-0.00310, -0.00139}
q_3	-0.03358	0.04032	{-0.11340, 0.04624}
c_3	0.43093	0.13511	{0.16349, 0.69836}
b_3	-0.04525	0.10586	{-0.25480, 0.16430}
a_3	21.0000	0.00263	{20.9948, 21.0052}
R^2	0.96284		

establish 15 environmental quality objectives, where green energy was prioritised with increasing prices on carbon and fossil fuels. Moreover, the positive shocks for nuclear energy may be related to six new nuclear reactors that entered commercial service in the 1980s (NPS, 2018).

The market potential of the second phase ($\hat{m}_\beta = 4088.32$ Mtoe) is about three times of the first phase ($\hat{m}_\alpha = 1457.43$ Mtoe). Indeed, the length of the first phase is extremely short. In the second phase, the innovative effect of CGO sources ($\hat{p}_{1\beta} = 0.00875$) and renewables ($\hat{p}_{2\beta} = 0.00255$) are notably larger than the effect of nuclear ($\hat{p}_3 = -0.00225$). By substituting the parameter estimates in the second phase of model (A.4), we obtain

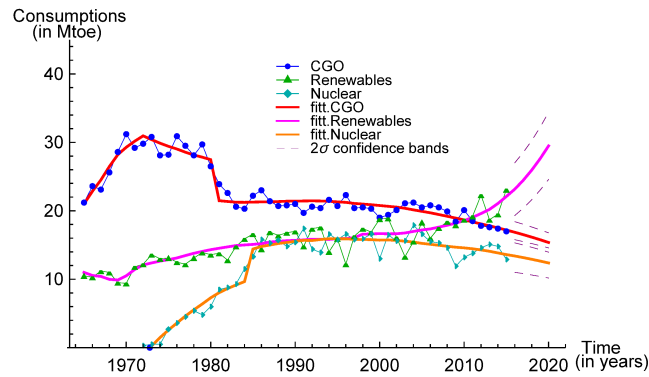


FIGURE 3.4: Sweden, 3CM. Energy consumption (Mtoe) from CGO sources (circles), renewables (triangles) and nuclear (diamonds). The solid lines correspond to the restricted UCRCF fitted model with three shocks (one for each competitor). The broken lines represent 2σ predictions' confidence bands.

the following three equations:

$$\begin{aligned} z'_1(t) &\propto 0.00875 - 0.02387 z_1(t)/m_\beta + 0.04038 z_2(t)/m_\beta + 0.04038 z_3(t)/m_\beta \\ z'_2(t) &\propto 0.00255 + 0.02969 z_1(t)/m_\beta - 0.03456 z_2(t)/m_\beta + 0.02969 z_3(t)/m_\beta \\ z'_3(t) &\propto -0.00225 + 0.03067 z_1(t)/m_\beta + 0.03067 z_2(t)/m_\beta - 0.03358 z_3(t)/m_\beta. \end{aligned}$$

The within-product WOM effects of all three sources are negative ($\hat{q}_{1\beta} + \hat{\delta}_\beta = -0.02387$ for CGO, $\hat{q}_{2\beta} + \hat{\delta}_\beta = -0.03456$ for renewables and $\hat{q}_3 = -0.03358$ for nuclear). However, the cross-product WOM effects of each product are positive. For instance, CGO sources cross-product effects by renewables and nuclear are the same, at $\hat{q}_{1\beta} = 0.04038$. The corresponding effect of renewables by CGO and nuclear energy is $\hat{q}_{2\beta} = 0.02969$, and that of nuclear energy by its competitors is $\hat{q}_3 - \hat{\delta}_\beta = 0.03067$. This means none of the energy sources can be sustained by their internal consumptions, but they support each other to be further sustained.

In Figures 3.3 and 3.4, the fitted lines go through the middle points of the scattered observed path, and the predictions from 2016 to 2020 follow the previous trend. The predictions suggest a rapid rise of renewables against a gradual decline of other energy sources in 2016–2020. Since the first three estimated values of the nuclear series are quite far from their observed path, we excluded them in computing the scaled residuals' variance. The scaled residuals follow a Gaussian distribution, which is verified by the Kolmogorov–Smirnov test. The standard deviations of scaled residuals ($\hat{\sigma}_u$) using the 2CM are 0.05115 for CGON and 0.08742 for renewables. Those with 3CM are 0.04591, 0.08319 and 0.08890 for CGO, renewables and nuclear, respectively. Accordingly, we computed the 2σ confidence bands of 2CM and 3CM predictions, represented by dashed

lines (see Figures 3.3 and 3.4), and the corresponding band width shown in Table 3.6. As we anticipated in Subsection 1.4.2, the band width results require a specific comment. The 3CM apparently results in a reduction in terms of confidence band width for only the first two prediction years. However, both $\hat{\sigma}_u$ values and the predicted trajectories highlight that the slight increase for the remaining three years is due to the steep increase in the predicted trajectory for the 3CM in contrast to a mild increase in the 2CM fitted trajectory. Conversely, the $\hat{\sigma}_u$ has a lower value for the 3CM, showing greater precision.

One of the aims of this thesis is developing models that can be used for forecasting future energy consumptions of the three types of sources. At this stage, we estimate the forecasting accuracy (FA) of the 2CM and 3CM models through a set of out-of-sample or test datasets. It should be noted that different datasets were used to estimate the FA for the 2CM and 3CM models (except for renewables). Hence, the various error measures (as mentioned below) of FA for the two models are not comparable. Conversely, we consider the forecasting error measures obtained through the random walk (RW) method as a benchmark (or naïve forecast method). The forecasting accuracies of both the models (2CM and 3CM) are then compared with the FA of the benchmark method.

Using the rolling-origin estimation procedure, we fix the origin t of the forecasting period at 2008 and forecasts until 2015. In the procedure, at least 86% of the available data are used for training, and the rest are kept for testing the prediction performance. Thus, we achieve seven 1-year-ahead and three 5-year-ahead forecasts. The forecasting accuracy is assessed using the forecasting error measures: RMSE, MAPE, sMAPE, MASE, UMBRAE and % Better (for details, see Subsection 1.4.3).

The measures evaluated here, except for MASE and UMBRAE, have no threshold for choosing a good fit model. Hence, we mainly focus on the MASE and UMBRAE measures for assessing a model's FA. In our study, the CGON and renewables have

TABLE 3.6: Sweden. Confidence band width of 2CM and 3CM predictions in 2016–2020.

Year	2CM		3CM		
	CGON ($\hat{\sigma}_u=0.05115$)	Renewables ($\hat{\sigma}_u=0.08742$)	CGO ($\hat{\sigma}_u=0.04591$)	Renewables ($\hat{\sigma}_u=0.08319$)	Nuclear ($\hat{\sigma}_u=0.08890$)
2016	6.23919	7.94242	3.09704	7.70788	4.76385
2017	6.11291	8.25599	3.03326	8.13855	4.68028
2018	5.97605	8.57684	2.96649	8.63140	4.59246
2019	5.82688	8.89427	2.89637	9.18911	4.49981
2020	5.66358	9.19494	2.82244	9.81229	4.40155

TABLE 3.7: Sweden. Forecasting accuracy measures for CGON predictions by 2CM and RW.

Measure	2CM (USC with 2 shocks)					RW				
	1-step	2-step	3-step	4-step	5-step	1-step	2-step	3-step	4-step	5-step
RMSE	6.110	3.707	4.571	3.356	3.814	5.730	3.897	2.488	2.278	2.276
MAPE	0.046	0.042	0.056	0.038	0.065	0.052	0.037	0.026	0.025	0.033
sMAPE	0.044	0.041	0.054	0.037	0.062	0.050	0.037	0.026	0.025	0.032
MASE	0.834	0.787	1.030	0.717	1.182	0.939	0.688	0.477	0.451	0.581
UMBRAE	0.834	1.317	1.370	0.508	0.811	1.000	0.840	0.668	0.315	0.334
% Better	43%	33%	60%	75%	67%	0%	67%	80%	100%	100%

TABLE 3.8: Sweden. Forecasting accuracy measures for CGO and nuclear predictions by 3CM and RW.

Measure	3CM (restricted UCRCO with 3 shocks)					RW				
	1-step	2-step	3-step	4-step	5-step	1-step	2-step	3-step	4-step	5-step
	CGO									
RMSE	1.705	1.519	0.552	0.575	0.445	2.903	2.486	1.814	0.854	0.490
MAPE	0.025	0.024	0.013	0.016	0.013	0.048	0.043	0.034	0.021	0.015
sMAPE	0.025	0.024	0.013	0.016	0.013	0.048	0.043	0.033	0.021	0.015
MASE	0.389	0.377	0.192	0.234	0.193	0.760	0.676	0.524	0.317	0.225
UMBRAE	0.577	0.696	0.211	0.172	0.099	1.000	0.990	0.485	0.223	0.137
% Better	86%	67%	100%	100%	100%	0%	67%	60%	100%	100%
	Nuclear									
RMSE	3.974	2.553	1.967	1.620	1.363	3.732	2.577	2.225	2.142	1.987
MAPE	0.094	0.069	0.058	0.048	0.054	0.089	0.066	0.060	0.064	0.067
sMAPE	0.090	0.068	0.058	0.049	0.055	0.086	0.066	0.058	0.062	0.064
MASE	1.021	0.790	0.683	0.575	0.638	0.970	0.754	0.687	0.733	0.754
UMBRAE	1.119	0.771	0.573	1.059	1.029	1.000	0.679	0.481	0.972	0.945
% Better	43%	67%	60%	75%	33%	0%	83%	80%	50%	33%

different lifecycles. Hence, simultaneously achieving smaller errors of out-of-sample forecasts for both the competitors is less likely. The situation is even more vulnerable when three competitors (CGO, renewables and nuclear) are assessed simultaneously. In this case, we assessed forecasting accuracies of the two models, namely the CGON time series in the 2CM and CGO time series in the 3CM. According to the data level, these two series are relatively more consistent than the other time series are.

Table 3.7 represents the 1- to 5-year-ahead forecasting error measures for CGON predictions in Sweden. Only the measures of 1-year-ahead forecasts (except the RMSE measure) and the RMSE measure at the 1-year-ahead forecasts using the 2CM are smaller than those from the RW method. This may be an example that, on occasions, the simpler models can perform better than the more sophisticated, complex models (Makridakis and Hibon, 2000). However, the value of the MASE measure at the 1-, 2- and 4-year-ahead forecasts and that of the UMBRAE measures at the 1-, 4- and 5-year-ahead forecasts using the 2CM are smaller than 1. This means that the 2CM

TABLE 3.9: Sweden. Comparison of forecasting accuracy measures for renewables predictions by 2CM and 3CM.

Measure	2CM					3CM				
	1-step	2-step	3-step	4-step	5-step	1-step	2-step	3-step	4-step	5-step
RMSE	7.024	9.087	7.485	6.616	7.548	6.071	7.497	7.595	5.046	1.923
MAPE	0.120	0.148	0.144	0.137	0.160	0.092	0.119	0.136	0.081	0.045
sMAPE	0.121	0.151	0.149	0.150	0.182	0.090	0.113	0.133	0.087	0.046
MASE	1.661	2.119	2.119	2.021	2.423	1.288	1.662	2.031	1.224	0.654
UMBRAE	1.503	1.604	3.450	1.309	1.908	1.069	1.249	3.531	0.614	0.602
% Better	29%	17%	0%	25%	0%	57%	50%	20%	50%	67%

forecasting errors are not too large.

For all the 1- to 5-year-ahead forecasts of CGO consumption, in contrast, the estimated values of the forecasting error measures using the 3CM are smaller than those obtained for the RW method (Table 3.8). In addition, all the 3- to 5-year-ahead forecasting error measures (except the UMBRAE measures) for the consumption of energy from nuclear sources through 3CM are smaller than those obtained by the RW method. Apparently, the 3CM produces better forecasts (smaller error measures) than those achieved through the RW method. Moreover, all 1- to 5-year ahead measures of MASE and UMBRAE for CGO are smaller than 1. Further, the MASE measures of 2- to 5-year-ahead forecasts and the UMBRAE measures of 2- and 3-year-ahead forecasts for nuclear energy are smaller than 1. This means that the forecasting errors obtained through the 3CM are smaller than those obtained using the RW method. Hence, both models (2CM and 3CM), and especially the 3CM, prove to be powerful for achieving reasonably accurate forecasts for these data.

Beyond the above discussions, our main concern is observing any improvement of the 3CM over 2CM assessed by FA measures. In this case, we focus on renewables findings, as only the renewables data are common to both the models. As shown in Table 3.9, all 1- to 5-year-ahead forecasting error measures (except RMSE and UMBRAE at 3-year-ahead forecasts) by the 3CM are smaller than those obtained for the 2CM. We can conclude that, with respect to the 2CM, the 3CM model is more accurate in forecasting the energy data for Sweden.

3.3.3 Switzerland

The Swiss energy policies are oriented toward reviewing the CO₂ law to fulfil the goals being debated in Europe and worldwide. According to source-specific data (British Petroleum, 2016), in 1965, Switzerland consumed about 6 Mtoe of energy from renewables, when CGON consumption amounted nearly to 11 Mtoe. From the beginning,

TABLE 3.10: Switzerland, 2CM. Estimates, standard errors and marginal linearised 95% confidence interval of the USC model with two shocks (one for each competitor).

Parameter	Estimate	Standard error	95% Confidence interval
m	2223.16	59.1183	{2105.71, 2340.61}
p_1	0.00435	0.00016	{0.00403, 0.00468}
q_1	0.09558	0.02256	{0.05076, 0.14040}
δ	-0.09620	0.03237	{-0.16052, -0.03189}
c_1	0.20395	0.04937	{0.10587, 0.30204}
b_1	-0.26374	0.09854	{-0.45950, -0.06798}
a_1	6.72128	0.00266	{6.71600, 6.72655}
p_2	0.00290	0.00013	{0.00264, 0.00316}
q_2	-0.05919	0.02294	{-0.10476, -0.01361}
c_2	0.14114	0.08460	{-0.02692, 0.30921}
b_2	0.13846	0.19591	{-0.25074, 0.52767}
a_2	47.1195	0.00165	{47.1162, 47.1228}
R^2	0.98874		

hydropower was the most important domestic source of Swiss renewable energy. Other renewable energy sources are geothermal and biomass (launched in 1978), solar (1990) and wind (1996). Figure 3.5 shows that CGON consumption sharply increased for the first decade. After a short decline, it increased notably, with regular fluctuations, until 2002, after which time it decreased. Conversely, the use of renewables gradually increased, with larger variations, over time.

In 1969, Switzerland started to consume nuclear energy, and the consumption substantially increased until 1985 (see Figure 3.6). It was almost stable or increased trivially

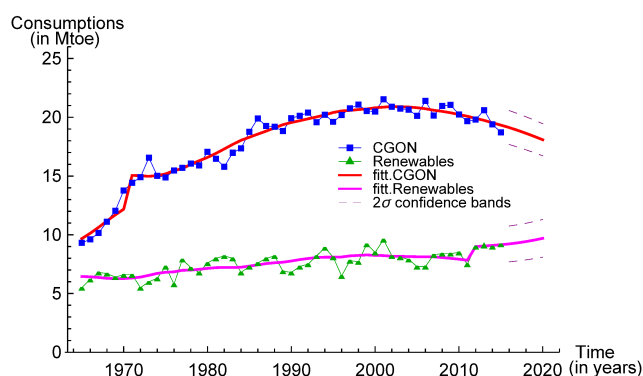


FIGURE 3.5: Switzerland, 2CM. Energy consumption (Mtoe) from CGON sources (squares) and renewables (triangles). The solid lines correspond to the USC fitted model with two shocks (one for each competitor). The broken lines represent 2σ predictions' confidence bands.

TABLE 3.11: Switzerland, 3CM. Estimates, standard errors and marginal linearised 95% confidence intervals of the restricted UCRC model with three shocks (one for each competitor).

Parameter	Estimate	Standard error	95% Confidence interval
m_α	566.398	$2.52 * 10^{-8}$	{566.398, 566.398}
$p_{1\alpha}$	0.01618	0.00075	{0.01470, 0.01765}
$q_{1\alpha}$	0.03845	0.01447	{0.00982, 0.06708}
$p_{2\alpha}$	0.01002	0.00075	{0.00854, 0.01149}
$q_{2\alpha}$	0.02654	0.01447	{-0.00209, 0.05517}
m_β	2605.15	138.442	{2331.20, 2879.10}
$p_{1\beta}$	0.00490	0.00025	{0.00441, 0.00538}
$q_{1\beta}$	0.02503	0.00582	{0.01351, 0.03655}
δ_β	-0.02542	0.01007	{-0.04534, -0.00550}
c_1	0.26752	0.15234	{-0.03393, 0.56896}
b_1	-1.89115	1.86736	{-5.58632, 1.80401}
a_1	8.65531	0.07707	{8.50280, 8.80781}
$p_{2\beta}$	0.00235	0.00013	{0.00209, 0.00262}
$q_{2\beta}$	0.01466	0.00313	{0.00846, 0.02086}
c_2	0.12913	0.06338	{0.00372, 0.25454}
b_2	0.08712	0.19123	{-0.29129, 0.46553}
a_2	47.5553	0.00070	{47.5539, 47.5567}
p_3	-0.00027	0.00015	{-0.00057, 0.00003}
q_3	-0.01174	0.00822	{-0.02801, 0.00454}
c_3	0.41973	0.12489	{0.17260, 0.66686}
b_3	-0.10201	0.05289	{-0.20668, 0.00265}
a_3	20.0000	0.00530	{19.9894, 20.0106}
R^2	0.98710		

for the next two decades, and then it narrowly declined after 2006. In May 2011, the Swiss Federal Council approved the nuclear phase-out, that is, nuclear plants will not be replaced after their working lifetimes expire. However, nuclear energy is still the second most consumed energy source in Switzerland (Redondo and van Vliet, 2015). The consumption of CGO sources declined with the increase of renewables and nuclear energy. Both per capita and per gross domestic product (GDP), the energy and CO₂ intensities of Switzerland are some of the lowest among the IEA countries owing to the structure of the Swiss economy and energy supply (IEA, 2007).

Model (A.2), USC, with two exponential shocks (one for each competitor) is applied to the Swiss energy data, which are partitioned as CGON sources and renewables. The shocks are significant, as the value of F -ratio, comparing the fitted model with the USC

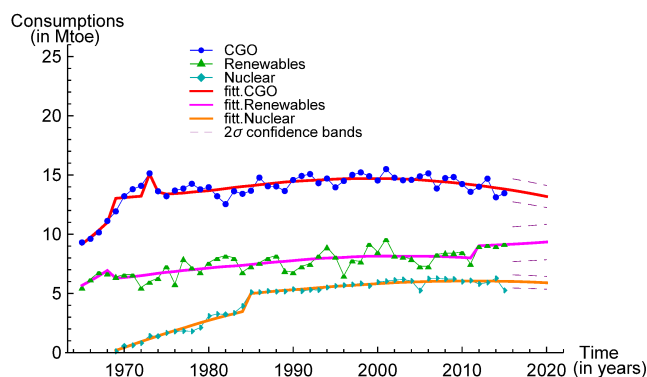


FIGURE 3.6: Switzerland, 3CM. Energy consumption (Mtoe) from CGO sources (circles), renewables (triangles) and nuclear (diamonds). The solid lines correspond to the restricted UCRCF fitted model with three shocks (one for each competitor). The broken lines represent 2σ predictions' confidence bands.

without shocks, is large ($\hat{F} = 6.09854$).

When the data are separated into three sources (CGO, renewables and nuclear), they offer a diachronic competition, as CGO and renewables exist from the beginning and nuclear enters the market at a later time. Model (A.4), with $\delta_\alpha = 0$ for the first phase, which is extremely short (only 4 years), representing a restricted UCRCF model with three exponential shocks (one for each competitor), is fitted. The fitting is good overall ($R^2 = 0.98710$). The value of the F -statistic obtained by the fitted model with and without shocks is large ($\hat{F} = 4.95781$). This proves that the shocks are significant. The shocks occurred at time $1965 + \hat{a}_1 \simeq 1974$ for the CGO time series, time $1965 + \hat{a}_2 \simeq 2013$ for renewables and time $1965 + \hat{a}_3 \simeq 1985$ for nuclear. All three shocks were estimated as positive ($\hat{c}_1 = 0.26752$, $\hat{c}_2 = 0.12913$ and $\hat{c}_3 = 0.41973$). The shock for renewables has not yet decayed (positive \hat{b}_2), while those for CGO and nuclear sources ceased their effect over time (negative \hat{b}_1 and \hat{b}_3). The positive shock for CGO sources may be the cause of sharply increased fossil fuel consumptions from 1965 to 1974. However, the shock rapidly vanished ($\hat{b}_1 = -1.89115$), as the 1973 global oil crisis caused energy consumption in Switzerland to decrease from 1974 to 1977⁵. The shock of renewables may be the effect of the Kyoto Protocol, where Switzerland committed to reducing its GHG emissions by 8% below the 1990 level in 2008–2012 (REEEP, 2014).

Now, we concentrate on the estimated parameters of the second phase. We see that the innovative effects of CGO ($\hat{p}_{1\beta} = 0.00490$) and renewables ($\hat{p}_{2\beta} = 0.00235$) are higher than the effect of nuclear energy ($\hat{p}_3 = -0.00027$). By substituting the estimated parameter values in the second phase of model (A.4), the following three equations can

⁵Global Tenders. Economy of Switzerland. www.globaltenders.com/economy-switzerland.htm

be obtained:

$$z_1'(t) \propto 0.00490 - 0.00039 z_1(t)/m_\beta + 0.02503 z_2(t)/m_\beta + 0.02503 z_3(t)/m_\beta$$

$$z_2'(t) \propto 0.00235 + 0.01466 z_1(t)/m_\beta - 0.01076 z_2(t)/m_\beta + 0.01466 z_3(t)/m_\beta$$

$$z_3'(t) \propto -0.00027 + 0.01369 z_1(t)/m_\beta + 0.01369 z_2(t)/m_\beta - 0.01174 z_3(t)/m_\beta.$$

All three products experience a negative within-product WOM effect. That is, none of the sources sustain its further consumptions ($\hat{q}_{1\beta} + \hat{\delta}_\beta = -0.00039$ for CGO, $\hat{q}_{2\beta} + \hat{\delta}_\beta = -0.01076$ for renewables and $\hat{q}_3 = -0.01174$ for nuclear). In contrast, the cross-product WOM effects of each product through its competitors are positive. The effect of CGO sources by renewables and nuclear is $\hat{q}_{1\beta} = 0.02503$. The corresponding effects of renewables and nuclear by their competitors are $\hat{q}_{2\beta} = 0.01466$ and $\hat{q}_3 - \hat{\delta}_\beta = 0.01369$, respectively. Since all the cross-product measures are substantially large, the diffusion of Swiss energy reveals three separate sources strongly supporting each other to further evolve.

The estimated trajectories in Figures 3.5 and 3.6 adequately describe the observed data; consequently, the predictions from 2016 to 2020 are reliable. The predictions suggest a moderate increase of renewables against substantial stability of other energy sources in 2016–2020. Since the first two estimated values of nuclear series are quite far from the observed values, we ignored them in computing the variance of scaled residuals. The Kolmogorov–Smirnov test confirmed the normality assumption of scaled residuals. The standard deviations of scaled residuals ($\hat{\sigma}_u$) using the 2CM are 0.03772 and 0.08269 for CGON and renewables, and those obtained with the 3CM are 0.03540, 0.08009 and 0.04602 for CGO, renewables and nuclear, respectively. Thus, we computed the 2σ confidence bands of predictions, represented by dashed lines in Figures 3.5 and

TABLE 3.12: Switzerland. Confidence band width of 2CM and 3CM predictions in 2016–2020.

Year	2CM		3CM		
	CGO ($\hat{\sigma}_u=0.03772$)	Renewables ($\hat{\sigma}_u=0.08269$)	CGO ($\hat{\sigma}_u=0.03540$)	Renewables ($\hat{\sigma}_u=0.08009$)	Nuclear ($\hat{\sigma}_u=0.04602$)
2016	2.88587	3.04972	1.94055	2.93491	1.10693
2017	2.85009	3.07992	1.92358	2.94783	1.10296
2018	2.81193	3.11599	1.90564	2.96182	1.09818
2019	2.77151	3.15853	1.88673	2.97702	1.09258
2020	2.72884	3.20809	1.86686	2.99360	1.08618

TABLE 3.13: Switzerland. Forecasting accuracy measures for CGON predictions by 2CM and RW.

Measure	2CM (USC with 2 shocks)					RW				
	1-step	2-step	3-step	4-step	5-step	1-step	2-step	3-step	4-step	5-step
RMSE	1.672	1.677	0.999	0.867	1.288	1.894	1.892	1.710	1.612	1.607
MAPE	0.027	0.026	0.020	0.014	0.033	0.031	0.036	0.035	0.036	0.046
sMAPE	0.027	0.026	0.020	0.014	0.033	0.031	0.035	0.034	0.036	0.045
MASE	0.800	0.759	0.580	0.420	0.964	0.910	1.041	1.009	1.050	1.336
UMBRAE	0.952	0.429	0.562	0.302	0.633	1.000	0.727	0.845	0.782	0.904
% Better	43%	83%	60%	75%	67%	0%	67%	60%	50%	67%

TABLE 3.14: Switzerland. Forecasting accuracy measures for CGO and nuclear predictions by 3CM and RW.

Measure	3CM (restricted UCRCO with 3 shocks)					RW				
	1-step	2-step	3-step	4-step	5-step	1-step	2-step	3-step	4-step	5-step
CGO										
RMSE	1.517	1.461	1.409	1.233	1.291	2.005	2.003	1.914	1.797	1.744
MAPE	0.037	0.040	0.043	0.041	0.051	0.045	0.052	0.054	0.055	0.064
sMAPE	0.036	0.039	0.042	0.040	0.050	0.044	0.051	0.053	0.054	0.062
MASE	0.875	0.943	1.012	0.956	1.198	1.075	1.228	1.270	1.303	1.490
UMBRAE	0.913	0.663	0.852	1.387	1.321	1.000	0.859	0.971	1.708	1.332
% Better	57%	83%	60%	50%	67%	0%	50%	60%	25%	67%
Nuclear										
RMSE	1.036	1.038	1.030	1.152	0.885	1.151	1.151	1.130	1.126	1.088
MAPE	0.050	0.062	0.064	0.090	0.074	0.053	0.062	0.067	0.080	0.091
sMAPE	0.048	0.059	0.061	0.086	0.070	0.051	0.059	0.064	0.076	0.085
MASE	1.160	1.440	1.486	2.095	1.672	1.241	1.448	1.556	1.851	2.069
UMBRAE	1.206	1.140	1.180	1.053	0.915	1.000	0.967	1.199	0.825	1.348
% Better	43%	17%	20%	25%	33%	0%	50%	40%	50%	33%

TABLE 3.15: Switzerland. Comparison of forecasting accuracy measures for renewables predictions by 2CM and 3CM.

Measure	2CM					3CM				
	1-step	2-step	3-step	4-step	5-step	1-step	2-step	3-step	4-step	5-step
RMSE	1.604	1.976	2.260	2.763	2.368	1.287	1.653	1.891	2.225	1.959
MAPE	0.059	0.075	0.100	0.149	0.150	0.043	0.064	0.085	0.121	0.124
sMAPE	0.061	0.078	0.106	0.162	0.162	0.044	0.066	0.088	0.129	0.132
MASE	0.831	1.066	1.446	2.213	2.220	0.590	0.905	1.210	1.796	1.836
UMBRAE	2.095	2.042	1.146	1.713	2.044	0.994	1.759	0.779	1.404	1.689
% Better	29%	33%	40%	0%	0%	71%	33%	60%	25%	0%

3.6, and the corresponding band width (see Table 3.12). Compared with the 2CM, the 3CM gives narrower confidence bands of predictions for renewables. This means that the 3CM predictions are more reliable.

Now, we assess the FA of the fitted models. Table 3.13 shows the error measures of 1- to 5-year-ahead forecasts for CGON predictions by the 2CM and RW method applied to the data from Switzerland. It shows that all error measures (RMSE, MAPE, sMAPE,

MASE, UMBRAE and % Better) of 1- to 5-year-ahead forecasts by the 2CM are smaller than those obtained using the RW method – the benchmark. It should be noted that the MASE and UMBRAE measures of the 1- to 5-year-ahead forecasts are less than 1.

In contrast, the error measures of the 1- to 5-year-ahead forecasts for CGO by the 3CM are smaller than those of RW method (see Table 3.14). The corresponding measures (except for 4-year-ahead forecasts and the UMBRAE of 1- and 2-year-ahead forecasts) for nuclear using the 3CM are also smaller than those obtained through the RW method. Furthermore, for CGO, the MASE measures of 1-, 2- and 4-year-ahead forecasts and the UMBRAE measures of 1- to 3-year-ahead forecasts using the 3CM are smaller than 1. Above all, in relation to RW method, the fitted models (2CM and 3CM) provide smaller errors for the test datasets.

As underlined in the previous subsection, we are concerned with any improvement of the 3CM over the 2CM assessed through FA measures. For this, we focus on renewables predictions that are common in both the models. The results show that all the error measures of 1- to 5-year-ahead forecasts for renewables by the 3CM are smaller than those obtained by the 2CM (see Table 3.15). This implies that, compared with the 2CM, the 3CM is more accurate in forecasting the Swiss energy data.

3.3.4 The United Kingdom

The United Kingdom's electricity is generated from several different fuel sources and technologies. Hence, the country has a constant supply, and it is not excessively dependent on a single type of power generation. However, the share of renewables in the UK energy mix is limited. In 1965, the United Kingdom consumed about 197 Mtoe energy from CGON sources and only 1 Mtoe from renewables. Initially, hydroelectricity was the sole renewable energy source. Solar, wind and geothermal and biomass sources were added to the renewable energy mix in 1984, 1989 and 1990, respectively (British Petroleum, 2016). According to Figure 3.7, the consumption of CGON was always exceedingly higher than that of renewables. In fact, for a long time, the United Kingdom extensively used mainly fossil fuels (94% of total energy consumption in 1970), such that it ranked among the world's largest GHG producers. Still, its per capita CO₂ emissions from fuel burning are higher than the European average (7.2 tonnes in 2012, compared to an EU average of 6.9 tonnes; Planete-energies, 2015c). Figure 3.7 also shows that, after 2005, the use of renewables substantially increased against a sharp decline of CGON consumption. Basically, the United Kingdom's economic restructuring is engendering huge energy savings and lower carbon emissions.

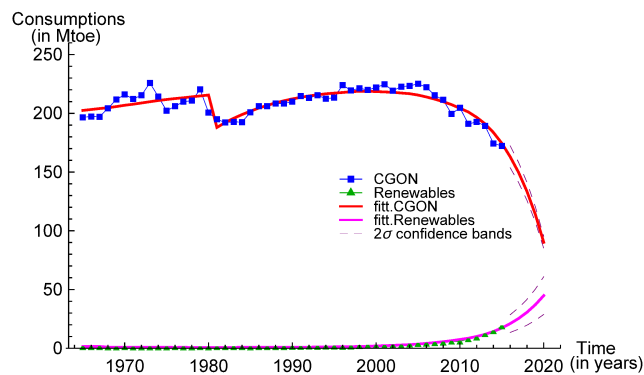


FIGURE 3.7: The United Kingdom, 2CM. Energy consumption (Mtoe) from CGON sources (squares) and renewables (triangles). The solid lines correspond to the UUC fitted model with two shocks (one for each competitor). The broken lines represent 2σ predictions' confidence bands.

TABLE 3.16: The United Kingdom, 2CM. Estimates, standard errors and marginal linearised 95% confidence interval of the UUC model with two shocks (one for each competitor).

Parameter	Estimate	Standard error	95% Confidence interval
m	42007.3	16641.2	{8941.53, 75073.1}
p_1	0.00482	0.00187	{0.00110, 0.00854}
q_1	-0.90160	0.08658	{-1.07363, -0.72957}
δ	0.91531	0.08804	{0.74037, 1.09025}
c_1	-0.15016	0.01492	{-0.17981, -0.12051}
b_1	-0.13940	0.03387	{-0.20669, -0.07211}
a_1	16.0000	0.00031	{15.9994, 16.0006}
p_2	0.00004	0.00006	{-0.00009, 0.00016}
q_2	0.32519	1.36356	{-2.38417, 3.03454}
γ	0.32675	1.36899	{-2.3934, 3.04689}
c_2	-0.37090	1.83206	{-4.01115, 3.26936}
b_2	-0.02740	0.86414	{-1.74443, 1.68962}
a_2	3.58748	0.01862	{3.55048, 3.62448}
R^2	0.99837		

The United Kingdom established the world's first civil nuclear programme by launching a nuclear power station in 1956 (Financial Times, 2013). In Figure 3.8, we see that the consumption of nuclear energy increased almost continuously for the first three decades. Hence, in the late 1990s, nuclear power plants contributed around one-fourth of the total annual electricity generation in the United Kingdom. However, since 1998, the consumption of nuclear energy has been gradually declining, since old plants have been shut down and aging-related problems affect plants' capability. The consumption

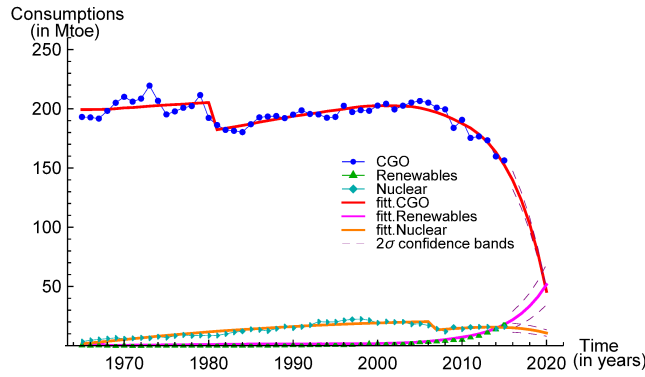


FIGURE 3.8: The United Kingdom, 3CM. Energy consumption (Mtoe) from CGO sources (circles), renewables (triangles) and nuclear (diamonds). The solid lines correspond to the USC fitted model with three shocks (one for each competitor). The broken lines represent 2σ predictions' confidence bands.

of CGO sources slowly declined until 2005, as most of the United Kingdom's electricity is produced by burning fossil fuels. However, it has been sharply declining in recent years.

First, the data from the UK have been partitioned as CGON and renewables and model (A.1), UUC, with two exponential shocks (one for each source) is applied. A notably large value of R^2 (0.99837) proves that the model is well fitted. The shocks are significant, since the F -statistic, comparing the fitted model with the UUC model without shocks, gives an adequately large value ($\hat{F} = 23.05760$).

Subsequently, the data have been partitioned into three sources, as follows: CGO, renewables and nuclear. Since all three sources were launched simultaneously, model (A.6), USC, with three exponential shocks (one for each competitor) is fitted. A notably large value of R^2 (0.99859) proves that the fitting is good. The shocks are significantly incorporated into the model, as the value of the F -test, comparing the fitted model with the USC without shocks, is large ($\hat{F} = 17.40843$). The shocks occurred at time $1965 + \hat{a}_1 \simeq 1981$ for the CGO time series, time $1965 + \hat{a}_2 = 1969$ for renewables and time $1965 + \hat{a}_3 \simeq 2008$ for nuclear energy. All three shocks were estimated to have a negative effect ($\hat{c}_1 = -0.11774$, $\hat{c}_2 = -0.90652$ and $\hat{c}_3 = -0.34769$ respectively) that was absorbed over time (negative \hat{b}_1 , \hat{b}_2 and \hat{b}_3).

The shock for CGO sources may have arisen because the UK economy and energy industries have been affected by the evolution in oil and gas prices; from the 1970s' oil price hikes to the 1986 price collapse and the increased price instability (Institute of Engineering Technology (IET), 2012). The shock for nuclear sources can be explained in that, since 1997, several reactors have been closed; thus, the share of nuclear energy in the UK energy mix has notably declined.

TABLE 3.17: The United Kingdom, 3CM. Estimates, standard errors and marginal linearised 95% confidence interval of the USC model with three shocks (one for each competitor).

Parameter	Estimate	Standard error	95% Confidence interval
m	33247.9	14934.8	{3707.45, 62788.4}
p_1	0.00560	0.00269	{0.00068, 0.01132}
q_1	0.11769	0.08228	{-0.04506, 0.28044}
ε	-0.10694	0.08117	{-0.26749, 0.05360}
η	-1.34682	0.23844	{-1.81844, -0.87519}
c_1	-0.11774	0.01381	{-0.14505, -0.09043}
b_1	-0.04098	0.02386	{-0.08817, 0.00621}
a_1	16.0698	0.00007	{16.0697, 16.0700}
p_2	$4.68 * 10^{-6}$	0.00007	{-0.00013, 0.00014}
q_2	-0.09308	0.08656	{-0.26429, 0.07813}
θ	0.09272	0.09124	{-0.08775, 0.27320}
ξ	1.41632	0.34781	{0.72836, 2.10428}
c_2	-0.90652	0.27968	{-1.45973, -0.35332}
b_2	-0.00446	0.00726	{-0.01882, 0.00991}
a_2	4.00000	0.00113	{3.99777, 4.00223}
p_3	0.00005	0.00005	{-0.00005, 0.00015}
q_3	-0.00984	0.02466	{-0.05862, 0.03894}
c_3	-0.34769	0.12872	{-0.60228, -0.09310}
b_3	-0.07467	0.22585	{-0.52139, 0.37205}
a_3	43.0000	0.00334	{42.9934, 43.0066}
R^2	0.99859		

By substituting the estimated parameter values in model (A.6), the following three equations can be obtained:

$$z_1'(t) \propto 0.00560 + 0.01075 z_1(t)/m - 1.22913 z_2(t)/m + 0.11769 z_3(t)/m$$

$$z_2'(t) \propto 4.68 * 10^{-6} - 0.00036 z_1(t)/m + 1.32324 z_2(t)/m - 0.09308 z_3(t)/m$$

$$z_3'(t) \propto 0.00005 + 0.00438 z_1(t)/m - 0.07934 z_2(t)/m - 0.00984 z_3(t)/m.$$

The innovative component of CGO sources is large ($\hat{p}_1 = 0.00560$) compared with the components of renewables ($\hat{p}_2 = 4.68 * 10^{-6}$) and nuclear sources ($\hat{p}_3 = 0.00005$). Turning to the imitative component, the within-product WOM effect of CGO is positive ($\hat{q}_1 + \hat{\varepsilon} = 0.01075$), and its cross-product WOM effects by renewables and nuclear sources are negative ($\hat{q}_1 + \hat{\eta} = -1.22913$) and positive ($\hat{q}_1 = 0.11769$), respectively. This means that the level of diffusion of CGO is enhanced by its spread and that of nuclear energy,

but it is decreased by renewables' spread. The renewables' within-product effect is positive ($\hat{q}_2 + \hat{\xi} = 1.32324$), and their cross-product effects by both CGO sources ($\hat{q}_2 + \hat{\theta} = -0.00036$) and nuclear ($\hat{q}_2 = -0.09308$) are negative. That is, the diffusion of renewables is enhanced by their spread but discharged by that of the competitors. The nuclear within-product ($\hat{q}_3 = -0.00984$) and cross-product effects by renewables ($\hat{q}_3 - \hat{\eta} - \hat{\xi} = -0.07934$) are negative, while the cross-product effect by CGO sources ($\hat{q}_3 - \hat{\varepsilon} - \hat{\theta} = 0.00438$) is positive. This denotes that the level of diffusion of nuclear energy is reduced by its spread and that of renewables but increased by CGO's spread. CGO and renewables are sustained by further internal consumptions, whereas nuclear energy has no internal support to further sustain it. Renewables and nuclear sources are mutually exclusive to further sustain, as they are quite strong in their positions. That is, the share of nuclear energy in the UK energy mix is substantially large. Conversely, nowadays, the use of renewables is markedly increasing.

The estimated trajectories shown in Figures 3.7 and 3.8 adequately follow the observed path, especially at the last part of each time series. Hence, the predictions from 2016 to 2020 are trustworthy and suggest a rapid increase for the renewables against a steep decline of other energies, especially CGO sources. It should be observed that estimated values in the first part of the renewables series in the 3CM do not satisfactorily follow the observed data. Thus, we excluded the first 12 residuals for renewables obtained with 3CM. To maintain consistency between the 2CM and 3CM confidence bands, all these residuals are also ignored from the 2CM. Due to the lack of fit, we also omitted the first five values of the nuclear series in estimating the scaled residuals' variance. The Kolmogorov–Smirnov test confirmed the normality assumption of scaled residuals. The standard deviations of scaled residuals ($\hat{\sigma}_u$) obtained with the 2CM are 0.02856 and 0.17900 for CGON and renewables, and those from the 3CM are 0.02767,

TABLE 3.18: The United Kingdom. Confidence band width of 2CM and 3CM predictions in 2016–2020.

Year	2CM		3CM		
	CGON ($\hat{\sigma}_u=0.02856$)	Renewables ($\hat{\sigma}_u=0.17900$)	CGO ($\hat{\sigma}_u=0.02767$)	Renewables ($\hat{\sigma}_u=0.16514$)	Nuclear ($\hat{\sigma}_u=0.12663$)
2016	18.61456	15.06058	15.45041	14.46406	7.64444
2017	17.09520	18.16938	13.63603	17.83507	7.34031
2018	15.25245	21.94720	11.38197	22.06343	6.89061
2019	13.01813	26.53902	8.57551	27.37995	6.26170
2020	10.30804	32.12262	5.07208	34.08372	5.40996

0.16514 and 0.12663 for CGO, renewables and nuclear, respectively. Thus, we computed the 2σ confidence bands of predictions, represented by broken lines in Figures 3.7 and 3.8, and the corresponding band width, shown in Table 3.18. Apparently, the 3CM results in a reduction in terms of the confidence band width for only the first two prediction years. However, both $\hat{\sigma}_u$ values and the band width for renewables using the 2CM and 3CM highlight that a slight increase for the next 3 years is due to the rapid growth in the predicted trajectory for the 3CM with respect to a mild growth in the 2CM fitted trajectory. Conversely, the $\hat{\sigma}_u$ has a lower value for the 3CM, showing greater precision.

3.3.5 The United States

According to the Energy Information Administration's statistics, the per capita energy consumptions in the United States have been somewhat consistent since 1970. Between 1980 and 2010, the average energy consumption has been estimated as 334 million British thermal units (BTUs) per person. Geothermal and biomass sources with hydroelectricity have been contributing as renewables since 1965; solar and wind technologies were simultaneously launched in 1983. However, the share of renewables is still less than 10% in the US energy mix. In Figure 3.9, we observe that the consumption of CGON sources described two waves during the study period, but the level of consumption in the former wave is somewhat lower than that of the latter. A rapid decline in 1981–1986 and further in 2008–2009 represents the years of financial crises, when oil consumptions reduced and gas consumptions were stable; the delayed positive trend in these years only is due to shale gas extraction (source-specific data in British Petroleum,

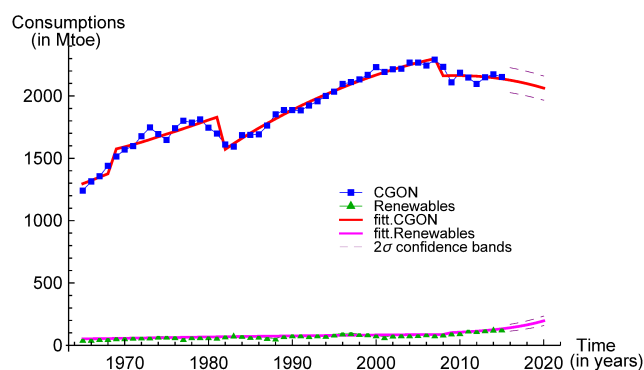


FIGURE 3.9: The United States, 2CM. Energy consumption (Mtoe) from CGON sources (squares) and renewables (triangles). The solid lines correspond to the BSC fitted model with four shocks (three for CGON and one for renewables). The broken lines represent 2σ predictions' confidence bands.

TABLE 3.19: The United States, 2CM. Estimates, standard errors and marginal linearised 95% confidence intervals of the BSC model with four shocks (three for CGON sources and one for renewables).

Parameter	Estimate	Standard error	95% Confidence interval
m	272997.0	70072.4	{133674.0, 412320.0}
p_1	0.00475	0.00119	{0.00238, 0.00712}
q_1	0.02474	0.00485	{0.01510, 0.03438}
c_1	0.12586	0.01993	{0.08623, 0.16549}
b_1	-0.10034	0.07294	{-0.24536, 0.04468}
a_1	4.66597	0.00025	{4.66547, 4.66647}
c_2	-0.16026	0.01567	{-0.19141, -0.12910}
b_2	-0.11071	0.03896	{-0.18817, -0.03324}
a_2	17.7119	0.00028	{17.7114, 17.7125}
c_3	-0.06316	0.01274	{-0.08850, -0.03783}
b_3	0.06260	0.03163	{-0.00028, 0.12548}
a_3	43.4611	0.00005	{43.4610, 43.4612}
p_2	0.00019	0.00006	{0.00008, 0.00030}
q_2	0.00089	0.00028	{0.00032, 0.00145}
c_4	0.14276	0.22252	{-0.29966, 0.58518}
b_4	0.17970	0.25574	{-0.32879, 0.68819}
a_4	44.1508	0.00571	{44.1395, 44.1622}
R^2	0.99899		

2016). The use of renewables was almost constant or trivially increased over the years. In fact, renewables mostly come from hydroelectricity, which produces almost a fixed amount of energy. O'Connor and Cleveland (2014) observed that wind and solar power are expanding rapidly for electricity generation on a large scale.

Nuclear energy was launched in the United States in 1965 (British Petroleum, 2016). According to Nuclear Power in the USA (NPUS; 2018), today, the United States is the world's largest nuclear energy producer, accounting for more than 30% of the global nuclear energy generation. In 2016, the United States' 100 nuclear reactors produced 805 billion kWh, almost 20% of the total energy production. Figure 3.10 shows that nuclear consumption almost continuously increased until 1995 and slightly declined after that year. In fact, by the late 1990s, 28 nuclear reactors permanently closed before their 40-year working licenses expired. Various factors (including cost escalation, slower growth of electricity demand and a changing regulatory environment) played a role in this. CGO consumptions fluctuated widely in the first two decades, and later, they formed a second wave.

TABLE 3.20: The United States, 3CM. Estimates, standard errors and marginal linearised 95% confidence intervals of the BSC model with five shocks (three for CGO sources, one for renewables and one for nuclear).

Parameter	Estimate	Standard error	95% Confidence interval
m	197260.0	8284.92	{180871.0, 213650.0}
p_1	0.00665	0.00026	{0.00614, 0.00717}
q_1	0.02996	0.00149	{0.02702, 0.03291}
c_1	0.15234	0.04350	{0.06629, 0.23838}
b_1	-0.56366	0.23664	{-1.03179, -0.09552}
a_1	7.25068	0.00373	{7.24329, 7.25806}
c_2	-0.18752	0.01181	{-0.21087, -0.16416}
b_2	-0.03990	0.00998	{-0.05965, -0.02015}
a_2	16.3727	0.00009	{16.3725, 16.3729}
c_3	-0.05770	0.01169	{-0.08082, -0.03458}
b_3	-0.08237	0.07509	{-0.23091, 0.06618}
a_3	45.0000	0.00006	{44.9999, 45.0001}
p_2	0.00025	0.00005	{0.00016, 0.00034}
q_2	0.00115	0.00024	{0.00068, 0.00162}
c_4	0.19635	0.21172	{-0.22248, 0.61517}
b_4	0.17497	0.18660	{-0.19416, 0.54411}
a_4	44.3532	0.00727	{44.3388, 44.3675}
p_3	-0.00011	0.00005	{-0.00021, -0.00002}
q_3	0.00433	0.00025	{0.00383, 0.00483}
c_5	-0.03262	0.11891	{-0.26785, 0.20261}
b_5	0.08754	0.51223	{-0.92576, 1.10085}
a_5	42.1567	0.00034	{42.1560, 42.1574}
R^2	0.99889		

For the US energy data separated as CGON sources and renewables, model (A.3), BSC, with four exponential shocks (three for CGON and one for renewables) is fitted. The shocks are significant, as the F -ratio, comparing the fitted model with the BSC without shocks, offers a large value ($\hat{F} = 30.07433$).

When the data have been separated into three sources, namely CGO, renewables and nuclear, we see that all three products are launched simultaneously. Hence, model (A.7), BSC, with five exponential shocks (three for CGO, one for renewables and one for nuclear) is applied. The shocks are significantly incorporated into the model, as the value of the F -test obtained by the fitted model with and without shocks is large ($\hat{F} = 27.57070$). A notably large value of R^2 (0.99889) is a proof of a good-fitting model.

The three shocks arose for CGO sources at times $1965 + \hat{a}_1 \simeq 1972$, $1965 + \hat{a}_2 \simeq 1981$

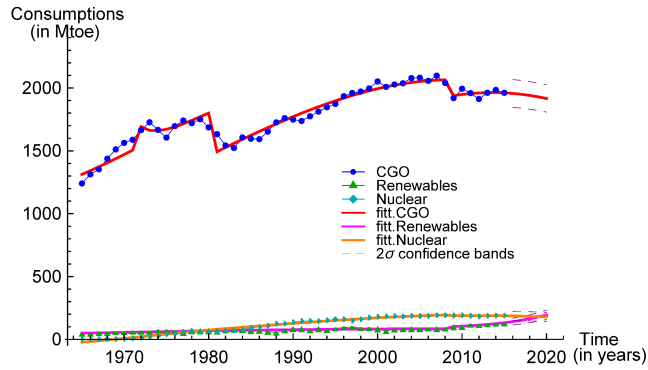


FIGURE 3.10: The United States, 3CM. Energy consumption (Mtoe) from CGO sources (circles), renewables (triangles) and nuclear (diamonds). The solid lines correspond to the BSC fitted model with five shocks (three for CGO, one for renewables and one for nuclear). The broken lines represent 2σ predictions' confidence bands.

and $1965 + \hat{a}_3 \simeq 2010$. The first shock was estimated as positive ($\hat{c}_1 = 0.15234$) and the next two as negative ($\hat{c}_2 = -0.18752$ and $\hat{c}_3 = -0.05770$), but none decayed over time (positive \hat{b}_1 , \hat{b}_2 and \hat{b}_3). The first shock can be explained in that, in the early 1970s, the US oil consumption, in the form of gasoline and other products, was rising while the domestic oil production declined, leading to an increasing dependence on imported oil⁶. The second shock may be due to the 1979 energy crisis – the second of two oil-price hikes in the 1970s – when the United States reduced its fossil fuel consumption. The third shock may be because, recently, the United States has increased the cost of fossil fuels to reduce its widespread consumption, as the use of fossil fuels continues to impose massive environmental costs. A positive shock ($\hat{c}_4 = 0.19641$) arose for renewables at time $1965 + \hat{a}_4 \simeq 2009$, and this has not yet been absorbed in time (positive \hat{b}_4). This may be because, in 2009–2010, the US government approved several incentives (e.g. production tax credit [PTC], energy investment tax credit [ITC] and renewable production incentive [REPI]) to increase renewables' growth and consumption. Conversely, a negative shock ($\hat{c}_5 = -0.03262$) occurred for nuclear at time $1965 + \hat{a}_5 \simeq 2007$. This negative shock is quite unexpected, as nuclear consumption plateaued between 2007 and 2010. This may be the trend of nuclear decline after 2010, since the shock has not faded over time (positive \hat{b}_5).

The innovative coefficient of CGO sources ($\hat{p}_1 = 0.00665$) is much larger than those of the other sources. By substituting the estimated parameter values in the BSC model,

⁶Energy Crisis (1970s). <http://www.history.com/topics/energy-crisis>.

TABLE 3.21: The United States. Confidence band width of 2CM and 3CM predictions in 2016–2020.

Year	2CM		3CM		
	CGON ($\hat{\sigma}_u=0.02350$)	Renewables ($\hat{\sigma}_u=0.09739$)	CGO ($\hat{\sigma}_u=0.02823$)	Renewables ($\hat{\sigma}_u=0.09564$)	Nuclear ($\hat{\sigma}_u=0.09934$)
2016	199.89091	55.01620	220.94707	54.06655	74.20643
2017	198.68395	59.06870	220.17926	58.01955	73.62590
2018	197.28804	63.89289	219.16304	62.68527	72.91027
2019	195.69755	69.64031	217.90067	68.18687	72.05794
2020	193.90967	76.49056	216.39779	74.66669	71.06575

we obtain the following three equations:

$$z'_1(t) \propto 0.00665 + 0.02996 z(t)/m$$

$$z'_2(t) \propto 0.00025 + 0.00115 z(t)/m$$

$$z'_3(t) \propto -0.00011 + 0.00433 z(t)/m.$$

All three products exploit the WOM effect of the whole category. Although nuclear experiences a negative innovative effect, the imitative component (WOM effect) of each product is positive. However, the spread of CGO sources diffusion is extremely fast ($\hat{q}_1 = 0.02996$), and those of the other sources are also considerable ($\hat{q}_2 = 0.00115$ for renewables and $\hat{q}_3 = 0.00433$ for nuclear).

In Figures 3.9 and 3.10, we see that the fitted lines by the 2CM and 3CM satisfactorily follow the observed path. The predictions suggest a gradual increase for the renewables and a small decline of the other energies in 2016–2020. It should be observed that the fitted values in the first part of the nuclear series are somewhat more scattered from the observed data. Thus, we omitted the first nine residuals of nuclear energy in computing the scaled residuals' variance. The standard deviations of the scaled residuals ($\hat{\sigma}_u$) using the 2CM are 0.02350 for CGON and 0.09739 for renewables. Those obtained from the 3CM are 0.02823 for CGO, 0.09564 for renewables and 0.09934 for nuclear sources. The Kolmogorov–Smirnov test confirmed that the scaled residuals follow a Gaussian distribution. Accordingly, we computed the 2σ confidence bands for predictions, represented by broken lines in Figures 3.9 and 3.10, and the corresponding band width (see Table 3.21). The confidence bands of renewables predictions through the 3CM is narrower than those obtained with the 2CM. That is, the 3CM is more appropriate for reliably producing forecasts on the US energy market.

3.4 Remarks

In this chapter, we have analysed energy consumption data through diffusion models in a competitive environment. First, the existing diffusion models were applied to two-competitor data, namely those of depleting energies (CGON) and renewables. The form of the model is quite straightforward, as both the competitors generated consumptions from the beginning of the observed period. The models were then extended to three competitors (CGO, renewable and nuclear). To incorporate possible regime changes in the diffusion framework, the extended model demands a relatively complex mathematical form. Both models were fitted to the total annual energy consumption data from 10 developed and 2 developing countries. The countries were selected based on the availability of data for the period from 1965 to 2015.

The competitors considered in the models were at different stages of their lifecycle and the competition dynamics were different among the competitors. Hence, instead of confining ourselves to a specific model, we initially considered a set of diffusion models for competition. Then, based on the model fitting performance, we chose the model with the best fit for the data from each of the studied countries. To minimise the errors globally and locally, one or more shocks were incorporated into the models. The overall fit of the models was satisfactory for most cases.

According to the observed data, the financial crisis in 2008–2009 had an inverse effect on the energy sectors of Europe, Japan and the United States. This resulted in the reduction of total energy consumptions (especially CGON sources) in these countries in recent years, although the US consumptions are relatively stable now. In the interim, all these countries approved incentives to promote green energies, which were deemed a partial substitution for the reduction of CGON consumption. Conversely, during the financial crisis, the energy consumptions of China and India, especially those depending on CGON sources, showed an increasing trend. This may be due to the developing stage of the energy sector. In all the selected countries, the 2016–2020 predictions for the consumption of CGON sources demonstrate a declining trend, whereas a moderate increasing trend is observed in the predicted renewables consumption.

In the case of three competitors, the consumption of CGO sources has undergone a trend similar to the trend of CGON consumption. Nuclear energy has already reached the top of its growth. After the Fukushima accident in 2011, nuclear consumptions have been declining around the globe. Japan is the frontrunner in this declining track, followed by Europe and the United States. The rising trend in nuclear energy consumption is still observed in China and India. The 2016–2020 predictions for nuclear consumption

suggest a declining trend for all the other studied countries.

We now focus on the estimated parameters obtained from 3CM models. The findings from the fitted 3CM models are more specific and informative than those relating to the 2CM. Eight of 12 countries were analysed with an unbalanced model that can split the WOM coefficients into within-product and cross-product effects. The within-product effects of all three sources (CGO, renewables and nuclear) for China and Germany are positive, and for Finland, Sweden and Switzerland, they are negative. The corresponding effects for France, Japan and the United Kingdom are positive (or negative) for one or two sources. The cross-product effects of each source by its competitors are positive for Finland, Sweden and Switzerland, and in all the cases, CGO strongly supports spreading its competitors' diffusion. An opposite situation is observed for China, that is, all the cross-product effects (excluding the effect of nuclear energy by CGO) are negative. Although each source is acting as a competitor to energy sources in China, nuclear strongly opposes spreading its competitors' diffusion. Not all the cross-product effects are positive (or negative) for France, Germany, Japan, and the United Kingdom, where nuclear energy has a larger support to sustain its competitors, followed by CGO and renewables. In contrast, a balanced model is suitably fitted to the data from Belgium, India, Spain and the United States. The WOM effect of each source for all four countries is found to be positive. However, the effect is extremely strong for CGO, followed by nuclear (except for India) and renewables. Apparently, the different countries gave different results about the sign and the magnitude of WOM coefficients, thereby describing different competition/substitution patterns. Our results show some similarities to the findings reported by Csereklyei *et al.* (2017). These authors performed cluster analyses with energy data from the 28 member states of the European Union for the period 1971–2010 and found several distinct energy paths and profiles. The energy profiles were ranked from the highest to lowest combined fossil fuel share. The researchers noticed that it takes a long time to make relevant changes in the energy paths. Usually, countries stay in a specific cluster for decades before moving to other clusters. This may be due to the consequence of energy policies, financial development or the availability of a new dominant energy form.

Notable variations in the 2σ confidence bands of the predictions are observed in the 2CM and 3CM. The renewables data are the same in both models, but the two models produced different confidence bands for the predictions. For 10 of the 12 studied countries, narrower confidence bands are observed for 3CM than those obtained with 2CM. Since narrower confidence bands correspond to a reduced forecasting uncertainty, we can say that our extended 3CM allows more precise forecasting.

For two countries, the performance of the two models (2CM and 3CM) is also compared using FA measures. The FA measures for Sweden and Switzerland give results in the same direction as those pertaining to the confidence band width. That is, like the confidence band width, the FA measures corresponding to renewables by 3CM are found to be almost uniformly smaller than those in the 2CM. Hence, we can say that the proposed 3CM produces a concrete advantage in forecasting the energy dynamics.

Chapter 4

The three-competitor diffusion model with dynamic market potential

4.1 Introduction

In Chapter 2, we proposed a diffusion model for three competing products with the assumption that the market potential is fixed (constant) throughout the diffusion process. In the application of that model (Chapter 3), we observed that, capturing the wide variety of shapes of diffusion requires incorporating intervention functions (i.e. external shocks) in the model. For some datasets, the required number of shocks proved to be relevant. However, this approach may not be the proper way to follow the lifecycle of products, and it generates a load of extra parameters. Such models cannot describe communication networks that spread knowledge and generate awareness of products in a marketplace. Knowledge and awareness of products are not instantly dispersed to all the eligible adopters upon the entrance of new products into the market. In addition, the entrance of new products in the same category may increase awareness of the previously existing products. In fact, awareness is a latent adoption criterion, and the amount of incursion of a product into the market is controlled by the amount of diffusion of knowledge concerning its survival and characteristics (Guseo and Mortarino, 2015). Such a behaviour may concern almost all types of goods or services in a social system.

Energy may be considered as a good until its production stage (produced by the electric utility company), or it may be a service when it is distributed (as electricity) to consumers. Energy sources have been measured with coherent data for decades, and long

time series of consumptions are available. In all 12 countries analysed here, we see that renewable and nonrenewable energy sources have been available since 1965. Moreover, there is a competition among energy sources (discussed in detail in the Introduction). Consequently, the lifecycle of one source may be affected by its competitors. These interactions among energy sources may differ from country to country, depending on country-specific characteristics, such as the market structure, political tendency and people's openness to technological change and substitution.

A relevant point is that the size of the energy market has been increasing over time. For instance, a rising trend in overall energy consumption was observed in all 12 countries in the period of 1965–2015. According to World Bank Development Indicators, the use of energy is strongly related to almost every possible aspect of development (Lloyd, 2017). Hence, energy demands are increasing day by day, and the demand for consumption of energy is not fixed; instead, it rises with time. This feature is comparable to the evolution of a product, as the number of adopters grows over time. For this reason, an interesting question is investigating whether the description of this increasing market could benefit from the use of a diffusion model with a dynamic market potential (DMP).

Although diffusion of innovations has a long practice in model building and corresponding applications, the contributions of such models relaxing the fixed m assumption are limited in the literature. As mentioned in Chapter 1, only in recent years Guseo and Guidolin (2009) did propose a univariate diffusion model, and even more recently, Guseo and Mortarino (2015) proposed a bivariate model that describes diffusion in a competitive environment (for details, see Subsections 1.2.3 and 1.3.2).

In this chapter, we contribute to the diffusion of innovations literature by proposing a model for three products competing for the same customers in a marketplace, assuming a DMP. For models with a large number of competitors, which entail extra parameters, the inference with an actual diagnosis of feasibility may be more complicated. Thus, the relevant point is the study of the feasibility of such a model and the assessment of the gain in terms of fitting performance and forecasting reduability. Specifically, a key question is whether the increase in flexibility due to the DMP (and proven for a single product or two competitors) could reduce the need for introducing many shocks.

4.2 The Model

In building the model, we follow the model structure and corresponding assumptions proposed by Guseo and Mortarino (2015). The diffusion of innovations modelling for three competing products with the assumption of DMP requires a large number

of parameters. The model may not have any closed-form solution. Thus, it is necessary to represent the model through differential equations that can suitably be used to instantaneous data.

As we are building a diffusion model extended for three competitors, the repetition of notations (discussed in Chapter 2) is avoided. We assume that the competition is performed in two phases: two products partake in the first phase and a third enters in the second phase. Therefore, the model can be expressed with the following system of differential equations:

$$\begin{aligned}
z_1'(t) &= m(t) \left\{ \left[p_{1\alpha} + (q_{1\alpha} + \delta_\alpha) \frac{z_1(t)}{m(t)} + q_{1\alpha} \frac{z_2(t)}{m(t)} \right] (1 - I_{t > c_2}) + \right. \\
&\quad \left. + \left[p_{1\beta} + (q_{1\beta} + \varepsilon_\beta) \frac{z_1(t)}{m(t)} + (q_{1\beta} - \eta_\beta) \frac{z_2(t)}{m(t)} + q_{1\beta} \frac{z_3(t)}{m(t)} \right] I_{t > c_2} \right\} \left[1 - \frac{z(t)}{m(t)} \right] + \\
&\quad + z_1(t) \frac{m'(t)}{m(t)}, \\
z_2'(t) &= m(t) \left\{ \left[p_{2\alpha} + (q_{2\alpha} - \gamma_\alpha) \frac{z_1(t)}{m(t)} + q_{2\alpha} \frac{z_2(t)}{m(t)} \right] (1 - I_{t > c_2}) + \right. \\
&\quad \left. + \left[p_{2\beta} + q_{2\beta} \frac{z_1(t)}{m(t)} + (q_{2\beta} + \theta_\beta) \frac{z_2(t)}{m(t)} + (q_{2\beta} - \xi_\beta) \frac{z_3(t)}{m(t)} \right] I_{t > c_2} \right\} \left[1 - \frac{z(t)}{m(t)} \right] + \\
&\quad + z_2(t) \frac{m'(t)}{m(t)}, \\
z_3'(t) &= m(t) \left\{ \left[p_3 + (q_3 - \mu) \frac{z_1(t)}{m(t)} + q_3 \frac{z_2(t)}{m(t)} + (q_3 + \lambda) \frac{z_3(t)}{m(t)} \right] I_{t > c_2} \right\} \left[1 - \frac{z(t)}{m(t)} \right] + \\
&\quad + z_3(t) \frac{m'(t)}{m(t)}, \\
m(t) &= m_\alpha(t)(1 - I_{t > c_2}) + m_\beta(t)I_{t > c_2}, \\
z(t) &= z_1(t) + z_2(t) + z_3(t)I_{t > c_2},
\end{aligned} \tag{4.1}$$

where $z(t) \leq m(t)$, for all t . System (4.1) is a general structure for a diffusion model, describing a competition among three products in two phases. Observe that system (2.1), in Chapter 2, is a restricted version of (4.1), while both are unbalanced models, letting the within-product WOM be different from the cross-product WOM in phase α . That is, the number of discrimination parameters of this model is larger than model (2.1), since this model also assumes $\delta_\alpha = \gamma_\alpha$ (besides $m = m(t) \forall t$). Thus, model (4.1) may be more flexible to express the within-product and the cross-product WOM effects.

In model (4.1), $m(t)$ is the common market potential, which is defined by the structure (1.11), proposed by Guseo and Guidolin (2009; for details, see Subsection 1.2.3). Guseo and Mortarino (2015) have also proposed two alternative structures of $m(t)$ that are defined by Equations (1.15) and (1.16), respectively (see Subsection 1.3.2). In this

study, we will consider all three structures of $m(t)$. That is, all three structures are used for model fitting. Finally, we choose the one that performs better than the two alternative structures. Since (4.1) is a two-phase model, $m(t)$ equals $m_\alpha(t)$ in the first phase and is allowed to change to $m_\beta(t)$ in the second phase. The last additive terms in the first three equations of (4.1) represent the self-reinforcing component, which would obviously vanish for a constant $m(t)$, that is, when $m(t) = m$. The mean sales of all three products are increased when $m(t)$ increases faster, that is, when awareness of the product category spreads rapidly. Since $m(t)$ could be also a nonmonotonic function (for structures different from (1.11), (1.15) and (1.16)), the self-reinforcing term could be negative when the market potential reduces, and the mean sales would suffer a further reduction.

It should be noted that, for the first phase, the sum of the first two equations of model (4.1) with consideration of their last terms is equal to a GGM (see model (1.12)). This is also the case for the second phase. For convenience, system (4.1) is called the competition dynamic market potential (CDMP) model for three competitors. A similar version of model (4.1) has been proposed and applied in Furlan *et al.* (2018c).

Chapter 5

Applications of the three-competitor diffusion model with dynamic market potential

5.1 Introduction

Guseo and Mortarino (2015) proved that the CDMP model designed for two products performed better than fixed market potential (FMP) in the pharmaceutical market, and they opined that the model may play a valuable role in the diffusion of innovations literature. However, the application of CDMP models is still lacking for energy markets. In this chapter, we apply CDMP models of two competitors to energy data, with potential extension to three competitors.

All available energy sources and how they are partitioned have been discussed in Chapter 3. Here, we consider all those energy sources with the same partitioning to keep uniformity throughout the study. However, we apply the two- and three-competitor CDMP models and other similar models with FMP to the energy data from four countries (Belgium, Finland, France and Germany) instead of to the data from all 12 countries studied in Chapter 3. Indeed, we conduct a comparative study of CDMP models and the models with FMP. In addition, we compare CDMP models with two and three competitors.

5.2 Analysis

In Chapter 4, we discussed the observed behaviour of energy sources partitioned into two competitors, coal, gas, oil and nuclear (CGON) and renewables (hydro, solar, wind,

geothermal and biomass), and three competitors, where CGO and nuclear are analysed separately and contrasted to renewables. Here, we skip those discussions and focus only on the model-fitting performance and flexibility of the CDMP models over the models with FMP. For assessing the real performance of the CDMP models, we avoid incorporating control functions (i.e. external shocks) into the models. Indeed, models with a dynamic market potential (DMP) may be able to capture the wide variety of structures of diffusion (see Guseo and Guidolin, 2009; Guseo and Mortarino, 2015). Here, we conjecture that increased flexibility of DMP could make the improvement due to shocks' inclusion less useful than we observed for fixed m . (This topic is discussed further below).

5.2.1 Belgium

5.2.1.1 2CM and 3CM DMP

To describe the diffusion of energy consumptions in Belgium as two competing products, model (1.14), UUC with DMP, is applied to the data partitioned as CGON and renewables. The model gives a large value of R^2 (0.99526); hence we can assert that the fitting is good. The estimation results are shown in Table 5.1. For this case, structure (1.11) for the DMP performs better than the other two structures do. (In this case, the R^2 values obtained with structures (1.15) and (1.16) are 0.99364 and 0.99396, respectively).

For three-way comparison, the data are split into three sources (CGO, renewables and nuclear). Since all three products simultaneously entered the market, model (C.2), UUC with DMP (see Appendix C), is suitably fitted to the data. For this, structure (1.11) is found again to perform better ($R^2 = 0.99254$) than the alternative structures (1.15) and (1.16) of DMP do, giving R^2 values 0.99155 and 0.98944, respectively. The parameter estimates are shown in Table 5.2.

For this model, \hat{K} (5406.12 Mtoe) represents an estimate of the aggregate size of the energy market, which is about one-third of the estimate obtained with the 2CM-DMP (16722.3 Mtoe). Figures 5.1(a) and 5.1(b) depict the estimated evolution of the common DMP, $m(t)$, of the 2CM and 3CM, respectively. A linear increase in the market potential is observed in the 2CM. Both lines are exceedingly far from the fixed m pattern. That is, the demand for energy consumption seems to have grown in a regular way in Belgium.

If we focus on the innovation parameters in the 3CM, it is apparent that this component does not play a significant role for nuclear and renewables, and this may explain their slow start. The innovation effect of both nuclear and renewables could not compete

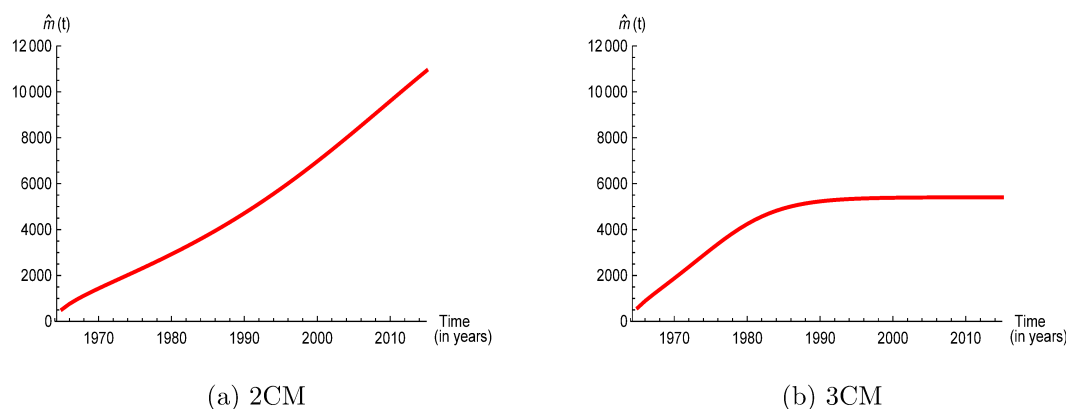


FIGURE 5.1: Belgium. Plot of estimated market potential function, $\hat{m}(t)$, for two and three competitors.

with the corresponding term for CGO sources. For interpreting imitative parameters, we substitute estimates in model (C.2) and obtain the following three equations:

$$\begin{aligned} z_1'(t) - z_1(t) \frac{m'(t)}{m(t)} &\propto 0.03527 - 0.22750 \frac{z_1(t)}{m(t)} + 3.30950 \frac{z_2(t)}{m(t)} + 1.29702 \frac{z_3(t)}{m(t)}, \\ z_2'(t) - z_2(t) \frac{m'(t)}{m(t)} &\propto -0.00002 - 0.00047 \frac{z_1(t)}{m(t)} + 0.43831 \frac{z_2(t)}{m(t)} - 0.00169 \frac{z_3(t)}{m(t)}, \\ z_3'(t) - z_3(t) \frac{m'(t)}{m(t)} &\propto -0.00090 + 0.01484 \frac{z_1(t)}{m(t)} - 0.99334 \frac{z_2(t)}{m(t)} + 0.00839 \frac{z_3(t)}{m(t)}. \end{aligned}$$

CGO is sustained by a strong innovative effect, and its cycle initiates with a relatively higher pace than the competitors' cycle does. However, CGO experiences a negative within-product WOM effect (-0.22750), in contrast with the positive effects

TABLE 5.1: Belgium, 2CM-DMP. Estimates, standard errors and marginal linearised 95% confidence intervals of the UUC model with DMP for two competitors.

Parameter	Estimate	Standard error	95% Confidence interval
K	16722.3	8151.83	{534.333, 32910.2}
p_c	0.00096	0.00006	{0.00085, 0.00107}
q_c	0.08075	0.00314	{0.07452, 0.08698}
p_1	0.04571	0.02445	{-0.00285, 0.09427}
δ	1.46873	0.58421	{0.30860, 2.62885}
q_1	-1.65262	0.58218	{-2.80872, -0.49653}
p_2	0.00007	0.00105	{-0.00202, 0.00215}
q_2	0.26049	0.14459	{-0.02663, 0.54762}
γ	0.26117	0.14558	{-0.02792, 0.55026}
R^2	0.99526		

TABLE 5.2: Belgium, 3CM-DMP. Estimates, standard errors and marginal linearised 95% confidence intervals of the UUC model with DMP for three competitors.

Parameter	Estimate	Standard error	95% Confidence interval
K	5406.12	1426.55	{2585.39, 8226.84}
p_c	0.01105	0.00166	{0.00778, 0.01433}
q_c	0.20628	0.01400	{0.17859, 0.23397}
p_1	0.03527	0.00881	{0.01785, 0.05269}
ε	-1.52452	0.15280	{-1.82665, -1.22240}
η	2.01248	0.36996	{1.28097, 2.74400}
q_1	1.29702	0.12718	{1.04555, 1.54849}
p_2	-0.00002	0.00117	{-0.00233, 0.00228}
θ	0.43878	0.25524	{-0.06591, 0.94346}
ξ	0.00122	0.04823	{-0.09416, 0.09659}
q_2	-0.00047	0.00877	{-0.01781, 0.01686}
p_3	-0.00090	0.00123	{-0.00333, 0.00152}
μ	-1.00818	0.22866	{-1.46031, -0.55604}
λ	1.00173	0.22785	{0.55121, 1.45225}
q_3	-0.99334	0.22633	{-1.44086, -0.54582}
R^2	0.99254		

of renewables (0.43831) and nuclear (0.00839) sources. Substantial variations in the cross-product WOM effect of a product by its competitors have been observed for the energy sources. For instance, CGO's cross-product effects from its competitors are strongly positive (3.3095 from renewables and 1.29702 from nuclear). Conversely, the cross-product effects of renewables from the competitors are weakly negative (-0.00047 from CGO and -0.00169 from nuclear). Nuclear sources receive a positive cross-product effect from CGO (0.01484) and a negative one from renewables (-0.99334).

5.2.1.2 Comparison between models with two and three competitors

Now, we want to prove the efficacy of the extension from two to three competitors in the CDMP models. In other words, as we showed that 3CM models were generally more performant than their corresponding 2CM versions in Chapter 3, here, we want to make a similar comparison for DMP models. Moreover, while the observed flexibility stands in favour of models with DMP, $m(t)$, it should be tested whether fitted, such a model really improves the fitting. For these purposes, the model proposed by Guseo and Mortarino (2014) is fitted, as it can be obtained from the model (1.14) with the restriction $m(t) = m$. Since model (1.14) for two competitors and (C.2) for three competitors are fitted to the data from Belgium, we fitted similar models with fixed m . It should be noted that, excluding the restriction $m(t) = m$, all the features related to

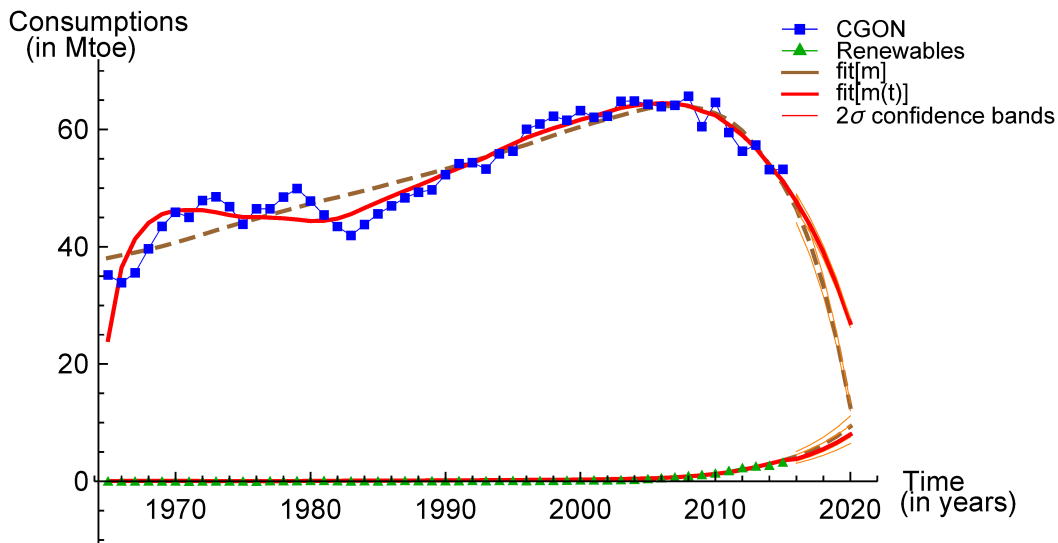
TABLE 5.3: Belgium. Values of R^2 of the 2CM and 3CM with FMP and DMP. The F -ratio values to compare DMP models with the corresponding FMP version are also shown.

	FMP	DMP
2CM	$R^2 = 0.99365$	$R^2 = 0.99526$ ($\hat{F} = 15.72549$)
3CM	$R^2 = 0.98876$	$R^2 = 0.99254$ ($\hat{F} = 34.93917$)

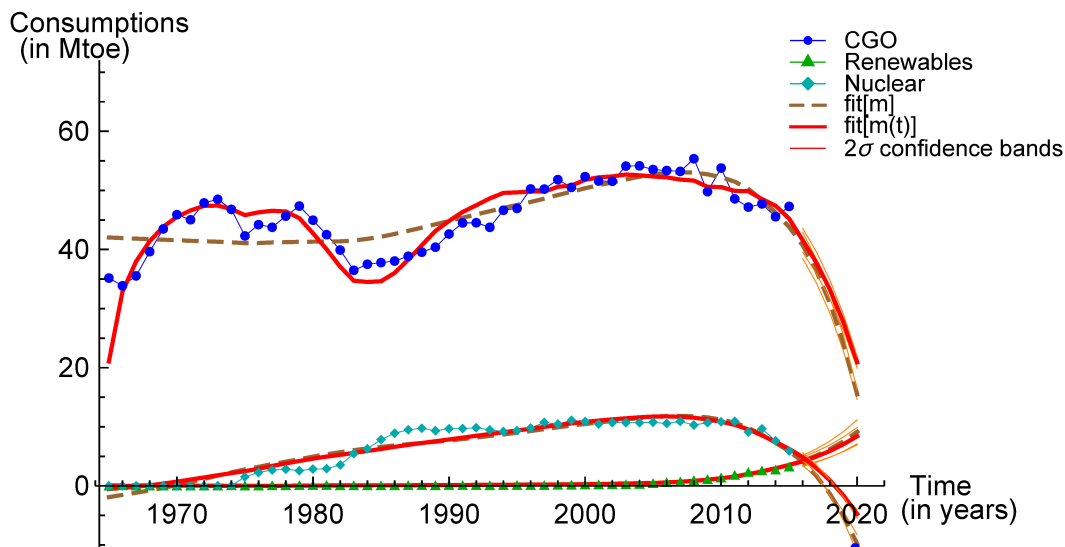
the evolution of the process are the same for both CDMP models and the models with FMP. Thus, we can assert that, if a CDMP model performs significantly better than the model with fixed m , this proves that the market potential for this category formed in a way that differs significantly from the constant path. Observe that the 2CM and 3CM with FMP compared here are not the ones discussed in Chapter 3, because here, we did not incorporate external shocks (to avoid introducing a further confounding element).

The R^2 values of models (1.14) and (C.2) with fixed m are 0.99365 and 0.98876, respectively (see Table 5.3). Since the models with fixed m are nested in the similar models with DMP, an F test (for details, see Subsection 1.4.4) can be used to detect whether the gain of the complex model (say, M_1) from the relatively simple model (say, M_2) is significant. The test comparing model (1.14) and model (C.2) with their respective fixed m pattern models assign large values of \hat{F} , which are 15.72549 and 34.93917, respectively, demonstrating the relevance of CDMP models presented by (1.14) for two competitors and (C.2) for three competitors. Both the results of the F test and the graphical comparisons for both two and three competitors demonstrate that a DMP is more suitable for describing the Belgium energy consumption data than the corresponding FMP version is.

Now, as anticipated, to assess whether 3CM really performs better than 2CM from a forecasting point of view in the context of the CDMP models, we proceed as we did in Chapter 3. We make a short-term prediction (for the 5 years from 2016 to 2020) for each time series using the CDMP models (and the models with fixed m). To obtain the predictions and corresponding confidence bands, we follow the procedure mentioned in Subsection 1.4.2. Figure 5.2(a) represents the predictions using 2CM with DMP and fixed m , and Figure 5.2(b) represents those obtained by 3CM with DMP and fixed m . We observe worse fit in the first part of each series, especially for models with fixed m . Since the purpose is to build plausible confidence bands for the future assessment of each series, we excluded the first 17 residuals from each time series of all 2CM and 3CM in computing the scaled residuals' variance. The Kolmogorov–Smirnov test for goodness



(a) 2CM



(b) 3CM

FIGURE 5.2: Belgium. Observed data and fitted trajectories with predictions' 2σ confidence bands (thin lines): (a) 2CM, (b) 3CM.

of fit confirmed the assumption that scaled residuals follow a Gaussian distribution. The estimated standard deviation of the scaled residuals ($\hat{\sigma}_u$) and p -value for each series using all the fitted models are shown in Table 5.4. Hence, using the properties of normal distributions, we computed the 2σ confidence bands for predictions of each source (competitor), represented by thin (orange) lines in Figure 5.2, and the corresponding band width, shown in Table 5.4.

TABLE 5.4: Belgium. Comparison among all 2CM and 3CM models: predictions' confidence band width.

		2CM-FMP			2CM-DMP		
		CGON	Renewables		CGON	Renewables	
	$\hat{\sigma}_u$	0.05163	0.19237		0.02908	0.19339	
	p -value	0.48942	0.46047		0.97551	0.63522	
Confidence band width	2016	4.67631	1.64194		2.73143	1.47439	
	2017	4.09088	1.99584		2.50663	1.76943	
	2018	3.35310	2.42784		2.23933	2.12696	
	2019	2.42896	2.95522		1.92264	2.56099	
	2020	1.27693	3.59904		1.54796	3.08899	
		3CM-FMP			3CM-DMP		
		CGO	Renewables	Nuclear	CGO	Renewables	Nuclear
	$\hat{\sigma}_u$	0.05517	0.22090	0.15362	0.04870	0.17495	0.14963
	p -value	0.87889	0.67030	0.67123	0.99016	0.55906	0.51164
Confidence band width	2016	4.48915	1.87098	1.26488	4.04761	1.45356	1.46009
	2017	4.01374	2.26635	0.51796	3.67898	1.73535	0.92130
	2018	3.41164	2.74690	–	3.23102	2.06967	0.27657
	2019	2.65491	3.33098	–	2.69007	2.46742	–
	2020	1.70957	4.04093	–	2.03793	2.94286	–

Confidence band width is not shown when the fitted trajectory is negative.

In Table 5.4, we see that the confidence band width for predictions of CGON using 2CM-DMP is smaller than that obtained with 2CM-FMP for 4 out of 5 years (the rapid reduction in the fit of the 2CM-FMP reduces the final width). Conversely, the 2CM-DMP gives a slightly larger residuals' variance for renewables, but the corresponding band width is smaller due to a milder increase in the fitted trajectory.

We now compare 3CM-FMP with 3CM-DMP. Since $\hat{\sigma}_u$ values for all sources through 3CM-DMP models are smaller than the 3CM-FMP, we conclude that CDMP models are more suitable for evaluating forecasts about Belgium's energy market.

Finally, we compared the predictive performance between 2CM-DMP and 3CM-DMP models. The focus of the comparison was renewables, as these elements are common in both models. Narrower confidence band width for predictions was obtained for 3CM-DMP. The reduced forecasting uncertainty (narrower confidence band width) indicates more reliable predictions for the 3CM-DMP model.

5.2.1.3 Comparison among the alternative 3CM models

In Chapter 3, the 3CM model with an FMP and shocks was fitted to Belgium's energy data. A comparison of the different fitted models with three competitors evaluated in this study may be of interest. In Table 5.5, we see that, among the models, the 3CM-FMP with shocks (results described in Subsection 3.3.1) has the highest R^2 value (0.99514). However, it entails a large number of parameters (22) compared with the parameters of the other two models (15 of 3CM-DMP and 13 of 3CM-FMP). According to the diffusion parameters, only the innovative components are common in 3CM-DMP and 3CM-FMP with shocks. While we observe some similarities between the findings, the innovative effect for renewables using 3CM-DMP (-0.00002) is opposite to that obtained with 3CM-FMP (0.00001). In addition, the innovative effect for CGO with 3CM-DMP is extremely large (0.03527) compared with 3CM-FMP (0.00600). This may be due to the fact that models with DMP are more proficient in describing the products under competition, considering their weight.

The agreement between the observed and fitted values for three competitors can be assessed by observing Figure 5.3. The continuous (red) line represents fitted values obtained by a DMP model, the dashed (brown) line shows the model with fixed m and the dotted (orange) line describes the model with fixed m incorporating shocks. In Figure 5.3, the estimated profiles of CGO and renewables through 3CM-DMP are found to be more flexible to account for the observed data, but the profile of nuclear sources deviates from the observations for the period 1965–1990. The estimated profiles using 3CM-FMP with shocks are also flexible to follow the observed path. However, even with shocks, the 3CM-FMP is unable to minimise the deviation between the observed and estimated values for the period 1965–1990. Moreover, the model (3CM-FMP with shocks) is quite rigid for the last few points of nuclear energy. Although the estimated profiles of renewables and nuclear through 3CM-DMP and 3CM-FMP are almost overlapping, the profile of CGO using 3CM-FMP is extremely stiff and unable to follow the observed path.

TABLE 5.5: Belgium, 3CM. Comparison among models with DMP, fixed m and fixed m with shocks.

Name of model	No. of parameters	R^2 value
3CM-DMP	15	0.99254
3CM-FMP	13	0.98876
3CM-FMP with shocks	22	0.99514

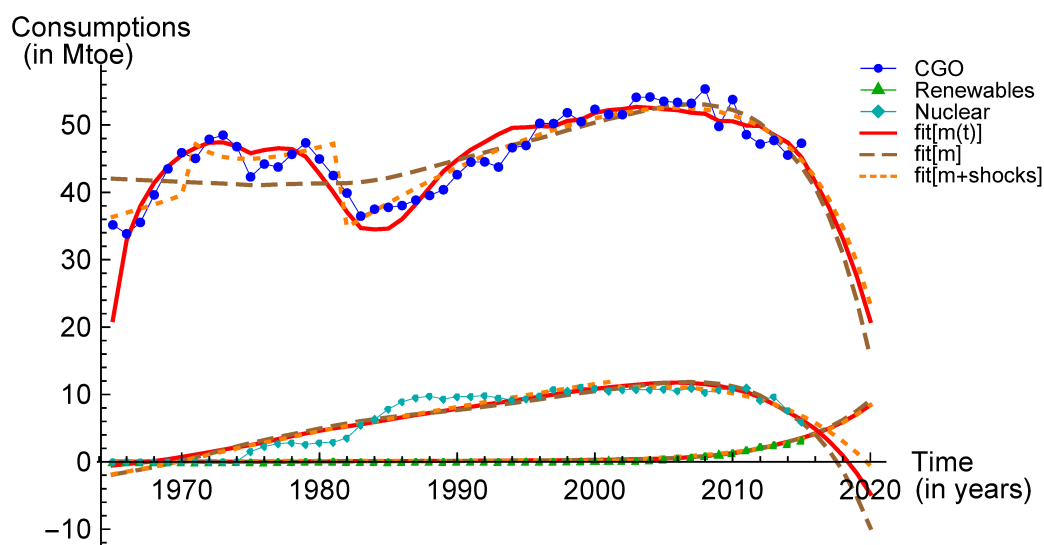


FIGURE 5.3: Belgium, 3CM. Energy consumption (in Mtoe) from CGO sources (circles), renewables (triangles) and nuclear (diamonds). Solid (red) lines for the model with DMP, dashed (brown) lines for the model with fixed m and dotted (orange) lines for the model with fixed m and shocks.

5.2.2 Finland

5.2.2.1 2CM and 3CM DMP

For modelling purposes, first, we partitioned the total energy consumptions in Finland into CGON and renewable sources. The diffusion of these two competing products is described by model (C.1) (see Appendix C), USC with DMP. Estimated values of the fitted parameters, their standard errors and 95% confidence intervals are presented in Table 5.6. With the model (C.1), the structure (1.16) for DMP, which is proportional to the cumulative distribution function of a Gamma random variable, is found to be a better performer ($R^2 = 0.98919$) than the alternative structures (1.11) ($R^2 = 0.98897$) and (1.15) are ($R^2 = 0.98863$). However, we notice small differences among these values.

When the data are partitioned into three sources (CGO, renewables and nuclear), a diachronic competition is observed. In the competition, the CGO and renewables compete from the beginning, and nuclear enters the market at a later stage. In such a situation, model (4.1), the unrestricted UCRCF with DMP, is suitably fitted. A larger value of R^2 (0.99441) also confirms that the model fits well to the energy data in Finland. In model (4.1), the structure (1.11) for DMP performs relatively better than the alternative structures (1.15) and (1.16), giving R^2 values 0.98955 and 0.98848, respectively. The outputs of the model are presented in Table 5.7.

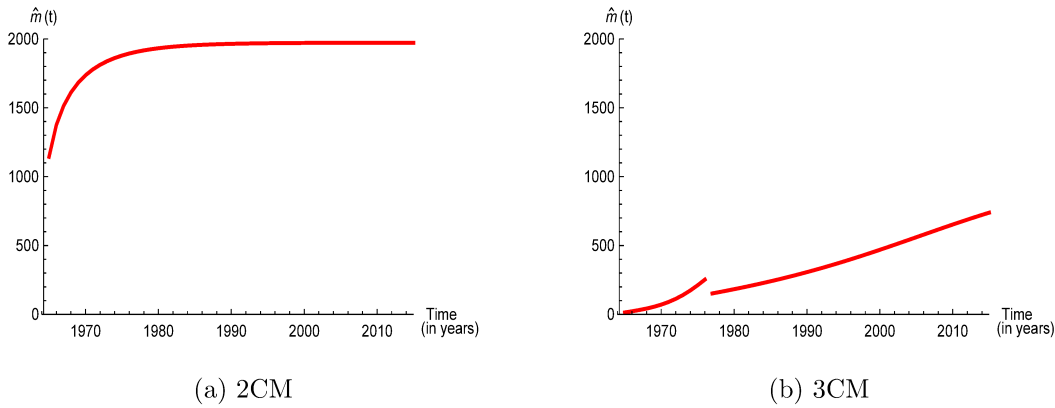


FIGURE 5.4: Finland. Plot of estimated market potential function, $\hat{m}(t)$, for two and three competitors.

The estimated aggregate consumptions of CGO, renewables and nuclear in the second phase ($\hat{K}_\beta=1009.540$ Mtoe) are more than double the aggregate CGO and renewables consumptions in the first phase ($\hat{K}_\alpha=474.193$ Mtoe). Figure 5.4(b) represents the estimated evolutions of the common DMP of both phases. The gap between the ultimate stage of the first phase DMP and initial stage of the second phase DMP designates discontinuity between the phases, as CGO consumptions abruptly declined immediately after launching nuclear energy in the market. The DMPs are extremely far from a fixed m pattern.

TABLE 5.6: Finland, 2CM-DMP. Estimates, standard errors and marginal linearised 95% confidence intervals of the USC model with DMP for two competitors.

Parameter	Estimate	Standard error	95% Confidence interval
K	1972.45	79.8796	{1813.85, 2131.06}
a	0.30582	0.11658	{0.07436, 0.53729}
b	7.69133	4.49272	{-1.22906, 16.6117}
p_1	0.00568	0.00017	{0.00536, 0.00601}
δ	0.15710	0.04792	{0.06196, 0.25225}
q_1	-0.09627	0.04140	{-0.17847, -0.01406}
p_2	0.00049	0.000157	{0.00018, 0.00080}
q_2	0.14329	0.04074	{0.06241, 0.22417}
R^2	0.98919		

TABLE 5.7: Finland, 3CM-DMP. Estimates, standard errors and marginal linearised 95% confidence intervals of the unrestricted UCRC model with DMP for three competitors.

Parameter	Estimate	Standard error	95% Confidence interval
K_α	474.193	52.0778	{371.055, 577.33}
$p_{c\alpha}$	0.00069	0.00022	{0.00026, 0.00113}
$q_{c\alpha}$	0.46511	0.02348	{0.41862, 0.51160}
$p_{1\alpha}$	0.53166	0.05435	{0.42403, 0.63929}
δ_α	-13.1734	2.84509	{-18.8079, -7.5388}
$q_{1\alpha}$	10.0140	2.31343	{5.43236, 14.5956}
$p_{2\alpha}$	0.15682	0.03315	{0.09118, 0.22246}
γ_α	2.21220	0.76280	{0.70152, 3.72289}
$q_{2\alpha}$	1.56006	0.61444	{0.34319, 2.77692}
K_β	1009.54	27.1152	{955.839, 1063.24}
$p_{c\beta}$	0.00092	0.00002	{0.00088, 0.00095}
$q_{c\beta}$	0.09278	0.00052	{0.09176, 0.09381}
$p_{1\beta}$	-2.34032	0.32187	{-2.97777, -1.70288}
ε_β	2.19500	0.40444	{1.39402, 2.99598}
η_β	-4.46217	0.79661	{-6.03981, -2.88452}
$q_{1\beta}$	-0.78713	0.18005	{-1.14371, -0.43055}
$p_{2\beta}$	-0.02829	0.10895	{-0.24405, 0.18748}
θ_β	-0.09914	0.14373	{-0.38379, 0.18552}
ξ_β	-0.00600	0.12081	{-0.24526, 0.23326}
$q_{2\beta}$	0.02996	0.06424	{-0.09727, 0.15718}
p_3	0.22212	0.10891	{0.00643, 0.43782}
μ_β	-0.58102	0.14906	{-0.87622, -0.28582}
λ_β	1.08410	0.26804	{0.55327, 1.61493}
q_3	-0.69963	0.20442	{-1.10446, -0.29479}
R^2	0.99441		

Now, substituting parameter estimates in the second phase of model (4.1), we obtain the following three equations:

$$\begin{aligned}
z'_1(t) - z_1(t) \frac{m'(t)}{m(t)} &\propto -2.34032 + 1.40787 \frac{z_1(t)}{m(t)} + 3.67504 \frac{z_2(t)}{m(t)} - 0.78713 \frac{z_3(t)}{m(t)}, \\
z'_2(t) - z_2(t) \frac{m'(t)}{m(t)} &\propto -0.02829 + 0.02996 \frac{z_1(t)}{m(t)} - 0.06918 \frac{z_2(t)}{m(t)} + 0.03596 \frac{z_3(t)}{m(t)}, \\
z'_3(t) - z_3(t) \frac{m'(t)}{m(t)} &\propto 0.22212 - 0.11861 \frac{z_1(t)}{m(t)} - 0.69963 \frac{z_2(t)}{m(t)} + 0.38447 \frac{z_3(t)}{m(t)}.
\end{aligned}$$

The innovation parameter estimate for nuclear energy is positive (0.22212), and those for CGO and renewables are negative (-2.34032 and -0.02829, respectively). This may be because, at phase β , the innovative effect for CGO and renewables had already

been exhausted. However, CGO experiences a strong positive within-product WOM effect (1.60665), and that for nuclear is also positive (0.38447), but for renewables, it is negative (-0.06918). According to the cross-product WOM effect, CGO is sustained by a strong positive push from renewables (3.67504) and a negative effect from nuclear (-0.78713). Renewables are sustained by positive effects from competitors (0.02996 from CGO and 0.03596 from nuclear), whereas nuclear obtains negative effects from its competitors (-0.11861 from CGO and -0.69963 from renewables).

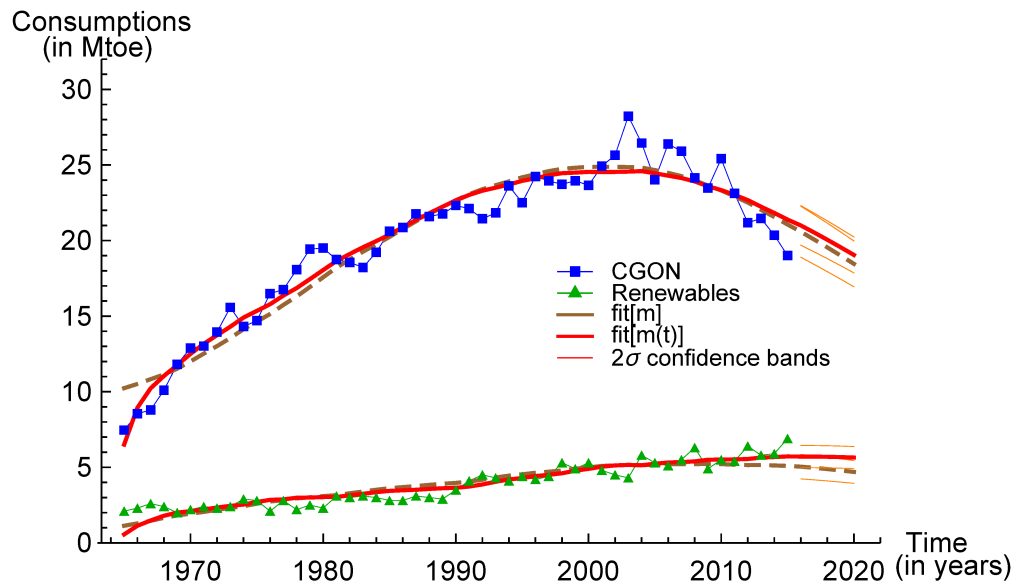
5.2.2.2 Comparison between models with two and three competitors

In this section, we want to assess the efficacy of two- and three-competitor DMP models over similar models with FMP (e.g. under the restriction $m(t) = m$). These models (2CM and 3CM) with FMP are not the same ones discussed in Chapter 3. The R^2 value using model (C.1) for FMP is 0.98619 and that obtained by model (4.1) for FMP is 0.98672. The F -ratio, comparing models (C.1) and (4.1) with the similar models with fixed m , assigns the values 11.83202 and 32.18180, respectively (see Table 5.8). Thus, we conclude that CDMP models significantly differ from the models with fixed m . Both the graphical representation (see Figure 5.5) and the F -test values show that an FMP is not as suitable as a DMP to describe the Finnish energy consumption data partitioned in two or three sources.

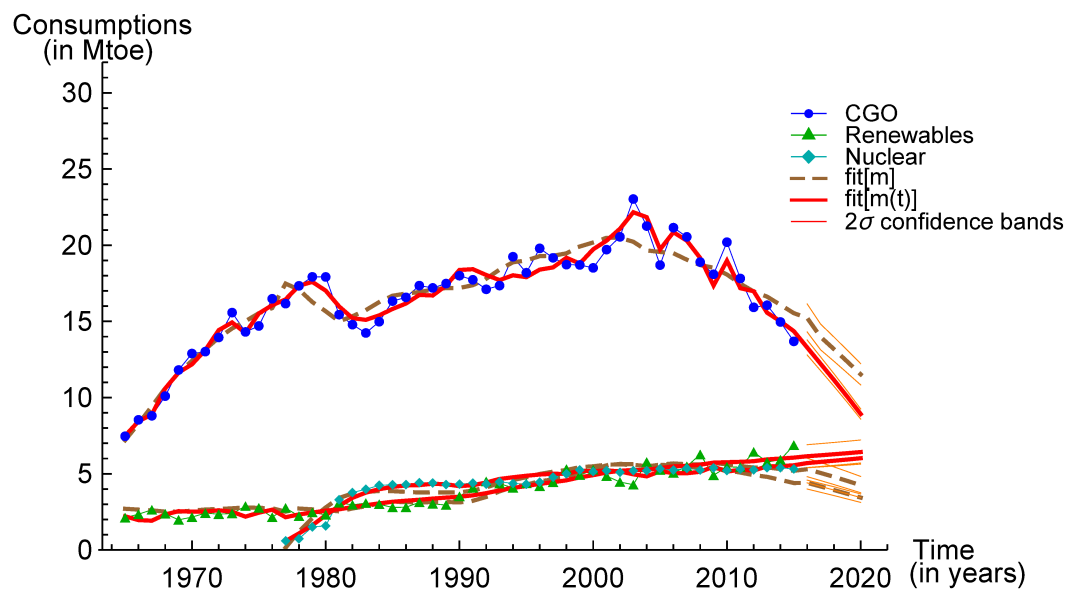
Now, to assess the performance of CDMP models in terms of the models with fixed m and in the context of CDMP models from a forecasting point of view, we make a short-term prediction for each time series from 2016 to 2020. Figures 5.5(a) and 5.5(b) represent the predictions for each source using DMP and FMP models for two and three competitors, respectively. We observe worse fit to the first part of renewables obtained with 2CM and 3CM and nuclear sources using 3CM. To obtain credible confidence bands for the predictions of each series, we ignored the first three residuals from renewables and four residuals from nuclear for all the models with DMP and fixed m in computing

TABLE 5.8: Finland. Values of R^2 of the 2CM and 3CM with FMP and DMP. The F -ratio values to compare DMP models with the corresponding FMP version are also shown.

	FMP	DMP
2CM	$R^2 = 0.98619$	$R^2 = 0.98919$ ($\hat{F} = 11.83202$)
3CM	$R^2 = 0.98672$	$R^2 = 0.99441$ ($\hat{F} = 32.18180$)



(a) 2CM



(b) 3CM

FIGURE 5.5: Finland. Observed data and fitted trajectories with predictions' 2σ confidence bands (thin lines): (a) 2CM, (b) 3CM.

the variance of scaled residuals.

The Kolmogorov–Smirnov test confirmed the normality assumption of scaled residuals. Table 5.9 represents the standard deviations ($\hat{\sigma}_u$) and p -values of scaled residuals for each series. Accordingly, we computed the 2σ confidence bands for predictions, shown in Figure 5.5, and the corresponding confidence band width (see Table 5.9).

From Table 5.9, we see that the confidence band width of predictions for each source

TABLE 5.9: Finland. Comparison among all 2CM and 3CM models: predictions' confidence band width.

		2CM-FMP			2CM-DMP		
		CGON	Renewables		CGON	Renewables	
	$\hat{\sigma}_u$	0.08208	0.16037		0.06235	0.12878	
	p -value	0.79144	0.99669		0.56241	0.53227	
Confidence band width	2016	3.37906	1.61718		2.61857	1.47041	
	2017	3.29517	1.59255		2.56053	1.46955	
	2018	3.20881	1.56563		2.50045	1.46653	
	2019	3.12040	1.53660		2.43861	1.46135	
	2020	3.03035	1.50565		2.37529	1.45403	
		3CM-FMP			3CM-DMP		
		CGO	Renewables	Nuclear	CGO	Renewables	Nuclear
	$\hat{\sigma}_u$	0.06041	0.13575	0.09225	0.03697	0.12331	0.05189
	p -value	0.68501	0.74630	0.40610	0.88992	0.84885	0.83002
Confidence band width	2016	1.83984	1.43891	0.81255	0.98242	1.51684	0.59173
	2017	1.68942	1.37212	0.76947	0.90368	1.53257	0.59979
	2018	1.59266	1.30314	0.72536	0.82498	1.54896	0.60764
	2019	1.49336	1.22992	0.68010	0.74360	1.56624	0.61593
	2020	1.39299	1.15385	0.63434	0.65971	1.58477	0.62482

using 2CM-DMP is smaller than those obtained with 2CM-FMP. Focussing on the 3CM, the confidence bands for CGO and nuclear sources through the model with DMP are smaller than those obtained by the model with FMP. In relation to the model with FMP, the confidence bands for renewables using the model with DMP are wider due to a steeper increase of predicted trajectories (the decreasing trend predicted by the 3CM-FMP for renewables is not reliable). Indeed, models with DMP for both two and three competitors give smaller residual variance for each source than the models with fixed m . This suggests that CDMP models are more suitable for providing reliable predictions for the Finnish energy market.

We now concentrate on predictions using the two- and three-competitor DMP models. To accomplish this, we consider only the findings for renewables that are common to both the models. We notice that 3CM predictions are more reliable since the residuals' variance using 3CM is smaller than 2CM.

5.2.2.3 Comparison among the alternative 3CM models

In Chapter 3, the 3CM model with FMP and shocks has been applied to the Finland energy consumption data. Here, we want to make a comparison among the different fitted models with three competitors. Among the models in Table 5.10, the 3CM-DMP has the highest R^2 value (0.99441), although the 3CM-FMP with shocks (results discussed in Subsection B.2) has a very high parameter dimension (26 parameters, whereas 3CM-DMP has 24 parameters). In addition, the R^2 value using 3CM-FMP is small (0.98672) in relation to the number of parameters (20). According to the diffusion parameters, only the innovative component for CGO using 3CM-DMP and 3CM-FMP with shocks shows a similar direction. For the imitative components, both the models give similar effects for renewables. The models (3CM-FMP and 3CM-DMP) suggest that renewables have no internal support to further sustain them, but CGO and nuclear sources support renewables' expansion. Moreover, renewables support CGO sources. All other

TABLE 5.10: Finland, 3CM. Comparison among models with DMP, fixed m and fixed m with shocks.

Name of model	No. of parameters	R^2 value
3CM-DMP	24	0.99441
3CM-FMP	20	0.98672
3CM-FMP with shocks	26	0.99080

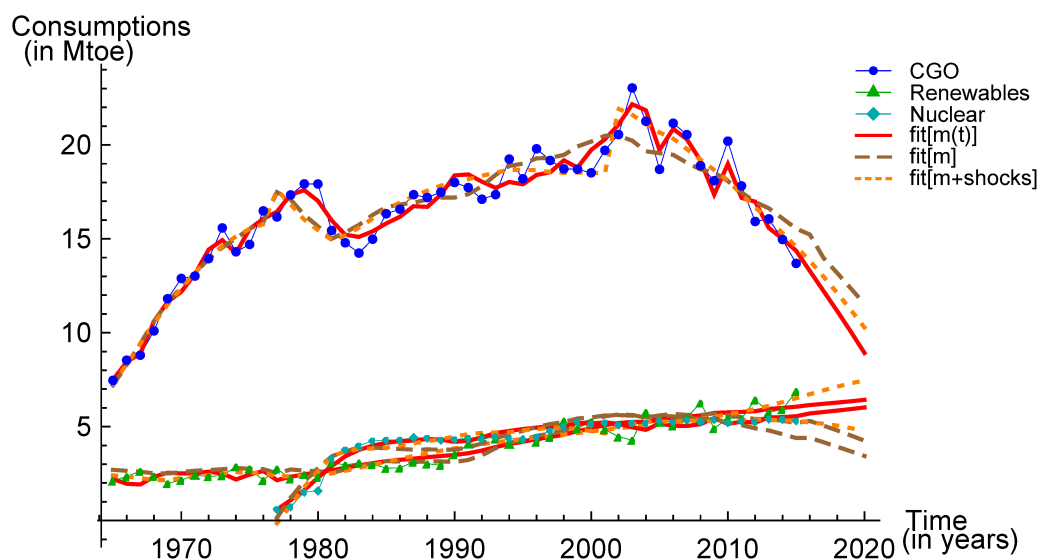


FIGURE 5.6: Finland, 3CM. Energy consumption (in Mtoe) from CGO sources (circles), renewables (triangles) and nuclear (diamonds). Solid (red) lines for the model with DMP, dashed (brown) lines for the model with fixed m and dotted (orange) lines for the model with fixed m and shocks.

imitative effects using 3CM-DMP are opposite to those obtained with 3CM-FMP. Notice that the values of the estimated parameter largely differ between the models. This may also happen because the WOM parameters multiply $z_i(t)/m$ in the FMP model and $z_i(t)/m(t)$ in the DMP model. In terms of 3CM-FMP, the 3CM-DMP findings may be more relevant to the data structure.

The agreement between the observed and estimated profiles for all three sources are shown in Figure 5.6. The dashed (brown) line for each source using 3CM-FMP is not flexible enough to follow the observed path, especially in the last part of each time series, which is heavily underestimated, resulting in totally unreliable predictions. Conversely, the continuous (red) line for of each series obtained by the CDMP model is flexible enough to follow the observed path. Although the dotted (orange) line for each source through 3CM-FMP with shocks is well flexible to follow the observed data, the estimated profile for CGO deviates in the final stage of the observed time series. Overall, the 3CM-DMP appears to be more appropriate for describing the Finland energy consumption data and providing reliable predictions.

5.2.3 France

5.2.3.1 2CM and 3CM DMP

The initial model was developed by partitioning the France's energy consumption data into CGON and renewable sources. The diffusion process of these two sources has been described by model (1.14), UUC with DMP. The adequately large value of R^2 (0.99703) suggests that the model is well fitted. Structure (1.15) of DMP performs better than structures (1.11), giving $R^2 = 0.99655$, and (1.16), giving $R^2 = 0.99530$. The findings are shown in Table 5.11.

Subsequently, the data have been partitioned into three sources, namely CGO, renewables and nuclear sources. We observe a synchronic competition among the sources as they are simultaneously launched. In this situation, model (C.2), UUC with DMP, is suitably fitted. For three competitors, structure (1.11) is found to be better performing ($R^2 = 0.99207$) than the other two structures of DMP ($R^2 = 0.99180$ for structure (1.15) and $R^2 = 0.98503$ for (1.16)). The parameter estimates, standard errors and 95% confidence intervals are shown in Table 5.12.

The aggregate size of the market potential using 3CM-DMP is smaller ($\hat{K} = 16793$ Mtoe) than that obtained by 2CM-DMP ($\hat{K} = 19374.6$ Mtoe). The estimated profiles for the DMP of both 2CM and 3CM, presented in Figure 5.7, are exceedingly far from a fixed m pattern.

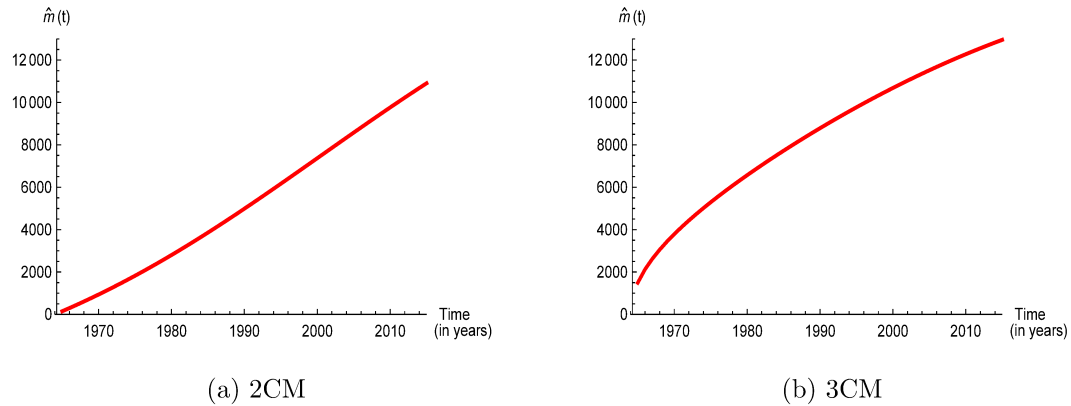


FIGURE 5.7: France. Plot of estimated market potential function, $\hat{m}(t)$, for two and three competitors.

Substituting the parameter estimates in model (C.2), we obtain the following three equations:

$$\begin{aligned} z_1'(t) - z_1(t) \frac{m'(t)}{m(t)} &\propto 0.04790 + 0.17940 \frac{z_1(t)}{m(t)} - 3.08287 \frac{z_2(t)}{m(t)} + 0.24298 \frac{z_3(t)}{m(t)}, \\ z_2'(t) - z_2(t) \frac{m'(t)}{m(t)} &\propto 0.00392 + 0.02827 \frac{z_1(t)}{m(t)} - 0.38942 \frac{z_2(t)}{m(t)} + 0.02853 \frac{z_3(t)}{m(t)}, \\ z_3'(t) - z_3(t) \frac{m'(t)}{m(t)} &\propto -0.00725 - 0.13498 \frac{z_1(t)}{m(t)} + 1.88821 \frac{z_2(t)}{m(t)} - 0.00182 \frac{z_3(t)}{m(t)}. \end{aligned}$$

The estimated innovation components of CGO and renewables are positive (0.04790 and 0.00392, respectively). This means these two sources benefitted from an impressive start, whereas nuclear started extremely slowly (-0.00097). Regarding the within-product

TABLE 5.11: France, 2CM-DMP. Estimates, standard errors and marginal linearised 95% confidence intervals of the UUC model with DMP for two competitors.

Parameter	Estimate	Standard error	95% Confidence interval
K	19374.6	707.765	{17969.1, 20780.1}
p_c	0.00748	0.00037	{0.00675, 0.00821}
q_c	0.03337	0.00233	{0.02874, 0.03800}
p_1	0.65873	0.04027	{0.57876, 0.73869}
δ	10.0764	1.62196	{6.85555, 13.2973}
q_1	-9.99472	1.49275	{-12.959, -7.03041}
p_2	0.06576	0.02572	{0.01468, 0.11684}
γ	-1.02469	0.574434	{-2.1654, 0.11603}
q_2	-1.01986	0.55271	{-2.11743, 0.07771}
R^2	0.99703		

TABLE 5.12: France, 3CM-DMP. Estimates, standard errors and marginal linearised 95% confidence intervals of the UUC model with DMP for three competitors.

Parameter	Estimate	Standard error	95% Confidence interval
K	16793.0	841.361	{15129.3, 18456.6}
p_c	0.00782	0.00290	{0.00208, 0.01355}
q_c	0.03566	0.01079	{0.01433, 0.05699}
p_1	0.04790	0.01050	{0.02713, 0.06867}
ε	-0.06358	0.02930	{-0.12152, -0.00565}
η	3.32585	0.51144	{2.31459, 4.33712}
q_1	0.24298	0.01951	{0.20440, 0.28156}
p_2	0.00392	0.00136	{0.00123, 0.00662}
θ	-0.41769	0.30648	{-1.0237, 0.18831}
ξ	-0.00026	0.01646	{-0.03280, 0.03228}
q_2	0.02827	0.02508	{-0.02132, 0.07785}
p_3	-0.00725	0.00214	{-0.01148, -0.00301}
μ	2.02319	0.36763	{1.29628, 2.75011}
λ	-1.89003	0.35426	{-2.59052, -1.18954}
q_3	1.88821	0.33960	{1.21671, 2.55971}
R^2	0.99207		

WOM effects, CGO experiences a positive effect (0.17940), but the other two sources experience a negative one (-0.38942 for renewables and -0.00182 for nuclear). For the cross-product WOM effects, CGO is sustained by the spread of nuclear sources (0.24298), but it is strongly adversely affected by renewables' spread (-3.08287). Conversely, renewables are supported by the competitors' diffusion spread (0.02827 from CGO and 0.02853 from nuclear). Although nuclear energy is opposed by CGO sources (-0.13498), it obtains strong support from renewables (1.88821).

5.2.3.2 Comparison between models with two and three competitors

Here, we want to assess the efficacy of CDMP models over the similar models with FMP (i.e. the models under the restriction $m(t) = m$). It should be noted that these FMP models are different from those we discussed in Chapter 3. The R^2 values of the 2CM (model (1.14) with FMP) and 3CM (model (C.2) with FMP) are 0.99531 and 0.98213, respectively (see Table 5.13). The F -test, obtained by the 2CM-DMP compared with 2CM-FMP, gives a large value of 26.90704. Furthermore, when the test is performed for the 3CM-DMP in comparison with the 3CM-FMP, we obtain a huge value of $F = 86.51318$. These validate that both the two- and three-competitor DMP models significantly differ from their respective similar models with fixed m . This

TABLE 5.13: France. Values of R^2 of the 2CM and 3CM with FMP and DMP. The F -ratio values to compare DMP models with the corresponding FMP version are also shown.

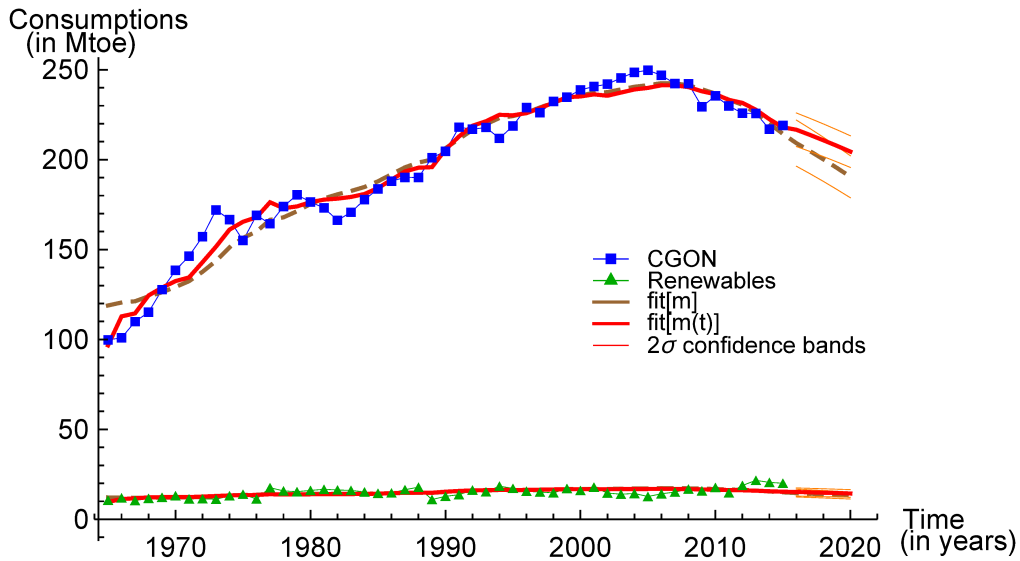
	FMP	DMP
2CM	$R^2 = 0.99531$	$R^2 = 0.99703$ ($\hat{F} = 26.90704$)
3CM	$R^2 = 0.98213$	$R^2 = 0.99207$ ($\hat{F} = 86.51318$)

TABLE 5.14: France. Comparison among all 2CM and 3CM models: predictions' confidence band width.

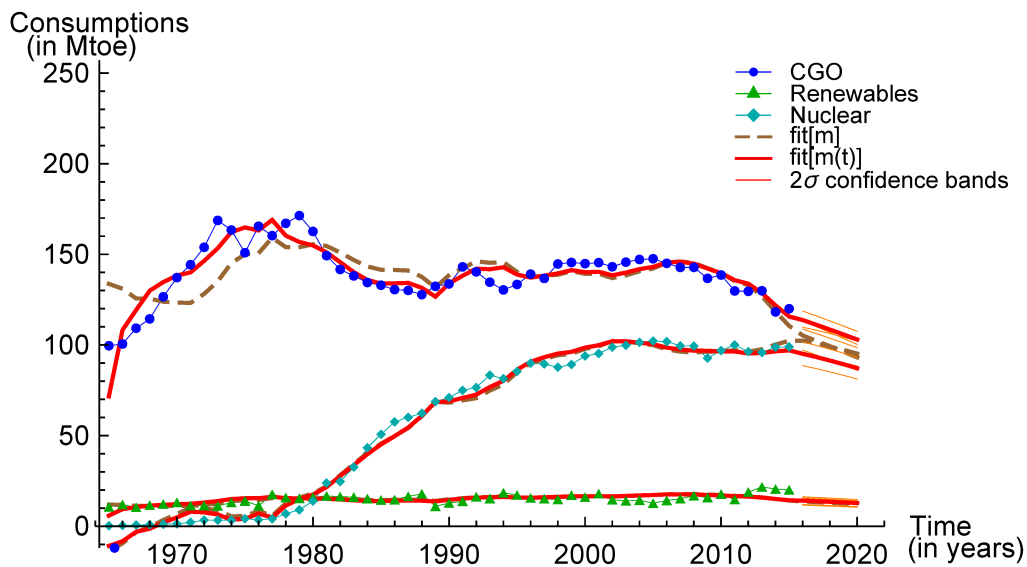
		2CM-FMP			2CM-DMP		
		CGON	Renewables		CGON	Renewables	
	$\hat{\sigma}_u$	0.06132	0.14857		0.04306	0.14784	
	p -value	0.27561	0.93777		0.81552	0.75257	
Confidence band width	2016	25.65349	4.33513		18.65833	4.49481	
	2017	25.11492	4.24048		18.41235	4.43567	
	2018	24.55186	4.14210		18.15551	4.37417	
	2019	23.96714	4.04043		17.88857	4.31049	
	2020	23.36360	3.93594		17.61226	4.24476	
		3CM-FMP			3CM-DMP		
		CGO	Renewables	Nuclear	CGO	Renewables	Nuclear
	$\hat{\sigma}_u$	0.07637	0.14602	0.07248	0.04402	0.15193	0.06845
	p -value	0.44420	0.77441	0.76200	0.54626	0.92200	0.75515
Confidence band width	2016	16.07373	3.97619	14.83264	10.01167	4.28108	13.02210
	2017	15.62368	3.88216	14.61179	9.78329	4.18697	12.77710
	2018	15.16555	3.78448	14.36533	9.54917	4.08952	12.51288
	2019	14.70113	3.68362	14.09530	9.31023	3.98921	12.23176
	2020	14.23219	3.58009	13.80384	9.06738	3.88651	11.93602

means that models with fixed m are less appropriate for describing the energy dynamics of France.

Now, to measure the gain due to the more realistic description of the market potential (for all the sources in 2CM and 3CM) and the improvement due to more specific data (only for renewables) based on predictions, we make a short-term forecast for each time series from 2016 to 2020. The predictions for each source obtained by the models with DMP and FMP for both two and three competitors are shown in Figure 5.8. It should be observed that, at the beginning of the CGO and nuclear time series, the estimated values using 3CM-FMP are quite far from their observed data. Hence, for



(a) 2CM



(b) 3CM

FIGURE 5.8: France. Observed data and fitted trajectories with predictions' 2σ confidence bands (thin lines): (a) 2CM, (b) 3CM.

having credible confidence bands for predictions, we ignored the first three residuals for CGO and the first 15 residuals for nuclear using 3CM-FMP. For a fair comparison, all these residuals for CGO and nuclear obtained with 3CM-DMP are also ignored in computing the scaled residuals' variance. In this computation, we also ignored the first three residuals for renewables from both the 2CM and 3CM, since at the beginning of the renewables time series, the estimated values obtained with the 3CM-DMP deviate

from the observed values.

The Kolmogorov–Smirnov test confirmed that scaled residuals follow a Gaussian distribution. The standard deviations ($\hat{\sigma}_u$) and p -values of scaled residuals for each series using the 2CM and 3CM are shown in Table 5.14. Using the properties of normal distributions, we computed the 2σ confidence bands for predictions, represented in Figure 5.8, and the corresponding confidence band width (see Table 5.14).

In Table 5.14, the confidence band width for predictions of CGON through 2CM-DMP is smaller than that obtained with the 2CM-FMP. Conversely, the confidence band width for predictions of renewables using the 2CM-DMP is larger than that obtained with the 2CM-FMP, whereas the 2CM-DMP has a smaller residual variance. This is because the predicted trajectories using the 2CM-DMP are larger than those obtained by the 2CM-FMP. In the case of 3CM, the confidence bands for CGO and nuclear predictions using the model with DMP are smaller than those obtained by the model with FMP. Conversely, compared with the model with FMP, the model with DMP provides larger confidence bands for renewables predictions. Overall, the predictions using CDMP models are more trustworthy, since the residuals' variance for each source (except for renewables in 3CM-DMP) using the models with DMP are smaller than the similar models with fixed m are.

Our main concern is perceiving any improvement of the 3CM-DMP over 2CM-DMP assessed by the renewables' predictions that are common in both models. With respect to this point, we observe a smaller confidence band width from the 3CM-DMP than the results obtained with the 2CM-DMP. However, the 3CM-DMP gives a relatively large residual variance. Hence, the 3CM-DMP may not be a good choice for predictions about the French energy market.

5.2.3.3 Comparison among the alternative 3CM models

In Chapter 3, the French energy consumption data were analysed through the 3CM model with FMP and shocks (results discussed in Subsection B.3). Here, it is interesting to compare the alternative fitted models for three competitors. The values in Table 5.15 highlight that the value of $R^2 = 0.98978$ using the 3CM-FMP with shocks is smaller than that obtained with the 3CM-DMP (0.99207). Conversely, 3CM-FMP with shocks has a higher parameter dimension (20) than the other two models do (15 parameters for the 3CM-DMP and 13 for the 3CM-FMP). Focussing on diffusion parameter estimates, the innovative and imitative components for each source using the 3CM-DMP have the same sign as those obtained with the 3CM-FMP with shocks.

The agreement of observed and estimated profiles of all the three sources (CGO,

TABLE 5.15: France, 3CM. Comparison among models with DMP, fixed m and fixed m with shocks.

Name of model	No. of parameters	R^2 value
3CM-DMP	15	0.99207
3CM-FMP	13	0.98213
3CM-FMP with shocks	20	0.98978

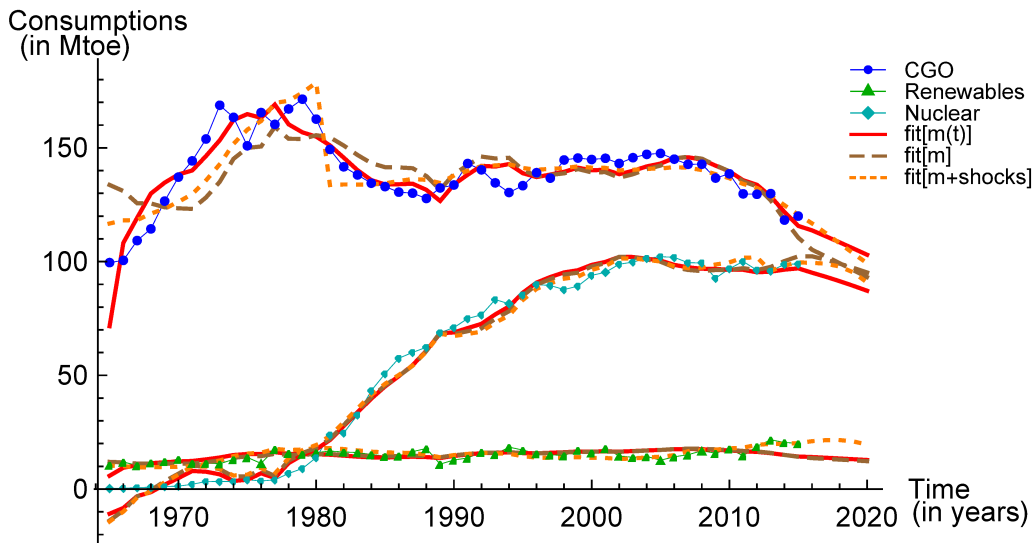


FIGURE 5.9: France, 3CM. Energy consumption (in Mtoe) from CGO sources (circles), renewables (triangles) and nuclear (diamonds). Solid (red) lines for the model with DMP, dashed (brown) lines for the model with fixed m and dotted (orange) lines for the model with fixed m and shocks.

renewables and nuclear) obtained by the alternative models is shown in Figure 5.9. The estimated profiles using the model with fixed m (the dashed brown line) are stiff and unable to follow the observed path; especially, in the last part, the estimated values are largely underestimated or overestimated in relation to the observed values. Conversely, the estimated profiles using the model with DMP (continuous red line) are flexible and follow the observed path well, except for the last part of the renewables series. Although, at the beginning, the estimated values through the model with fixed m and shocks (the dotted orange line) are somewhat stiff to the observed values, in the last part, they are more flexible in following the observed path. However, both the R^2 values and estimated profiles suggest that the 3CM-DMP is more appropriate for describing the French energy market.

5.2.4 Germany

5.2.4.1 2CM and 3CM DMP

First, model (C.1), USC with DMP, is fitted to the data from Germany to describe the diffusion of energy sources partitioned as CGON and renewables. The structure (1.11) for the DMP performs slightly better ($R^2 = 0.99647$) than the other two DMP structures do (structure (1.15) gives $R^2 = 0.99638$ and (1.16) gives $R^2 = 0.99627$). The findings are shown in Table 5.16.

Subsequently, the data were separated into three sources, as follows: CGO, renewables and nuclear. Since all three sources were launched simultaneously, model (C.2), UUC with DMP, is fitted. A notably large value of R^2 (0.99819) proves that the fitting is good overall. Structure (1.15) for DMP gives improved performance compared with structures (1.11) and (1.16), which have R^2 values of 0.99602 and 0.99707, respectively. Table 5.17 represents the findings of the fitted model.

The aggregate size of the market potential through 3CM-DMP is $\hat{K} = 40210$ Mtoe, which is about 1.5 times larger than that obtained with the 2CM-DMP ($\hat{K} = 28783.2$ Mtoe). The estimated profiles of the DMP, $m(t)$, from the 2CM and 3CM are shown in Figures 5.10(a) and 5.10(b), respectively. We observe a linear increase in the market potential in the 3CM, whereas the DMP quickly reaches its asymptotic value.

If we focus on the innovation parameters of 3CM, it is clear that this component for nuclear sources is not important compared with the other two sources' components. By substituting the parameter estimates in model (C.2), we obtain the following three

TABLE 5.16: Germany, 3CM-DMP. Estimates, standard errors and marginal linearised 95% confidence intervals of the USC model with DMP for two competitors.

Parameter	Estimate	Standard error	95% Confidence interval
K	28783.2	104209.0	$\{-178126.0, 235692.0\}$
p_c	1.57190	10.9229	$\{-20.1158, 23.2596\}$
q_c	-1.57190	11.9233	$\{-25.2459, 22.1021\}$
p_1	0.01011	0.00029	$\{0.00953, 0.01069\}$
δ	0.26623	0.04968	$\{0.16759, 0.36487\}$
q_1	-0.23923	0.04953	$\{-0.33757, -0.14089\}$
p_2	0.00002	0.00012	$\{-0.00022, 0.00026\}$
q_2	0.26397	0.04874	$\{0.16719, 0.36074\}$
R^2	0.99647		

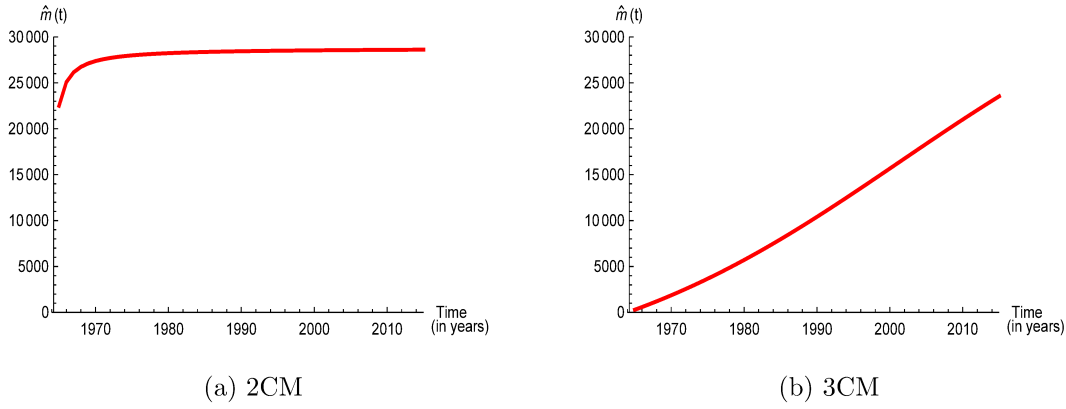


FIGURE 5.10: Germany. Plot of estimated market potential function, $\hat{m}(t)$, for two and three competitors.

TABLE 5.17: Germany, 3CM-DMP. Estimates, standard errors and marginal linearised 95% confidence intervals of the UUC model with DMP for three competitors.

Parameter	Estimate	Standard error	95% Confidence interval
K	40210.0	1855.95	{36540.2, 43879.7}
p_c	0.00704	0.00037	{0.00631, 0.00776}
q_c	0.03829	0.00249	{0.03337, 0.04321}
p_1	0.82137	0.02823	{0.76555, 0.87719}
ε	2.54962	0.22742	{2.09994, 2.99930}
η	-1.45686	0.69560	{-2.83226, -0.08145}
q_1	-3.52656	0.24588	{-4.01273, -3.04038}
p_2	0.01283	0.01413	{-0.01510, 0.04077}
θ	0.35825	0.10210	{0.15636, 0.56014}
ξ	0.00569	0.05176	{-0.09666, 0.10803}
q_2	-0.02090	0.01634	{-0.05320, 0.01139}
p_3	-0.02603	0.01431	{-0.05433, 0.00226}
μ	-0.22920	0.10266	{-0.43219, -0.02621}
λ	0.12437	0.11768	{-0.10832, 0.35705}
q_3	-0.17964	0.11093	{-0.39898, 0.03969}
R^2	0.99819		

equations:

$$\begin{aligned}
 z_1'(t) - z_1(t) \frac{m'(t)}{m(t)} &\propto 0.82137 - 0.97694 \frac{z_1(t)}{m(t)} - 2.06970 \frac{z_2(t)}{m(t)} - 3.52656 \frac{z_3(t)}{m(t)}, \\
 z_2'(t) - z_2(t) \frac{m'(t)}{m(t)} &\propto 0.01283 - 0.02090 \frac{z_1(t)}{m(t)} + 0.33735 \frac{z_2(t)}{m(t)} - 0.02659 \frac{z_3(t)}{m(t)}, \\
 z_3'(t) - z_3(t) \frac{m'(t)}{m(t)} &\propto -0.02603 + 0.04956 \frac{z_1(t)}{m(t)} - 0.17964 \frac{z_2(t)}{m(t)} - 0.05527 \frac{z_3(t)}{m(t)}.
 \end{aligned}$$

CGO sources are sustained by a large innovative effect (0.82137), that is, the cycle starts rapidly. The cycle of renewables also started rapidly (0.01283), whereas the large negative effect for nuclear (-0.02603) represents an extremely slow start of the nuclear cycle. Regarding the within-product WOM effects, only renewables experience a positive effect (0.33735), while the other two sources experience negative effects (-0.97694 for CGO and -0.05527 for nuclear). With respect to the cross-product WOM effect, the spread of CGO's diffusion is strongly opposed by both its competitors (-2.06970 from nuclear and -3.52656 from renewables). Renewables' diffusion spread is also limited by competitors (-0.02090 from CGO and -0.02659 from nuclear), while renewables sustain further internal consumptions. In contrast, nuclear energy's diffusion spread is supported by CGO sources (0.04956) but opposed by renewables (-0.17964).

5.2.4.2 Comparison between models with two and three competitors

In this subsection, we want to assess the efficacy of CDMP models with reference to similar models under the restriction $m(t) = m$. The R^2 values of the 2CM and 3CM with FMP are 0.99557 and 0.99699, respectively (see Table 5.18). In the case of the 2CM, the F -ratio, obtained by model (C.1) compared with the similar model with FMP, assigns a large value of $\hat{F} = 11.87971$. Furthermore, for the 3CM, the value of the F -test, comparing model (C.2) with the similar model with fixed m , is notably large ($\hat{F} = 45.65672$). The estimates of both F -ratios validate the significance of the CDMP models. Apparently, models with DMP are more appropriate for describing the German energy market.

Now, we make a short-term prediction for each time series, using the 2CM and 3CM, from 2016 to 2020, to assess the improvement of the models with DMP over the similar models with fixed m and further investigate the improvement of the 3CM-DMP over the 2CM-DMP. Figure 5.11 represents the predictions for each source obtained by the models with DMP and FMP for both two and three competitors. It should be observed that,

TABLE 5.18: Germany. Values of R^2 of the 2CM and 3CM with FMP and DMP. The F -ratio values to compare DMP models with the corresponding FMP version are also shown.

	FMP	DMP
2CM	$R^2 = 0.99557$	$R^2 = 0.99647$ ($\hat{F} = 11.87971$)
3CM	$R^2 = 0.99699$	$R^2 = 0.99819$ ($\hat{F} = 45.65672$)

TABLE 5.19: Germany. Comparison among all 2CM and 3CM models: predictions' confidence band width.

		2CM-FMP			2CM-DMP		
		CGON	Renewables		CGON	Renewables	
	$\hat{\sigma}_u$	0.04701	0.25644		0.04300	0.21834	
	p -value	0.98729	0.45740		0.99478	0.39267	
Confidence band width	2016	23.61976	17.79177		21.89753	16.87599	
	2017	22.94994	18.83600		21.27710	18.15474	
	2018	22.26948	19.89622		20.63837	19.49069	
	2019	21.58022	20.96809		19.98246	20.88153	
	2020	20.88397	22.04712		19.31058	22.32445	
		3CM-FMP			3CM-DMP		
		CGO	Renewables	Nuclear	CGO	Renewables	Nuclear
	$\hat{\sigma}_u$	0.04153	0.14271	0.12092	0.03104	0.13698	0.12846
	p -value	0.53371	0.95846	0.46210	0.96762	0.91070	0.48499
Confidence band width	2016	20.31696	10.98120	3.86159	15.12109	13.38838	3.76394
	2017	19.11660	10.76348	3.33125	14.82897	15.01720	2.84346
	2018	17.68847	10.30349	2.83808	14.51080	16.84014	1.83134
	2019	16.08775	9.63768	2.38994	14.16579	18.87882	0.71893
	2020	14.38377	8.81767	1.99144	13.79304	21.15694	–

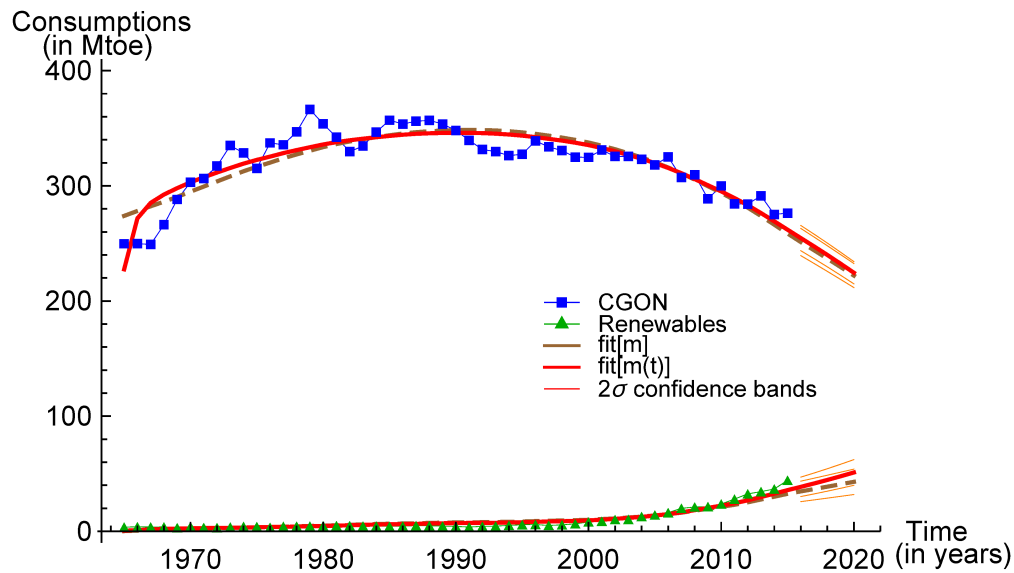
Confidence band width is not shown when the fitted trajectory is negative.

in the beginning, the estimated profiles for renewables using the 2CM- and 3CM-FMP and for nuclear energy using the 3CM-FMP deviated somewhat from their observed paths. To obtain reliable confidence bands for the predictions, we thus ignored the first 7 residuals for renewables in both 2CM- and 3CM-FMP and the first 12 residuals for nuclear in 3CM-FMP. To maintain consistency, all these residuals for renewables and nuclear in 2CM- and 3CM-DMP are also ignored in computing the scaled residuals' variance.

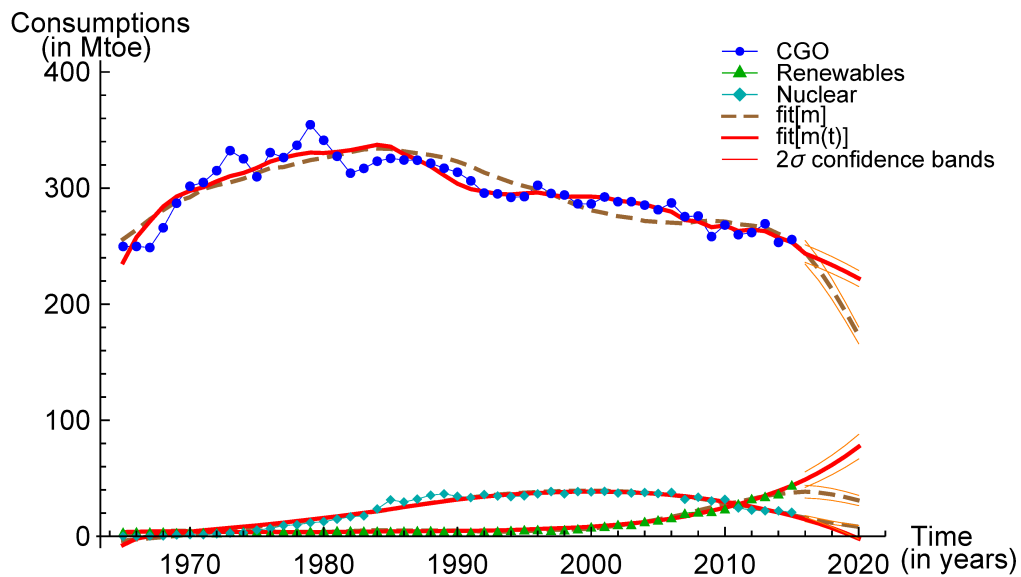
The Kolmogorov–Smirnov test for goodness of fit confirmed the normality assumption of the scaled residuals. Table 5.19 represents the standard deviations ($\hat{\sigma}_u$) and p -values of scaled residuals for each series using the 2CM and 3CM with DMP and fixed m . Accordingly, we computed the 2σ confidence bands for predictions' (see Figure 5.11) and the corresponding confidence band width (see Table 5.19).

In Table 5.19, the confidence band width for CGON predictions using the 2CM-DMP is smaller than those obtained with the 2CM-FMP. Moreover, the confidence band width for the first four-year predictions of renewables through the 2CM-DMP is smaller than

those obtained by 2CM-FMP. The larger confidence band width for the last-year prediction is due to a steeper predicted trajectory in the 2CM-DMP than in the 2CM-FMP. In contrast, the confidence band width for CGO predictions using the 3CM-DMP is smaller than that of the 3CM-FMP. In the case of the confidence band width for renewables predictions, 3CM-DMP, we observe larger bands for the 3CM-FMP. This is because the 3CM-DMP predictions suggest an increase of renewables in 2016–2020. According to the



(a) 2CM



(b) 3CM

FIGURE 5.11: Germany. Observed data and fitted trajectories with predictions' 2σ confidence bands (thin lines): (a) 2CM, (b) 3CM.

3CM-FMP predictions, renewables may be declining in 2016–2020, but this is not consistent with the observed data. Moreover, the smaller residual variance for renewables using the 3CM-DMP represents greater precision. Conversely, the confidence bands for nuclear predictions using the 3CM-FMP are more consistent than those obtained by the 3CM-DMP. Overall, the models with DMP are more appropriate for obtaining reliable predictions.

Beyond the above discussions, we are interested in finding any improvement of the 3CM-DMP model in comparison with the 2CM-FMP. In this case, we consider only the findings for renewables that are common to both models. Compared with the 2CM-DMP, the 3CM-DMP gives narrower confidence bands for the renewables' predictions. This means that the 3CM-DMP is more suitable for evaluating forecasts about the German energy market.

5.2.4.3 Comparison among the alternative 3CM models

In Chapter 3, the energy consumption data from Germany were analysed through the 3CM model with fixed m and shocks. Thus, it is important to make a comparison among the alternative fitted models for three competitors. In Table 5.20, we see that the 3CM-FMP with shocks has the largest R^2 value (0.99869). However, the value is narrowly larger than that obtained through the 3CM-DMP ($R^2 = 0.99819$). Notice that 3CM-FMP with shocks entails a large number of parameters (23) compared with the other two models (15 parameters for 3CM-DMP and 13 parameters for 3CM-FMP).

According to the diffusion parameter estimates, the innovative components using the 3CM-DMP and 3CM-FMP with shocks change in the same directions. Of all three within-product WOM effects using both models, we observe the same changing direction for renewables. Moreover, both models describe the decrease of the traditional energy (CGO sources) consumptions well. In addition to this, the models suggest that the diffusion of renewables is opposed by the spread of CGO sources. The direction of changes for all the remaining within- and cross-product WOM effects using the 3CM-DMP is the opposite of those obtained by the 3CM-FMP with shocks. It should be

TABLE 5.20: Germany, 3CM. Comparison among models with DMP, fixed m and fixed m with shocks.

Name of model	No. of parameters	R^2 value
3CM-DMP	15	0.99819
3CM-FMP	13	0.99699
3CM-FMP with shocks	23	0.99869

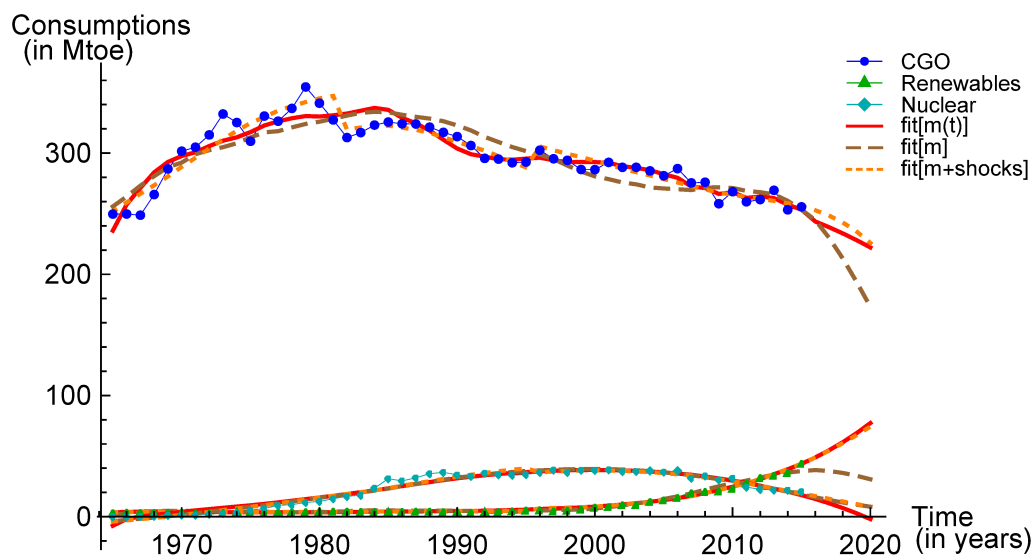


FIGURE 5.12: Germany, 3CM. Energy consumption (in Mtoe) from CGO sources (circles), renewables (triangles) and nuclear (diamonds). Solid (red) lines for the model with DMP, dashed (brown) lines for the model with fixed m and dotted (orange) lines for the model with fixed m and shocks.

observed that the values obtained by the 3CM-DMP vary widely from those obtained with 3CM-FMP with shocks. However, 3CM-DMP may be more reliable, as the model stands on a more realistic structure of market potential.

Figure 5.12 represents the agreement between the observed and estimated outlines for all three sources obtained by the alternative models with DMP. The dashed (brown) lines using 3CM-FMP are somewhat rigid to go through the data lines. Especially, we observe a weaker agreement between the observed and fitted values in the CGO time series. Conversely, the continuous (red) lines through 3CM-DMP are more flexible and able to follow the observed path. Although the dotted (orange) lines using 3CM-FMP with shocks are flexible enough to undergo the observed path, the model does not provide any significant improvement compared with the more parsimonious 3CM-DMP. Hence, we can say that 3CM-DMP is more suitable for describing energy dynamics in Germany.

5.3 Remarks

In this chapter, we applied existing diffusion models (e.g. CDMP models for two competitors) to energy consumption data, from 1965 to 2015, partitioned as CGON sources and renewables. To describe the diffusion process in a broader way, the models

were extended to three competitors (CGO, renewables and nuclear). The data were analysed using three different versions of the CDMP models, as follows: balanced, unbalanced and unrestricted unbalanced. Finally, we chose the best-fitting model. Other models with FMP have also been applied to prove the efficacy of CDMP models over the models with FMP. All these models have been fitted to the yearly energy consumption data from four countries, that is, Belgium, Finland, France and Germany.

Focussing on the estimate profiles of the market potential, we see that, for both the 2CM and 3CM, they are generally extremely far from the fixed m patterns. This means that the demand for energy consumption seems to have grown in a regular way in the energy market of the studied countries.

For the interpretation of parameter estimates, we focus only on CDMP models for three competitors, since some rich information may be hidden in the bivariate models. Here, all four countries were analysed using an unrestricted unbalanced model. The innovative component for nuclear sources in each country (excluding Finland) is negative. This means that we did not observe a good start of the nuclear cycle against other energies with almost positive innovative effects. Two out of three sources' within-product WOM effects at the maximum were positive (or negative) in each country. The cross-product WOM effects for renewables by competitors were positive in Finland and France, but they were negative in Belgium and Germany. CGO's cross-product effects by competitors were positive in Belgium but negative in Germany. Only in Finland the cross-product effects of nuclear energy by its competitors are negative. Of all other cross-product effects for each source in each country, it shows that both competitors have an opposite influence on the specific source. Indeed, the findings obtained by the CDMP models are somewhat similar to those we discussed in Chapter 3 using the models with FMP and shocks. This means that the competition/substitution patterns among energy sources differ from country to country.

The estimated profiles using models with fixed m are not flexible enough to follow the observed path. Conversely, the estimated profiles obtained with the CDMP models are flexible to undergo the observed path. Although the estimated profiles using models with fixed m and shocks are also flexible to follow the observed data, they have a high parameter dimension and do not provide any significant improvement over the models with DMP. Hence, CDMP models may be more appropriate for describing the energy dynamics, as these models consider a more realistic assumption about the market potential.

In almost all cases, the predictions for each source using models with DMP differ significantly from those obtained with the similar models with fixed m . According to the

2σ confidence bands for predictions, CDMP models are generally more precise. Beyond the above comparisons, our main concern is observing any improvement of the 3CM-DMP over the 2CM-DMP. Regarding this point, we focus on the renewables elements that are common to the two models. We see that for three of four countries (Belgium, Finland and Germany), the confidence band width using the 3CM-DMP is narrower than that obtained from the 2CM-DMP. Although, for France, the 2CM-DMP gives narrower confidence bands than the 3CM-DMP does, the 2CM-DMP fails to carefully follow the last few points of the renewables time series. Above all, the 3CM-DMP models are more appropriate for describing the evolution of energy sources and providing reliable predictions about the energy market.

Conclusions

Discussion

Research on the diffusion of innovations represents an attempt to explain the mechanism by which new ideas, products, technologies or trends spread in society. The new trends or innovations take time to diffuse. The basic paradox in the diffusion of innovations research is explore the reasons why there is often a long interim between the first appearance of an innovation and the time of its significant adoption. In fact, an innovation diffusion process is often affected by the existing technologies. Thus, it is important to structure a diffusion process of two or more products or technologies, targeting the main set of potential adopters or subgroups of potential adopters with possible interaction effects.

In Chapter 1 of this thesis, we discussed the fundamental diffusion models and the models of two products diffusion in a competitive environment that are already available in the literature. The BM (Bass, 1969) describes how an innovation is diffused or adopted in a society through interaction between early adopters and potential adopters (innovators and imitators). The GBM (Bass *et al.*, 1994) enables capturing the local extensions or contractions in the lifecycle of an innovation. Considering the structure of the market potential, the GGM (Guseo and Guidolin, 2009) is dissimilar from the BM and GBM. It allows the nature of the market potential to be dynamic, while in the BM and GBM, it is assumed to be constant throughout the diffusion process.

Existing diffusion models describe a competition between only two products. These models are not suitable in situations when there are several products competing in a homogeneous category. Typically, building a diffusion model for a substantial number of products is too tricky as it requires a high number of parameters to describe a composite structure of the interactions among the products. In this study, the models for competition are extended from two to three products.

Following the model proposed by Guseo and Mortarino (2014), in Chapter 2, we proposed a diffusion of innovations model to describe a market, where three products

compete for the same customers. The model separates competition into two phases. In the first phase, the competition is between two products, and in the second, it is extended from two to three products. The first phase is absent when all the three products are simultaneously launched. This model is described by a set of differential equations that may not have a closed-form expression; for this reason, they are suitable for instantaneous data. The flexibility of this model is that it can also be represented in some reduced forms (see Appendix A) by imposing restrictions on the discrimination parameters. Nonlinear estimation techniques are used to estimate the parameters.

Applications of the proposed model (3CM) to 12 countries' energy data, partitioned as CGO, renewables and nuclear sources, are discussed in Chapter 3. The existing bivariate model (2CM) is also applied to the data, where nuclear is added to CGO, that is, CGON is contrasted with renewables. The 2CM fitting is performed to perceive the improvement of the 3CM over the 2CM. Notice that the intervention functions (e.g. the external shocks) are incorporated with the models applied to all 12 countries (except for India) to capture the wide variety of shapes of data. The significance of shocks' inclusion in the model is verified by the F -test (see Subsection 1.4.4), where the model without shocks is considered the benchmark.

If we focus on the findings of 3CM, we see that for all 12 countries (excluding China), the innovative components corresponding to CGO sources are extremely large, followed by renewables and nuclear energy sources. This indicates that almost all countries are somewhat more motivated for the innovation of green energy (renewables) technology in comparison with nuclear technology. Of all 12 countries, a balanced model is fitted to the data from Belgium, India, Spain and the United States. According to the imitative component, referred to WOM effect, the diffusion spread of CGO is substantially larger than its competitors' spread. However, except for India, nuclear has a higher diffusion spread than renewables. An unbalanced model is fitted to the data from the remaining eight countries. In this case, the WOM effect is split into within-product and cross-product effect. For China and Germany, all three sources within-product effects are positive, and the analogous cross-product effects are mostly negative. We observe a reverse situation for Finland, Sweden and Switzerland and a mixed situation for France, Japan and the United Kingdom. Indeed, when energy sources sustain further internal consumptions, at that time they are more likely to be controlled by competitors, and vice-versa.

With respect to the 2CM, the 3CM is more flexible for representing the specific features of some of the products under competition. For instance, in the case of China, concerning the cross-product WOM effect using 2CM, CGON sources counteracted the

spread of renewables. According to 3CM, nonrenewables (CGO and nuclear) also negatively affected the spread of renewables, but the effect from nuclear is larger than that from CGO sources (see Subsection B.1). This means that nuclear energy is an intense threat for renewables' expansion in China. Using 3CM, we also obtained similar rich information for the remaining 11 countries, whereas the 2CM failed to be so specific. It should be noted that the countries' WOM components are different. That is, across countries different signs and magnitudes of WOM components describe different competition/substitution patterns.

The model fitting performance, that is, the model's goodness of fit was measured by the standard deviation, residual diagnostics and R^2 value. Since the two models (2CM and 3CM) use different data other than renewables, we decided to evaluate the improvement of the 3CM over 2CM, focussing on the renewables instead of the global goodness of fit measures. The focus is on the forecasting performance of the renewables. We see that among the 12 countries analysed, our proposed 3CM gives narrower confidence bands than the existing 2CM does for 10 countries. The predictions from 2016 to 2020 suggest an increase of renewables against declining other energies in all 12 countries except for India, where all sources of energy may be increased in 2016–2020, since India's energy sector is still developing.

The performance of the models was also assessed by FA measures that we computed for two countries (Sweden and Switzerland). The FA measures, for both countries, denoted the superiority of the 3CM compared with the 2CM. It should be noted that the confidence bands for renewables' predictions for Sweden and Switzerland using 3CM are also narrower than those obtained with the 2CM. That is, both FA measures and confidence band width agree, suggesting that 3CM performs better than 2CM.

Although the diffusion models proposed in Chapter 2 are more suitable for estimating the innovation and imitation effects of the products under competition, the application results show that the model often requires incorporating several intervention functions to have a good fit with reliable forecasts. In this case, the intervention functions may influence the estimates of diffusion parameters. Such influences may be more severe when there are larger variations in the lifecycle of products. Hence, it is crucial to define a model that can modify the evolutionary shapes of diffusion of innovations methodologies over time.

Energy sources, partitioned as two or three products, differ essentially in the persuasion effects exerted by the respective energy companies and in their acceptance through early adopters spreading WOM about their efficacy. The initial novelty of these influences of energy sources as two or three products suggests configuring diffusion models

that define the market potential as a dynamic structure. The model proposed in Chapter 4 is suitable for describing the diffusion of three competing products under the assumption of DMP. We suppose that awareness and adoption are two successive situations that subjects may experience. The first situation, awareness, is a latent criterion. As we have no data at the individual level, the description is combined, as a mean profile, that gives rise to the equations (1.11) or (1.15) or (1.16).

Our proposed CDMP model, in Equation (4.1), is suitable for analysing competition among three products, where two products exist from the beginning and the third enters the market later. The model stands only on its' second phase (see model (C.2) in Appendix C), when all three products enter the market simultaneously. In the case of two-product competition, we used the model proposed by Guseo and Mortarino (2015), but we considered its more general structure.

To prove the efficacy of CDMP models for both two and three products over the similar models with FMP, all these models were applied to four countries' energy data (see Chapter 5). The F -test proved that the CDMP models significantly differ from the models with FMP. Moreover, the confidence bands for predictions of each source using CDMP models are more precise compared with those obtained by the models with FMP. When we focussed on the context of two- and three-competitor CDMP models, we saw that only renewables are common in the two models. For three of the four studied countries, the confidence bands using the 3CM-DMP are narrower than those obtained with the 2CM-DMP. That is, the predictions about the energy market using the 3CM-DMP are more reliable.

Regarding the diffusion parameter estimates, the innovative component for nuclear sources in each country (except for Finland) is negative. This means that the nuclear cycle did not have a good start against other energies in Belgium, France and Germany. None of four countries' within-product effects are completely opposite to the corresponding cross-product effects. However, when an energy source is found to be diffused by its own spread, it is more likely to be opposed by competitors' spread. Apparently, there are some similarities in innovative and imitative components using the CDMP models compared with the models with FMP and shocks (see Chapter 3), although the values differ. That is, like the models with FMP and shocks, the CDMP models describe a diverse competition/substitution pattern among the countries. The 3CM-DMP predictions also suggest for increasing renewables in 2016–2020, when other energies may be declined in all four countries except for France, although there may have a gradual increase of nuclear sources in Finland. When comparing among all the alternative fitted models through the observed and estimated profiles, we see that the estimated profiles

using the models with FMP are often unable to follow the observed path. Conversely, the estimated profiles using the CDMP models and the models with FMP and shocks are flexible and adequately follow the observed path. Although both the CDMP model and the model with FMP and shocks are well fitted to the observed data, the CDMP model can preferably be used in describing the diffusion of energy dynamics and similar issues as the model has a more realistic structure of market potential.

Above all, the applications of the two models (i.e. the CDMP model and model with FMP and shocks) show the feasibility of the 3CM and highlight that a more accurate description of the market category through the data of three separate products gives better results than the 2CM for the common product, the renewables, in terms of out-of-sample accuracy.

As a final remark, the applications of the proposed models in this thesis seem to be interesting from two perspectives. First, the newly developed models are based on the latest bivariate diffusion models, which are more flexible in their framework compared with other similar models available in the literature. It is important to note that the models stand on the basic assumptions of the BM, which is the pioneer in the diffusion of innovations literature and has been widely used because it considers the internal rules of a social system. Second, the proposed models in the given structures are more flexible for interpreting the interaction effects of competing products. However, according to necessity, the models can be expressed in some reduced forms by imposing certain restrictions on the discrimination parameters. The applications of the proposed models to historical energy consumption data are indeed appropriate, as there is relatively complex competition among energy sources. The models can also be applied to describe the diffusion of three competing products with similar setups.

Future directions for research

This thesis described the diffusion dynamics of two and three products in a competitive framework. To obtain an improved description of mutual interactions among competitors, the thesis proposed some feasible extensions of the existing models that motivates further research directions.

Our proposed models are suitable in situations when the products under competition represent a homogeneous category competing for the same customers. That is, the products are similar enough to have a common market potential and common residual market. However, in other situations, a modified Lotka–Volterra approach may be preferable to our proposed models because it will allow more realistic residual market

potentials that are partially specific with latent ‘churn’ effects. One can find ideas about a modified Lotka–Volterra approach in Guidolin and Guseo (2015).

It should be observed that the models we considered under the assumption of a fixed market potential required incorporation of intervention or control functions to capture the wide variety of structures of products in diffusion processes. However, models with control functions may not be well fitted when the fluctuations are too intense. In this situation, a multi-wave (two or more waves) model may give a better fit, especially when there is a synchronic competition among the products. Discussions about a two-wave model are available in Furlan and Mortarino (2018). Furthermore, the concept of multi-wave modelling with the assumption of DMP may also be suitable in situations when the data are naturally waved. Nevertheless, in situations where models with DMP are also unable to capture the wide variety of shapes of data, a limited number of shocks with the DMP models may enrich the fitting and provide more reliable predictions, but the complexity of a DMP model with shocks may introduce identifiability problems.

The proposed diffusion models, which allow competition among a substantially large number of products, require a high number of parameters. Indeed, every additional product in a diffusion process generates a complex structure of interactions among competing products. Since there are open competitions in almost every marketplace, substitute products or services are increasing day by day. Thus, a model for more than three competitors may make important contributions to the diffusion literature.

Appendix A

Models with fixed m

For two products

In the case of two products (or competitors), if the products launch together, only the second phase of model (1.13) is applicable. Then, it is called the unrestricted unbalanced (synchronic) competition (UUC) model of two competitors and has the following form:

$$\begin{aligned}z_1'(t) &= m \left[p_1 + (q_1 + \delta) \frac{z_1(t)}{m} + q_1 \frac{z_2(t)}{m} \right] \left[1 - \frac{z(t)}{m} \right], \\z_2'(t) &= m \left[p_2 + (q_2 - \gamma) \frac{z_1(t)}{m} + q_2 \frac{z_2(t)}{m} \right] \left[1 - \frac{z(t)}{m} \right], \\z(t) &= z_1(t) + z_2(t).\end{aligned}\tag{A.1}$$

Under the restriction $\delta = \gamma$, (A.1) is called the unbalanced synchronic competition (USC) model and can be written as

$$\begin{aligned}z_1'(t) &= m \left[p_1 + (q_1 + \delta) \frac{z_1(t)}{m} + q_1 \frac{z_2(t)}{m} \right] \left[1 - \frac{z(t)}{m} \right], \\z_2'(t) &= m \left[p_2 + (q_2 - \delta) \frac{z_1(t)}{m} + q_2 \frac{z_2(t)}{m} \right] \left[1 - \frac{z(t)}{m} \right], \\z(t) &= z_1(t) + z_2(t).\end{aligned}\tag{A.2}$$

If the further restriction $\delta = \gamma = 0$ in (A.1) or $\delta = 0$ in (A.2) is imposed, it reduces to a balanced model, called the balanced synchronic competition (BSC) model, and this

can be expressed as

$$\begin{aligned}
z_1'(t) &= m \left[p_1 + q_1 \frac{z_1(t)}{m} + q_1 \frac{z_2(t)}{m} \right] \left[1 - \frac{z(t)}{m} \right], \\
z_2'(t) &= m \left[p_2 + q_2 \frac{z_1(t)}{m} + q_2 \frac{z_2(t)}{m} \right] \left[1 - \frac{z(t)}{m} \right], \\
z(t) &= z_1(t) + z_2(t).
\end{aligned} \tag{A.3}$$

For three products

In the case of three products, if two products exist from the beginning and the other one enters the market later, model (2.1) can suitably be used. However, sometimes, it requires to represent the model in a reduced form. If, in the second phase, we consider only one discriminant parameter instead of four, model (2.1) reduces the most restricted version of an unbalanced model, called the restricted unbalanced competition and regime change diachronic (restricted UCRC) model of three competitors and can be written in the following form:

$$\begin{aligned}
z_1'(t) &= m \left\{ \left[p_{1\alpha} + (q_{1\alpha} + \delta_\alpha) \frac{z_1(t)}{m} + q_{1\alpha} \frac{z_2(t)}{m} \right] (1 - I_{t>c_2}) + \right. \\
&\quad \left. + \left[p_{1\beta} + (q_{1\beta} + \delta_\beta) \frac{z_1(t)}{m} + q_{1\beta} \frac{z_2(t)}{m} + q_{1\beta} \frac{z_3(t)}{m} \right] I_{t>c_2} \right\} \left[1 - \frac{z(t)}{m} \right], \\
z_2'(t) &= m \left\{ \left[p_{2\alpha} + (q_{2\alpha} - \delta_\alpha) \frac{z_1(t)}{m} + q_{2\alpha} \frac{z_2(t)}{m} \right] (1 - I_{t>c_2}) + \right. \\
&\quad \left. + \left[p_{2\beta} + q_{2\beta} + \frac{z_1(t)}{m} + (q_{2\beta} + \delta_\beta) \frac{z_2(t)}{m} + q_{2\beta} \frac{z_3(t)}{m} \right] I_{t>c_2} \right\} \left[1 - \frac{z(t)}{m} \right], \\
z_3'(t) &= m \left\{ \left[p_3 + (q_3 - \delta_\beta) \frac{z_1(t)}{m} + (q_3 - \delta_\beta) \frac{z_2(t)}{m} + q_3 \frac{z_3(t)}{m} \right] I_{t>c_2} \right\} \left[1 - \frac{z(t)}{m} \right], \\
m &= m_\alpha (1 - I_{t>c_2}) + m_\beta I_{t>c_2}, \\
z(t) &= z_1(t) + z_2(t) + z_3(t) I_{t>c_2}.
\end{aligned} \tag{A.4}$$

Under the restriction $\delta_\alpha = 0$ in the first phase and $\varepsilon_\beta = \eta_\beta = \theta_\beta = \xi_\beta = 0$ in the second phase, model (2.1) reduces a balanced model, called the competition and regime change diachronic (CRC) model of three competitors, which can be expressed

as follows:

$$\begin{aligned}
z'_1(t) &= m \left\{ \left[p_{1\alpha} + q_{1\alpha} \frac{z_1(t)}{m} + q_{1\alpha} \frac{z_2(t)}{m} \right] (1 - I_{t>c_2}) + \right. \\
&\quad \left. + \left[p_{1\beta} + q_{1\beta} \frac{z_1(t)}{m} + q_{1\beta} \frac{z_2(t)}{m} + q_{1\beta} \frac{z_3(t)}{m} \right] I_{t>c_2} \right\} \left[1 - \frac{z(t)}{m} \right], \\
z'_2(t) &= m \left\{ \left[p_{2\alpha} + q_{2\alpha} \frac{z_1(t)}{m} + q_{2\alpha} \frac{z_2(t)}{m} \right] (1 - I_{t>c_2}) + \right. \\
&\quad \left. + \left[p_{2\beta} + q_{2\beta} \frac{z_1(t)}{m} + q_{2\beta} \frac{z_2(t)}{m} + q_{2\beta} \frac{z_3(t)}{m} \right] I_{t>c_2} \right\} \left[1 - \frac{z(t)}{m} \right], \\
z'_3(t) &= m \left\{ \left[p_3 + q_3 \frac{z_1(t)}{m} + q_3 \frac{z_2(t)}{m} + q_3 \frac{z_3(t)}{m} \right] I_{t>c_2} \right\} \left[1 - \frac{z(t)}{m} \right], \\
m &= m_\alpha (1 - I_{t>c_2}) + m_\beta I_{t>c_2}, \\
z(t) &= z_1(t) + z_2(t) + z_3(t) I_{t>c_2}.
\end{aligned} \tag{A.5}$$

If all three competitors enter the market together, then there is a synchronic competition. In this case, only the second phase of model (2.1) is appropriate; this is called the USC model, and it can be represented as

$$\begin{aligned}
z'_1(t) &= m \left[p_1 + (q_1 + \varepsilon) \frac{z_1(t)}{m} + (q_1 + \eta) \frac{z_2(t)}{m} + q_1 \frac{z_3(t)}{m} \right] \left[1 - \frac{z(t)}{m} \right], \\
z'_2(t) &= m \left[p_2 + (q_2 + \theta) \frac{z_1(t)}{m} + (q_2 + \xi) \frac{z_2(t)}{m} + q_2 \frac{z_3(t)}{m} \right] \left[1 - \frac{z(t)}{m} \right], \\
z'_3(t) &= m \left[p_3 + (q_3 - \varepsilon - \theta) \frac{z_1(t)}{m} + (q_3 - \eta - \xi) \frac{z_2(t)}{m} + q_3 \frac{z_3(t)}{m} \right] \left[1 - \frac{z(t)}{m} \right], \\
z(t) &= z_1(t) + z_2(t) + z_3(t).
\end{aligned} \tag{A.6}$$

Under the restriction $\varepsilon = \eta = \theta = \xi = 0$, (A.6) reduces a balanced model, called the BSC model of three competitors, and it can be written as

$$\begin{aligned}
z'_1(t) &= m \left[p_1 + q_1 \frac{z_1(t)}{m} + q_1 \frac{z_2(t)}{m} + q_1 \frac{z_3(t)}{m} \right] \left[1 - \frac{z(t)}{m} \right], \\
z'_2(t) &= m \left[p_2 + q_2 \frac{z_1(t)}{m} + q_2 \frac{z_2(t)}{m} + q_2 \frac{z_3(t)}{m} \right] \left[1 - \frac{z(t)}{m} \right], \\
z'_3(t) &= m \left[p_3 + q_3 \frac{z_1(t)}{m} + q_3 \frac{z_2(t)}{m} + q_3 \frac{z_3(t)}{m} \right] \left[1 - \frac{z(t)}{m} \right], \\
z(t) &= z_1(t) + z_2(t) + z_3(t).
\end{aligned} \tag{A.7}$$

Appendix B

Applications of the three-competitor diffusion model with a fixed m to other countries

B.1 China

Over the last few decades, China has been observing a consistent and remarkable expansion in the energy sector (Shen and Luo, 2015). With an average annual increase of 50%, the total energy consumption reached 2329 Mtoe in 2009 from 132 Mtoe in 1965. By this time, China become the world's largest energy consumer (see source-specific data in British Petroleum, 2016). To meet this rapidly rising demand, China produces huge amounts of energy from coal. Roughly 90% of the world's total coal is produced by 10 countries, with China in the lead (47%). Moreover, the country consumes more than half of the total global coal consumption¹. Lack of environmental consciousness over the decades leads China to depend heavily on coal (Crompton and Wu, 2005). However, in recent years, environmental awareness regarding the use of green energy has been developing among China's citizens. This trend has been acknowledged by policymakers, which is reflected in the respective public policies. For instance, since 2005, the Government of China has approved several policies to support the growth of renewables and reduce the CO₂ emissions (Shen and Luo, 2015). These policies were also underlined to sustain local industries (e.g. PV cell manufacturers). A faster growth in the consumption of CGON sources was observed between 2000 and 2010 (Figure B.1).

¹Worldatlas. The top 10 coal producers worldwide. <http://www.worldatlas.com/articles/the-top-10-coal-producers-worldwide.html>

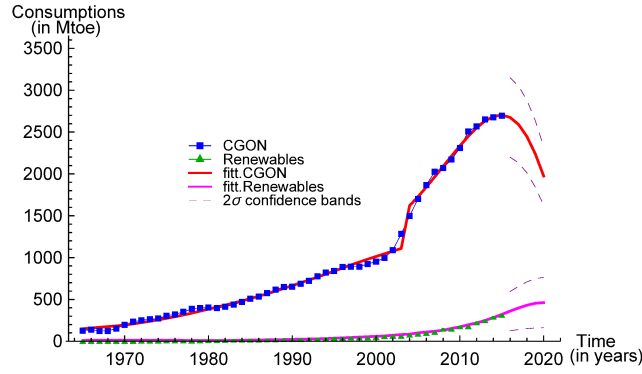


FIGURE B.1: China, 2CM. Energy consumption (Mtoe) from CGON sources (squares) and renewables (triangles). The solid lines correspond to the UUC fitted model with two shocks (one for each competitor). The broken lines represent 2σ predictions' confidence bands.

A substantial increase in the use of renewables has been observed since 2005.

Although China is quite young in the nuclear sector, its policy is to ‘go global’ with exporting nuclear technology, with heavy components in the supply chain (Nuclear Power in China (NPC), 2018). In 1993, China consumed only 0.4 Mtoe of energy from nuclear sources, against over 775 Mtoe from CGO and 35 Mtoe from renewable sources (British Petroleum, 2016). Nuclear and fossil fuel consumptions are separately presented in Figure B.2. The use of CGO and CGON sources follow a similar trend, as the use of nuclear energy has been increasing over time.

First, the energy data from China are partitioned as CGON sources and renewables. In this case, model (A.1), a UUC model, with two exponential shocks (one for each competitor) is applied. The fitting of the model is good overall, as the value of R^2 ($= 0.99822$) is adequately large. The shocks are significant, as the F -ratio, comparing the fitted models with and without shocks, provides a large value ($\hat{F} = 93.26312$).

When the data are partitioned into three sources (CGO, renewables and nuclear), a diachronic competition model is proposed, as the first two products exist from the beginning and the third enters the market at a later time. Thus, the UCRC model, in Equation (2.1), with two exponential shocks (one for the CGO time series and the other for renewables) is fitted. Parameter estimates are shown in Table B.2. A notably large value of R^2 (0.99852) is a proof of a well-fitted model. The shocks are significantly incorporated into the models, as the F -ratio, comparing the fit of the model with the UCRC without shocks, produces a large value ($\hat{F} = 28.15374$). The shock occurred at $1965 + \hat{a}_1 \simeq 2004$ for the CGO series and $1965 + \hat{a}_2 = 2006$ for renewables. The shocks were estimated as positive ($\hat{c}_1 = 0.32721$ and $\hat{c}_2 = 0.26777$) and did not fade over time (positive \hat{b}_1 and \hat{b}_2). The positive shock for CGO sources can be explained by the fact

TABLE B.1: China, 2CM. Estimates, standard errors and marginal linearised 95% confidence intervals of the UUC model with two exponential shocks (one for each competitor).

Parameter	Estimate	Standard error	95% Confidence interval
m	72383.6	5667.05	{61123.3, 83643.9}
p_1	0.00207	0.00024	{0.00159, 0.00254}
q_1	0.04959	0.36525	{-0.67614, 0.77532}
δ	0.01913	0.37891	{-0.73375, 0.77201}
c_1	0.41564	0.02368	{0.36859, 0.46270}
b_1	0.10764	0.01249	{0.08283, 0.13245}
a_1	40.0000	0.00106	{39.9979, 40.0021}
p_2	0.00015	0.00014	{-0.00013, 0.00043}
q_2	0.42129	0.23942	{-0.05444, 0.89702}
γ	0.43481	0.24954	{-0.06102, 0.93063}
c_2	0.09416	0.19070	{-0.28475, 0.47307}
b_2	0.19221	0.13706	{-0.08013, 0.46454}
a_2	40.7539	0.00345	{40.7471, 40.7608}
R^2	0.99822		

that, after 2002, the use of coal sharply increased in China, as it is relatively cheap to extract. A sharp increasing trend in the GHG emissions in China has been observed since the early 1990s, and by 2007, the emission exceeded the amount produced by the United States, the world's biggest carbon dioxide polluter. Moreover, the positive shock for renewables may indicate the country's policies with an alignment to the Paris Agreement, where China declared that it would cut the carbon intensity by 60–65% by 2030, compared with the 2005 level².

While focussing the findings of 3CM, we observe that the second phase of the market potential ($\hat{m}_\beta = 70932$ Mtoe) is about two times larger than that of the first phase ($\hat{m}_\alpha = 37405$ Mtoe). Since the innovative and imitative components of the first phase are similar to those with 2CM, we concentrate on the second phase only. Substituting the estimated parameters in the second phase of model (2.1), we obtain the following three equations:

$$z'_1(t) \propto -0.00055 + 0.09754 z_1(t)/m_\beta - 0.33685 z_2(t)/m_\beta - 0.45635 z_3(t)/m_\beta$$

$$z'_2(t) \propto 0.00037 - 0.01270 z_1(t)/m_\beta + 0.37428 z_2(t)/m_\beta - 0.09156 z_3(t)/m_\beta$$

$$z'_3(t) \propto 0.00054 - 0.00453 z_1(t)/m_\beta + 0.04288 z_2(t)/m_\beta + 0.62822 z_3(t)/m_\beta.$$

²www.nytimes.com/2017/06/02/world/asia/chinas-role-in-climate-change-and-possibly-in-fighting-it.html

The effect of CGO sources on the evolution of CGO, called the within-product WOM effect, is positive ($\hat{q}_{1\beta} + \hat{\varepsilon}_{\beta} = 0.09754$), while the evolution of renewables and nuclear, called cross-product WOM effects, have a negative influence on CGO ($\hat{q}_{1\beta} + \hat{\eta}_{\beta} = -0.33685$ and $\hat{q}_{1\beta} = -0.45635$, respectively). This means that the level of diffusion of CGO is increased by its own spread but reduced by the spread of its competitors. Like CGO, renewables' within-product effect is positive ($\hat{q}_{2\beta} + \hat{\xi}_{\beta} = 0.37428$), and the cross-product effects of both CGO ($\hat{q}_{2\beta} + \hat{\theta}_{\beta} = -0.01270$) and nuclear ($\hat{q}_{2\beta} = -0.09156$) are negative. That is, the level of diffusion of renewables is increased by their spread but reduced by that of competitors. Moreover, the within-product effect of nuclear is positive ($\hat{q}_{3\beta} = 0.62822$), while its cross-product effects by CGO sources and renewables are negative ($\hat{q}_{3\beta} - \hat{\varepsilon}_{\beta} - \hat{\theta}_{\beta} = -0.00453$) and positive ($\hat{q}_{3\beta} - \hat{\eta}_{\beta} - \hat{\xi}_{\beta} = 0.04288$), respectively. This means that the speed of nuclear diffusion is accelerated by its own and diffusion by renewables' spread but reduced by CGO diffusion.

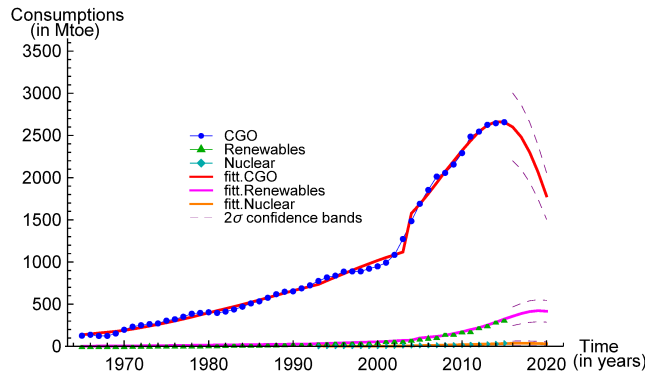


FIGURE B.2: China, 3CM. Energy consumption (Mtoe) from CGO sources (circles), renewables (triangles) and nuclear (diamonds). The solid lines correspond to the UCRCD fitted model with two shocks (one for CGO and the other for renewables). The broken lines represent 2σ predictions' confidence bands.

Regarding the within-product effects, all three sources of diffusion are sustained by their further internal consumptions. In terms of cross-product effects, none of the competing sources support CGO expansion, as the level of consumption is already excessively high, resulting in the world's biggest emitter of greenhouse gases from fossil fuels. The development of renewables is hindered because it competes with the relatively less expensive fossil fuels. With the aim of promoting investment in renewables, China has introduced FiT (Market Watch, 2016). Moreover, the higher productivity of nuclear sources makes those economically more attractive over renewables (China-dialogue, 2013). Considering that nuclear sources of energy has no claim for global warming, China is positively motivated to the use of nuclear energy sources. However,

TABLE B.2: China, 3CM. Estimates, standard errors and marginal linearised 95% confidence intervals of the UCRC model with two shocks (one for CGO sources and the other for renewables).

Parameter	Estimate	Standard error	95% Confidence interval
m_α	37405.2	9929.03	{17711.0, 57099.4}
$p_{1\alpha}$	0.00367	0.00084	{0.00200, 0.00534}
$q_{1\alpha}$	0.13909	0.75055	{-1.34963, 1.62781}
δ_α	-0.05968	0.77215	{-1.59123, 1.47186}
$p_{2\alpha}$	0.00008	0.00025	{-0.00043, 0.00058}
$q_{2\alpha}$	-0.05403	0.74527	{-1.53227, 1.42421}
m_β	70932.0	7204.58	{56641.7, 85222.2}
$p_{1\beta}$	-0.00055	0.00229	{-0.00509, 0.00399}
$q_{1\beta}$	-0.45635	3.17901	{-6.76190, 5.84921}
ε_β	0.55389	3.19182	{-5.77706, 6.88484}
η_β	0.11950	3.22989	{-6.28697, 6.52596}
c_1	0.32721	0.03217	{0.26340, 0.39102}
b_1	0.12754	0.01415	{0.09946, 0.15561}
a_1	39.1721	0.00134	{39.1694, 39.1747}
$p_{2\beta}$	0.00037	0.00279	{-0.00516, 0.00590}
$q_{2\beta}$	-0.09156	3.20178	{-6.44228, 6.25915}
θ_β	0.07886	3.21342	{-6.29495, 6.45268}
ξ_β	0.46584	3.31426	{-6.10797, 7.03966}
c_2	0.26777	0.60561	{-0.93346, 1.46899}
b_2	0.14337	0.20467	{-0.26259, 0.54934}
a_2	41.0000	0.02325	{40.9539, 41.0461}
p_3	0.00054	0.00140	{-0.00223, 0.00331}
q_3	0.62822	1.98373	{-3.30650, 4.56294}
R^2	0.99852		

the use of nuclear sources of energy is curbed by the use of CGO sources because of their long tradition and lower costs.

The solid lines (the fitted data) in Figures B.1 and B.2 accurately follow the respective observed paths. Hence, the models fit well to the data, and the predictions over the period from 2016 to 2020 may be considered reliable. According to the 2CM predictions, the consumption of CGON sources may decline sharply against a notable increase in the use of renewables. In contrast, the predictions using the 3CM models indicate a rapid decline of CGO sources, substantial increase of renewables and stable state or trivial increase of nuclear sources. This may be due to the continuous evolution of China's energy mix, with coal's dominance declining from 66% in 2014 to 47% in 2035, but

TABLE B.3: China. Confidence band width of 2CM and 3CM predictions in 2016–2020.

Year	2CM		3CM		
	CGON ($\hat{\sigma}_u=0.08869$)	Renewables ($\hat{\sigma}_u=0.32436$)	CGO ($\hat{\sigma}_u=0.07742$)	Renewables ($\hat{\sigma}_u=0.15474$)	Nuclear ($\hat{\sigma}_u=0.37148$)
2016	948.59818	468.13508	805.04921	221.20378	53.80993
2017	919.05892	516.44322	768.44861	240.71042	55.15661
2018	867.91948	559.11796	712.67286	255.32121	54.26001
2019	794.51652	589.58268	639.33230	261.96062	50.90648
2020	700.43216	600.06843	552.25140	257.83103	45.26108

natural gas more than doubling to 11%. Moreover, the share of oil remains consistent (at around 19%), and the share of nuclear energy increases by 12%. The target use of renewables is surprisingly high (+593%; see British Petroleum, 2016).

We computed the ‘scaled residuals’ for each of the products for both models (2CM and 3CM). The Kolmogorov–Smirnov test confirmed the normality assumption for scaled residuals. The standard deviations of scaled residuals ($\hat{\sigma}_u$) for CGON and renewables in the 2CM are 0.08869 and 0.32436, respectively, and those obtained with the 3CM are 0.07742 for CGO, 0.15474 for renewables and 0.37148 for nuclear. Accordingly, we computed the 2σ confidence bands, represented by broken lines in Figures B.1 and B.2, and the corresponding band width (see Table B.3). The confidence bands of the prediction for renewables obtained through the 3CM are almost half of those obtained through the 2CM. This means that the 3CM is more appropriate for providing reliable predictions about the energy market of China. Both models suggest an increasing trend in the consumption of renewables in 2016–2020. In 2014, a 32% increase from the previous year in the investments in renewables was reported, and the investment of China in this sector reached US\$ 89.5 billion (Bloomberg New Energy Finance (BNEF), 2015). China is the leading investor in renewables, and by 2020, the world’s largest energy operator plans to have 100 GW of solar and 200 GW of wind installed (China Analysis, 2015).

B.1.1 An alternative partition of energy sources as two competitors

Findings of the previous section conclude that the 3CM performs better than the 2CM. This is true in describing the lifecycle of energy sources and also in achieving reliable predictions. Further comparison of the performance of 3CM and 2CM with an

TABLE B.4: China, 2CM. Estimates, standard errors and marginal linearised 95% confidence intervals of the UUC model with two exponential shocks (one for each competitor) for an alternative partition of energy sources.

Parameter	Estimate	Standard error	95% Confidence interval
m	72357.7	5245.88	{61934.2, 82781.2}
p_1	0.00207	0.00022	{0.00163, 0.00252}
q_1	0.04961	0.29745	{-0.54141, 0.64064}
δ	0.01916	0.30882	{-0.59446, 0.63278}
c_1	0.41564	0.02778	{0.36045, 0.47084}
b_1	0.10738	0.01253	{0.08248, 0.13228}
a_1	40.0000	0.00124	{39.9975, 40.0025}
p_2	0.00015	0.00014	{-0.00013, 0.00043}
q_2	0.42124	0.18052	{0.06256, 0.77992}
γ	0.43486	0.18850	{0.06032, 0.80940}
c_2	0.08986	0.16166	{-0.23134, 0.41107}
b_2	0.18694	0.13086	{-0.07308, 0.44695}
a_2	41.0021	0.00272	{40.9967, 41.0075}
R^2	0.99812		

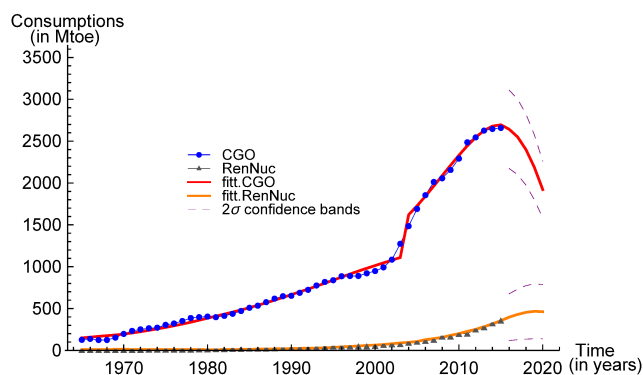


FIGURE B.3: China, 2CM. Energy consumption (Mtoe) from CGO sources (circles) and RenNuc (triangles). The solid lines correspond to the UUC fitted model with two shocks (one for each competitor). The broken lines represent 2σ predictions' confidence bands.

alternative partition of energy sources would help to arrive a stronger conclusion. If in the alternative partitioning, the predictions of leading products using 3CM produce smaller confidence bands (as compared to the 2CM), the findings of the previous section would be established with further evidence.

Now, we consider the following partition of energy sources from China as two competitors: CGO and RenNuc (renewables and nuclear). To this new partitioned energy data from China, model (A.1), a UUC model, with two exponential shocks (one for

TABLE B.5: China. Confidence band width of 2CM (CGO and RenNuc) and 3CM predictions in 2016–2020.

Year	2CM		3CM		
	CGO ($\hat{\sigma}_u=0.08855$)	RenNuc ($\hat{\sigma}_u=0.35136$)	CGO ($\hat{\sigma}_u=0.07742$)	Renewables ($\hat{\sigma}_u=0.15474$)	Nuclear ($\hat{\sigma}_u=0.37148$)
2016	935.63688	558.57264	805.04921	221.20378	53.80993
2017	903.42727	604.04859	768.44861	240.71042	55.15661
2018	849.93114	638.81646	712.67286	255.32121	54.26001
2019	774.95722	656.22851	639.33230	261.96062	50.90648
2020	680.61999	649.62854	552.25140	257.83103	45.26108

each competitor) is applied. A substantially large value of R^2 (0.99812) proves that the fitting is good (see Table B.4). The shocks are significantly incorporated into the model, as the F -ratio, comparing the fitted models with and without shocks, provides a large value ($\hat{F} = 84.88399$). The fitted lines in Figure B.3 accurately follow the observed paths, consequently, the predictions from 2016 to 2020 are reliable. The scaled residuals of CGO and RenNuc energy sources follow a Gaussian distribution, which is verified by the Kolmogorov–Smirnov test. Hence, the 2σ confidence bands for predictions are computed and represented by broken lines in Figure B.3. The band width for predictions is also computed and shown in Table B.5.

In both 2CM and 3CM, only CGO sources are common, hence, the corresponding findings are considered in making a comparison between the two models. We see that the band width for CGO sources using 2CM is larger than that obtained with 3CM. This means that the 2CM predictions are less reliable than the 3CM predictions. This result confirms the conclusion reached when nuclear energy was added to CGO sources. That is, the 3CM models are more suitable for reducing the forecasting uncertainty along with describing the more specific features of products.

B.2 Finland

Among the EU member states, Finland stands at the second position (after Luxembourg) in per capita energy consumption. In 2003, the per capita energy consumption of Finland (188.3) was much higher than the EU-25 average (100) and Japanese (107.2) levels. The consumption is comparable with that of the United States (207.3; Eurostat, 2006). With an alignment to the Kyoto Protocol, the Government of Finland has developed a national strategy ensuring the reduction of the emission of gases responsible

for global warming. The key feature of the policy includes technological development. The availability of sufficient funding remains at the center of the policy (Academy of Finland, 2006). The two main foci of the development are the promotion of renewable sources and gain of efficiency. In terms of renewables, the development and utilisation of bio-energy and bio-fuels are encouraged, whereas efficiency refers to the cogeneration, production through industries, decentralisation and supply system (Academy of Finland, 2006).

Renewables have a significant share in the total energy consumption of Finland. For instance, in 1965, the country consumed 7.5 Mtoe of energy from CGON sources and 2.1 Mtoe from renewables (British Petroleum, 2016). Until 1989, the only renewable source of energy was hydroelectricity. The three other sources of renewables are currently geothermal and biomass (launched in 1990), solar (1991) and wind (1992). From Figure B.4, we observe a sharp increasing trend in the consumption of CGON until 2006. From this timepoint, the use of the source declines drastically. This may be due to the Finnish policies targeting a 16% reduction (compared to 2005) of non-emission trading scheme (ETS) emission by 2020. The estimated reduction in the emissions during 2005–2011 was 9% (Eclareon, 2014). With minor fluctuations, the consumption of energy from renewables observed a substantially increasing trend over time. The ambitious renewable energy programmes in Finland were designed to meet 38% total energy consumption from renewables by 2020. Since Finland is the most forested country in Europe, biomass may play the major role in meeting the target.

The first nuclear reactor in Finland came into operation in 1977, with a generation capacity of about 0.5 Mtoe of energy (Nuclear Power in Finland (NPF), 2018). Over

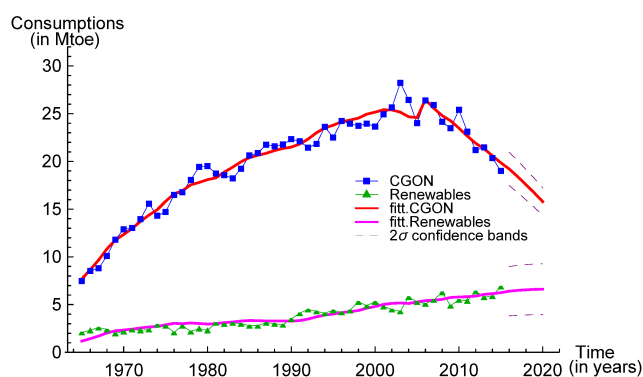


FIGURE B.4: Finland, 2CM. Energy consumption (Mtoe) from CGON sources (squares) and renewables (triangles). The solid lines correspond to the UUC fitted model with two shocks (one for each competitor). The broken lines represent 2 σ predictions' confidence bands.

TABLE B.6: Finland, 2CM. Estimates, standard errors and marginal linearised 95% confidence interval of the UUC model with two exponential shocks (one for each competitor).

Parameter	Estimate	Standard error	95% Confidence interval
m	1557.53	31.9551	{1494.04, 1621.03}
p_1	0.00495	0.00022	{0.00451, 0.00538}
q_1	0.62850	0.10026	{0.42928, 0.82771}
δ	-0.67291	0.11578	{-0.90297, -0.44285}
c_1	0.08640	0.02857	{0.02963, 0.14318}
b_1	-0.23836	0.24100	{-0.71723, 0.24051}
a_1	41.9413	0.00059	{41.9401, 41.9425}
p_2	0.00076	0.00029	{0.00018, 0.001332}
q_2	0.22994	0.09540	{0.04038, 0.41949}
γ	0.25943	0.11047	{0.03993, 0.47893}
c_2	0.04333	0.09696	{-0.14933, 0.23600}
b_2	0.07989	0.05801	{-0.03538, 0.19516}
a_2	16.0000	0.00034	{15.9993, 16.0007}
R^2	0.99305		

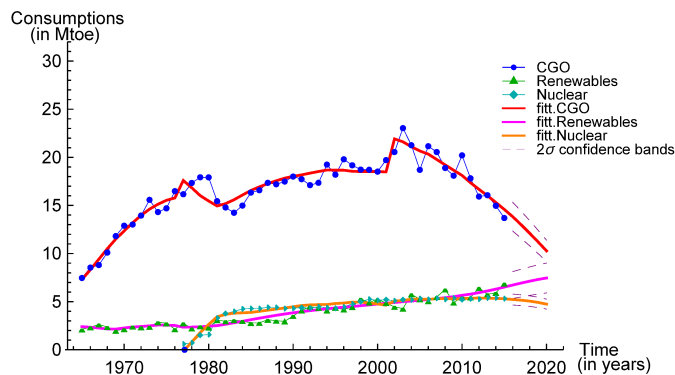


FIGURE B.5: Finland, 3CM. Energy consumption (Mtoe) from CGO sources (circles), renewables (triangles) and nuclear (diamonds). The solid lines correspond to the UCRCF fitted model with three shocks (one for each competitor). The broken lines represent 2σ predictions' confidence bands.

time, the country's dependency on nuclear sources of energy has been increasing noticeably. The four nuclear reactors functioning (about 2700 Megawatts electric, MWe, net total) in Finland are considered among the world's most efficient, in terms of average lifetime and average capacity factor (over 85%; NPF, 2018). In Figure B.5, we see that, after a rapid increase in the initial years, the consumption of nuclear energy sources became almost constant. A rapidly increasing trend in the consumption of CGO sources is observed at the beginning, while between 1981 and 2004, it follows a U-shape. A sharp

TABLE B.7: Finland, 3CM. Estimates, standard errors and marginal linearised 95% confidence interval of the UCRC model with three shocks, one for each competitor.

Parameter	Estimate	Standard error	95% Confidence interval
m_α	415.510	88.3780	{240.450, 590.570}
$p_{1\alpha}$	0.01757	0.00351	{0.01063, 0.02452}
$q_{1\alpha}$	0.30491	0.21822	{-0.12734, 0.73716}
δ_α	-0.22818	0.27058	{-0.76415, 0.30778}
$p_{2\alpha}$	0.00579	0.00135	{0.00311, 0.00847}
$q_{2\alpha}$	-0.17941	0.22732	{-0.62968, 0.27086}
m_β	1499.39	97.9620	{1305.35, 1693.44}
$p_{1\beta}$	0.01813	0.00222	{0.01374, 0.02253}
$q_{1\beta}$	0.41368	0.07792	{0.25933, 0.56802}
ε_β	-0.47725	0.08317	{-0.64200, -0.31250}
η_β	-0.33901	0.18450	{-0.70446, 0.02645}
c_1	0.19662	0.03180	{0.13363, 0.25961}
b_1	0.00899	0.06386	{-0.11751, 0.13549}
a_1	37.9798	0.08955	{37.8024, 38.1571}
$p_{2\beta}$	0.00169	0.00211	{-0.00250, 0.00587}
$q_{2\beta}$	0.06223	0.07833	{-0.09293, 0.21739}
θ_β	-0.05986	0.08175	{-0.22178, 0.10206}
ξ_β	-0.06988	0.19678	{-0.45968, 0.31991}
c_2	0.00391	0.01273	{-0.02129, 0.02912}
b_2	0.16175	0.05223	{0.05830, 0.26521}
a_2	14.9531	12.6061	{-10.0173, 39.9235}
p_3	-0.00741	0.00159	{-0.01055, -0.00427}
q_3	-0.22710	0.05179	{-0.32969, -0.12451}
c_3	0.10944	0.07572	{-0.04056, 0.25943}
b_3	0.18317	0.04077	{0.10242, 0.26392}
a_3	37.8745	0.57089	{36.7437, 39.0053}
R^2	0.99080		

declining trend in the use of such sources has been observed since then.

Model (A.1), UUC, with two exponential shocks (one for each competitor) is applied to the data from Finland, partitioned as CGON sources and renewables. An adequately large value of R^2 (0.99305) suggests that the fitting is good overall. The fitted model significantly differs from the UUC model without shocks, as the value of the F -ratio ($\hat{F} = 4.457255$) is larger than the threshold of 4.

When the data are partitioned into three sources (CGO, renewables and nuclear), we consider that CGO and renewables exist from the beginning, while nuclear enters

the market later. Thus, the model in Equation (2.1), a UCRC model with three exponential shocks (one for each competitor), is suitably fitted. The shocks are significant, since the value of the F -ratio, comparing the fitted model with the UCRC model without shocks, is large ($\hat{F} = 9.85032$). The shocks rose at time $1965 + \hat{a}_1 \simeq 2003$ for the CGO time series, time $1965 + \hat{a}_2 \simeq 1980$ for renewables and time $1965 + \hat{a}_3 \simeq 2003$ for nuclear. All three shocks were estimated to be positive ($\hat{c}_1 = 0.19662$, $\hat{c}_2 = 0.16175$ and $\hat{c}_3 = 0.10944$) and not yet faded in time (\hat{b}_1 , \hat{b}_2 and \hat{b}_3 are positive). The shock of renewables may be motivated by the incentives provided by the government to increase renewable consumption in 1980–81, when CGO consumptions abruptly declined. Moreover, the shock of nuclear may be linked to Finland's parliamentary vote in May 2002, approving the building of a fifth nuclear power reactor (NPF, 2018).

The market potential of the second phase ($\hat{m}_\beta = 1499.39$) is more than three times that of the first phase ($\hat{m}_\alpha = 415.51$). Now, by substituting the estimated parameters in the second phase of model (2.1), the following three equations can be obtained:

$$\begin{aligned} z'_1(t) &\propto -0.00741 - 0.06357 z_1(t)/m_\beta + 0.07467 z_2(t)/m_\beta + 0.41368 z_3(t)/m_\beta \\ z'_2(t) &\propto 0.00169 + 0.12209 z_1(t)/m_\beta - 0.00765 z_2(t)/m_\beta + 0.06223 z_3(t)/m_\beta \\ z'_3(t) &\propto -0.00741 + 0.31001 z_1(t)/m_\beta + 0.18179 z_2(t)/m_\beta - 0.22710 z_3(t)/m_\beta. \end{aligned}$$

The innovative effect of CGO ($\hat{p}_1 = 0.01813$) is far larger than that of nuclear ($\hat{p}_3 = -0.00741$), and the effect of renewables is also considerable ($\hat{p}_2 = 0.00169$). The within-product WOM effect of CGO is negative ($\hat{q}_{1\beta} + \hat{\varepsilon}_\beta = -0.06357$), and its cross-product effects by both renewables and nuclear are positive ($\hat{q}_{1\beta} + \hat{\eta}_\beta = 0.07467$ and $\hat{q}_{1\beta} = 0.41368$, respectively). Similarly, renewables and nuclear have negative within-product effects ($\hat{q}_{2\beta} + \hat{\xi}_\beta = -0.00765$ for renewables and $\hat{q}_{3\beta} = -0.22710$ for nuclear) and positive cross-product effects. More specifically, renewables' cross-product effects by CGO and nuclear are $\hat{q}_{2\beta} + \hat{\theta}_\beta = 0.12209$ and $\hat{q}_{2\beta} = 0.06223$, respectively. The corresponding effects of nuclear by CGO and renewables are $\hat{q}_{3\beta} - \hat{\varepsilon}_\beta - \hat{\theta}_\beta = 0.31001$ and $\hat{q}_{3\beta} - \hat{\eta}_\beta - \hat{\xi}_\beta = 0.18179$, respectively. That is, none of the products' diffusion is sustained by further internal consumptions; however, they are supported by the spread of their competitors. Specifically, nuclear receives strong support from its competitors, followed by CGO sources and renewables.

In Figure B.5, the fitted lines accurately follow the observed path. The predictions suggest a steep decline of CGO sources and a narrower increase of renewables in 2016–2020, with a minor decline of nuclear. Observe that the fitted and observed values are not well matched in the first part of the nuclear series. Therefore, we removed

TABLE B.8: Finland. Confidence band width of 2CM and 3CM predictions in 2016–2020.

Year	2CM		3CM		
	CGON ($\hat{\sigma}_u=0.04537$)	Renewables ($\hat{\sigma}_u=0.20138$)	CGO ($\hat{\sigma}_u=0.05406$)	Renewables ($\hat{\sigma}_u=0.10394$)	Nuclear ($\hat{\sigma}_u=0.05438$)
2016	3.48633	5.16328	2.99068	2.79693	1.13561
2017	3.34114	5.22772	2.80906	2.88174	1.12100
2018	3.18870	5.27605	2.62009	2.96363	1.09977
2019	3.03080	5.31633	2.42428	3.03839	1.07049
2020	2.86565	5.32438	2.22249	3.10090	1.03197

the first four residuals of nuclear when computing the scaled residuals' variance. The Kolmogorov–Smirnov test confirmed the assumption that scaled residuals of 2CM and 3CM follow a Gaussian distribution. The standard deviations of scaled residuals ($\hat{\sigma}_u$) using 2CM are 0.04537 and 0.20138 for CGON and renewables, and those using 3CM are 0.05406, 0.10394 and 0.05438 for CGO, renewables and nuclear, respectively. We computed 2σ confidence bands of predictions for both models, see Figures B.4 and B.5, and the corresponding band width, shown in Table B.8. With respect to the 2CM, the confidence bands of renewables predictions with the 3CM are much narrower. This means that the 3CM is more appropriate to make forecasts on the Finnish energy market.

B.3 France

France has the second largest electricity generation capacity of the EU member states, and the second ‘less-carbonised’ electricity generation mix after Sweden (Deloitte, 2015b). Of the French primary energy consumption, nuclear energy accounts for the greatest share today, while fossil fuels still play an important role. Biomass is the leading source of renewable energy in France (more than 50% of renewable consumption, second in Europe after Germany), ahead of hydroelectricity, wind and solar energy³. Despite having a high-volume electricity generation capacity, France imports almost half of its energy demands and uses around 2.5% of the global energy supply (Planete-energies, 2015a). According to source-specific data (British Petroleum, 2016), in 1965, French total energy consumption was approximately 111 Mtoe, where the share of renewables, represented only by hydroelectric energy, was only 11 Mtoe. Geothermal and biomass were launched as renewables in 1966, and after more than two decades,

³Renewable energy research in France. campusfrance.org.

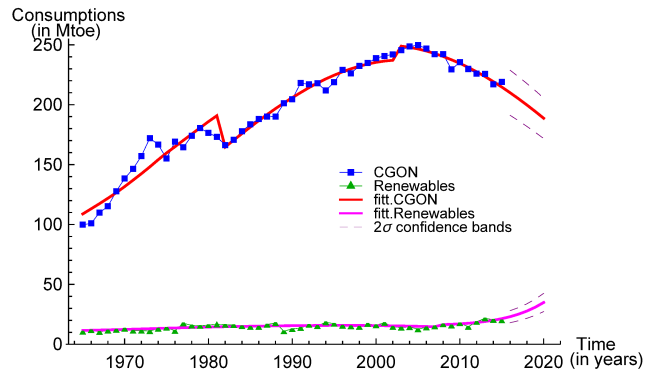


FIGURE B.6: France, 2CM. Energy consumption (Mtoe) from CGON sources (squares) and renewables (triangles). The solid lines correspond to the BSC fitted model with three exponential shocks (two for CGON and one for renewables). The broken lines represent 2σ predictions' confidence bands.

wind and solar energy were launched in 1990 and 1992, respectively. Figure B.6 shows that the consumption of CGON sources sharply increased between 1965 and 1974 and fluctuated widely for the next decade. Further, it sharply increased until 2006 and substantially declined after this year. Over time, the use of renewables narrowly increased with regular fluctuations.

France started to use nuclear energy in 1965, and nuclear power has been the leading energy sector since 2002 (British Petroleum, 2016). According to the Nuclear Power in France (NPF; 2018), France derives about 75% of its electricity from nuclear energy because of a long-standing policy based on energy security, and 17% of its' electricity comes from recycled nuclear fuel. Figure B.7 shows that the consumption of CGO sources sharply increased until 1977, when the use of nuclear was limited. Later, CGO sources rapidly reduced due to a rapid increase of nuclear capacity between 1978 and 1990. After some fluctuations, CGO sources have been declining in recent years, whereas nuclear has been running through a (roughly) constant path since 2005.

First, the energy data from France have been separated into two sources, namely CGON and renewables. Model (A.3), BSC, with three exponential shocks (two for CGON time series and one for renewables) is applied. The value of R^2 (0.99729) is adequate to conclude that the fitting is good. The F -ratio, obtained to compare the fitted models with and without shocks, gives a large value ($\hat{F} = 10.17812$). This means that the shocks are significant.

Next, the data were partitioned into three sources, as follows: CGO, renewables and nuclear. Since all three competitors enter the market simultaneously, model (A.6), USC, with three exponential shocks (one for each competitor) is applied. The shocks are found to be significant, as the F -test, comparing the fitted model with the USC without

TABLE B.9: France, 2CM. Estimates, standard errors and marginal linearised 95% confidence intervals of the BSC model with three shocks (two for CGON sources and one for renewables).

Parameter	Estimate	Standard error	95% Confidence interval
m	16508.4	748.777	{15020.4, 17996.5}
p_1	0.00659	0.00029	{0.00602, 0.00716}
q_1	0.04570	0.00208	{0.04156, 0.04983}
c_1	-0.15792	0.02047	{-0.19859, -0.11724}
b_1	-0.06897	0.02803	{-0.12466, -0.01327}
a_1	17.9545	0.03154	{17.8918, 18.0172}
c_2	0.04698	0.01866	{0.00990, 0.08407}
b_2	-0.07278	0.19762	{-0.46550, 0.31994}
a_2	38.9892	0.25129	{38.4898, 39.4886}
p_2	0.00070	0.00010	{0.00050, 0.00090}
q_2	0.00220	0.00047	{0.00126, 0.00313}
c_3	0.12657	0.17695	{-0.22508, 0.47823}
b_3	0.22943	0.20716	{-0.18227, 0.64113}
a_3	43.5560	$2.24 * 10^{-7}$	{43.5560, 43.5560}
R^2	0.99729		

shocks, provides the value of $\hat{F} = 12.74395$. The shocks occurred at $1965 + \hat{a}_1 = 1981$ for the CGO time series, $1965 + \hat{a}_2 \simeq 2008$ for renewables and $1965 + \hat{a}_3 \simeq 2014$ for nuclear. The shocks for CGO and nuclear sources were estimated to be negative ($\hat{c}_1 = -0.26083$ and $\hat{c}_3 = -0.08535$, respectively) and that of renewables was estimated to be positive ($\hat{c}_2 = 0.08360$). None of the three shocks decayed over time (positive \hat{b}_1 , \hat{b}_2 and \hat{b}_3). The shock for CGO sources may represent the effect of the second oil crisis in 1979, as France does not have significant oil resources on its territory. The shock of renewables can be explained in that the French renewable energy sector offers admirable investment opportunities owing to the FiT mechanism, announced in 2008, for boosting renewables growth. The shock of nuclear may be an effect of the French National Assembly's Deputies voting to reduce the country's reliance on nuclear power to reduce its 2012 electricity supply levels by half by the year 2050⁴.

⁴The Local. www.thelocal.fr/20141010/france-votes-to-reduce-reliance-on-nuclear-power

TABLE B.10: France, 3CM. Estimates, standard errors and marginal linearised 95% confidence intervals of the USC model with three shocks (one for each competitor).

Parameter	Estimate	Standard error	95% Confidence interval
m	19326.4	3577.46	{12250.3, 26402.5}
p_1	0.00604	0.00110	{0.00387, 0.00821}
q_1	0.06264	0.01942	{0.02424, 0.10104}
ε	0.07453	0.01892	{0.03711, 0.11195}
η	-1.15514	0.25088	{-1.65137, -0.65892}
c_1	-0.26083	0.02215	{-0.30464, -0.21702}
b_1	0.01144	0.01263	{-0.01353, 0.03642}
a_1	16.0000	0.00007	{15.9999, 16.0001}
p_2	0.00053	0.00016	{0.00022, 0.00085}
q_2	0.00859	0.01047	{-0.01213, 0.02931}
θ	0.02821	0.01237	{0.00374, 0.05268}
ξ	-0.36854	0.23114	{-0.82572, 0.08865}
c_2	0.08360	0.20395	{-0.31981, 0.48702}
b_2	0.29126	0.27815	{-0.25892, 0.84143}
a_2	42.5465	0.00497	{42.5367, 42.5563}
p_3	-0.00074	0.00016	{-0.00106, -0.00042}
q_3	-0.01491	0.01981	{-0.05409, 0.02429}
c_3	-0.08535	0.06751	{-0.21889, 0.04818}
b_3	0.18547	0.40291	{-0.61147, 0.98240}
a_3	48.9757	0.00107	{48.9736, 48.9778}
R^2	0.98978		

By substituting the estimated parameter values in model (A.6), the following three equations can be obtained:

$$z_1'(t) \propto 0.00604 + 0.13717 z_1(t)/m - 1.0925 z_2(t)/m + 0.06264 z_3(t)/m$$

$$z_2'(t) \propto 0.00053 + 0.03680 z_1(t)/m - 0.35995 z_2(t)/m + 0.00859 z_3(t)/m$$

$$z_3'(t) \propto -0.00074 - 0.11765 z_1(t)/m + 1.50877 z_2(t)/m - 0.01491 z_3(t)/m.$$

The innovative effect for CGO sources ($\hat{p}_1 = 0.00604$) and renewables ($\hat{p}_2 = 0.00053$) is remarkably larger than the effect for nuclear ($\hat{p}_3 = -0.00074$). Turning to the imitative components, the within-product WOM effect of CGO is positive ($\hat{q}_1 + \hat{\varepsilon} = 0.13717$). The cross-product effects on CGO by renewables and nuclear are negative ($\hat{q}_1 + \hat{\eta} = -1.0925$) and positive ($\hat{q}_1 = 0.06264$), respectively. This means the diffusion level of CGO is accelerated by both its spread and that of nuclear, but it is reduced by the spread of renewables. Renewables' within-product effect is negative ($\hat{q}_2 + \hat{\xi} = -0.35995$) and

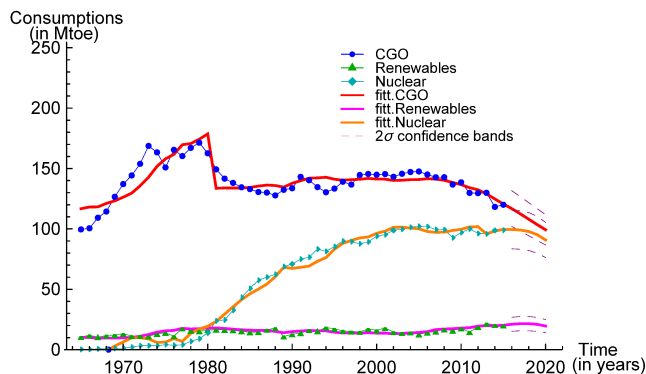


FIGURE B.7: France, 3CM. Energy consumption (Mtoe) from CGO sources (circles), renewables (triangles) and nuclear (diamonds). The solid lines correspond to the USC fitted model with three shocks (one for each competitor). The broken lines represent 2σ predictions' confidence bands.

cross-product effects by both CGO sources ($\hat{q}_2 + \hat{\theta} = 0.03680$) and nuclear ($\hat{q}_2 = 0.00859$) are positive. That is, renewables are contracted by their spread but supported by the spread of CGO sources and nuclear. The nuclear within-product effect is negative ($\hat{q}_3 = -0.01491$). Its cross-product effect by CGO sources is negative ($\hat{q}_3 - \hat{\varepsilon} - \hat{\theta} = -0.11765$) and by renewables is positive ($\hat{q}_3 - \hat{\eta} - \hat{\xi} = 1.50877$). This indicates that the level of diffusion of nuclear is reduced by the spread of its own and CGO but enhanced by renewables spread. Concerning the within-product WOM effect, the positive sign of CGO sources may be because there is still far more fossil fuel consumption than there is consumption of other sources. Moreover, the negative sign of renewables' within-product WOM may be due to the immature use of renewables over the years. Regarding the cross-product coefficient, the knowledge about the problems associated with the adoption of green technologies and the ample development of nuclear technology may support each other. CGO supports renewables expansion; however, renewables oppose further CGO consumption. Indeed, France is trying to phase out all oil and gas exploration and production through promoting renewable consumption. Nuclear supports further CGO consumptions, but CGO does not support nuclear.

The fitted lines in Figures B.6 and B.7 adequately follow the observed data. Especially in the last part of the time series, the observed and fitted paths overlap, suggesting that predictions from 2016 to 2020 may be reliable. The predictions suggest that the renewables may show a light increase or they may remain constant, while other energies may decline in 2016–2020. It should be observed that the first part of nuclear path shows reduced fitting. Thus, we ignored the first 15 residuals of nuclear in computing scaled residuals' variance. The Kolmogorov–Smirnov test confirmed the normality assumption of scaled residuals. The standard deviations of scaled residuals ($\hat{\sigma}_u$) obtained

TABLE B.11: France. Confidence band width of 2CM and 3CM predictions in 2016–2020.

Year	2CM		3CM		
	CGON ($\hat{\sigma}_u=0.04479$)	Renewables ($\hat{\sigma}_u=0.10900$)	CGO ($\hat{\sigma}_u=0.06340$)	Renewables ($\hat{\sigma}_u=0.13745$)	Nuclear ($\hat{\sigma}_u=0.08021$)
2016	37.61000	10.05058	29.61929	11.57386	31.91185
2017	36.71964	10.96417	28.53481	11.82726	31.79371
2018	35.78628	12.09893	27.40748	11.84782	31.39164
2019	34.81352	13.49955	26.27254	11.51641	30.56280
2020	33.80134	15.21805	25.17724	10.76650	29.14194

with 2CM are 0.04479 for CGON and 0.10900 for renewables. Those for 3CM products are 0.06340, 0.13745 and 0.08021 for CGO, renewables and nuclear, respectively. Accordingly, we computed 2σ confidence bands of 2CM and 3CM predictions, represented in Figures B.6 and B.7, and the corresponding band width, shown in Table B.11. The $\hat{\sigma}_u$ and Figures B.6 and B.7 highlight that predictions for renewables using the 2CM are more reliable than those obtained with the 3CM.

B.4 Germany

Germany is a huge energy consumer, with one of the world’s most powerful and competitive economy. Around four-fifths of German energy comes from fossil fuels, to which petroleum contributes the lion share, followed by coal and natural gas (Deloitte, 2015c). Despite having the largest energy system in Europe, Germany depends heavily on imported fossil fuels. However, the country has the largest share of renewable power (excluding hydroelectricity) in Europe in terms of installed capacity, which is the third largest in the world (REN21, 2014). To decarbonise the economy, the country has also introduced a transformative energy transition, called the *Energiewende*. Through this policy, Germany planned to phase out nuclear energy by 2022 (Agora Energiewende, 2015).

In 1965, Germany consumed about 250 Mtoe of energy from CGON sources and only 3.7 Mtoe from renewables (British Petroleum, 2015). Hydroelectricity has been representing renewables from the beginning. Geothermal and biomass, wind and solar energy were added to the renewable energy mix in 1979, 1986 and 1990, respectively. Figure B.8 depicts that the consumption of CGON sources sharply increased in the first few years. It was unstable during the period 1972–2000 and gradually declined after that

point. Conversely, the use of renewables was almost stable until 2010 and substantially increased after this year.

Germany strongly supported nuclear energy in the 1970s following the oil price hike of 1974 (Nuclear Power in Germany (NPG), 2018). However, doubt was cast on this policy after the Chernobyl disaster in 1986, and the last new nuclear power plant was custom

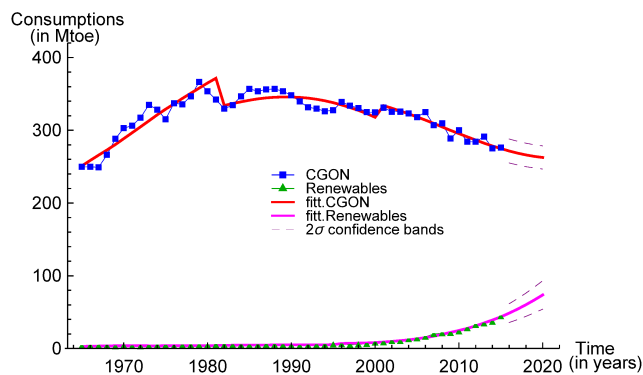


FIGURE B.8: Germany, 2CM. Energy consumption (Mtoe) from CGON sources (squares) and renewables (triangles). The solid lines correspond to the USC fitted model with three shocks (two for CGON and one for renewables). The broken lines represent 2σ predictions' confidence bands.

TABLE B.12: Germany, 2CM. Estimates, standard errors and marginal linearised 95% confidence intervals of the USC model with three shocks (two for CGON sources and one for renewables).

Parameter	Estimate	Standard error	95% Confidence interval
m	30715.7	10492.6	{9860.55, 51570.8}
p_1	0.00817	0.00272	{0.00276, 0.01359}
q_1	-0.21549	0.48746	{-1.18437, 0.75340}
δ	0.25718	0.49474	{-0.72617, 1.24054}
c_1	-0.11429	0.01843	{-0.15091, -0.07766}
b_1	0.04640	0.01280	{0.02096, 0.07184}
a_1	17.9202	0.03241	{17.8557, 17.9846}
c_2	0.05007	0.01456	{0.02113, 0.07901}
b_2	0.11558	0.02407	{0.06774, 0.16342}
a_2	36.9999	0.11061	{36.7800, 37.2197}
p_2	0.00009	0.00009	{-0.00009, 0.00028}
q_2	0.25438	0.48862	{-0.71680, 1.22556}
c_3	0.23627	0.83486	{-1.42312, 1.89565}
b_3	0.00754	0.31340	{-0.61539, 0.63046}
a_3	31.0592	$1.04 * 10^{-8}$	{31.0592, 31.0592}
R^2	0.99806		

built in 1989. Nevertheless, March 2011, Germany obtained one-fourth of its electricity from nuclear sources of energy using 17 reactors (NPG, 2018). According to source-specific data (British Petroleum, 2016), Germany started consuming nuclear energy in 1965. As Figure B.9 shows, initially, the amount of nuclear consumption was below 0.05 Mtoe, which was much lower than the renewables consumption (3.7 Mtoe). However, through a continuous rising trend, nuclear consumption outstripped renewables in 1973, reached a plateau between 1985 and 2007 and gradually declined after that point. With some instabilities, the consumption of CGO sources sharply increased until 1976. After this year, it substantially declined.

First, the data from Germany were partitioned as CGON sources and renewables, and model (A.2), USC, with three exponential shocks (two for CGON and one for renewables) was fitted. The shocks are significant, since the value of F -ratio, obtained by comparing the USC model with and without shocks, is large ($\hat{F} = 11.26911$). Subsequently, the data were separated into three sources, as follows: CGO, renewables and nuclear. Since all three products were simultaneously launched, model (A.6), USC, with four exponential shocks (two for CGO, one for renewables and one for nuclear) was fitted. A substantially large value of R^2 (0.99869) is a proof of a good model fit. The F -statistic, comparing the fitted model with the USC model without shocks, provides a large value ($\hat{F} = 24.94398$). That is, the shocks are significantly incorporated into the model. Two shocks occurred for the CGO time series, at times $1965 + \hat{a}_1 \simeq 1983$ and $1965 + \hat{a}_2 \simeq 1997$. The former shock was estimated as negative ($\hat{c}_1 = -0.08340$) and decaying over time (negative \hat{b}_1). The latter shock was found to be positive ($\hat{c}_2 = 0.07720$) and not yet faded over time (positive \hat{b}_2). The negative shock for CGO sources may be due to the second oil crisis of 1979, which notably reduced the German fossil fuel consumption, as occurred throughout Europe (Planete-energies, 2015b). However, the positive shock may be due to the energy regulation, passed in 1998, that marked full legal liberalisation of the German natural gas sector according to European Union orders (EIA, 2003). For renewables, a positive shock ($\hat{c}_3 = 0.34621$) rose at time $1965 + \hat{a}_3 \simeq 1995$, and this did not fade over time (positive \hat{b}_3). This shock may be due to numerous incentives, especially relating to the Renewable Energy Sources Act or *Erneuerbare-Energien-Gesetz* (EEG), that were approved; as a result of this, the share of renewables in the German energy mix has been growing rapidly since 1995. Furthermore, for nuclear energy, a negative shock ($\hat{c}_4 = -0.09755$) arose at time $1965 + \hat{a}_4 \simeq 1997$, but the shock did not decay over time (positive \hat{b}_4).

TABLE B.13: Germany, 3CM. Estimates, standard errors and marginal linearised 95% confidence intervals of the USC model with four shocks (two for CGO sources, one for renewables and one for nuclear).

Parameter	Estimate	Standard error	95% Confidence interval
m	22949.8	6599.82	{9892.83, 36006.8}
p_1	0.01096	0.00309	{0.00486, 0.01707}
q_1	-0.25658	0.16526	{-0.58352, 0.07036}
ε	0.30602	0.16523	{-0.02087, 0.63291}
η	-0.23910	0.19507	{-0.62502, 0.14682}
c_1	-0.08340	0.01840	{-0.11980, -0.04700}
b_1	-0.06659	0.10351	{-0.27138, 0.13819}
a_1	17.8534	0.04797	{17.7585, 17.9483}
c_2	0.07720	0.02163	{0.03441, 0.11998}
b_2	0.13240	0.00789	{0.11679, 0.14802}
a_2	31.9969	0.08593	{31.8269, 32.1669}
p_2	0.00015	0.00011	{-0.00007, 0.00038}
q_2	0.00050	0.01992	{-0.03891, 0.03992}
θ	-0.00312	0.02089	{-0.04444, 0.03820}
ξ	0.22807	0.31156	{-0.38831, 0.84444}
c_3	0.36661	0.91081	{-1.43533, 2.16854}
b_3	0.06381	0.10488	{-0.14367, 0.27130}
a_3	31.8230	0.94243	{29.9585, 33.6875}
p_3	-0.00018	0.00012	{-0.00040, 0.00005}
q_3	0.07318	0.03730	{-0.00062, 0.14698}
c_4	-0.09760	0.08549	{-0.26674, 0.07154}
b_4	0.06591	0.08614	{-0.10451, 0.23634}
a_4	31.7783	0.42105	{30.9453, 32.6113}
R^2	0.99869		

Now, substituting the parameter estimates in model (A.6), we obtain the following three equations:

$$z_1'(t) \propto 0.01096 + 0.04944 z_1(t)/m - 0.49568 z_2(t)/m - 0.25658 z_3(t)/m$$

$$z_2'(t) \propto 0.00015 - 0.00266 z_1(t)/m + 0.22935 z_2(t)/m + 0.00050 z_3(t)/m$$

$$z_3'(t) \propto -0.00018 - 0.22970 z_1(t)/m + 0.08341 z_2(t)/m + 0.07318 z_3(t)/m.$$

The innovative component of CGO sources is much larger ($\hat{p}_1 = 0.01096$) than that of nuclear ($\hat{p}_3 = -0.00018$) and renewables ($\hat{p}_2 = 0.00015$) sources. However, we see that Germany has a greater interest in the innovation of green energy technology than

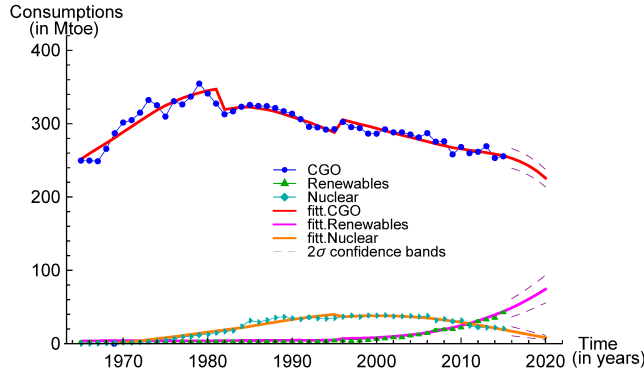


FIGURE B.9: Germany, 3CM. Energy consumption (Mtoe) from CGO sources (circles), renewables (triangles) and nuclear (diamonds). The solid lines correspond to the USC fitted model with four shocks (two for CGO, one for renewables and one for nuclear). The broken lines represent 2σ predictions' confidence bands.

nuclear technology. In the case of imitative components, the CGO sources' within-product WOM effect ($\hat{q}_1 + \hat{\varepsilon} = 0.04944$) is positive, and the cross-product WOM effects by both renewables ($\hat{q}_1 + \hat{\eta} = -0.49568$) and nuclear ($\hat{q}_1 = -0.25658$) are negative. This means that the diffusion of CGO is sustained by its own spread but restricted by the spread of its competitors (renewables and nuclear). Renewables' within-product effect ($\hat{q}_2 + \hat{\xi} = 0.22935$) and the cross-product effect by nuclear sources ($\hat{q}_2 = 0.00050$) are positive. The cross-product effect by CGO ($\hat{q}_2 + \hat{\theta} = -0.00266$) is negative. That is, the diffusion level of renewables is accelerated by their spread and that of nuclear sources, but it is decreased by the spread of CGO. The within-product effect of nuclear energy is positive ($\hat{q}_3 = 0.07318$), and its cross-product effects by CGO ($\hat{q}_3 - \hat{\varepsilon} - \hat{\theta} = -0.22970$) and renewables ($\hat{q}_3 - \hat{\eta} - \hat{\xi} = 0.08341$) are negative and positive, respectively. This means that the diffusion of nuclear is enhanced by the spread of its own and renewables but limited by the spread of CGO sources.

Regarding cross-product effects, CGO and renewables are rivals, since still the overall fossil fuel consumption is much higher, even if it has been declining since 1980. Notice that, since 1990, brown coal electricity production in Germany rose to its highest level in 2013 (Financial Times, 2014). However, as part of the government's Energiewende initiative to transition away from fossil fuels, Germany has been investing heavily in renewables. CGO sources and nuclear are also rivals, since both are at the phase-out stage. However, renewables and nuclear support each other as the Energiewende is directed toward an environmentally sound, reliable, and affordable energy supply.

The fitted lines in Figures B.8 and B.9 follow the observations well. Consequently, the predictions from 2016 to 2020 convincingly follow the previous trend. The predictions suggest a rapid rise of renewables and a substantial decline of other energies in

TABLE B.14: Germany. Confidence band width of 2CM and 3CM predictions in 2016–2020.

Year	2CM		3CM		
	CGON ($\hat{\sigma}_u=0.03030$)	Renewables ($\hat{\sigma}_u=0.13268$)	CGO ($\hat{\sigma}_u=0.02642$)	Renewables ($\hat{\sigma}_u=0.12681$)	Nuclear ($\hat{\sigma}_u=0.18326$)
2016	32.90884	25.82253	26.71890	24.79289	12.45192
2017	32.55353	28.76076	26.25334	27.66530	10.81685
2018	32.25193	31.95426	25.64824	30.78123	9.19791
2019	32.00931	35.40394	24.86544	34.13294	7.62200
2020	31.82991	39.10532	23.86324	37.70647	6.11711

2016–2020. Since the first five estimated values of the nuclear time series are not well matched with the observed data, we have ignored them in computing the scaled residuals' variance. The Kolmogorov–Smirnov test confirmed the normality assumption of the scaled residuals. The standard deviations of scaled residuals ($\hat{\sigma}_u$) for 2CM products are 0.03030 and 0.13268 for CGON and renewables, and those for 3CM products are 0.02642, 0.12681 and 0.18326 for CGO, renewables and nuclear, respectively. Thus, we computed the 2σ confidence bands, represented by broken lines in Figures B.8 and B.9, and the corresponding band width (see Table B.14). In comparison with the 2CM, the 3CM gives narrower confidence bands of predictions for renewables. This implies that the 3CM predictions may be more reliable.

B.5 India

In 2011, India became the world's fourth-largest energy consumer, following China, the United States and Russia. India's dependence on imported energy resources and the inconsistent restructuring of the energy sector are challenged to meet the rising demand. According to source-specific data (British Petroleum, 2016), in 1965, India's total energy consumption was only 53 Mtoe, and more than 48 Mtoe came from CGON sources. That is, initially, the share of renewables produced by hydroelectricity was extremely limited. Other renewable sources (geothermal, biomass and wind energy) were launched in 1990s, while solar power was launched in 1995. Figure B.10 depicts an exponential curve for the consumption of CGON sources and a slowly rising trend in the use of renewables. Indian Electricity Scenario (2016) reported some recent improvements in the renewable energy mix. For instance, even if 62.1% of the electricity still comes from coal thermal power, 27.4% comes from renewables. Before March 31, 2014, 21 318 (3.6%) villages in

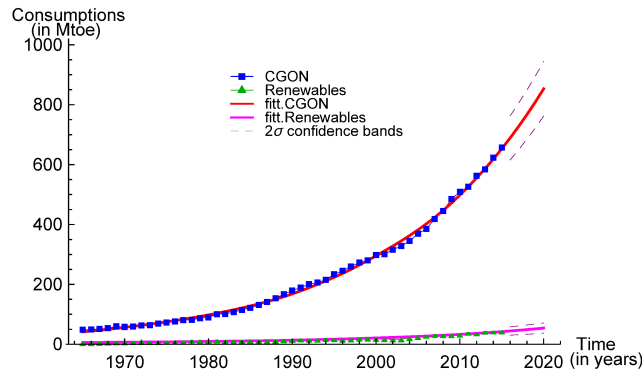


FIGURE B.10: India, 2CM. Energy consumption (Mtoe) from CGON sources (squares) and renewables (triangles). The solid lines correspond to the BSC fitted model. The broken lines represent 2σ predictions' confidence bands.

the remote areas had no access to electricity facilities, which made renewable energy a suitable and preferable choice (Tripathi *et al.*, 2016). In fact, the increase of the share of renewables in the energy mix has been promoted by the National Action Plan of 2008 to meet India's goal of reducing the CO₂ emissions (from the 2005 levels) by 20–25% by 2020 (Chandel *et al.*, 2016).

In 1969, India started to use nuclear energy (British Petroleum, 2016), which is now well established for civil use. Figure B.11 shows that the consumption of CGO sources exponentially increased. Nuclear consumption was almost fixed or negligibly increasing over time. This higher dependency on fossil fuels seems to be associated with the expansion of various types of local contaminants. For example, suspended particulate matter, such as sulphur or SO₂, contributes to health hazards, with effects mainly in cities, while acid rains mainly effect rural areas.

To India's energy data, partitioned as CGON sources and renewables, the model in Equation (A.3), BSC, is applied. The model is suitably fitted, as the F -test comparing the USC model (in which the BSC is nested) with the BSC fitted model provides a small

TABLE B.15: India, 2CM. Estimates, standard errors and marginal linearised 95% confidence intervals of the BSC model.

Parameter	Estimate	Standard error	95% Confidence interval
m	$6.04 * 10^6$	$8.01 * 10^5$	$\{4.45 * 10^6, 7.63 * 10^6\}$
p_1	$6.90 * 10^{-6}$	$9.37 * 10^{-7}$	$\{5.04 * 10^{-6}, 8.75 * 10^{-6}\}$
q_1	$5.18 * 10^{-2}$	$1.42 * 10^5$	$\{-2.81 * 10^5, 2.81 * 10^5\}$
p_2	$1.04 * 10^{-6}$	$1.34 * 10^7$	$\{-2.65 * 10^7, 2.65 * 10^7\}$
q_2	$3.06 * 10^{-3}$	$1.41 * 10^5$	$\{-2.81 * 10^5, 2.81 * 10^5\}$
R^2	0.99869		

value ($\hat{F} = 0.22257$).

When the data are separated into three competitors, CGO, renewables and nuclear, we observe a diachronic competition, as CGO and renewables exist from the beginning and nuclear enters the market at a later time. Thus, model (A.7), CRCDC, is fitted. The fitting is good, as the F -test comparing the UCRCD model (in which the CRCDC is nested) with the fitted CRCDC model, gives a small value ($\hat{F} = 1.92000$). Moreover, a notably large value of R^2 (0.99887) proves that the model is well fitted.

The marginally linearised 95% intervals of confidence hint that the parameter estimates are vulnerable. This situation typically arises when the lifecycle of all products is

TABLE B.16: India, 3CM. Estimates, standard errors and marginal linearised 95% confidence intervals of the CRCDC model.

Parameter	Estimate	Standard error	95% Confidence interval
m_α	$7.55 * 10^3$	$3.73 * 10^5$	$\{-7.30 * 10^5, 7.45 * 10^5\}$
$p_{1\alpha}$	$6.37 * 10^{-3}$	$3.15 * 10^{-1}$	$\{-6.16 * 10^{-1}, 6.28 * 10^{-1}\}$
$q_{1\alpha}$	$4.02 * 10^{-2}$	$3.67 * 10^{-1}$	$\{-6.86 * 10^{-1}, 7.66 * 10^{-1}\}$
$p_{2\alpha}$	$5.50 * 10^{-4}$	$2.76 * 10^{-2}$	$\{-5.41 * 10^{-2}, 5.52 * 10^{-2}\}$
$q_{2\alpha}$	$1.02 * 10^{-2}$	$2.25 * 10^2$	$\{-4.45 * 10^2, 4.45 * 10^2\}$
m_β	$3.00 * 10^6$	$3.31 * 10^5$	$\{2.34 * 10^6, 3.65 * 10^6\}$
$p_{1\beta}$	$1.36 * 10^{-5}$	$1.55 * 10^{-6}$	$\{1.05 * 10^{-5}, 1.66 * 10^{-5}\}$
$q_{1\beta}$	$5.14 * 10^{-2}$	$2.20 * 10^{-4}$	$\{5.09 * 10^{-2}, 5.18 * 10^{-2}\}$
$p_{2\beta}$	$2.20 * 10^{-6}$	$4.52 * 10^6$	$\{-8.94 * 10^6, 8.94 * 10^6\}$
$q_{2\beta}$	$3.02 * 10^{-3}$	$1.12 * 10^5$	$\{-2.22 * 10^5, 2.22 * 10^5\}$
p_3	$-7.84 * 10^{-8}$	$1.03 * 10^8$	$\{-2.03 * 10^8, 2.03 * 10^8\}$
q_3	$6.80 * 10^{-5}$	$1.75 * 10^5$	$\{-3.47 * 10^5, 3.48 * 10^5\}$
R^2	0.99887		

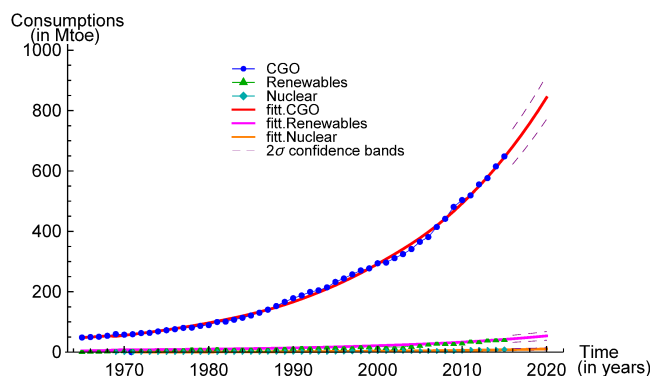


FIGURE B.11: India, 3CM. Energy consumption (Mtoe) from CGO sources (circles), renewables (triangles) and nuclear (diamonds). The solid lines correspond to the CRCDC fitted model. The broken lines represent 2σ predictions' confidence bands.

still far from reaching maturity. If we focus on the second phase findings (Table B.16), the innovative components of all three competitors are extremely small ($\hat{p}_{1\beta} = 1.36 * 10^{-5}$ for CGO, $\hat{p}_{2\beta} = 2.20 * 10^{-6}$ for renewables and $\hat{p}_3 = -7.84 * 10^{-8}$ for nuclear), especially for nuclear sources. By substituting the parameter estimates in the second phase of the CRCDD model, we obtain the following three equations:

$$\begin{aligned} z'_1(t) &\propto 1.36 * 10^{-5} + 5.14 * 10^{-2} z(t)/m_\beta \\ z'_2(t) &\propto 2.20 * 10^{-6} + 3.02 * 10^{-3} z(t)/m_\beta \\ z'_3(t) &\propto -7.84 * 10^{-8} + 6.80 * 10^{-5} z(t)/m_\beta. \end{aligned}$$

Here, the nuclear imitative effect (WOM) is negligible ($\hat{q}_3 = 6.80 * 10^{-5}$). This is linked to the low spread of nuclear diffusion. Conversely, the spread of CGO diffusion is high ($\hat{q}_{1\beta} = 5.14 * 10^{-2}$), and that of renewables is also considerable ($\hat{q}_{2\beta} = 3.02 * 10^{-3}$).

The observed and fitted values, in Figures B.10 and B.11, are extremely close to each other, resulting in reliable predictions from 2016 to 2020. According to the trend of predictions, all sources of energy may increase in 2016–2020. In fact, in the 12th 5-year plan of the Planning Commission, the estimated total domestic energy production reaches 669.6 Mtoe by 2016–17 and 844 Mtoe by 2021–22 (Kumar and Vimala, 2012). Moreover, India's energy consumption is set to grow 4.2% per year by 2035, faster than that of all the world's major economies (British Petroleum, 2016).

Through a close inspection, we can see that, in the first part of the nuclear series, the fitted values do not satisfactorily follow the observed data. Thus, we removed the first eight residuals when computing the scaled residuals. The Kolmogorov–Smirnov test confirmed that scaled residuals follow a Gaussian distribution. The standard deviations of scaled residuals ($\hat{\sigma}_u$) using 2CM are 0.05350 for CGON and 0.15818 for renewables. Those obtained with 3CM are 0.04282, 0.13245 and 0.19164 for CGO, renewables and

TABLE B.17: India. Confidence band width of 2CM and 3CM predictions in 2016–2020.

Year	2CM		3CM		
	CGON ($\hat{\sigma}_u=0.05350$)	Renewables ($\hat{\sigma}_u=0.15818$)	CGO ($\hat{\sigma}_u=0.04282$)	Renewables ($\hat{\sigma}_u=0.13245$)	Nuclear ($\hat{\sigma}_u=0.19164$)
2016	147.435381	28.139080	116.68254	23.40227	6.35929
2017	155.530653	29.551810	123.08152	24.56385	6.74071
2018	164.066746	31.041335	129.82638	25.78821	7.14275
2019	173.065060	32.611787	136.93542	27.07867	7.56650
2020	182.553412	34.267516	144.42786	28.43874	8.01310

nuclear, respectively. Thus, we computed 2σ confidence bands of 2CM and 3CM predictions, represented by broken lines in Figures B.10 and B.11, and the respective band width, shown in Table B.17. The confidence bands of renewable predictions by 3CM are narrower than those of 2CM. That is, the 3CM predictions are more trustworthy.

B.6 Japan

Japan is the frontrunner in energy technology development and a major exporter in that sector. However, the security of the energy supply has customarily been critical to Japan, as it depends on imported energies, especially in terms of its entire fossil fuel supply (IEA, 2016b). In 1965, Japan consumed only 16 Mtoe of energy from renewables (represented by hydroelectricity) against about 138 Mtoe CGON consumption. The 2015 Key World Energy Statistics reported that hydroelectricity (including pumped storage) is the leading renewable energy source of Japan, with an installed capacity of about 50 GWs. Geothermal and biomass started being exploited in 1970, and after more than two decades, solar (in 1990) and wind (in 1993) were added to the renewable energy mix. Figure B.12 shows that the consumptions of CGON sources sharply increased in the first few years. After some fluctuations, it further increased in the period 1984–2006 and rapidly declined after that. The use of renewables was almost stable or increased trivially over time.

Japan is the sole country that suffered overwhelming effects from nuclear the World War II, with over 100 000 deaths. However, the country embraced the peaceful use of nuclear technology to afford a significant portion of its electricity (Nuclear Power in Japan (NPJ), 2018). Japan's first commercial nuclear power reactor started operating in mid-1966. Initially, the consumption of nuclear was extremely low (< 0.05 Mtoe), against extremely large fossil fuel (about 138 Mtoe) and substantial renewable (about 16 Mtoe) consumptions (see source-specific data in British Petroleum, 2016). Figure B.13 shows that, through a continuously increasing trend, the consumption of nuclear overlapped with renewables in 1982. However, it suddenly declined in 2010, and it ceased in 2014 (this is naturally connected with the Fukushima accident occurred in March 2011). The CGO consumption exhibits a trend similar to that of CGON sources, but it has become unstable in recent years.

When the data from Japan are partitioned as CGON sources and renewables, model (A.3), BSC, with four exponential shocks (three for CGON and one for renewables) is applied. The shocks are significant, as the F -ratio, comparing the fitted model with the BSC without shocks, provides an adequately large value ($\hat{F} = 24.02300$).

TABLE B.18: Japan, 2CM. Estimates, standard errors and marginal linearised 95% confidence intervals of the BSC model with four shocks (three for CGON sources and one for renewables).

Parameter	Estimate	Standard error	95% Confidence interval
m	34395.0	4947.19	{24558.7, 44231.4}
p_1	0.00455	0.00063	{0.00329, 0.00580}
q_1	0.05179	0.00768	{0.03652, 0.06707}
c_1	0.39699	0.05090	{0.29577, 0.49820}
b_1	-0.12728	0.06178	{-0.25011, -0.00445}
a_1	4.60010	0.00257	{4.59499, 4.60522}
c_2	-0.19941	0.02593	{-0.25097, -0.14785}
b_2	-0.08143	0.05424	{-0.18926, 0.02641}
a_2	16.6034	0.00042	{16.6026, 16.6043}
c_3	-0.01421	0.02008	{-0.05413, 0.02571}
b_3	0.13092	0.04920	{0.03310, 0.22874}
a_3	32.0000	0.00004	{31.9999, 32.0001}
p_2	0.000446	0.00011	{0.00024, 0.00066}
q_2	0.00172	0.00055	{0.00062, 0.00281}
c_4	0.01042	0.04930	{-0.08761, 0.10844}
b_4	0.27690	0.31498	{-0.34937, 0.90316}
a_4	35.9616	0.00014	{35.9613, 35.9618}
R^2	0.99779		

Afterward, the data have been separated into three products (CGO sources, renewables and nuclear). Since all three products were launched simultaneously, the second phase of model (A.6), USC, with five exponential shocks (three for CGO, one for renewables, and one for nuclear) is applied. The fitting is good overall ($R^2 = 0.99688$). The F -ratio, obtained by the USC model with and without shocks, gives a large value ($\hat{F} = 25.27788$). Hence, the shocks are significantly incorporated into the model. Three shocks occurred for CGO sources, at times $1965 + \hat{a}_1 \simeq 1970$, $1965 + \hat{a}_2 \simeq 1982$ and $1965 + \hat{a}_3 \simeq 2002$. The first shock was estimated as positive ($\hat{c}_1 = 0.32869$) and the next two were found to be negative ($\hat{c}_2 = -0.19301$ and $\hat{c}_3 = -0.01534$), but all three shocks decayed over time (negative \hat{b}_1 , \hat{b}_2 and \hat{b}_3). The positive shock may be due to a rapid industrial growth; Japan's energy consumption grew much faster than its gross national product (GNP) in 1960–1972. However, the negative shocks can be explained in that, after the oil shocks of the 1970s, Japan offered strong incentives to reduce the reliance on fossil fuels in relation to its economic growth. The country also possessed the advanced technology and ample capital to grow non-fossil energy (Ishida, 2013). A

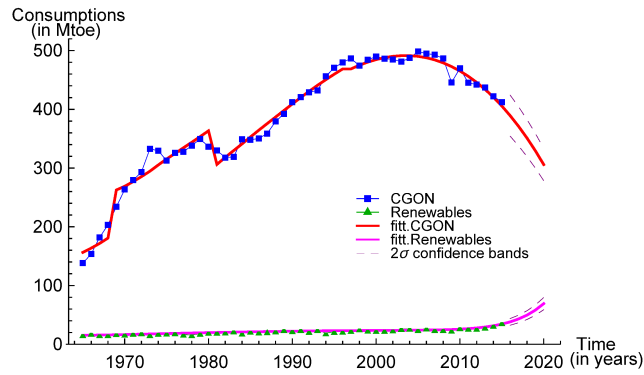


FIGURE B.12: Japan, 2CM. Energy consumption (Mtoe) from CGON sources (squares) and renewables (triangles). The solid lines correspond to the BSC fitted model with three shocks (three for CGON and one for renewables). The broken lines represent 2σ predictions' confidence bands.

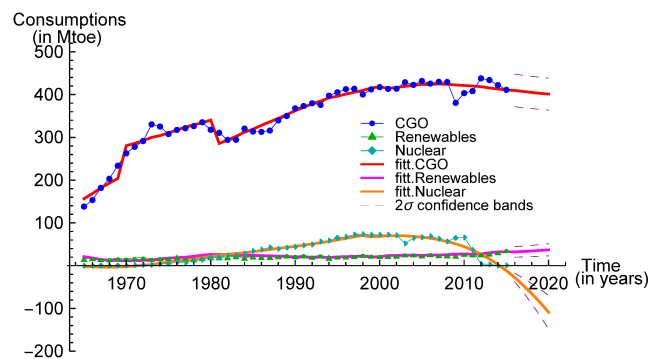


FIGURE B.13: Japan, 3CM. Energy consumption (Mtoe) from CGO sources (circles), renewables (triangles) and nuclear (diamonds). The solid lines correspond to the USC fitted model with five shocks (three for CGO, one for renewables and one for nuclear). The broken lines represent 2σ predictions' confidence bands.

positive shock ($\hat{c}_4 = 0.12406$) is estimated for the renewables at time $1965 + \hat{a}_4 \simeq 2002$, and this has not yet dissipated over time (positive \hat{b}_4). In some way, the shock is related to the Kyoto Protocol (adopted in Kyoto, Japan, on 11 December 1997) to reduce GHG emissions. Under this practice, Japan reduced its CO_2 by 1.9% between 2002 and 2014. While the amount is almost negligible, in 2012, Japan introduced a FiT system for renewables expansion. A negative ($\hat{c}_5 = -0.07580$) shock rose for nuclear sources at time $1965 + \hat{a}_5 \simeq 1999$, but the shock not yet diminished in time (positive \hat{b}_5).

TABLE B.19: Japan, 3CM. Estimates, standard errors and marginal linearised 95% confidence intervals of the USC model with five shocks (three for CGO sources, one for renewables and one for nuclear).

Parameter	Estimate	Standard Error	Lower 95% Confidence interval
m	34478.8	2357.33	{29814.0, 39143.5}
p_1	0.00454	0.00033	{0.00390, 0.00519}
ε	-0.03224	0.03711	{-0.10566, 0.04118}
η	0.76943	0.26760	{0.23990, 1.29896}
q_1	0.03154	0.02730	{-0.02248, 0.08557}
c_1	0.32869	0.05277	{0.22426, 0.43312}
b_1	-0.13858	0.08949	{-0.31566, 0.03851}
a_1	5.35307	0.00240	{5.34831, 5.35783}
c_2	-0.19301	0.02043	{-0.23344, -0.15257}
b_2	-0.03467	0.04445	{-0.12263, 0.05329}
a_2	16.7768	0.00014	{16.7766, 16.7771}
c_3	-0.01534	0.01581	{-0.04663, 0.01595}
b_3	-0.05327	0.42367	{-0.89165, 0.78510}
a_3	37.0000	0.00001	{37.0000, 37.0000}
p_2	0.00061	0.00017	{0.00029, 0.00094}
θ	0.06173	0.02775	{0.00682, 0.11665}
ξ	-0.46364	0.23496	{-0.92859, 0.00130}
q_2	-0.02761	0.01913	{-0.06546, 0.01024}
c_4	0.12406	0.26593	{-0.40217, 0.65028}
b_4	0.15919	0.12504	{-0.08824, 0.40661}
a_4	37.0000	0.00525	{36.9896, 37.0104}
p_3	-0.00005	0.00016	{-0.00037, 0.00027}
q_3	0.05180	0.01927	{0.01366, 0.08994}
c_5	-0.07580	0.03446	{-0.14398, -0.00761}
b_5	0.16412	0.03024	{0.10429, 0.22395}
a_5	34.4843	0.00043	{34.4834, 34.4851}
R^2	0.99688		

If we substitute the parameter estimates in model (A.6), we obtain the following three equations:

$$z'_1(t) \propto 0.00454 - 0.0007 z_1(t)/m + 0.80097 z_2(t)/m + 0.03154 z_3(t)/m$$

$$z'_2(t) \propto 0.00061 + 0.03412 z_1(t)/m - 0.49125 z_2(t)/m - 0.02761 z_3(t)/m$$

$$z'_3(t) \propto -0.00005 + 0.02231 z_1(t)/m - 0.25399 z_2(t)/m + 0.0518 z_3(t)/m.$$

The innovative effect of CGO sources ($\hat{p}_1 = 0.00454$) is notably larger than the effect of

nuclear ($\hat{p}_3 = -0.00005$) and renewables ($\hat{p}_2 = 0.00061$) as well. Turning to the imitative component, the within-product effect of CGO ($\hat{q}_1 + \hat{\varepsilon} = -0.0007$) is negative, while its cross-product effects by renewables ($\hat{q}_1 + \hat{\eta} = 0.80097$) and nuclear ($\hat{q}_1 = 0.03154$) are positive. This means that the diffusion of CGO is reduced by its spread but enhanced by that of its competitors. Regarding within-product effects, according to the Paris climate agreement, Japan is under pressure to carry out a public pledge to reduce fossil fuel consumptions to reduce GHG emissions by 26% by 2030 compared with the 2013 level. Regarding cross-product effects, after the Fukushima disaster in 2011, Japan largely reduced the nuclear consumption, resulting in a shift in Japan's energy mix toward oil and natural gas (EIA, 2013). Moreover, biomass and geothermal energy steadily supported the increase of the use of fossil fuels, mainly gas, in combined heat and power (CHP) generation (Greenpeace, 2008). Renewables' within-product effect ($\hat{q}_2 + \hat{\xi} = -0.49125$) is negative, and their cross-product effect by CGO ($\hat{q}_2 + \hat{\theta} = 0.03412$) and nuclear ($\hat{q}_2 = -0.02761$) are positive and negative, respectively. That is, the level of diffusion of renewables is delayed by their spread and that of nuclear sources but increased by the spread of CGO. The within-product effect can be explained as a reflection of Japan's geothermal, wind, and solar energy potential, which could easily power the world's third-largest economy. The recent growth of solar PV in Japan is indebted to strong policies promoting its adoption (Treehugger, 2011). Regarding cross-product effects, after the Fukushima accident, nuclear power has faced higher security standards, and therefore, higher costs. Thus, Japan has a greater interest in renewable energy. In addition to this, Japan planned to reduce long-term reliance on imported fossil fuels (CGO sources) through larger investments in renewable energy. Nuclear within-product ($\hat{q}_3 = 0.0518$) and cross-product effects by CGO sources ($\hat{q}_3 - \hat{\varepsilon} - \hat{\theta} = 0.02231$) are positive, while the cross-product effect by renewables ($\hat{q}_3 - \hat{\eta} - \hat{\xi} = -0.25399$) is negative. That is, the diffusion of nuclear sources is positively associated with its spread and that of CGO, but it is inversely associated with renewables. Regarding within-product effects, Japan relies heavily on nuclear energy, as it is resources poor for other energy forms. Regarding cross-product effects, the extent to which renewable energy sources enjoys public support through subsidies may also related to concern over traditional energy because of the Fukushima disaster, whereas green energies can be an alternative source to nuclear power.

The fitted lines in Figures B.12 and B.13 adequately follow the observed data. Consequently, the predictions (except for nuclear), from 2016 to 2020, satisfactorily follow the previous trend. The predictions for nuclear sources are unrealistic, but this is essentially a consequence of the dramatic decline observed after 2010 (the fitted model

TABLE B.20: Japan. Confidence band width of 2CM and 3CM predictions in 2016–2020.

Year	2CM		3CM		
	CGON ($\hat{\sigma}_u=0.04485$)	Renewables ($\hat{\sigma}_u=0.07479$)	CGO ($\hat{\sigma}_u=0.04647$)	Renewables ($\hat{\sigma}_u=0.19068$)	Nuclear ($\hat{\sigma}_u=0.18020$)
2016	69.81056	11.41988	76.14831	24.52651	–
2017	66.55990	12.90362	75.71014	25.34581	–
2018	63.00063	14.85018	75.29020	26.24335	–
2019	59.11447	17.39510	74.90513	27.21071	–
2020	54.87917	20.71285	74.57093	28.23823	–

Confidence band width is not shown when the fitted trajectory is negative.

follows the trend of the final part of the observed data). Both 2CM and 3CM predictions suggest increasing renewables and declining other energies in 2016–2020. In fact, Japan’s green innovation goals for 2020 are to create over 50 trillion yen (JPY) in new environmental-related markets and 1.4 million new jobs in the environment sector, as well as reducing CO₂ emissions by using Japan’s private sector technology (Global Energy Network Institute (GENI), 2012). It should be observed that the first four estimated values of nuclear are far from their observed data, so we ignored them in estimating the scaled residuals’ variance. The Kolmogorov–Smirnov test confirmed that the scaled residuals follow a Gaussian distribution. The standard deviations of scaled residuals ($\hat{\sigma}_u$) obtained with 2CM are 0.04485 for CGON and 0.07479 for renewables, and those with 3CM are 0.04647 for CGO, 0.19068 for renewables and 0.18020 for nuclear. Accordingly, we computed the 2σ confidence bands of predictions, shown by broken lines in Figures B.12 and B.13, and the corresponding band width, represented in Table B.20. The confidence band width of predictions for renewables with 3CM is much larger than those obtained with 2CM. This means that the 2CM gives more reliable predictions for this dataset.

B.7 Spain

In 1965, Spain’s energy consumption from CGON sources was 24 Mtoe and that from renewables it was about 5 Mtoe (British Petroleum, 2016). For the first few years, hydroelectricity uniquely represented the renewables. Other renewable sources, such as geothermal and biomass, were launched in 1970, and wind and solar power were launched simultaneously in 1989. In Figure B.14, we observe that the consumption of CGON sources markedly increased for a long period, but they sharply declined from

2007. With regular fluctuations, the use of renewables was almost constant until 2000 and increased notably after that point.

Spain's first commercial nuclear power reactor started operating in 1969 (British Petroleum, 2016). The country is distinct in terms of its power plant upgrades. It has a program to add 810 MWe (11%) to its nuclear capacity by promoting its nine reactors by up to 13%. For instance, the Almaraz nuclear plant is being upgraded by more than 5% at a cost of US\$ 50 million (Nuclear Power in Spain (NPS), 2017). In Figure B.15, we see that nuclear and renewables crossed each other twice over the years. Especially, nuclear consumption was almost constant until 1983, and after this time, it reached a plateau after a short-period of increase. Conversely, an opposite path is observed for renewables consumption. The consumption of CGO sources follows the same trend as CGON sources.

With Spain's energy data partitioned into two sources (CGON and renewables), model (A.1), UUC, with two exponential shocks (one for each source) is applied. The shocks are significantly incorporated into the model, since the F -ratio, comparing the UUC model with and without shocks, gives a large value ($\hat{F} = 22.90880$).

When the data are partitioned into three sources (CGO, renewables and nuclear), we see that CGO sources and renewables exist from the beginning and nuclear enters the market later. Hence, model (A.5), CRCD, with three exponential shocks (one for each competitor) is applied. The fitting is good overall ($R^2 = 0.99193$). As before, the shocks are significant, as the value of F -ratio, obtained by comparing the fitted model with CRCD model without shocks, is notably large ($\hat{F} = 30.24205$). The shocks occurred at time $1965 + \hat{a}_1 \simeq 1999$ for the CGO time series, time $1965 + \hat{a}_2 \simeq 1995$ for renewables and time $1965 + \hat{a}_3 \simeq 2009$ for nuclear sources. All three shocks were

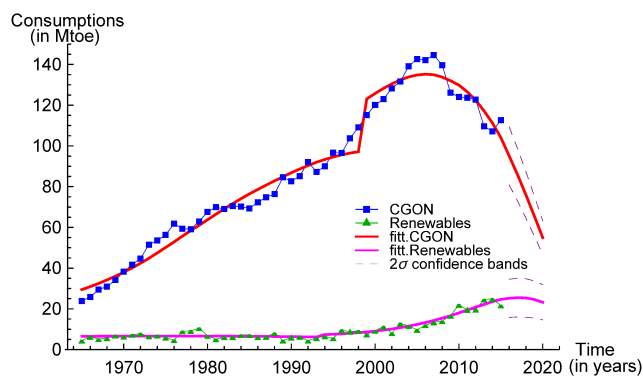


FIGURE B.14: Spain, 2CM. Energy consumption (Mtoe) from CGON sources (squares) and renewables (triangles). The solid lines correspond to the UUC fitted model with two shocks (one for each competitor). The broken lines represent 2σ predictions' confidence bands.

estimated to have a positive effect ($\hat{c}_1 = 0.31927$, $\hat{c}_2 = 0.21799$ and $\hat{c}_3 = 0.10978$), and they have not yet been absorbed (positive \hat{b}_1 , \hat{b}_2 and \hat{b}_3). The shock for CGO sources may be because, after facing some instabilities, the CGO consumption increased incredibly during the period of economic boom from 1997 to 2007. The shock for renewables may be related to the diffusion of on-shore wind power, during the period 1995–2004, that made Spain reach second rank in wind power installed capacity, behind only Germany and on par with the United States (Montoya *et al.*, 2014). Moreover, the shock for nuclear sources can be explained in that, although the fossil fuel consumption radically declined in the Spanish economic recession of 2009–2013, nuclear energy increased over the period.

The market potential of the first phase ($\hat{m}_\alpha=399.23$ Mtoe) is extremely small with respect to the second phase ($\hat{m}_\beta=5404.72$ Mtoe). This is because the period of the first phase is short, and \hat{m}_α may not be reliable. In the second phase, the innovative component of CGO is impressive ($\hat{p}_1 = 0.00658$), as is that of renewables ($\hat{p}_2 = 0.00136$), compared with nuclear ($\hat{p}_3 = -0.00069$). This means that Spain is well motivated for the innovation of green energy technology in place of nuclear technology.

TABLE B.21: Spain, 2CM. Estimates, standard errors and marginal linearised 95% confidence intervals of the UUC model with two shocks (one for each competitor).

Parameter	Estimate	Standard error	95% Confidence interval
m	5622.46	199.376	{5226.31, 6018.62}
p_1	0.00524	0.00037	{0.00450, 0.00597}
q_1	0.03186	0.07933	{-0.12576, 0.18948}
δ	0.02936	0.08791	{-0.14532, 0.20403}
c_1	0.25919	0.03072	{0.19814, 0.32023}
b_1	0.09418	0.01956	{0.05531, 0.13304}
a_1	34.8787	0.06197	{34.7555, 35.0018}
p_2	0.00116	0.00030	{0.00057, 0.00175}
q_2	0.00336	0.07948	{-0.15455, 0.16128}
γ	0.00214	0.08891	{-0.17452, 0.17880}
c_2	0.20901	0.37141	{-0.52896, 0.94699}
b_2	0.18766	0.05889	{0.07065, 0.30466}
a_2	29.9352	0.96753	{28.0127, 31.8576}
R^2	0.99284		

TABLE B.22: Spain, 3CM. Estimates, standard errors and marginal linearised 95% confidence intervals of the CRCDC model with three shocks (one for each competitor).

Parameter	Estimate	Standard error	95% Confidence interval
m_α	399.233	$1.14 * 10^{-6}$	{399.233, 399.233}
$p_{1\alpha}$	0.05990	0.00739	{0.04526, 0.07453}
$q_{1\alpha}$	0.07759	0.05077	{-0.02286, 0.17805}
$p_{2\alpha}$	0.01307	0.00739	{-0.00157, 0.02770}
$q_{2\alpha}$	0.00409	0.05077	{-0.09637, 0.10454}
m_β	5404.72	96.428	{5213.92, 5595.52}
$p_{1\beta}$	0.00658	0.00028	{0.00602, 0.00714}
$q_{1\beta}$	0.04494	0.00158	{0.04182, 0.04806}
c_1	0.31927	0.02470	{0.27038, 0.36815}
b_1	0.10705	0.01035	{0.08656, 0.12753}
a_1	33.9995	0.00084	{33.9978, 34.0011}
$p_{2\beta}$	0.00136	0.00029	{0.00079, 0.00193}
$q_{2\beta}$	0.00087	0.00156	{-0.00222, 0.00397}
c_2	0.21799	0.15686	{-0.09239, 0.52836}
b_2	0.20347	0.02123	{0.16144, 0.24545}
a_2	29.8929	0.00696	{29.8791, 29.9066}
p_3	-0.00069	0.00024	{-0.00117, -0.00021}
q_3	0.01166	0.00098	{0.00973, 0.01359}
c_3	0.10978	0.12799	{-0.14347, 0.36303}
b_3	0.32666	0.19112	{-0.05149, 0.70481}
a_3	43.9918	0.00459	{43.9827, 44.0009}
R^2	0.99193		

By substituting the parameter estimates in the second phase of the CRCDC model, the following three equations can be obtained:

$$z'_1(t) \propto 0.00658 + 0.04494 z(t)/m_\beta$$

$$z'_2(t) \propto 0.00136 + 0.00087 z(t)/m_\beta$$

$$z'_3(t) \propto -0.00069 + 0.01166 z(t)/m_\beta.$$

Here, nuclear exploited the WOM of the whole category. Although the innovative effect of nuclear is negative, it is experienced by a strong positive imitative (WOM) effect. The other two sources also have positive imitative effects. The spread of renewables diffusion is extremely low ($\hat{q}_2 = 0.00087$).

The fitted lines in Figures B.14 and B.15 adequately follow the observed data. Especially, the fitted lines of the renewables follow the observed path well, resulting in

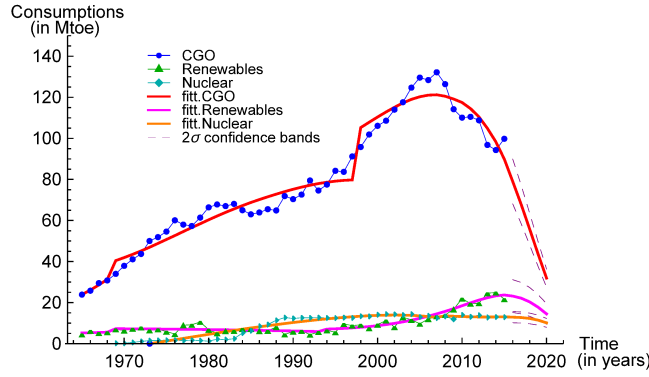


FIGURE B.15: Spain, 3CM. Energy consumption (Mtoe) from CGO sources (circles), renewables (triangles) and nuclear (diamonds). The solid lines correspond to the CRCRD fitted model with three shocks (one for each competitor). The broken lines represent 2σ predictions' confidence bands.

TABLE B.23: Spain. Confidence band width of 2CM and 3CM predictions in 2016–2020.

Year	2CM		3CM		
	CGON ($\hat{\sigma}_u=0.07495$)	Renewables ($\hat{\sigma}_u=0.18594$)	CGO ($\hat{\sigma}_u=0.06916$)	Renewables ($\hat{\sigma}_u=0.17257$)	Nuclear ($\hat{\sigma}_u=0.10588$)
2016	28.497511	18.73658	21.8502	15.99526	5.46833
2017	25.731339	18.980368	18.7546	15.29872	5.39171
2018	22.758277	18.852743	15.4482	14.05259	5.20618
2019	19.64896	18.291691	12.08048	12.26240	4.85636
2020	16.491825	17.258839	8.83802	10.01616	4.29882

reliable predictions. The predictions suggest a decline in all energies in 2016–2020. It should be observed that, in the first part of the nuclear series, the fitted values are quite far from their observed path. Hence, we ignored the first 15 residuals in computing the variance of scaled residuals. The Kolmogorov–Smirnov test confirmed the hypothesis that scaled residuals follow a normal distribution. The standard deviations of scaled residuals ($\hat{\sigma}_u$) obtained with the 2CM are 0.07495 and 0.18594 for CGON and renewables, and those with the 3CM are 0.06916, 0.17257 and 0.10588 for CGO, renewables and nuclear, respectively. Accordingly, we computed the 2σ confidence bands of predictors, represented by broken lines in Figures B.14 and B.15, and the corresponding band width (in Table B.23). For renewables predictions, the 3CM provides narrower confidence bands than the 2CM does. That is, the 3CM is more appropriate for reliable forecasting of the Spanish energy market.

Appendix C

Models with dynamic market potential

For two products

Model (1.14) is the general structure of two products, when the products launch together, and the model is called the UUC model with DMP. Under the restriction $\delta = \gamma$, it is called the USC model with DMP, and it can be expressed as

$$\begin{aligned} z_1'(t) &= m(t) \left[p_1 + (q_1 + \delta) \frac{z_1(t)}{m(t)} + q_1 \frac{z_2(t)}{m(t)} \right] \left[1 - \frac{z(t)}{m(t)} \right] + z_1(t) \frac{m'(t)}{m(t)}, \\ z_2'(t) &= m(t) \left[p_2 + (q_2 - \delta) \frac{z_1(t)}{m(t)} + q_2 \frac{z_2(t)}{m(t)} \right] \left[1 - \frac{z(t)}{m(t)} \right] + z_2(t) \frac{m'(t)}{m(t)}, \\ z(t) &= z_1(t) + z_2(t). \end{aligned} \quad (\text{C.1})$$

For three products

If all three products enter the market simultaneously, only the second phase of model (4.1) is applicable. Then, it is called the UUC model with DMP of three competitors,

and can be written in the following form:

$$\begin{aligned}
z_1'(t) &= m(t) \left[p_1 + (q_1 + \varepsilon) \frac{z_1(t)}{m(t)} + (q_1 - \eta) \frac{z_2(t)}{m(t)} + q_1 \frac{z_3(t)}{m(t)} \right] \left[1 - \frac{z(t)}{m(t)} \right] + \\
&\quad + z_1(t) \frac{m'(t)}{m(t)}, \\
z_2'(t) &= m(t) \left[p_2 + q_2 \frac{z_1(t)}{m(t)} + (q_2 + \theta) \frac{z_2(t)}{m(t)} + (q_2 - \xi) \frac{z_3(t)}{m(t)} \right] \left[1 - \frac{z(t)}{m(t)} \right] + \\
&\quad + z_2(t) \frac{m'(t)}{m(t)}, \\
z_3'(t) &= m(t) \left[p_3 + (q_3 - \mu) \frac{z_1(t)}{m(t)} + q_3 \frac{z_2(t)}{m(t)} + (q_3 + \lambda) \frac{z_3(t)}{m(t)} \right] \left[1 - \frac{z(t)}{m(t)} \right] + \\
&\quad + z_3(t) \frac{m'(t)}{m(t)}, \\
z(t) &= z_1(t) + z_2(t) + z_3(t).
\end{aligned} \tag{C.2}$$

Appendix D

A short essential bibliography

Bass, F. M. (1969) A new product growth model for consumer durables. *Management Science* 15, 215–227.

Bass, F. M., Krishnan, T. V. and Jain, D. C. (1994) Why the Bass model fits without decision variables. *Marketing Science* 13(3), 203–223.

Guseo, R. and Guidolin, M. (2009) Modelling a dynamic market potential: A class of automata networks for diffusion of innovations. *Technological Forecasting and Social Change* 76, 806–820.

Guseo, R. and Mortarino, C. (2012) Sequential market entries and competition modelling in multi-innovation diffusions. *European Journal of Operational Research* 216(3), 658–667.

Guseo, R. and Mortarino, C. (2014) Within-brand and cross-brand word-of-mouth for sequential multi-innovation diffusions. *IMA Journal of Management Mathematics* 25(3), 287–311.

Guseo, R. and Mortarino, C. (2015) Modeling competition between two pharmaceutical drugs using innovation diffusion models. *The Annals of Applied Statistics* 9(4), 2073–2089.

Bibliography

- Abramson, G. and Zanette, D. H. (1998) Statistics of extinction and survival in Lotka–Volterra systems. *Physical Review E* **57**(4), 4572–4577.
- Academy of Finland (2006) Energy research in Finland 1999–2005. Available <https://www.aka.fi/en/about-us/publications/publication-series/>.
- Agora Energiewende (2015) Country profile Germany. Report on the German power system. Available <https://www.agora-energiewende.de/en/publications/report-on-the-german-power-system/>.
- Aguilera, R. F. and Aguilera, R. (2012) World natural gas endowment as a bridge towards zero carbon emissions. *Technological Forecasting and Social Change* **79**(3), 579–586.
- Akaike, H. (1974) A new look at the statistical model identification. *IEEE Transactions on Automatic Control* **19**(6), 716–723.
- Apergis, N. and Payne, J. E. (2012) Renewable and non-renewable energy consumption-growth nexus: Evidence from a panel error correction mode. *Energy Economics* **34**(3), 733–738.
- Armstrong, J. S. and Collopy, F. (1992) Error measures for generalizing about forecasting methods: Empirical comparisons. *International Journal of Forecasting* **8**(1), 69–80.
- Armstrong, J. S. and Fildes, R. (1995) Correspondence on the selection of error measures for comparisons among forecasting methods. *Journal of Forecasting* **14**(1), 67–71.
- Atkinson, K. E. (1962) *An Introduction to Numerical Analysis*. 2nd ed. Wiley: New York.
- Bass, F. M. (1969) A new product growth model for consumer durables. *Management Science* **15**, 215–227.

- Bass, F. M., Jain, D. C. and Krishnan, T. V. (2000) Modeling the marketing-mix influence in new-product diffusion. In *New-product Diffusion Models*, eds V. Mahajan, E. Muller and Y. Wind. pp. 99–122. Kluwer Academic Publishers: Boston, MA.
- Bass, F. M., Krishnan, T. V. and Jain, D. C. (1994) Why the Bass model fits without decision variables. *Marketing Science* **13**(3), 203–223.
- BNEF (2015) Bloomberg New Energy Finance. Rebound in clean energy investment in 2014 beats expectations. Available <https://about.bnef.com/blog/rebound-clean-energy-investment-2014-beats-expectations/>.
- Boswijk, H. P. and Franses, P. H. (2005) On the econometrics of the Bass diffusion model. *Journal of Business and Economic Statistics* **23**(3), 255–268.
- Brandt, A. R. (2007) Testing Hubbert. *Energy Policy* **35**(5), 3074–3088.
- British Petroleum (2015) BP statistical review of world energy 2015. Available <https://www.bp.com>.
- British Petroleum (2016) BP statistical review of world energy 2016. Available <https://www.bp.com>.
- Brook, B. W., Alonso, A., Meneley, D. A., Misak, J., Bles, T. and Van Erp, J. B. (2014) Why nuclear energy is sustainable and has to be part of the energy mix. *Sustainable Materials and Technologies* **1**, 8–16.
- Centrone, F., Goia, A. and Salinelli, E. (2007) Demographic processes in a model of innovation diffusion with dynamic market. *Technological Forecasting and Social Change* **74**(3), 247–266.
- Chakravorty, U., Magné, B. and Moreaux, M. (2006) A Hotelling model with a ceiling on the stock of pollution. *Journal of Economic Dynamics and Control* **30**(12), 2875–2904.
- Chakravorty, U., Magné, B. and Moreaux, M. (2012) Resource use under climate stabilization: Can nuclear power provide clean energy? *Journal of Public Economic Theory* **14**(2), 349–389.
- Chandel, S. S., Shrivastva, R., Sharma, V. and Ramasamy, P. (2016) Overview of the initiatives in renewable energy sector under the national action plan on climate change in India. *Renewable and Sustainable Energy Reviews* **54**, 866–873.

- Chen, C., Twycross, J. and Garibaldi, J. M. (2017) A new accuracy measure based on bounded relative error for time series forecasting. *PloS ONE* **12**(3), 1–23.
- China Analysis (2015) China's fast track to a renewable future. Available <https://www.theclimategroup.org/sites/default/files/archive/files/RE100-China-analysis.pdf>.
- Chinadialogue (2013) Chinese nuclear versus renewables: Who is winning? Available <https://www.chinadialogue.net/article/show/single/en/6215-Chinese-nuclear-versus-renewables-who-is-winning->.
- Cohen, W. M. and Levinthal, D. A. (1990) Absorptive capacity: A new perspective on learning and innovation. *Administrative Science Quarterly* **35**(1), 128–152.
- Crompton, P. and Wu, Y. (2005) Energy consumption in China: Past trends and future directions. *Energy Economics* **27**(1), 195–208.
- Csereklyei, Z., Thurner, P. W., Langer, J. and Küchenhoff, H. (2017) Energy paths in the European Union: A model-based clustering approach. *Energy Economics* **65**, 442–457.
- Dalla Valle, A. and Furlan, C. (2011) Forecasting accuracy of wind power technology diffusion models across countries. *International Journal of Forecasting* **27**(2), 592–601.
- Davies, S. W. and Diaz-Rainey, I. (2011) The patterns of induced diffusion: Evidence from the international diffusion of wind energy. *Technological Forecasting and Social Change* **78**(7), 1227–1241.
- Davydenko, A. and Fildes, R. (2013) Measuring forecasting accuracy: The case of judgmental adjustments to SKU-level demand forecasts. *International Journal of Forecasting* **29**(3), 510–522.
- Deloitte (2015a) European energy market reform. Country profile: Belgium. Available <https://www2.deloitte.com/content/dam/Deloitte/global/Documents/Energy-and-Resources/gx-er-market-reform-belgium.pdf>.
- Deloitte (2015b) European energy market reform. Country profile: France. Available <https://www2.deloitte.com/content/dam/Deloitte/global/Documents/Energy-and-Resources/gx-er-market-reform-france.pdf>.
- Deloitte (2015c) European energy market reform. Country profile: Germany. Available <https://www2.deloitte.com/content/dam/Deloitte/global/Documents/Energy-and-Resources/gx-er-market-reform-germany.pdf>.

- Duan, H. B., Zhu, L. and Fan, Y. (2014) A cross-country study on the relationship between diffusion of wind and photovoltaic solar technology. *Technological Forecasting and Social Change* **83**, 156–169.
- Eclareon (2014) Assessment of climate change policies in the context of the European semester. Country report: Finland. Ecologic Institute. Available https://www.ecologic.eu/sites/files/publication/2014/countryreport_fi.ecologicelclareon_jan2014_0.pdf.
- EIA (2003) Country analysis briefs: Germany. Available https://www.geni.org/global-energy/library/national_energy_grid/germany/GermanyCountryAnalysisBrief.shtml.
- EIA (2013) Today in Energy. Japan is the second largest net importer of fossil fuels in the world. Available <https://www.eia.gov/todayinenergy/detail.php?id=13711>.
- EIA (2017) The US Energy Information Administration. International energy outlook 2017. Available [https://www.eia.gov/outlooks/ieo/pdf/0484\(2017\).pdf](https://www.eia.gov/outlooks/ieo/pdf/0484(2017).pdf).
- Energy Outlook (2013) The Belgian electricity market: Overview, analysis of today's issues and suggestions to fix it. Available <http://energy.sia-partners.com/belgian-electricity-market-overview-analysis-todays-issues-and-suggestions-fix-it>.
- Energy Transition (2016) The Global Energiewende. Renewable energy in Belgium. Available <https://energytransition.org/2016/10/renewable-energy-in-belgium/>.
- Eurostat (2006) EU integration seen through statistics. Available <https://www.lu.lv/materiali/biblioteka/es/pilnieteksti/statistika/EU%20integration%20seen%20through%20statistics.pdf>.
- Financial Times (2013) Osborne hails UK nuclear deal with China as 'new dawn'. Available <https://www.ft.com/content/9ffdb6a-367c-11e3-aaf1-00144feab7de>.
- Financial Times (2014) German coal use at highest level since 1990. Available <https://www.ft.com/content/e6470600-77bf-11e3-807e-00144feabdc0>.
- Furlan, C., Guidolin, M. and Guseo, R. (2016) Has the Fukushima accident influenced short-term consumption in the evolution of nuclear energy? An analysis of the world and seven leading countries. *Technological Forecasting and Social Change* **107**, 37–49.
- Furlan, C. and Mortarino, C. (2018) Forecasting the impact of renewable energies in competition with non-renewable sources. *Renewable and Sustainable Energy Reviews* **81**(2), 1879–1886.

- Furlan, C., Mortarino, C. and Zahangir, M. S. (2018a) A new diffusion model for competition among three actors. Proceedings of the 33rd International Workshop of Statistical Modelling, July 16–20, 2018, Bristol, UK, Vol. II, 50–55.
- Furlan, C., Mortarino, C. and Zahangir, M. S. (2018b) Interaction among three competitors: an extended innovation diffusion model. Working Paper Series 03/2018. Department of Statistical Sciences, University of Padova (submitted for publication to an international journal).
- Furlan, C., Mortarino, C. and Zahangir, M. S. (2018c) An extended diffusion model applied to competition between renewables and alternative energies. Proceedings of the 3rd Renewable Energy Sources – Research and Business (RESRB) 2018 conference, June 18–20, 2018, Brussels, Belgium, Book of ‘Abstract’, 63–64.
- GENI (2012) Global Energy Network Institute. How is 100% renewable energy possible in Japan by 2020? Available https://www.geni.org/globalenergy/research/renewable-energy-potential-of-japan/renewable_energy_potential_of_Japan_by_2020.pdf.
- Goodwin, P. and Lawton, R. (1999) On the asymmetry of the symmetric MAPE. *International Journal of Forecasting* **15**(4), 405–408.
- Greenpeace (2008) The energy revolution scenario for Japan. Available <https://www.greenpeace.org/archive-international/en/publications/reports/energy-revolution-scenario-japan/>.
- Guidolin, M. and Guseo, R. (2012) A nuclear power renaissance? *Technological Forecasting and Social Change* **79**(9), 1746–1760.
- Guidolin, M. and Guseo, R. (2015) Technological change in the US music industry: Within-product, cross-product and churn effects between competing blockbusters. *Technological Forecasting and Social Change* **99**, 35–46.
- Guidolin, M. and Guseo, R. (2016) The German energy transition: Modeling competition and substitution between nuclear power and renewable energy technologies. *Renewable and Sustainable Energy Reviews* **60**, 1498–1504.
- Guidolin, M. and Mortarino, C. (2010) Cross-country diffusion of photovoltaic systems: Modelling choices and forecasts for national adoption patterns. *Technological Forecasting and Social Change* **77**(2), 279–296.
- Guseo, R. (2011) Worldwide cheap and heavy oil productions: A long-term energy model. *Energy Policy* **39**(9), 5572–5577.

- Guseo, R. and Dalla Valle, A. (2005) Oil and gas depletion: Diffusion models and forecasting under strategic intervention. *Statistical Methods and Applications* **14**(3), 375–387.
- Guseo, R., Dalla Valle, A. and Guidolin, M. (2007) World oil depletion models: Price effects compared with strategic or technological interventions. *Technological Forecasting and Social Change* **74**(4), 452–469.
- Guseo, R. and Guidolin, M. (2009) Modelling a dynamic market potential: A class of automata networks for diffusion of innovations. *Technological Forecasting and Social Change* **76**, 806–820.
- Guseo, R. and Guidolin, M. (2010) Cellular automata with network incubation in information technology diffusion. *Physica A: Statistical Mechanics and its Applications* **389**(12), 2422–2433.
- Guseo, R. and Guidolin, M. (2011) Market potential dynamics in innovation diffusion: Modelling the synergy between two driving forces. *Technological Forecasting and Social Change* **78**(1), 13–24.
- Guseo, R. and Mortarino, C. (2012) Sequential market entries and competition modelling in multi-innovation diffusions. *European Journal of Operational Research* **216**(3), 658–667.
- Guseo, R. and Mortarino, C. (2014) Within-brand and cross-brand word-of-mouth for sequential multi-innovation diffusions. *IMA Journal of Management Mathematics* **25**(3), 287–311.
- Guseo, R. and Mortarino, C. (2015) Modeling competition between two pharmaceutical drugs using innovation diffusion models. *The Annals of Applied Statistics* **9**(4), 2073–2089.
- Guseo, R., Mortarino, M. and Darda, M. A. (2015) Homogeneous and heterogeneous diffusion models: Algerian natural gas production. *Technological Forecasting and Social Change* **90**(B), 366–378.
- Hauser, J., Tellis, G. J. and Griffin, A. (2006) Research on innovation: A review and agenda for marketing science. *Marketing Science* **25**(6), 687–717.
- Horsky, D. (1990) A diffusion model incorporating product benefits, price, income and information. *Marketing Science* **9**(4), 342–365.

- Huh, S. Y. and Lee, C. Y. (2014) Diffusion of renewable energy technologies in South Korea on incorporating their competitive interrelationships. *Energy Policy* **69**, 248–257.
- Hyndman, R. J. and Koehler, A. B. (2006) Another look at measures of forecast accuracy. *International Journal of Forecasting* **22**(4), 679–688.
- IEA (2007) International Energy Agency. Energy policies of IEA countries – Switzerland 2007 review. Available <https://webstore.iea.org/energy-policies-of-iea-countries-switzerland-2007-review>.
- IEA (2016a) International Energy Agency. Energy policies of IEA countries – Belgium 2016 review. Available https://www.iea.org/publications/freepublications/publication/Energy_Policies_of_IEA_Countries_Belgium_2016_Review.pdf.
- IEA (2016b) International Energy Agency. Energy policies of IEA countries – Japan 2016 review. Available <https://www.iea.org/publications/freepublications/publication/EnergyPoliciesofIEACountriesJapan2016.pdf>.
- IET (2012) The Institute of Engineering Technology. UK energy policy 1980–2010: A history and lessons to be learnt. Available <http://sro.sussex.ac.uk/38852/1/uk-energy-policy.pdf>.
- Ishida, H. (2013) Causal relationship between fossil fuel consumption and economic growth in Japan: A multivariate approach. *International Journal of Energy Economics and Policy* **3**(2), 127–136.
- Jain, D. C. and Rao, R. C. (1990) Effect of price on the demand for durables: Modeling, estimation, and findings. *Journal of Business and Economic Statistics* **8**(2), 163–170.
- Kalinowski, P. and Fidler, F. (2010) Interpreting significance: the differences between statistical significance, effect size, and practical importance. *Newborn and Infant Nursing Reviews* **10**(1), 50–54.
- Kalish, S. (1985) A new product adoption model with price, advertising, and uncertainty. *Management Science* **31**(12), 1569–1585.
- Kalish, S., Mahajan, V. and Muller, E. (1995) Waterfall and sprinkler new-product strategies in competitive global markets. *International Journal of Research in Marketing* **12**(2), 105–119.

- Kamakura, W. A. and Balasubramanian, S. (1988) Long-term view of the diffusion of durables a study of the role of price and adoption influence processes via tests of nested models. *International Journal of Research in Marketing* **5**(1), 1–13.
- Katz, E. and Lazarsfeld, P. F. (1955) *Personal Influence: The Part Played by People in the Flow of Mass Communication*. Free Press: Glencoe, IL.
- Kijek, A. and Kijek, T. (2010) Modelling of innovation diffusion. *Operations Research and Decisions* **20**(3-4), 53–68.
- Kim, N., Bridges, E. and Srivastava, R. K. (1999) A simultaneous model for innovative product category sales diffusion and competitive dynamics. *International Journal of Research in Marketing* **16**(2), 95–111.
- Klein, S. J. W. and Whalley, S. (2015) Comparing the sustainability of U.S. electricity options through multi-criteria decision analysis. *Energy Policy* **79**, 127–149.
- Krishnan, T. V., Bass, F. M. and Kumar, V. (2000) Impact of a late entrant on the diffusion of a new product/service. *Journal of Marketing Research* **37**(2), 269–278.
- Kumar, V. K. R. and Vimala, M. (2012) Energy consumption in India-recent trends. *Asia Pacific Journal of Research* **1**(36), 140–151.
- Libai, B., Muller, E. and Peres, R. (2009) The role of within-brand and cross-brand communications in competitive growth. *Journal of Marketing* **73**(3), 19–34.
- Lloyd, P. J. (2017) The role of energy in development. *Journal of Energy in Southern Africa* **28**(1), 54–62.
- Mahajan, V. (1986) Innovation diffusion models of new product acceptance. In *Innovation Diffusion Models of New Product Acceptance: A Reexamination*, eds V. Mahajan and Y. Wind. Ballinger: Cambridge, MA.
- Mahajan, V. and Muller, E. (1979) Innovation diffusion and new product growth models in marketing. *Journal of Marketing* **43**(Fall), 55–68.
- Mahajan, V., Muller, E. and Bass, F. M. (1990) New product diffusion models in marketing: A review and directions for research. *Journal of Marketing* **54**(January), 1–26.
- Mahajan, V., Muller, E. and Bass, F. M. (1995) Diffusion of new products: Empirical generalizations and managerial uses. *Marketing Science* **14**(3), G79–G88.

- Mahajan, V., Muller, E. and Wind, Y. (2000) *New-product Diffusion Models*. Springer Verlag: Switzerland.
- Mahajan, V. and Peterson, R. A. (1978) Innovation diffusion in a dynamic potential adopter population. *Management Science* **24**(15), 1589–1597.
- Mahajan, V., Sharma, S. and Buzzell, R. D. (1993) Assessing the impact of competitive entry on market expansion and incumbent sales. *Journal of Marketing* **57**, 39–52.
- Makridakis, S. (1993) Accuracy measures: Theoretical and practical concerns. *International Journal of Forecasting* **9**(4), 527–529.
- Makridakis, S. and Hibon, M. (2000) The M3-competition: Results, conclusions and implications. *International Journal of Forecasting* **16**(4), 451–476.
- Marchetti, C. (1980) Society as a learning system: Discovery, invention, and innovation cycles revisited. *Technological Forecasting and Social Change* **18**(4), 267–282.
- Market Watch (2016) China's growth in renewable energy raises 'overcapacity' concerns: IEA. Available <https://www.marketwatch.com/story/chinas-growth-in-renewable-energy-raises-overcapacity-concerns-iea-2016-10-25>.
- Meade, N. and Islam, T. (2001) Forecasting the diffusion of innovations: Implications for time-series extrapolation. In *Principles of Forecasting*, ed. J. S. Armstrong, pp. 577–595. Springer: Boston, MA.
- Meade, N. and Islam, T. (2006) Modelling and forecasting the diffusion of innovation—A 25-year review. *International Journal of Forecasting* **22**, 519–545.
- Melikoglu, M. (2014) Shale gas: Analysis of its role in the global energy market. *Renewable and Sustainable Energy Reviews* **37**, 460–468.
- Meyer, P. S. and Ausubel, J. H. (1999) Carrying capacity: A model with logistically varying limits. *Technological Forecasting and Social Change* **61**(3), 209–214.
- Montoya, F. G., Aguilera, M. J. and Manzano-Agugliaro, F. (2014) Renewable energy production in Spain: A review. *Renewable and Sustainable Energy Reviews* **33**, 509–531.
- Muller, E., Peres, R. and Mahajan, V. (2009) *Innovation Diffusion and New Product Growth*. Marketing Science Institute: Cambridge, MA.

- Norton, J. A. and Bass, F. M. (1987) A diffusion theory model of adoption and substitution for successive generations of high-technology products. *Management Science* **39**(9), 1069–1086.
- NP (2017) World Energy Needs and Nuclear Power. World Nuclear Association. Available <http://www.world-nuclear.org/information-library/current-and-future-generation/world-energy-needs-and-nuclear-power.aspx>.
- NPB (2018) Nuclear Power in Belgium. World Nuclear Association. Available <http://www.world-nuclear.org/information-library/country-profiles/countries-a-f/belgium.aspx>.
- NPC (2018) Nuclear Power in China. World Nuclear Association. Available <http://www.world-nuclear.org/information-library/country-profiles/countries-a-f/china-nuclear-power.aspx>.
- NPF (2018) Nuclear Power in Finland. World Nuclear Association. Available <http://www.world-nuclear.org/information-library/country-profiles/countries-a-f/finland.aspx>.
- NPG (2018) Nuclear Power in Germany. World Nuclear Association. Available <http://www.world-nuclear.org/information-library/country-profiles/countries-g-n/germany.aspx>.
- NPJ (2018) Nuclear Power in Japan. World Nuclear Association. Available <http://www.world-nuclear.org/information-library/country-profiles/countries-g-n/japan-nuclear-power.aspx>.
- NPS (2017) Nuclear Power in Spain. World Nuclear Association. Available <http://www.world-nuclear.org/information-library/country-profiles/countries-o-s/spain.aspx>.
- NPS (2018) Nuclear Power in Sweden. World Nuclear Association. Available <http://www.world-nuclear.org/information-library/country-profiles/countries-o-s/sweden.aspx>.
- NPUS (2018) Nuclear Power in the USA. World Nuclear Association. Available <http://www.world-nuclear.org/information-library/country-profiles/countries-t-z/usa-nuclear-power.aspx>.
- O'Connor, P. A. and Cleveland, C. J. (2014) U.S. energy transitions 1780–2010. *Energies* **7**(12), 7955–7993.

- Pao, H. T. and Fu, H. C. (2013) Renewable energy, non-renewable energy and economic growth in Brazil. *Energy Economics* **25**, 381–392.
- Parker, P. M. (1992) Price elasticity dynamics over the adoption life cycle. *Journal of Marketing Research* **29**(3), 358–367.
- Parker, P. M. (1993) Choosing among diffusion models: Some empirical evidence. *Marketing Letters* **4**(1), 81–94.
- Parker, P. M. and Gatignon, H. (1994) Specifying competitive effects in diffusion models: An empirical analysis. *International Journal of Research in Marketing* **11**(1), 17–39.
- Peres, R., Muller, E. and Mahajan, V. (2010) Innovation diffusion and new product growth models: A critical review and research directions. *International Journal of Research in Marketing* **27**(2), 91–106.
- Peterson, R. A. and Mahajan, V. (1978) Multi-product growth models. *Research in Marketing* **1**(20), 1–23.
- Planete-energies (2015a) The history of energy in France. Available <https://www.planete-energies.com/en/medias/saga-energies/history-energy-france>.
- Planete-energies (2015b) The history of energy in Germany. Available <https://www.planete-energies.com/en/medias/saga-energies/history-energy-germany>.
- Planete-energies (2015c) The history of energy in the United Kingdom. Available <https://www.planete-energies.com/en/medias/saga-energies/history-energy-united-kingdom>.
- Rao, K. U. and Kishore, V. V. N. (2009) Wind power technology diffusion analysis in selected states of India. *Renewable Energy* **34**(4), 983–988.
- Rao, K. U. and Kishore, V. V. N. (2010) A review of technology diffusion models with special reference to renewable energy technologies. *Renewable and Sustainable Energy Reviews* **14**(3), 1070–1078.
- Redondo, P. D. and van Vliet, O. (2015) Modelling the energy future of Switzerland after the phase out of nuclear power plants. *Energy Procedia* **76**, 49–58.
- REEEP (2014) Renewable Energy and Energy Efficiency Partnership. Switzerland (2013). Available <https://www.reeep.org/switzerland-2013>.

- REN21 (2014) Renewable Energy Policy Network for the 21st Century. Renewables 2014 global status report. Available http://www.ren21.net/Portals/0/documents/Resources/GSR/2014/GSR2014_full%20report_low%20res.pdf.
- REN21 (2016) Renewable Energy Policy Network for the 21st Century. Renewables 2016 global status report. Available http://www.ren21.net/wp-content/uploads/2016/05/GSR_2016_Full_Report_lowres.pdf.
- Rogers, E. M. (2003) *Diffusion of Innovation*. 4th ed. Free Press: New York.
- Savin, S. and Terwiesch, C. (2005) Optimal product launch times in a duopoly: Balancing life-cycle revenues with product cost. *Operations Research* **53**(1), 26–47.
- Schwarz, G. (1978) Estimating the dimension of a model. *The annals of Statistics* **6**(2), 461–464.
- Seber, G. A. F. (1980) *The Linear Hypothesis: A General Theory*. 2nd ed. Griffin: London.
- Seber, G. A. F. and Wild, C. J. (1989) *Nonlinear Regression*. Wiley: New York.
- Shaikh, N. I., Rangaswamy, A. and Balakrishnan, A. (2006) Modeling the diffusion of innovations using small-world network. Technical Report, Penn State University.
- Sharif, M. N. and Ramanathan, K. (1981) Binomial innovation diffusion models with dynamic potential adopter population. *Technological Forecasting and Social Change* **20**(1), 63–87.
- Shen, J. and Luo, C. (2015) Overall review of renewable energy subsidy policies in China—Contradictions of intentions and effects. *Renewable and Sustainable Energy Reviews* **41**, 1478–1488.
- Sweden.se (2018) Energy use in Sweden. Available <https://sweden.se/society/energy-use-in-sweden/>.
- Sydow, J. and Schreyogg, G. (2013) *Self-Reinforcing Processes in and among Organizations*. Palgrave Macmillan: New York.
- Tarde, G. (1890) *Les lois de l'imitation*. Kimé: Paris.
- Tashman, L. J. (2000) Out-of-sample tests of forecasting accuracy: An analysis and review. *International Journal of Forecasting* **16**, 437–450.

- Treehugger (2011) Is now the time to rethink Japan's energy future? Available <https://www.treehugger.com/clean-technology/is-now-the-time-to-rethink-japans-energy-future.html>.
- Tripathi, L., Mishra, A. K., Dubey, A. K., Tripathi, C. B. and Baredar, P. (2016) Renewable energy: An overview on its contribution in current energy scenario of India. *Renewable and Sustainable Energy Reviews* **60**, 226–233.
- Tsur, Y. and Zemel, A. (2003) Optimal transition to backstop substitutes for nonrenewable resources. *Journal of Economic Dynamics and Control* **27**(4), 551–572.
- Van den Bulte, C. (2002) The Bass diffusion model is not a mixture of innovators and imitators. Technical Report, Wharton School, University of Pennsylvania.
- Van der Ploeg, F. and Withagen, C. (2012) Is there really a green paradox? *Journal of Environmental Economics and Management* **64**(3), 342–363.
- Vengosh, A., Jackson, R. B., Warner, N., Darrah, T. H. and Kondash, A. (2014) A critical review of the risks to water resources from unconventional shale gas development and hydraulic fracturing in the United States. *Environmental Science and Technology* **48**, 8334–8348.
- Vestrucci, P., Schiavi, S. and Orlandelli, C. M. (2015) Long term dynamics of energy systems: The Italian case. *Technological Forecasting and Social Change* **96**, 266–276.
- Wang, J., Feng, L., Zhao, L. and Snowden, S. (2013) China's natural gas: Resources, production and its impacts. *Energy Policy* **55**, 690–698.
- Wang, Q., Chen, X., Jha, A. N. and Rogers, H. (2014) Natural gas from shale formation—the evolution, evidences and challenges of shale gas revolution in United States. *Renewable and Sustainable Energy Reviews* **30**, 1–28.
- Wang, Z. and Krupnick, A. (2015) A retrospective review of shale gas development in the United States: What led to the boom? *Economics of Energy and Environmental Policy* **4**(1), 5–17.

Mohammad Salim Zahangir

CURRICULUM VITAE

Contact Information

University of Padova
Department of Statistics
via Cesare Battisti, 241-243
35121 Padova. Italy.

Tel. +39 049 827 4174
e-mail: mohammadsalim.zahangir@studenti.unipd.it

Current Position

Since October 2015; (expected completion: March 2019)

PhD Student in Statistical Sciences, University of Padova.

Thesis title: Competition and Substitution in Energy: Old Scenarios and Emerging Technologies

Supervisor: Prof. Cinzia Mortarino

Research interests

- Diffusion of Innovations Modelling
- Nonlinear Regression
- Demography

Education

September 2010 – August 2011

Master of Science in Demography.

Department of Sociology (including SUDA)

University of Stockholm, Sweden.

Title of dissertation: “Early and Very Early Family Formation in Bangladesh”

Supervisor: Prof. Gunnar Andersson

Final mark: Good

July 1995 – June 1996 (Exam. held in 2000)

Master of Science in Statistics.

Department of Statistics

University of Chittagong, Bangladesh.

Final mark: 389.

July 1992 – June 1995 (Exam. held in 1997)

Bachelor of Science with Honours in Statistics.

Department of Statistics

University of Chittagong, Bangladesh.

Final mark: 660.

Work experience

January 2006 – Till date (on study leave since October 2015)

Department of Statistics
University of Chittagong, Bangladesh.
Academic Staff.

August 2003 – January 2006

Cantonment College, Comilla Cantonment, Bangladesh.
Lecturer (Statistics).

July 2001 – August 2003

City Royal College, Dhaka, Bangladesh.
Lecturer (Statistics).

Awards and Scholarship

October 2015 – September 2018

PhD Scholarship, Università di Padova, Italy.

1995

Merit Scholarship for Undergraduate Results, University of Chittagong, Bangladesh.

1996

Merit Scholarship for Postgraduate Results, University of Chittagong, Bangladesh.

Computer skills

- Statgraphics
- Mathematica
- R
- SPSS
- L^AT_EX

Language skills

Bangla: native; English: fluent.

Publications

Articles in journals

Zahangir, M. S. (2015). Patterns in early and very early family formation in Bangladesh. *Asian Profile* **42**(2), 123–140.

Zahangir, M. S. and Chan, C. H. Y. (2015). Son preference and gender composition of children in Bangladesh. *Journal of Family Welfare* **61**(2), 25–42.

Nahar, M. Z. and Zahangir, M. S. (2013). Patterns and determinants of age at first birth in Bangladesh. *Turkish Journal of Population Studies* **35**, 63–77.

Zahangir, M. S. and Nahar, M. Z. (2013). Fertility in rural and urban Bangladesh: A comparative study. *Demografie* **55**(2), 132–144.

Nahar, M. Z. and Zahangir, M. S. (2013). Age at first marriage and its relation to fertility in Bangladesh. *Chinese Journal of Population, Resources and Environment* **11**(3), 227–235.

Zahangir, M. S. and Kamal, M. M. (2011). Several attributes linked with child marriage of females in Bangladesh. *International Journal of Statistics and Systems* **6**(1), 107–117.

Zahangir, M. S. and Balasundaram, N. (2011). Factors affecting employees' performance in ready-made garments (RMGs) sector in Chittagong, Bangladesh. *Petroleum-Gas University of Ploiesti BULLETIN, Economic Sciences Series* **LXIII**(1), 9–15.

Zahangir, M. S., Karim, M. A., Zaman, M. R., Hussain, M.I. and Hossain M. S. (2008). Determinants of age at first marriage of rural women in Bangladesh: A cohort analysis. *Trends in Applied Sciences Research* **3**(4), 335–343.

Zaman, M. R., Zahangir, M. S., Hussain, M. I. and Hossain M. S. (2008). Genotypic variability of the components and their effects on the rice yield: correlation and path analysis study. *Italian Journal of Agronomy/ Riv. Agron.* **3**(2), 131–134.

Work in progress

Furlan, C., Mortarino, C. and Zahangir, M. S. (2018). A new diffusion model for competition among three actors.

Working paper

Furlan, C., Mortarino, C. and Zahangir, M. S. (2018). Interaction among three competitors: An extended innovation diffusion model. *Working papers series* 03/2018. Department of Statistical Sciences, University of Padova.

Conference presentations

Furlan, C., Mortarino, C. and Zahangir, M. S. (2018). An extended diffusion model applied to competition between renewables and alternative energies. (oral presentation) *3rd Renewable Energy Sources – Research and Business (RESRB) 2018 conference*, Brussels, Belgium, June 18–20.

References

Prof. Cinzia Mortarino

Department of Statistical Sciences
University of Padova
Via Cesare Battisti 241
35121 Padua, Italy
Phone: +39 049 827 4184
e-mail: mortarino@stat.unipd.it

Prof. Claudia Furlan

Department of Statistical Sciences
University of Padova
Via Cesare Battisti 241
35121 Padua, Italy
Phone: +39 049 827 4129
e-mail: claudia.furlan@unipd.it

Gunnar Andersson

Professor in Demography
Department of Sociology (including SUDA)
University of Stockholm
106 91 Stockholm, Sweden
Phone: 0046 8 163261
e-mail: gunnar.andersson@sociology.su.se

Juho Harkonen

Professor of Sociology
Department of Political and Social Sciences
European University Institute
Via dei Roccettini, 9
50014 San Domenico di Fiesole (FI), Italy
Phone: +39 055 4685 426
e-mail: Juho.Harkonen@eui.eu